

NEW MATERIAL, SURFACE COATINGS
AND BIODEGRADABLE OILS FOR
INDUSTRIAL GEARS

Ramiro Carneiro Martins

Faculdade Engenharia da Universidade do Porto
Departamento de Engenharia Mecânica e Gestão Industrial

NEW MATERIALS, SURFACE COATINGS
AND BIODEGRADABLE OILS FOR
INDUSTRIAL GEARS

Ramiro Carneiro Martins

PhD thesis presented to
Faculdade de Engenharia da Universidade do Porto

Thesis supervised by
Dr. Jorge Humberto Oliveira Seabra
Associated Professor of FEUP

Porto, March of 2008

Acknowledgements

I would like to express my sincere gratitude to my supervisor Prof. Jorge Seabra for his patient guidance and permanent support throughout the course of this work.

I wish to thank to my remarkable colleagues and friends at CETRIB: Armando Campos, Beatriz Graça, Joana Claro, Jorge Castro, José Brandão, Luís Magalhães, Nuno Cardoso, Paulo Moura, Ricardo Ribeiro and Rui Amaro.

I'm beholden to my parents, brothers, nephews and closest friends for his permanent availability and encouragement.

I'm thankful to INEGI (Instituto Nacional de Engenharia e Gestão Industrial), FEUP (Faculdade de Engenharia da Universidade do Porto) and FCT (Fundação para a Ciência e a Tecnologia) for their support to this work.

This work has been performed within three european research projects supported by the European Commission, in which an enormous amount of persons and entities participated.

I would like to thank the European Commission for the economical support to these projects and to all the partners and their representatives involved in those projects, namely:

On CRAFT project:

- Shuton S.A.
- Teer Coatings Ltd.
- A. Brito - Industria Portuguesa de Engrenagens Lda.
- Equipamientos Tecnicos Comerciales S.A.
- Fundación TEKNIKER
- INEGI

On EREBIO project:

- Fundación TEKNIKER
- Centrale Recherche S.A.
- Ingenieurgesellschaft Fuer Auto und Verkehr GMBH
- Ferespe - Fundação de Ferro e Aço Lda.
- TARABUSI S.A.

- A. Brito - Industria Portuguesa de Engrenagens Lda.
- REGIENOV - Renault Recherche et Innovation
- GUASCOR Investigacion y Desarrollo S.A.
- Federal Institute for Material Research and Testing
- FALEX Tribology N.V.
- FUCHS Petrolub AG
- INEGI

On BIOMON project:

- ROWE Mineralolwerk GMBH
- A.BRITO - Industria Portuguesa de Engrenagens Lda.
- Fundación TEKNIKER
- SHUTON S.A.
- MONITION Ltd.
- INEGI

to my family

Abstract

Ever since gears were first used there has been a constant demand for increasing the power density in gear transmissions, to reduce the power losses, to increase the life time and also to decrease their weight. To satisfy these demands new solutions have been developed, such as the use of new materials, the application of surface coatings, improved surface finishing, different hardening treatments, and the use of new lubricants.

There is also a growing environmental awareness that leads to an increasing interest in biodegradable non-toxic oils. Of course, higher lubricant performance in what concerns friction, wear, lifetime, etc. has also major impact in the environmental compatibility, because premature wear, high energy needs and low lifetime are also harmful to the environment.

Any new solution presented must have technical performance advantages for its industrial application, and the technical performance must be proved in dedicated tests.

Nowadays some of the main concerns in gear applications are scuffing failures, micropitting fatigue damage (contact fatigue wear phenomenon observed in combined rolling and sliding contacts operating under elastohydrodynamic lubrication (EHL) or mixed EHL/Boundary lubrication conditions) and power loss or efficiency. These were some of the main concerns during this work for the evaluation of new material, surface coatings and lubricants for gears.

The applicability of multilayer composite surface coatings (providing coefficients of friction close to those obtained with solid lubricants like MoS₂ and graphite) in gear tooth is discussed in this work, mainly in what concerns to gear efficiency at normal operating conditions and to scuffing load capacity. The average friction coefficient between gear tooth is also discussed and compared with a conventional solution (carburized steel gears).

The use of Austempered Ductil Iron (ADI), austempered at 300°C, as a gear material is also discussed, mainly in what concerns fatigue life, both pitting and micropitting, and power loss behaviour.

Two new environmentally friendly lubricants blended for industrial gear applications were investigated in this work. These oils are based on fully or highly saturated esters and are produced from harvestable raw materials. Both oils are biodegradable and have low toxicity and were formulated to replace mineral lubricants in industrial gears, accomplishing CLP specification according to DIN51517.

The overall performance and applicability of the biolubricants was assessed in this work, their tribological performance has been evaluated in combination with the different materials and surface coatings, as well as with the classical carburized steel gears. This will give an overview of the range of tribological systems where ester oils could be used. This research focussed on the scuffing load capacity, micropitting protection and power loss.

The influence of lubricants and material / surface coating combinations on the friction coefficient between gear tooth is discussed and evaluated. A numerical model for the energetic balance of the FZG gearbox has been developed for that purpose, integrating the mechanisms of power loss and heat evacuation. The model also calculates the equilibrium temperature of the gearbox as well as the influence of gearbox com-

ponents in the overall power loss, providing a better understanding of the variation of the churning and friction losses and their influence in the total power loss.

The ADI material has very interesting properties and presents a behaviour similar to steel, although lower contact pressures must be used.

The surface coatings, specially the MoS₂/Ti presented an outstanding increase of scuffing load capacity and also a considerable improvement in the energetic efficiency of gears.

The biodegradable non-toxic lubricants proved to be an advantageous solution for replacing mineral lubricants. They form a better tribological system than the mineral lubricant with all the materials and surface coatings tested.

So, the ester lubricants tested are environmentally compatible not only due to their biodegradability and low-toxicity but also due to the lower power consumption, better load carrying capacity and equal or better micropitting protection.

Sumário

A utilização de engrenagens tem sofrido uma pressão constante desde o início da sua utilização no sentido de aumentar a potência transmitida, de melhorar o seu rendimento, aumentar a sua vida útil e simultaneamente diminuir o seu peso. A satisfação destes requisitos tem ocorrido através de novas soluções, que vão desde novos materiais, à aplicação de revestimentos superficiais, super acabamento superficial, novos tratamentos térmicos e a utilização de novos lubrificantes.

A crescente preocupação ambiental conduz a um interesse crescente em óleos biodegradáveis e de baixa toxicidade, mas o elevado desempenho dos lubrificantes no que diz respeito ao atrito, desgaste, tempo de vida, etc. também tem um elevado impacto na protecção ambiental, uma vez que o desgaste prematuro, o elevado consumo energético e um tempo de vida curto são altamente prejudiciais ao ambiente.

Qualquer nova solução deve apresentar vantagens técnicas para a sua aplicação industrial, e esse incremento de desempenho precisa de ser comprovado em testes específicos.

Algumas das principais preocupações no uso de engrenagens continuam a ser a avaria por gripagem, a fadiga superficial sob a forma de *micropitting* (fenómeno de fadiga superficial que ocorre em condições de lubrificação EHL ou mista EHL / lubrificação limite) e a dissipação de potência ou rendimento energético. Estas foram também algumas das principais preocupações ao longo deste trabalho na avaliação dos novos materiais, revestimentos superficiais e lubrificantes.

A aplicabilidade de revestimentos superficiais compostos multi-camada em engrenagens (com coeficientes de atrito próximos dos obtidos com MoS₂ ou grafite) será discutida neste trabalho, especialmente no que diz respeito à eficiência energética das engrenagens em condições normais de funcionamento e à capacidade de carga à gripagem. O coeficiente de atrito médio no contacto dos dentes da engrenagem será também discutido e comparado com o obtido para a solução convencional (rodas em aço cementadas).

A aplicabilidade do ferro fundido nodular austemperado (ADI) a 300 °C em engrenagens também é discutido neste trabalho, especialmente no que se refere à vida à fadiga (pitting e micropitting) e ao desempenho energético, sendo em ambos os casos comparado com a solução clássica, o aço cementado.

Neste trabalho foi também investigado o comportamento tribológico de duas novas formulações de óleos “amigos do ambiente”. Ambos os óleos são biodegradáveis e de baixa toxicidades, possuindo uma base ester muito ou totalmente saturada, produzida a partir de óleos vegetais provenientes de materias primas cultiváveis. Estes dois óleos foram formulados para aplicações industriais de modo a cumprir a especificação CLP DIN 51517, e também de modo a substituir os óleos minerais nessas aplicações.

A performance global e a aplicabilidade dos bio-lubrificantes em engrenagens foram estudadas neste trabalho. O estudo foi efectuado combinando os óleos com vários materiais, revestimentos superficiais em engrenagens cementadas, permitindo deste modo, uma visão geral sobre os tipos de sistemas tribológicos onde os esters podem ser usados. Os aspectos principais considerados foram a capacidade de carga à gripagem, a protecção contra o micropitting e o desempenho energético.

A influência do conjunto lubrificante/material ou lubrificante/revestimento superficial no coeficiente de atrito entre os dentes das engrenagens foi estudado e avaliado,

sendo para esse efeito desenvolvido um modelo numérico do balanço energético da caixa FZG, modelo esse que integra os mecanismos de dissipação de potência e de evacuação de calor. Este modelo energético também permite estimar a temperatura de estabilização do banho de óleo sendo conhecidas as condições de funcionamento, permite também estimar a influência dos diversos componentes constituintes da caixa na dissipação total de potência, permitindo deste modo uma melhor compreensão da origem da potência dissipada assim como da variação das perdas por chapinagem e das perdas devidas à carga e qual a sua proporção na perda total de potência.

O ADI possui propriedades muito interessantes e apresenta um desempenho semelhante ao obtido com aço cementado, no entanto é necessário usar pressões de contacto inferiores.

Os revestimentos superficiais, em especial o MoS_2/Ti , apresentaram um incremento enorme da capacidade de carga à gripagem e também uma melhoria considerável da eficiência energética das engrenagens.

Os lubrificantes biodegradáveis e não tóxicos mostraram ser uma solução vantajosa na substituição dos lubrificantes minerais. Mostraram formar um melhor sistema tribológico com todos os materiais e revestimentos superficiais testados.

Portanto, os esters testados são “amigos do ambiente” devido à sua biodegradabilidade e toxicologia e são-no também devido a promover menor consumo de energia, maior capacidade de carga à gripagem e igual ou mesmo melhor protecção em relação ao micropitting.

Sommaire

L'exigence d'un progrès vers des densités de puissance croissantes en transmissions par engrenages s'est faite sentir depuis toujours, à la fois pour augmenter leur vie utile et pour diminuer leur poids. De manière à satisfaire ces exigences, de nouvelles solutions ont été développées, telles que l'utilisation de nouveaux matériaux, l'application de revêtements de surface, l'amélioration de la finition de surface, l'usage de différents traitements de durcissement et l'emploi de nouveaux lubrifiants.

Plus récemment, des préoccupations d'ordre écologique ont fait surface et prennent une importance croissante. En conséquence les huiles non toxiques et biodégradables sont l'objet d'un intérêt considérable. Néanmoins, il ne faut pas oublier qu'une meilleure performance des lubrifiants en ce qui concerne la friction, l'usure, la vie etc. a aussi un impact majeur sur la compatibilité avec l'environnement, puisque l'usure prématurée, un grand besoin énergétique et une vie courte sont aussi néfastes à l'environnement.

Ainsi, toute solution présentée doit avoir des avantages au niveau de la performance technique dans les applications industrielles et cette performance doit être prouvée à travers d'essais spécifiques.

Quelques unes des préoccupations principales au sujet des applications des engrenages sont le grippage, la dégradation de fatigue de micropitting (un phénomène d'usure de fatigue de contact observé pendant les contacts avec roulement et glissement combinés, opérant en lubrification élasto-hydro-dynamique (EHL) ou en conditions de lubrification mixte EHL/limite) et la dissipation de puissance ou rendement. Ceci ont été quelques uns des principaux sujets d'attention de ce travail, pour l'évaluation de nouveaux matériaux, revêtements de surface et lubrifiants.

L'adéquation des revêtements de surface composites, à plusieurs couches, (à coefficient de frottement proche de ceux des lubrifiants solides tels que MoS₂ et la graphite) sur les dents d'engrenages est discutée dans ce travail, surtout en ce qui concerne le rendement des engrenages en conditions d'opération normales et la capacité de charge de grippage. Le coefficient de frottement moyen entre les dents d'engrenages est aussi discuté et comparé avec des solutions conventionnelles (acier d'engrenage de cémentation).

L'utilisation de la fonte sphéroïdale, austemprée à 300 °C, comme matériau pour engrenages est également discutée, surtout en ce qui concerne la vie à la fatigue, tant du point de vue du micropitting comme de celui du pitting, et le comportement de perte de puissance.

Deux nouvelles huiles eco-compatibles formulées pour l'utilisation en transmission d'engrenages ont été étudiées pendant ce travail. Les huiles ont une base ester complètement ou très saturée et sont produites à partir de matières premières cultivables. Toutes deux sont biodégradables et non toxiques et ont été formulées dans le but de remplacer les lubrifiants minéraux pour engrenages industriels et pour respecter la spécification CLP d'après la norme DIN51517.

La performance globale et l'adéquation des bio-lubrifiants ont été évaluées pendant ce travail. Leur performance tribologique a été évaluée en considérant plusieurs combinaisons de matériaux et de revêtements de surface (l'une de ces combinaisons est l'engrenage classique en acier de cémentation). Ceci devrait offrir un aperçu global des domaines d'utilisation des huiles ester.

Ce travail s'est concentré sur la capacité de charge au grippage, sur la protection

contre le micropitting et sur les pertes de puissance.

L'influence du lubrifiant et de la combinaison matériau / revêtement de surface sur le coefficient de frottement entre dents d'engrenages est discutée et évaluée. Dans ce but, un modèle numérique de l'équilibre énergétique d'une boîte d'engrenages FZG, qui intègre les mécanismes de dissipation de puissance et d'évacuation de chaleur, a été développé.

Ce modèle permet aussi de déterminer la température d'équilibre d'une boîte d'engrenages aussi bien que de connaître l'influence de chaque composant de la transmission sur la perte de puissance totale. Autrement dit, il permet de mieux comprendre les variations des pertes par barbotage et par friction et leur influence sur la perte globale de puissance.

L'ADI est un matériel avec des propriétés tribologiques très intéressantes, avec un comportement semblable à l'acier. Toutefois, il ne tolère que des pressions superficielles bien moins hautes.

Les revêtements de surface, en particulier le MoS₂/Ti, démontrent une remarquable augmentation de la capacité de charge au grippage et une amélioration considérable de l'efficacité énergétique des engrenages.

Il a été démontré que les lubrifiants biodégradables et non toxiques sont une solution avantageuse pour remplacer les lubrifiants minéraux. Ils forment un système tribologique avec les matériaux et revêtements testés mieux que les lubrifiants minéraux.

Ainsi, les lubrifiants ester testés sont eco-compatibles non seulement grâce à leur biodégradabilité et basse toxicité mais aussi grâce à leur faible consommation d'énergie, à leur meilleure capacité de charge et à leur protection contre le micropitting similaire ou même supérieure à l'acier de cémentation.

Keywords

Gears
ADI
Scuffing
Pitting
Micropitting
Power losses
Friction coefficient
Biodegradable oils
Surface coatings
Composite surface coating
Non-toxic lubricants

Palavras chave

Engrenagens
ADI
Gripagem
Pitting
Micropitting
Perda de potência
Coeficiente de atrito
Óleo biodegradável
Revestimentos superficiais
Revestimentos superficiais compostos
Óleos não tóxicos

Mots-clés

Engrenages
ADI
Grippage
Piqûres
Micro-piqûres
Perte de puissance
Coefficient de frottement
Lubrifiant biodégradable
Revêtement de surface
Revêtement de surface composé
Lubrifiants Non-toxic

Appended papers

R. Martins, R. Amaro, and J. Seabra, "Influence of low friction coatings on the scuffing load capacity and efficiency of gears ", *Tribology International*, vol. 41, pp. 234-243, Apr 2008.

R. Martins and J. Seabra, "Micropitting performance of mineral and biodegradable ester gear oils". *Industrial Lubrication and Tribology*, (6) 2008 (to be published).

R. Martins, J. Seabra, A. Brito, C. Seyfert, R. Luther, and A. Igartua, "Friction coefficient in fzg gears lubricated with industrial gear oils: Biodegradable ester vs. mineral oil", *Tribology International*, vol. 39, no. 6, pp. 512-521, 2006.

R. C. Martins, P. S. Moura, and J. O. Seabra, "MoS₂/Ti low-friction coating for gears", *Tribology International*, vol. 39, no. 12, pp. 1686-1697, 2006.

R. Martins, J. Seabra, and L. Magalhães, "Austempered Ductile Iron (ADI) Gears: Power Loss, Pitting and Micropitting", *WEAR*, Vol.264 no. 9-10, pp. 838-849, 2008.

R. Martins, P. Moura, and J. Seabra, "Power loss in fzg gears: Mineral oil vs. biodegradable ester and carburized steel vs. austempered ductile iron vs. MoS₂-Ti coated steel", *VDI Berichte*, no. 1904 II, pp. 1467-1486, 2005.

R. Amaro, R. Martins, F. Seabra, S. Yang, D. G. Teer, and N. M. Renevier, "Carbon/chromium low friction surface coating for gears application", *Industrial Lubrication and Tribology*, vol. 57, no. 6, pp. 233-242, 2005.

R. Martins, N. Cardoso, and J. Seabra, "Influence of lubricant type in gear scuffing". *Industrial Lubrication and Tribology*, (6) 2008 (to be published).

R. Martins, N. Cardoso, and J. Seabra, "Gear power loss performance of biodegradable low-toxicity ester based oils", *IMech Part J*. (to be published).

Contents

Acknowledgements	v
Abstract	ix
Sumário	xi
Sommaire	xiii
Keywords	xv
Appended papers	xvi
Table of contents	xvii
Table of Figures	xxi
List of Tables	xxiii
1 Introduction	1
1.1 Surface coatings	2
1.2 Gear materials	2
1.3 Biolubricants	3
1.3.1 Biodegradability and ecotoxicological evaluation	5
1.3.2 Environmental seals	5
1.3.3 Biodegradable Base Oils	6
1.3.4 Discussion	7
1.4 Aim and thesis outline	9
2 Gearboxes test procedures	11
2.1 Introduction	11
2.2 FZG gear tests	11
2.2.1 FZG gear test rig	11
2.2.2 Test gears	11
2.2.3 Scuffing tests	13
2.2.4 Micropitting tests	16
2.2.5 Pitting tests	16
2.2.6 Power loss tests	17
2.3 Transfer gearbox test rig, gearbox and tests	20
2.3.1 Gearbox power loss tests	20
2.4 Pre and post test analysis	22
2.4.1 Gears weight loss	22
2.4.2 Roughness measurements and topographies	22
2.4.3 Lubricant analysis	23
2.5 Summary	23
3 Gearbox power loss and a thermal equilibrium model	25
3.1 Introduction	25
3.2 Power loss tests	25

3.3	Energetic balance model of a gearbox	26
3.3.1	Model structure	28
3.4	Discussion	29
4	Gear Materials	31
4.1	Introduction	31
4.2	Scuffing protection	32
4.3	Pitting	33
4.4	Micropitting protection	34
4.5	Gear power loss	35
4.5.1	Friction coefficient	37
4.6	Discussion	37
5	Surface coatings	41
5.1	Introduction	41
5.2	Scuffing protection	42
5.2.1	Friction coefficient in scuffing conditions	42
5.3	Power loss	44
5.3.1	Friction coefficient	47
5.4	Discussion	49
6	Influence of lubricants in gears behaviour	51
6.1	Introduction	51
6.1.1	Lubricants properties	51
6.2	Scuffing	53
6.2.1	Critical lubricant temperature scuffing criterion	54
6.3	Micropitting	55
6.3.1	Visual inspection	56
6.3.2	Mass loss and oil analysis	58
6.3.3	Surface roughness and surface analysis	59
6.4	Power losses	60
6.4.1	Equilibrium oil bath temperature	61
6.4.2	Wear behaviour and oil degradation	63
6.4.3	Optimized friction coefficient between gear tooth	63
6.4.4	Prediction of lubricant behaviour for different operating conditions using the energetic model	66
6.5	Discussion	67
6.5.1	Scuffing	67
6.5.2	Micropitting	69
6.5.3	Power loss	70
7	Conclusions and future work	73
7.1	Conclusions	73
7.2	Future work	76
	Bibliography	77
	A Appended Papers	83

A.1	Paper A	87
A.2	Paper B	99
A.3	Paper C	113
A.4	Paper D	125
A.5	Paper E	139
A.6	Paper F	153
A.7	Paper G	175
A.8	Paper H	187
A.9	Paper I	207

List of Figures

1.1	Some international and national eco-labels.	6
1.2	Global Eco-labeling Network.	6
2.1	Schematic representation of FZG test rig.	12
2.2	Flank geometry of FZG type A20 (left) and type C14 (right) gears. Hertzian contact pressure (P0), curvature radius (R), sliding rate (Ve) and Flash temperature (Tflash) for both geometries at $n_{wheel}=2000$ rpm and $T_{wheel}=2000$ rpm.	14
2.3	Input power in power loss tests [kW].	19
2.4	Schematic view of the transfer gearbox test rig.	20
2.5	Photography of the transfer gearbox.	21
3.1	Evolution of oil bath temperature during a power loss test.	26
3.2	Schematic view of FZG gearbox and the different mechanisms of power dissipation and heat evacuation.	27
3.3	Algorithm for the energetic balance of gearboxes.	28
4.1	Procedure of ADI austempering heat treatment.	32
4.2	Graphite nodules on the surface (left) and a microstructure (right) of ADI material.	32
4.3	Gear pitting tests. Contact pressure v.s. number of cycles	33
4.4	Pictures of ADI and steel (CM, AM*) pinion tooth flanks after standard load stages of gear micropitting tests.	34
4.5	Pictures of ADI (AM, AE) pinion tooth flanks after modified micropitting tests.	35
4.6	Equilibrium temperature in power loss tests: ADI v.s. carburized steel.	36
4.7	Numerical friction coefficient for ADI and carburized steel gears ($T_{oil} = 90$ °C; 2000 rpm).	38
5.1	Scuffing load stage (or maximum load stage) of uncoated and surface coated gears on FZG scuffing tests with additive free ISO VG 100 lubricant.	43
5.2	Friction coefficient between gear tooth, in scuffing conditions, at 1500 rpm and 3000 rpm.	45
5.3	Efficiency of transfer gearbox with uncoated, C/Cr and MoS ₂ /Ti coated gears.	46
5.4	Equilibrium temperature (ΔT) on power loss tests of uncoated and MoS ₂ /Ti coated gears lubricated with ester lubricant in FZG test rig.	46

5.5	Equilibrium temperature (ΔT) on power loss tests of uncoated and MoS ₂ /Ti coated gears lubricated with mineral oil. * - test reached the limit temperature after 133 minutes and was stopped.	47
5.6	Total weigh loss after the power loss tests. * - not performed the tests at 3000 rpm.	47
5.7	Friction coefficient measurements (Hohn et al.) and numerical results considering the XL parameters mentioned in Table 5.1 (Toil=90 °C , p _H =1.1 GPa).	48
5.8	Numerical results for the friction coefficient considering the XL parameters mentioned in Table 5.1 (Toil=90 °C , pinion speed = 2000 rpm).	49
6.1	Scuffing load stage.	53
6.2	FZG type A gear geometry, reference points (A, I, V, W, B), normal force (F _n) and sliding speed (V _s) along pinion tooth.	55
6.3	Representation of scuffing criteria as function of oil bath temperature for pinion tip - wheel root contact point.	55
6.4	Pictures of pinion teeth flanks and micropitting area.	57
6.5	Mass loss during micropitting tests for M1 and E1 lubricants.	58
6.6	CPUC wear index during micropitting tests.	58
6.7	R _{pk} , R _k and R _{vk} roughness parameters [μm] of the measurements performed below the pitch line during: a) CM micropitting test; b) CE micropitting test.	60
6.8	Magnification of a micropit observed in the topography of CM pinion. All units in μm	61
6.9	Topography after CM and CE micropitting tests performed bellow the pitch line of a pinion tooth and analysis of the micropitting area with depth larger than 6 μm (at black). All units in μm	62
6.10	Oil bath temperature evolution for M1 and E1 oils at 3000 rpm for the 4 load conditions tested.	64
6.11	Oil bath equilibrium temperature.	64
6.12	Variation of lubricants viscosity with temperature.	64
6.13	CPUC and ISUC evolution during power loss tests for M1 and E1 oils.	65
6.14	Comparison of model and experimental oil bath temperatures for oil M1.	68
6.15	Comparison of model and experimental oil bath temperatures for oil E1.	68
6.16	Distribution of power losses as function of load stage for oils M1 and E1. The values inside chart represent the power losses in Watts.	68

List of Tables

2.1	Geometry of the FZG test gears: Types A10, A20, C14, C14 ^R	12
2.2	Operating conditions of biodegradable lubricants scuffing tests.	15
2.3	Gear micropitting test conditions.	17
2.4	Operating conditions used in ADI gear pitting tests (values for gear wheel).	17
2.5	Wheel operating conditions used in gear power loss tests (load arm of 0.5 m). * - 4.32×10^6 for ADI gears	18
2.6	Wheel operating conditions of the power loss gear tests (load arm of 0.35 m).	19
2.7	Geometric characteristics of the transfer gearbox gears and oil properties.	21
2.8	Operating conditions in the transfer gearbox efficiency tests with coated gears.	22
4.1	Mechanical properties of Austempered Ductil Iron.	33
4.2	ADI gears mass loss in micropitting modified test for ester (AE) and mineral (AM) oil	35
4.3	Lubricant factor exponent b_1 of X_L parameter ($n_{wheel} \leq 2000$ rpm).	37
5.1	Lubricant factor exponent b_1 for uncoated, ADI and MoS ₂ /Ti coated gears lubricated with both mineral and ester lubricant ($n_{wheel} \leq 2000$ rpm and $T_{wheel} \leq 275$ Nm).	48
6.1	Main properties of the tested lubricants.	52
6.2	Resume of scuffing tests results (* - load stage K12 performed after scuffing)	54
6.3	Critical lubricant temperatures (TCR) determined for each lubricant.	56
6.4	Test reference, lubricant and surface roughness of gear micropitting tests.	56
6.5	Roughness parameters in gear micropitting tests	59
6.6	Viscosity properties and Iron content measured before and after the power loss test for both lubricants.	65
6.7	Optimized lubricant factor exponent b_1 for oils M1 and E1. ($1000 \leq n_{wheel} \leq 3000$ rpm and $5 \leq T_{wheel} \leq 323$ Nm)	66

1 Introduction

The research work presented in this thesis has been developed and performed during the participation of the author, and the research center in which he collaborates, in three research projects supported by the European Commission.

The projects were:

- **Reduction of the fluid lubricant use in heavy loaded motion transmission systems through the application of self-lubricant coatings;** whose aim was to reduce dramatically the hydraulic fluids used for loaded motion transmission systems and by decreasing the lubrication failure risks by mean of low friction high resistant coatings. (Contract reference n. BRST-CT-97-5263, CRAFT Project BE-S2-5389).
- **EREBIO - Emission reduction from engines and transmissions substituting harmful additives in biolubricants by triboreactive materials;** whose aim was to substitute petrol based oils by new compatible low viscosity biodegradable engine and gear oils based on harvestable polyolesters or water based polyalkylen glycols, eliminating toxic triboactive additives, thus allowing to reduce CO₂ emissions, fuel consumption and particles emission. (Contract reference n. G3RD-CT-2002-00796 - EREBIO).
- **BIOMON - Toward long-life biolubricants using advanced design and monitoring tools;** whose aim was to develop long life biolubricants based on high performance native esters and high temperature and oxidation resistant biodegradable greases based on polyurea thickeners mixed with native esters. It was expected to increase 10 to 20 % the speed limits and performance, to reduce 20 % the wear and improve proportionally the life by comparison to actual lubricants. The use of advanced tools and the reduction of a 10 % the quantity of used lubricant, should help to decrease the maintenance cost around 30 %. (Contract reference n. BIOMON-COOP-508208).

The research papers appended to this thesis were written based on the work developed in these projects and also with the purpose of projects dissemination.

Those projects intended to develop new materials, new lubricants and new surface coatings with the purpose of improving the overall behaviour of gears and also to decrease the impact of their use on the environment. Power transmission equipments employing gears dissipate significant amounts of power and any improvement in their performance represents a significant reduction in energy consumption, beside, the demands of modern mechanical transmissions require higher operating torques, higher speeds, lower operating noise, lower weight, lower wear and higher life.

The next paragraphs present a brief introduction to the main research areas of this thesis and the guidelines followed to address the objectives in those areas.

1.1 Surface coatings

In the last decades, surface coating technology was important to achieve increased energetic performance, allowing lower friction coefficients, higher protection against surface failures and higher load capacity.

In applications with frequent start-stop operations such protection against failures, mainly scuffing, is very important. The application of low-friction surface coatings to power transmission equipments is expected to improve their efficiency and might represent a significant reduction of energy consumption. Other aim to be attained with the surface coatings was the reduction of the amount of lubricant used in the gearboxes, maintaining or increasing the scuffing protection and also reducing the churning losses, by reducing the oil level.

Another important objective that might be accomplished by surface coatings was the reduction or even elimination of some toxic lubricant additives and consent the use of biodegradable and low toxicity lubricants.

There are several types of coatings that can be used in gears, for instance, WC/C (tungsten carbide / carbon) [1], B₄C (boron carbide/carbon) [1,2] or MoS₂/Ti (molybdenum disulphide/titanium) [3–8], among others [9,10]. DLC (diamond-like carbon) coatings are very hard and have a lower friction coefficient but tend to be brittle and have poor adhesion. The DLC metallic-carbon coatings tend to be less brittle but are also softer. In order to provide a better wear protection it is interesting that the coating behaves like a true solid lubricant [6] like graphite or MoS₂ (molybdenum disulphide) [11].

Two sputtered multilayer composite surface coatings were selected to evaluate its tribological performance in gear applications, once these coatings appear to behave like a solid lubricant, have high hardness, low friction coefficient and a good adhesion potentially conducting to low wear rates.

So in this work the tribological application of the sputtered surface coatings to gear applications was tested and discussed, helping to improve the surface coatings for gear applications.

1.2 Gear materials

Carburized steel is a material with widespread and successfully use for gear application, although other materials have potential application in gears, such as nitriding steel [12] and the Austempered Ductile Iron (ADI), among others.

The Austempered Ductile Iron (ADI) has been used since the late 1970s and significant developments have been made since then, being now possible to produce high-resistance ADIs. Among the Fe-C alloys products, ADI presents a very interesting combination of mechanical properties. Actually, some ADIs are only surpassed by high-resistance alloyed steels when tensile strength is considered [13]. Replacing conventional steel parts by ADIs results in several advantages which strongly promoted the acceptance and use of these materials, namely in the automotive industry.

The first economical reason to use ADIs is that the base material (nodular iron) is cheaper than steel, the second is that ADIs are casting materials, thus products can be moulded, allowing significant cost reduction of the manufacturing process

when compared to conventional steel machining [14]. The heat-treatments are also low-energy consumers (austempering is done at about 300 °C) and allowing cost-savings when compared to steel quenching or other conventional heat-treatments [14]. ADI's are also very interesting for the automotive industry as they allow considerable weight reduction (10 % lighter than steel), high vibration absorption, more than 6 dB attenuation can be achieved in a gearbox, per instance [15], and a very high wear and scuffing resistance, avoiding malfunctions under unpredicted unfavorable working conditions, like a momentaneous failure of a lubrication system, per instance [16].

The use of ADI's is limited when extreme tensile strength is required (most of the power-transmission gears are still made of steel) but some ADIs can now reach more than 1600MPa (ultimate tensile strength), according to ASTM normalization, thus being able to support the efforts imposed by the majority of the mechanical applications.

ADI's tribological performance is only slightly dependent on the presence of AW and EP additives in the lubricants, allowing the use of low doped mineral oils [17,18]. This property is also very promising for the combination of ADI with biodegradable lubricants with low or non toxic additivation.

In this work the application of ADI cast iron to gearboxes is discussed, for that purpose a cast iron composition proposed by H. Santos et al. [19] was used to produce the ADI. The austenitization temperature for the production of ADI was choose based on the work performed by Magalhães et al. [16]. The austempering temperature selected was 300 °C , that appear to have a better compromise between toughness and strength for gear applications.

The ADI gears were tested with two gear lubricants, a mineral oil and a biodegradable ester, and both combinations were compared with carburizing steel gears. The comparison ranged from fatigue tests, pitting and micropitting, to power loss tests in order to evaluate the friction coefficient of the combinations. The wear behaviour was also analysed and the results were compared with carburized gears.

1.3 Biolubricants

The use and knowledge about the different biodegradable lubricants isn't very widespread, so a deeper attention will be paid to the introduction of biolubricants, such as the ways of testing the environmental compatibility, the toxicity, the types of biolubricants and some ecolabels available for the technical certification of biodegradable products.

Vegetable based lubrication is a 4000 years old science, it goes back to the Egypt, Sumer and India, where vegetable oils where widely available and used [20]. In the beginning of 20th century the vegetable oils kept being used, the work performed by Sir Otto Walach on vegetable based oils was awarded with a Nobel prize in chemistry in 1910.

During the two world wars, vegetable based oils and fuels were critical to the military, specially in the second world war in which Germany had limited access to petroleum, thus taking the lead in the research of synthetic oil and fuels, ending in the discovery of ester based lubricants around 1937 [20].

The lower price of petroleum based lubricants did not allowed a considerable market

share to the vegetable based oils, although the military and aviation use synthetic esters for a long time.

The biodegradable's started to be talked again during the 70's because of the oil embargo and in the 80's because of the environmental concerns in Europe.

Nowadays, the ecological aspects and the environmental awareness are gaining importance in our society. Our environment is being increasingly contaminated with all type of pollutants, so any reduction is desirable and welcome. The lubricants could not be the most severe problem, but are also a problem, because there are total loss lubricants, there are leaks, spillages and other problems that thrown lubricants to the environment, although in some cases this is technically desirable, such as in the case of total loss lubricants [21]. According to Mang et al. [21], every year around 40 to 50 % of the 5 million tonnes of used lubricants in Europe end up polluting the environment.

So, for environmental reasons the use of environmental compatible lubricants is desirable, although there are other factors that are pushing the use of biodegradable products, like politics, commercials and technical, once there is a need to decrease emissions, toxicity, spill liabilities and oil disposal hazards, there is also a need to decrease the maintenance cost, by using products with lower power losses, higher drain intervals and there is also interest in decreasing the dependence of petrol based products. All of these reasons are leading industry to search for highly efficient and less carbon-intensive biodegradable fluids and additives, and if possible that work with existing machinery with small or any modification [20].

Other advantages of using rapidly biodegradable products are the reduction of expense of oil spillages as well as the complying with health and safety regulations that are reduced. Usually these products are also skin compatible and non toxic that also reduces the requirements for their manipulation [21].

Nowadays, the major disadvantage of using rapidly biodegradable lubricant products is their higher acquisition price, although it is necessary to make an overall cost analysis, once the total cost results from the interaction of several characteristics such as: ageing and temperature stability, operating costs, machine investments/compatibility, maintenance measures, storage cost, emission reduction, cost of preventive health, etc. [21].

The expression *environment friendly* or *environment compatible* are widely used although they represent subjective criterion about the impact of the lubricant on the environment. The objective criteria (measurable) that must be used for classifying the lubricants are expressed in the following list:

- Biodegradability;
- Water solubility, water pollution;
- Ecological toxicity and physiological safety;
- Performance, approvals, oil change intervals;
- Efficiency improvements, lower energy consumptions;
- Emission reductions on use;

- Compatibility with conventional lubricant and materials;
- Use of renewable raw materials;
- Environment awards.

1.3.1 Biodegradability and ecotoxicological evaluation

There are already a group of test to evaluate those biotic potential of lubricants, being some of the most used those established by OECD. Some of the most important objective criteria are those that allow to classify the biodegradability and the toxicity of lubricants.

The biodegradability or biodegradation, that is the capability of being decomposed by biological agents or being absorbed by the environment, can be measured by the tests OECD 301B, OECD 301C, OECD 301D, OECD 301F and OECD 302B. To consider a lubricant rapidly biodegradable, it must pass the limit of $\geq 60\%$ in 28 days, rule valid for all the OECD tests listed above. Other biodegradability test is CEC-L-33-A-93, although it's becoming more and more obsolete.

The ecotoxicity intends to measure the impact of the lubricants in life, specially in aquatic organisms. Among the most used tests for evaluating the ecotoxicity are: OECD 201, OECD 202, OECD 209.

1.3.2 Environmental seals

In order to give a sense of security to the users of environmental compatible products and to combine the environmental behaviour and the technical properties of lubricants some countries have introduced the so called eco-labels. The lubricants are included in some of those eco-labelling system. To use an eco-label a product must accomplish the criteria established by that eco-labelling institution. Those criteria are based on the life cycle considerations.

International Organisation for Standardisation (ISO) states that the overall goal of these labels is: *through communication of verifiable and accurate information, that is not misleading, on environmental aspects of products and services, to encourage the demand for and supply of those products and services that cause less stress on the environment, thereby stimulating the potential for market-driven continuous environmental improvement.*

Some of the most important eco-labels are represented in Figure 1.1, being the European eco-label used in the European Union, the Blue Angel is used in Germany and is one of the oldest eco-label, the White Swan is used in the Nordic countries, at last the Green Seal that is used in the United States of America.

During the 90's a Global Eco-labelling Network was created, a non-profit association of third-party, environmental performance labelling organizations, whose purpose is to promote, improve and develop the eco-labelling of products and services. This organization already aggregates over 20 labelling organizations, among them are the cited above. The label of GEN is presented in Figure 1.2.

Nowadays we assist to an increasing international concern about the environmental compatibility of products, being the lubricants among them. These labelling organizations prove this, and also indicate a path to the future.



Figure 1.1: Some international and national eco-labels.



Figure 1.2: Global Eco-labeling Network.

1.3.3 Biodegradable Base Oils

The biodegradable fluids could be aggrouped in three main families: vegetal oils (or triglycerides), polyglycols and synthetic fluids (esters and polyalphaolefins) [20]. But the biodegradable lubricants have a main chemistry based in different ester oils. The ester oil could have by origin vegetable harvestable raw materials (soybean, rapeseed etc), semi-saturated transesterified ester oils with natural fatty acids and fully saturated esters (synthetic esters based on chemical modified vegetable or mineral oils) [21].

The other biodegradable base oils, mostly not present in the market for different reasons, are the Poly(alkylene glycol) (PAG), the low viscosity polyalphaolefins (PAO2) and some special types of synthetic hydrocarbon up to a viscosity of $6 \text{ mm}^2/\text{s}$ at $100 \text{ }^\circ\text{C}$ [21].

Vegetable oils or triglycerides

Natural fatty oils such as castor oil, palm oil, rapeseed oil, soybean oil, sunflower oil, lard, tallow and sperm oil have been used in lubricants for years and compared to mineral oils show excellent tribological qualities (low friction coefficient, good wear protection). They are more or less unsaturated fatty esters.

Their limitation is the low stability against thermal oxidative and hydrolytic stress and partly inferior cold flow properties, although, those limitations can be improved gradually either with additives, or with the cultivation selection, or genetically modification of new types of plants.

There are high oleic sunflower oils and high oleic soybeans oils (from genetically engineered seed) that allow to formulate oils for higher performance levels [20, 21].

Synthetic Esters

The synthetic esters covers a broad range of chemicals with different qualities and prices, among them are the diesters, monobasic esters, polyol esters, trimethylolpropane-tri-oleates, etc. Basically they are the reaction product of fatty acids from natural oils and alcohols from petrochemical and oleochemical industries. The chemical engineering offers a wide range of possibilities for the production of synthetic esters, being at present the polyolesters such as trimethylolpropane esters (TMP-esters) that dominate the market.

Basically the esters have better thermal-oxidative resistance, better low temperature behaviour and better resistance to hydrolysis than natural fatty oils. Those properties have made them traditionally indicated for jet engines lubrication and other applications that require extreme low or high temperature operation [20].

The hydrolytic stability of normal polyolesters is not very different from rapeseed oil, while the difference in oxidation resistance is much greater, though both characteristics are significantly improved with complex esters. The ester properties could be improved using some chemical reaction, among them the most important are: transesterification, hydrogenation, ozonolysis, dimerization [21].

Polyglycols

The polyglycols are lubricants based on polyalkyleneglycols (PAG), which can have very good technical properties and are well-known in long-term use. Polyethylene glycols (PEG) are mostly biodegradable, although they are not miscible with mineral oils or esters and are water-soluble. So, if PEG is released it will migrate quickly in the ground or in the water.

Polypropylene glycols (PPG) are partially miscible with mineral oils or esters, but in general not easily biodegradable. The PAGs are one of the product in development on the industry, it is being attempted to develop biodegradable, non-water soluble PAG's that could be an alternatives to esters.

Polyglycols have some material incompatibility with common coatings, seals and gaskets, being for example recommended the use of viton seals.

Polyalphaolefins

Low viscous polyalphaolefins (PAO 2) are biodegradable, but these base stocks have only limited application in the formulation of lubricants. The new types of biodegradable, higher viscosity synthetic hydrocarbons may have a greater influence in the future [21].

The polyalphaolefins with lower biodegradability are more widely used, especially blended into synthetic formulations of automotive lubricants, although the PAO have limited additive solubility and incompatibility with some seals [20].

1.3.4 Discussion

The vegetable and synthetic esters display excellent lubricity under boundary lubrication conditions, mainly due to the high degree of polarity of these fluids. The

1 Introduction

friction coefficient of vegetable and ester oils in twin disc machine is usually half of those of mineral oils [22].

Vegetable oils and synthetic esters show a high polarity, that also applies to corrosion inhibitors and can result in a competitive reaction on the metal surface.

The oxidation stability of vegetable oils is poor, although TMP complex esters display excellent oxidative stability [22,23].

The viscosity-temperature behaviour (Viscosity Index) of the vegetable and ester lubricants is much higher than those of mineral oils. Typically the viscosity index is above 150 [22].

The evaporation loss of vegetable and ester oils is also much smaller than those of conventional lubricants [22].

Biodegradability is reached by using a suitable biodegradable base fluid, although a fully formulated product has also additives and low toxicity requires an additivation that is environmentally friendly [21], too. The acceptance of biodegradable lubricants also depends on costs, and the cost of a biodegradable oil is between three to eight times higher than a mineral oil, meaning that this products must offer considerable advantages over the traditional products. So, the suppliers of biodegradables must provide products that beside having improved biodegradability must also have superior technical performance [22].

Biodegradable lubricants offer the best way to minimise pollution in industrial and automotive use, and their use in equipments still has potential to improve. The ester based products might represent a significant cost-saving element if the complete process cost is analysed [21–24].

The key aspect for any industrial application is the technical performance and technical advantages proved in dedicated tests. The lubricant performance (friction, wear, lifetime, load bearing, efficiency, etc.) has a major impact on its overall environmental compatibility, since premature wear or high energy needs are as well harmful to the environment.

So in this work we test and compare biodegradable ester oils with a conventional mineral oil to evaluate the vantages and disadvantages in what concerns to gear applications. For that purpose scuffing, micropitting and power loss tests were performed. Being also analysed the influence of different materials and surface coatings combination with the lubricants.

1.4 Aim and thesis outline

The main aim of this work was to investigate the influence of new materials, new surface coatings and new biodegradable lubricants in industrial gear performance. This main objective was approached in three parts.

The objective for the study of new multi-layer composite surface coatings was to understand if a considerably hard surface coating could be applied to gears, what was the potential of its application, specially what will be the increase of safety against scuffing failure and what was the decrease of power losses inside a gearbox.

The aim for the new material studied (ADI austempered at 300 °C) was to understand what are the implications of using it in gears in what concerns to fatigue resistance and power loss behaviour in comparison to the traditional carburized steel.

In what concerns to the biodegradable low-toxicity lubricants the objective was to study their influence in the overall behaviour of gears, in particular when combined with different gear materials or surface coatings and also what was their influence in the fatigue failures and in the power loss behaviour of gears and gearboxes.

To complement the analysis mentioned above, an additional objective consisted in developing a numerical model for the energetic behaviour of gearboxes, establishing the equilibrium between power loss inside the the gearbox and heat evacuated from the gearbox to the surrounding environment. Based on experimental gear test results, such model should allow the evaluation of the friction coefficient between gear tooth for different combinations of gear material or surface coating with lubricants and, when the friction coefficient is known, predict the gearbox operating temperature for a given speed / torque input.

This thesis is composed by 7 chapters, including this introductory Chapter, explaining the need to search for new solutions for materials, lubricants and surface coatings in gear applications.

This thesis resulted from a large amount of experimental work, thus Chapter 2 is dedicated to present the experimental tests performed, test rigs used, as well as the test procedures and the pre and post test analysis performed.

The third Chapter is dedicated to introduce and explain the objectives of a new type of gear tests, with the purpose of studying the efficiency or power loss behaviour of gears and gearboxes. In this chapter the model developed for study the energetic balance of the FZG gearbox, is also presented and used to determine the friction coefficient between gear tooth based on experimental power loss tests, and to estimate the stabilisation temperature of the FZG test gearbox for different operating conditions.

Chapter 4 is dedicated to show the applicability of ADI (Austempered Ductile Iron) material for gear applications, mainly its anti-scuffing, pitting and micropitting fatigue resistance. Other very important property for gear applications is the power loss behaviour of ADI gears, as well as the friction coefficient between gear tooth promoted by this material. The mechanical and tribological behaviour of ADI gears is, whenever possible, compared with carburized steel.

The fifth chapter is dedicated to present two multi-layer composite surface coatings and to discuss the applicability of those surface coatings to gears. In this chapter

1 Introduction

the outstanding scuffing capacity presented by these surface coatings when applied to gears is presented and discussed, as well as the power loss behaviour of surface coated gears compared to carburized gears.

In Chapter 6 the influence of biolubricants in gear behaviour is discussed. This discussion summarizes the comparison of a mineral fully formulated gear lubricant with biodegradable low-toxicity ester based lubricants, being this comparison performed in a wide range of conditions. The scuffing load carrying capacity, the micropitting protection, as well as the energetic behaviour of both lubricants are compared.

The seventh and last chapter presents the main conclusions of this work and presents some ideas for future work.

In appendix, nine research papers are presented which were the basis of this thesis, all published in high quality scientific journals in the field of tribology.

2 Gearboxes test procedures

2.1 Introduction

In this chapter an overview of the equipments, tests procedures and analysis techniques used during this work will be presented.

The test rigs where almost all tests were performed will be described as well as the gears used and their characteristics. The test procedures and the post-test analysis techniques will be presented and described in detail.

2.2 FZG gear tests

2.2.1 FZG gear test rig

The FZG test rig [25] is a well known back-to-back spur gear test rig with “power circulation”, shown in Figure 2.1. The test pinion (1) and the test wheel (2) are connected by two shafts to the driving gears (3). The front shaft is divided in two parts with the load clutch in-between (4). One half of the load clutch can be fixed to the foundation by a locking pin (5) while the other part can be twisted using a load lever and weights (6). After bolting the clutch together the load can be removed and the shaft unlocked. Now a static torque is applied to the system that can be measured by the torque measuring clutch (7). The maximum speed of the AC-motor is 3000 rpm. The test gears can be dip lubricated or jet lubricated. When dip lubrication is used, the oil may be heated using the electrical heaters mounted in the test gearbox. The heater and cooling coil allows the settling of a constant oil temperature measured by the temperature sensor (8).

Several types of standard gear tests [25] may be performed on the FZG gear test rig:

- Gear scuffing tests,
- Gear pitting tests,
- Gear micropitting tests.

2.2.2 Test gears

Several different types of test gears might be used in the FZG test rig:

- Type A20 for standard gear scuffing tests [25–28],
- Type A10 for more severe gear scuffing tests [27],

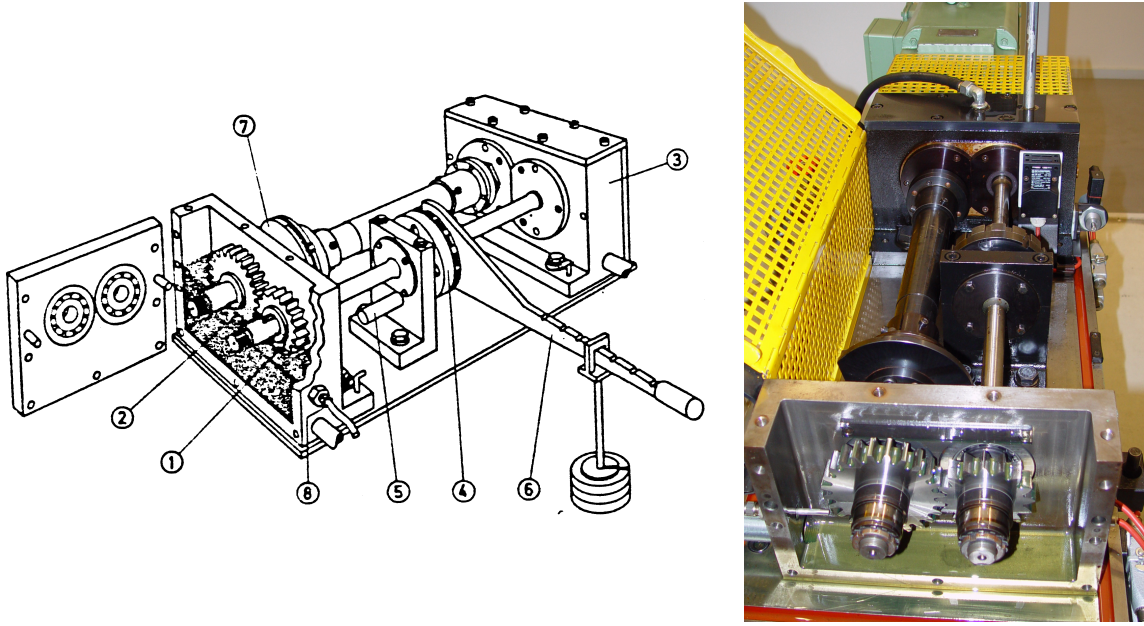


Figure 2.1: Schematic representation of FZG test rig.

- Type C14 for gear pitting tests [25, 29],
- Type C14R with increased surface roughness for gear micropitting tests [25, 29, 30].

The geometric characteristics of the different types of FZG test gears are presented in Table 2.1.

The gears used in the FZG tests are not of the same gear accuracy grade of those proposed in the standards [25–29], having lower manufacturing quality and yielding higher surface roughness and consequently lower specific film thickness. Another significant difference is the grinding direction on FZG type A gears that according to the standard should be MAAG criss-cross grinding (15° method) and the available gears are grinded at 0°. Figure 2.2 shows photographs of the teeth flanks in FZG

Gear type	A20		A10		C14		
	Pinion	Wheel	Pinion	Wheel	Pinion	Wheel	
Number of teeth	16	24	16	24	16	24	
Module [mm]	4.5		4.5		4.5		
Centre distance [mm]	91.5		91.5		91.5		
Pressure angle [°]	20		20		20		
Face width [mm]	20		10	20	14		
Addendum modification	+0.85	-0.50	+0.85	-0.50	+0.18	+0.17	
Addendum diameter [mm]	88.68	112.50	88.68	112.50	82.64	118.54	
Flank roughness ¹ [μm]	0.35	0.30	0.35	0.30	0.30		
Flank roughness ^R [μm]						0.50	

Table 2.1: Geometry of the FZG test gears: Types A10, A20, C14, C14^R.

type A and type C gears, as well as the hertzian contact pressure (P_0), curvature radius (R), sliding rate (Ve) and Flash temperature (T_{flash}) for both geometries at $n_{wheel}=2000$ rpm and $T_{wheel}=2000$ rpm.

2.2.3 Scuffing tests

The standard FZG gear scuffing test (ISO14635-1 - FZG test method A20/8.3/90 [26]) uses 20 mm wide type A gears, allowing very high sliding rates at the end of the meshing line (pinion tip / wheel root). The operating speed (wheel) is 1500 rpm, under dip lubrication. To obtain more severe operating conditions the standard FZG scuffing test for high scuffing load capacity lubricants (ISO14635-2 - FZG step load test A10/16, 6R/120 [27]) is also available and uses 10 mm wide gears with higher initial oil bath temperature (120 °C) and higher operating speed. Beside these standards, there are also other gear scuffing tests reported in the literature, like A10/8.3/90 or A20/16.6/140 [31] also developed for testing high scuffing load capacity lubricants.

The standard FZG scuffing test A20/8.3/90 [26] has the following procedure, which is similar for the other scuffing tests mentioned:

The torque is applied progressively, from load stage 1 to load stage 12, until scuffing occurs. Each load stage lasts for 15 minutes. Table 2.2 shows the wheel torque corresponding to each load stage in the standard FZG gear scuffing test. Each load stage corresponds to an increase of $\Delta p_H \approx 0.164$ GPa in the maximum Hertzian pressure at point W^1 of the gear meshing line.

Gear running-in takes place during the first 4 load stages, as indicated in Table 2.2. This running-in period was very important, since it avoids premature scuffing failure of the FZG gear. In the first 4 load stages the initial oil temperature is not imposed, typically is equal to the ambient temperature. From load stage 4 onward the initial oil temperature is set to 90 ± 2 °C. During each load stage, the oil temperature increases from the initial value to a final temperature, which is mainly dependent on the applied torque and lubricant properties. At the end of load stage 12 the oil temperature might reach over 140 °C , even if scuffing does not occur.

The pinion weight loss during scuffing test is evaluated, being the gears cleaned in a solvent ultrasonic bath before weighing. The roughness is also measured before and after scuffing tests. After each load test the gears are visually inspected for scuffing assessment and photographed at the end of the test.

Scuffing tests of coated gears

It was expected that surface coatings promoted a significant increase of the load capacity, over load stage $K=12$ on standard scuffing test (ISO14635-1), beside only type C coated gears where available.

So, for the scuffing tests of coated gears, the test procedure was considerably different, as detailedly explained on **Paper A** [32], **Paper D** [33] and **Paper G** [34]. The gears used were type C, instead of type A. The oil bath temperature was kept constant at 90°C during the scuffing test procedure. The scuffing test procedure was

¹W - transition point of the gear meshing line from one pair to two pairs of tooth engaged, where the Hertzian pressure reaches its maximum value.

2 Gearboxes test procedures

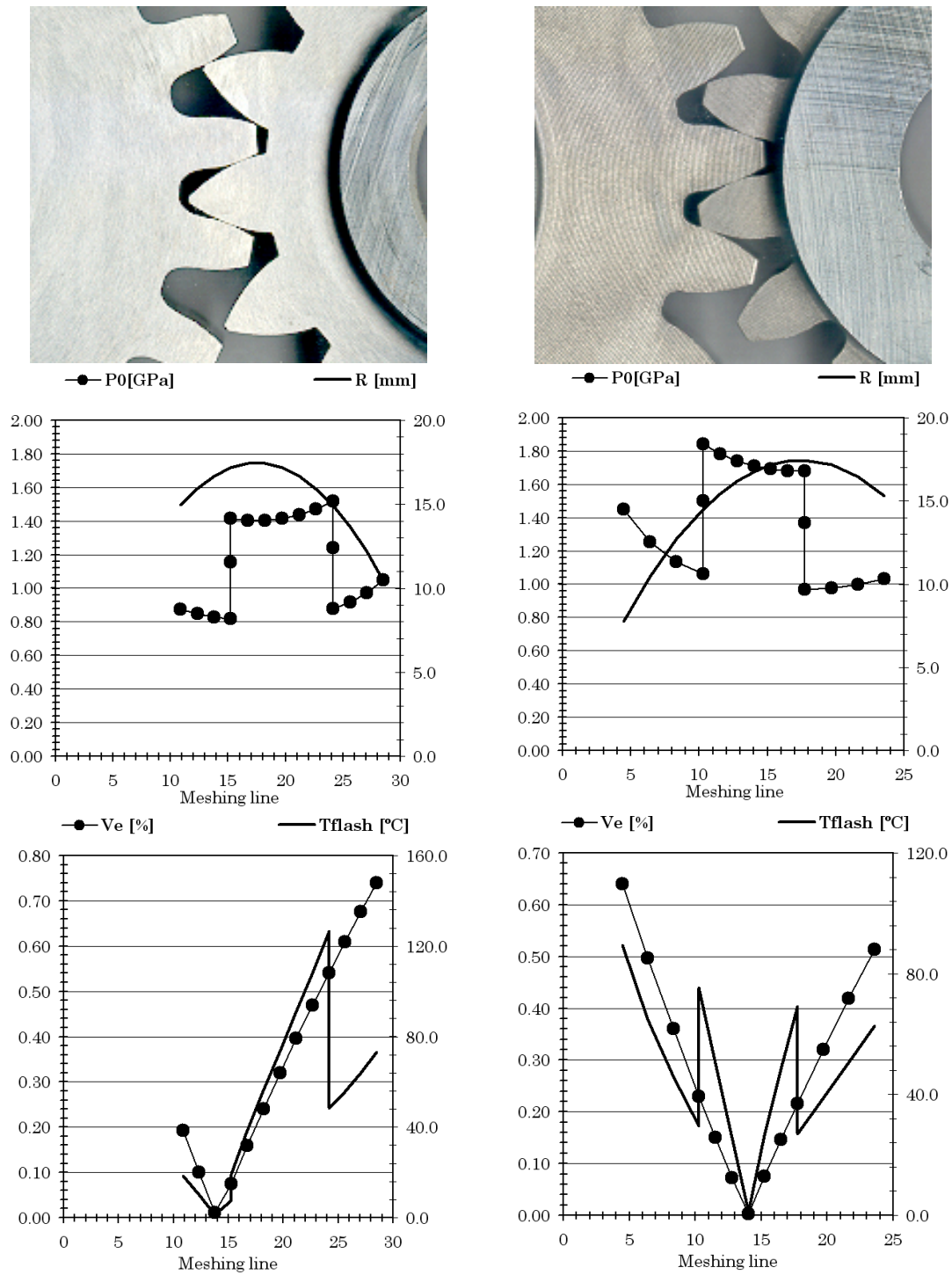


Figure 2.2: Flank geometry of FZG type A20 (left) and type C14 (right) gears. Hertzian contact pressure (P_0), curvature radius (R), sliding rate (Ve) and Flash temperature (T_{flash}) for both geometries at $n_{wheel}=2000$ rpm and $T_{wheel}=2000$ rpm.

FZG stage K_{FZG}	Stage time min	Wheel speed rpm	Wheel torque N.m	FZG A20/16.6/90		FZG A10/16.6/90	
				Max. Hertz pressure GPa	Initial temp. °C	Max. Hertz pressure GPa	Initial temp. °C
1	15	3000	5	0.15	free	0.22	free
2	15	3000	20.6	0.31	free	0.44	free
3	15	3000	53	0.5	free	0.71	free
4	15	3000	91.2	0.66	free	0.93	free
5	15	3000	141.2	0.82	90	1.16	90
6	15	3000	203	0.99	90	1.39	90
7	15	3000	275.1	1.15	90	1.62	90
8	15	3000	359	1.31	90	1.85	90
9	15	3000	453	1.47	90	2.08	90
10	15	3000	558.9	1.64	90	2.31	90
11	15	3000	675.2	1.8	90	2.54	90
12	15	3000	801.75	1.96	90	2.77	90

Table 2.2: Operating conditions of biodegradable lubricants scuffing tests.

performed at 1500 rpm and 3000 rpm (wheel speed). The running-in in these tests was performed on load stage 6 during 4h.

The FZG type C geometry was choose instead of FZG type A due to the difficulty of coating deposition in FZG type A wheel (see Figure 2.2). It was expected that the scuffing capacity of coated gears increased significantly, so an additive free lubricant has been choose to perform the tests, and due to the lack of additives a constant oil bath temperature of 90 °C was used. The scuffing test procedure at a wheel speed of 3000 rpm was also performed in order to increase the severity of the tests performed to allow a clear distinction between coatings.

Each load stage had a duration of 15 minutes and the loads were those defined in the standard scuffing test ISO14635-1.

Scuffing tests of biodegradable gear oils

The test procedure used in the scuffing tests with bio-oils was modified in relation to standard ISO14635-1. The main reason was the high load capacity of the industrial gear lubricants used, that increase the scuffing load stage over load stage 12 on standard test. ISO14635-2 standard could have been used but it might be to severe to the mineral reference lubricant, since the starting temperature is 120 °C. The scuffing tests were performed with an initial oil bath temperature of 90 °C at a pitch speed of 16.6 m/s. And beside the increased speed, gears with a teeth width of 10 mm, were also tested in order to allow an increase of 41.4 % of the maximum hertzian pressure between the contacting teeth.

The duration of each load stage was 15 minutes. Table 2.2 presents the operating conditions used in the two tests performed. After each load stage the teeth were visually inspected for detection of scuffing marks. The test procedure followed the ISO14635-1 standard in what concerns to all the other parameters and procedures.

2.2.4 Micropitting tests

The gear micropitting tests were based on the DGMK-FZG micropitting short test procedure (abbreviated as GFKT-C/8.3/90) [30], which is a short term test, able to classify candidate lubricants in what concerns to gear micropitting, analogous to FVA-FZG micropitting test [29].

The tested gears had a quality grade considered "current" while standard gears (according to DGMK-FZG) have a "fine" quality grade, and this difference was expressed in the larger average roughness (Ra) of the tooth flanks.

Dip lubrication was used during the gear micropitting tests, using the operating conditions presented in Table 2.3. The standard DGMK-FZG micropitting test has three stages, the first one lasting one hour in load stage K3, that works as a running-in period, followed by two load stages lasting 16 hours each, one in load stage K7 and another in load stage K9 (see Table 2.3).

The test procedure can be resumed as follows:

1. Load stage K3 (running-in);
2. Collect a lubricant sample for analysis;
3. Load stage K7;
4. Collect a lubricant sample for analysis;
5. Dismount gears, weight, roughness measurement and surface photography;
6. Mounting gears with fresh lubricant;
7. Load stage K9;
8. Repeating steps 4 and 5;

In the case of micropitting tests of ADI gears, the standard procedure was also used but proved to be excessively severe, because ADI gears had higher surface roughness and lower contact pressure resistance than carburized gears. So, the standard procedure was adapted for ADI gears and load stages K7 and K9 were replaced by load stages K5 and K7, that is, two load stages below the standard test. The running-in stage was still performed in load stage K3. The contact pressure for ADI and steel gears is also indicated in Table 2.3.

2.2.5 Pitting tests

Gear pitting tests were performed with ADI gears, using FZG type C profile, to evaluate the contact fatigue performance of ADI gears and determine its Wöhler curve.

The gear pitting tests were carried out in dip lubrication conditions, using 1.5 litre of fully saturated ester gear oil. The gears were of current quality grade with higher roughness than the defined by standard pitting test [35]. Each test was performed twice, except the test at 1000 rpm that was only performed once. Table 2.4 shows the operating conditions used in the gear pitting tests. The tests at 3000 rpm were

	Torque Stages							
	$K_{FZG}=3$		$K_{FZG}=5$		$K_{FZG}=7$		$K_{FZG}=9$	
	pinion wheel		pinion wheel		pinion wheel		pinion wheel	
Temperature [°C]	80				90			
Torque [Nm]	28.8	43.2	70	104.9	132.5	198.8	215.6	323.4
Rot speed [rpm]	2250	1500	2250	1500	2250	1500	2250	1500
Vt [m/s]	8.3							
Maximum Hertzian stress along the meshing line								
ADI [Mpa]	487		760		1046		1334	
Steel [Mpa]	550		857		1180		1505	
Power [kW]	6.8		16.5		31.2		50.8	
Duration [h]	1		16		16		16	
N cycles [$\times 10^3$]	135	90	2160	1440	2160	1440	2160	1440
ADI	X				X		X	
Carb. Steel	X				X		X	
ADI*	X		X		X			

Table 2.3: Gear micropitting test conditions.

Input Speed [rpm]	Input Torque [Nm]	Input Power [kW]	Hertz pressure [GPa]	Initial temperature [°C]	N° of repetitions [/]
3000 rpm	198.7	62.4	1.046	90 (± 2)	2
3000 rpm	257.4	80.9	1.19	90 (± 2)	2
3000 rpm	323.3	101.6	1.334	90 (± 2)	2
3000 rpm	397.5	124.9	1.479	90 (± 2)	2
1000 rpm	453	47.44	1.578	40 (± 2)*	1

Table 2.4: Operating conditions used in ADI gear pitting tests (values for gear wheel).

* - temperature evolution set free

all performed at constant temperature (90°C), and in the test at 1000 rpm, the oil temperature was set free.

Each test is carried out until pitting failure occurs, or up to 20 million cycles. During the pitting test regular stops were done to perform a visual inspection of tooth surface.

2.2.6 Power loss tests

Gear power loss tests were performed on the FZG test rig, using type C gears and dip lubrication, considering wide ranges for the operating conditions. The input power ranged from 0.5 kW to 142 kW. The operating conditions used are detailed in Table 2.5. The gears were runned-in before performing the power loss tests.

At the beginning of each test the oil temperature is set at 40(± 2) °C. The tests lasted 4 hours, which is the time necessary to reach a stabilized operating temperature. If the oil temperature reaches 180°C the test was stopped for safety reasons (damage of the gearbox seals). The tests performed at very low torques (0.5 to 1.5

Test type	Speed [rpm]	Torque [Nm]	Input Power [kW]	Initial temp. [°C]	Test time [hours]	Number of cycles [x10 ⁶]	Oil samples
No load tests	1000	4.95	0.52	Room temp.	2	0.12	
	2000	4.95	1.04		2	0.24	
	3000	4.95	1.56		2	0.36	/
Load tests	1000	141.15	14.78	40 (±2)	5	0.3	
	1000	275.1	28.81	40 (±2)	5	0.3	
	1000	453	47.44	40 (±2)	5	0.3	80 ml
	2000	141.15	29.56	40 (±2)	5	0.6	
	2000	275.1	57.62	40 (±2)	5	0.6	
	2000	453	94.88	40 (±2)	5	0.6	80 ml
	3000	141.15	44.34	40 (±2)	5	0.9	
	3000	275.1	86.43	40 (±2)	5	0.9	
	3000	453	142.31	40 (±2)	5	0.9	1500 ml
Total						6.12*	

Table 2.5: Wheel operating conditions used in gear power loss tests (load arm of 0.5 m).
* - 4.32×10^6 for ADI gears

kW) lasted only 2 hours, which was enough to reach a constant operating temperature. In this case the tests started at ambient temperature ($\pm 20^\circ\text{C}$), since, at low speed, the stabilized operating temperature is slightly above 40°C .

Air extraction and inflation were used during the tests in order to keep the ambient temperature constant.

During the tests the oil temperature was monitored (but not controlled). The gearbox wall, base plate and room temperatures were registered.

Each test is performed at constant input speed and torque. The torque was imposed at the beginning of the test and the speed was continuously monitored and controlled during the test. The same lubricant was used during the 12 test stages that compose the full power loss test procedure, two lubricant samples were collected during the tests and all the lubricant was collected at the end of the tests. The test was performed by the order displayed in Table 2.5. Each operating condition (pair speed - torque) was performed in a different day. The lubricant samples collected during tests were analysed by direct reading ferrometry and ferrography, the gears were weighted for mass loss evaluation and roughness measurements were made on the teeth surface. This test procedure was used in **Paper C** and **Paper F**.

Figure 2.3 displays graphically the operating conditions of the power loss tests. The circles area are proportional to the input power of that test.

This test procedure was quite time consuming and was changed later on, in order to perform three test stages in one day. In this modified test procedure each load level tested starts at 1000 rpm, being the speed increased to 2000 rpm immediately after 4 hours and to 3000 rpm after another 4 hours. This sequential procedure allows a time reduction, once three test stages are performed each day and the test performed at higher speed will start at an oil bath temperature closer to the final temperature than if it started at 40°C , although the same number of cycles was performed. The

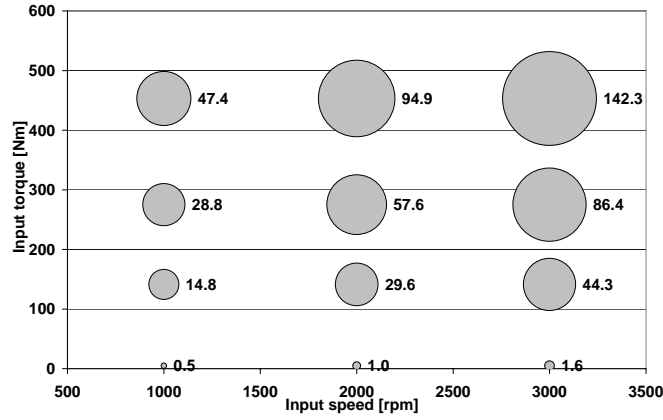


Figure 2.3: Input power in power loss tests [kW].

Test type	Speed [rpm]	Torque [Nm]	Input Power [kW]	Initial temp. [°C]	Test time [hours]	Number of cycles [$\times 10^6$]	Oil samples
No load tests	1000	4.95	0.52	Room	4	0.24	
	2000	4.95	1.04	temp.	4	0.48	
	3000	4.95	1.56		4	0.72	40ml
Load tests	1000	105.0	11.0	40 (± 2)	4	0.24	
	1000	198.8	22.0	40 (± 2)	4	0.24	
	1000	323.4	33.0	40 (± 2)	4	0.24	40 ml
	2000	105.0	20.8	40 (± 2)	4	0.48	
	2000	198.8	41.7	40 (± 2)	4	0.48	
	2000	323.4	62.5	40 (± 2)	4	0.48	40 ml
	3000	105.0	33.8	40 (± 2)	4	0.72	
	3000	198.8	67.6	40 (± 2)	4	0.72	
	3000	323.4	101.5	40 (± 2)	4	0.72	540 ml
Total					48	5.76	

Table 2.6: Wheel operating conditions of the power loss gear tests (load arm of 0.35 m).

test time on the load stages at low torque was also increased to four hours and a lubricant sample was collected at the end, thus all the load stages have the same procedure

Another change was the decrease of the load level, being performed the same load stages (same weight) but applying the weigh at a smaller distance in the load lever (0.35 m instead of 0.5 m), resulting in lower torque, thus lower contact pressures and lower input power. This reduction of torque is important because the maximum input power has a reduction of near 40 kW and the maximum hertzian contact pressure decreases from 1.78 GPa (load stage K9) to 1.50 GPa, thus avoiding excessive wear.

Table 2.6 displays the operating conditions of the updated test procedure. This procedure was used in the work presented on **Paper I**.

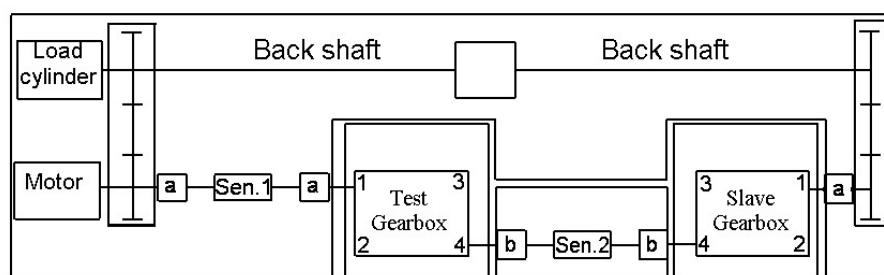


Figure 2.4: Schematic view of the transfer gearbox test rig.

2.3 Transfer gearbox test rig, gearbox and tests

For the MoS₂/Ti and C/Cr surface coated gears power loss tests were performed in a transfer gearbox test rig that is represented schematically in Figure 2.4. The test rig operates by the same principle as the FZG test rig, although it allows to test instead of gear pair, a complete gearbox.

The gearbox test rig is a back-to-back test rig with re-circulating power, where the driving electrical motor only supplies the power needed to overcome inertia, frictional and churning losses and to reach and maintain the desired operating speed, resulting in a significant reduction of energy consumption. A hydraulic cylinder displaces a helical gear pinion over a shaft and, consequently, the closed kinematic system twists applying the desired torque.

Figure 2.5 shows a cross section of a two speeds transfer gearbox used in four wheel drive light trucks. The transfer gearbox is mounted after the conventional gearbox of the vehicle, allowing it to have 2 drive axles and an auxiliary power output. This transfer gearbox used 5 gears mounted in three shafts employing gibs. The gears mounted on the input and output shafts were supported by needle roller bearings. The gears were manufactured with DIN 15CrNi6 steel. After machining, the gears were case hardened, quenched in oil and annealed. The geometric characteristics of the gears are presented in Table 2.7.

The reference lubricant for this transfer gearbox was a mineral based industrial gear oil with viscosity grade ISO VG 150, containing EP and AW additives. The transfer gearbox was filled up with 2.85 litre of lubricant oil, as recommended by the gearbox manufacturer. The most significant properties of the lubricant are displayed in Table 2.7 and are detailedly presented in section 6.1.1, where this lubricant is designated by M1.

2.3.1 Gearbox power loss tests

Two different gearboxes, one with C/Cr coated gears and another with MoS₂/Ti coated gears, were tested in a wide range of operating conditions (input torque and speed) in order to measure their efficiency. The running-in of each gearbox lasted approximately half million cycles, applying increasing input power, from 7.5 kW to 41 kW. After running-in the lubricant oil was replaced.

Each power loss test was performed at constant speed and torque, during which the oil temperature was free and continuously measured. The initial oil temperature

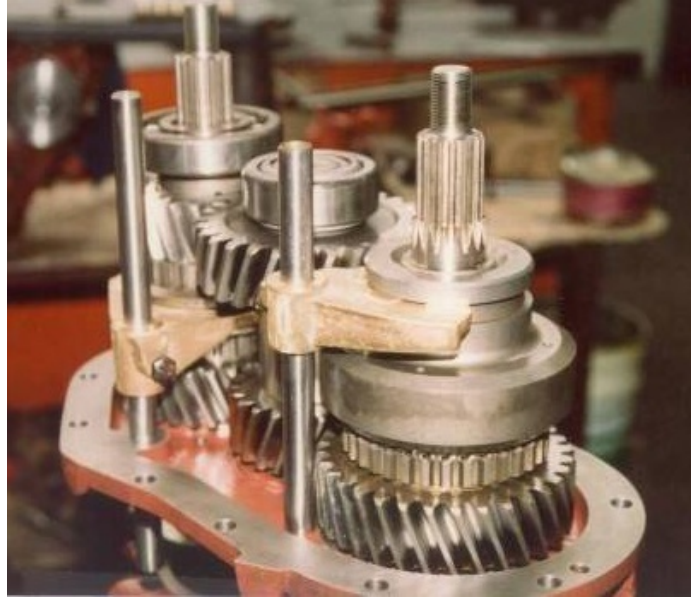


Figure 2.5: Photography of the transfer gearbox.

Parameter [units]	Design.	Gear wheel n°				
		1	3	2	4	6
Module [mm]	m	4	4	3.5	3.5	3.5
Number of teeth [/]	Z	17	28	27	23	32
Profile shift factor [/]	x	0.051	-0.24	0.161	0.415	0.381
Width [mm]	b	35	33.5	35	35	35
Pressure angle [°]	α	20	20	20	20	20
Helix angle [°]	β	20	20	20	20	20
Max. addendum diameter [mm]	da_{max}	80.7	125.2	108.4	95.3	128.6
Oil Type	-	ISO VG 150 mineral oil				
Viscosity @ 40°C [mm ² /s]	ν_{40}	150				
Viscosity @ 100°C [mm ² /s]	ν_{100}	14.5				
Specific gravity @ 15°C [/]	Sp Gr	0.896				
Viscosity Index [/]	VI	95				
FZG Rating [/]	K_{FZG}	12+				

Table 2.7: Geometric characteristics of the transfer gearbox gears and oil properties.

Parameter [units]		Design.	Stages				
Vehicle speed [km/h]		V	5.7	13.6	21.5	29.4	37.4
Transfer gearbox input speed [rpm]		n	573	1376	2178	2981	3784
P @ 36 kW	Input torque [N.m]	T _{in}	600	250	160	120	90

Table 2.8: Operating conditions in the transfer gearbox efficiency tests with coated gears.

was 40 °C and the test was stopped if the lubricant temperature exceeds 120 °C. The test duration was 120 minutes and the final oil temperature depends on the operating conditions (torque and speed). Table 2.8 shows the test programme where the operating conditions are defined as well as the corresponding speed of the vehicle using this transfer gearbox.

The results of the power loss results are presented in **Paper A** and in **Paper G**.

2.4 Pre and post test analysis

2.4.1 Gears weight loss

The weighing of components along this work were done in an electronic *Metler-Toledo PR1203* balance with 1210 g of capacity and a precision of 1 mg. The mass loss evaluation concerns the amount of material that was lost during a period of the test or during all test and results from the subtraction of the weight before the test by the weight after the test. Before any weighing, the component was washed in an ultrasonic bath of solvent and cleaned in order to remove oil and any other type of particles that might be glued to the surface.

2.4.2 Roughness measurements and topographies

The roughness measurements presented during this work were performed on a *Hommwerke T4000* controller. Two pick-ups were available for surface roughness measurements, one with a vertical range of measurement of $\pm 100 \mu\text{m}$ and other with $\pm 300 \mu\text{m}$, designated by TK100 and TK300, respectively, having both a tip radius of $5 \mu\text{m}$ and a cone angle of 90° .

The determination of the roughness parameters were performed by the *Hommwerke* controller T4000 according to the standards DIN4762, DIN4768 and DIN4776 [36]. The teeth surface roughness in general was measured in the axial direction, although in some cases the surface measurements were also performed in the radial direction. The roughness profiles presented along the work are of type R (DIN4777) or type K (DIN4776), being both filtered profiles that have removed the surface curvature.

The roughness measurement equipment also performs surface topography, although this is a very time consuming operation. The topographies performed are basically parallel roughness measurements at a well defined distance. The distance between points in the direction of measurement was $2.5 \mu\text{m}$ and the distance between measurements was $5 \mu\text{m}$. The topographies proved to be very interesting to observe the micropitting cavities generated during micropitting tests.

2.4.3 Lubricant analysis

The analysis of particles contained in lubricant samples gives a quite good indication about the wear of lubricated parts, since those particles in a closed box are generated in the contacting surfaces. All the tests performed during this work were followed by regular oil analysis. The oil samples were collected at pre-defined intervals, according to the test type. These oil samples are usually diluted with a solvent, being the dilution a function of the contamination level. Two main techniques were always used, direct reading ferrometry and analytical ferrography [37, 38].

These analysis allow the identification and characterizations of the wear particles present in the oil samples during the tests. This allows the comparison of lubricants, materials etc. in what concerns to wear behaviour, such as the size of wear particles, the amount of wear particles and the process that originated those wear particles.

Direct reading ferrometry

Direct reading ferrometry (DRIII) is performed on a diluted sample of lubricant, that is forced to pass through a optical system in which opacity measurements are performed in order to measure the ferrometric parameters D_L (large wear particles index - particles with size greater than $5\mu m$) and D_S (small wear particles index - particles with size smaller than $5\mu m$).

The values of D_L and D_S are used to evaluate the concentration of wear particles index - $CPUC$ and the severity of wear particles index - $ISUC$, defined as, $CPUC = \frac{D_L + D_S}{d}$, $ISUC = \frac{D_L^2 - D_S^2}{d^2}$, where d stands for the oil sample dilution. The CPUC index grows when the sum of large and small particles increase, while the ISUC index grows when the number of large particles is greater than the number of small particles.

Analytical Ferrography

Analytical ferrography is performed on a diluted oil sample that is passed through a slide submitted to a magnetic field, being the wear particles positioned along the slide as function of its magnetic sensibility and its size. This slide with the wear particles deposited, designated as ferrogram, is then observed on a microscope with bichromatic light (also known as ferroscope). The analytical ferrography provides information concerning the size of the wear particles, their morphologies, the particles concentration, the type of wear that originates the particle, the material / component of provenience of the particles allowing a more complete knowledge of the wear process.

2.5 Summary

In this chapter the gear and gearbox test procedures were presented and, the pre and post testing analysis were described.

Nine different gear testing procedures were developed and / or adapted to the gears materials, surface coatings and lubricants under evaluation and several different pre and post test analysis were used.

3 Gearbox power loss and a thermal equilibrium model

3.1 Introduction

The power losses of gearboxes are of capital importance in the majority of the applications, because they define the operating temperature which, in general, should be within a given range in order to avoid failures and to improve the lubricant performance. The environment compatibility also depends of lower power losses, because the equipment needs less energy to operate, thus needs less raw materials. During the years it has been observed an increase of power density in gear applications that has contributed to the development of new lubricants, new materials and new surface coatings in order to avoid failures and also to lower the energy consumption by those devices.

The introduction of these new solutions lead to the update or development of models to predict the overall behaviour of the equipment using those solutions. The development of models should be based on real component testing and should take in account the specific interactions between the lubricants and materials. An additivated lubricant might have a completely different behaviour than the base lubricant from which it was made, specially when it uses complex and new additivation.

To predict the power losses in a gearbox, or its operating temperature, it is necessary to know the friction properties of the lubricant in combination with the material or surface coating used, and such knowledge is only achieved in real component tests.

In this work a method for determining the influence of the pair lubricant / material combination on the friction coefficient between gear tooth is proposed, based in FZG gear power loss tests. The evaluation of the friction coefficient between gear tooth is done using a numerical model of the energetic balance of the FZG gearbox [32,39–42].

3.2 Power loss tests

The power loss tests consisted of a set of tests performed at a wide range of speed and torque operating conditions. The objective is to evaluate the behaviour of the combinations of lubricants, materials and surface coatings.

The tests are performed at several levels of input speed (1000, 2000 and 3000 rpm), and for each input speed the torque ranges from almost zero (no load condition where the churning losses are predominant) to a very high torque condition where the friction losses are very important. Roughly the contact pressure in these tests range from 0.016 GPa to 1.8 GPa.

The power loss tests are performed at constant operating conditions, i.e. at constant speed and torque, being the oil bath temperature free. Each test lasts for a

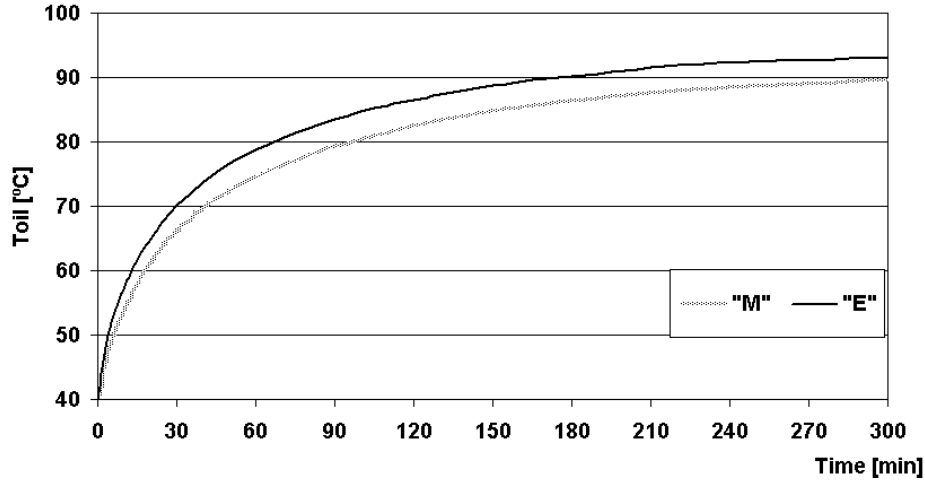


Figure 3.1: Evolution of oil bath temperature during a power loss test.

long period, two to four hours for the tests at very low load and four to five hours for the other tests, in order to allow the equilibrium temperature to be reached. The equilibrium temperature is reached when the oil bath temperature no longer changes with time, becoming almost constant. Figure 3.1 shows an example of the evolution of the oil bath temperature for two different lubricants (“M” and “E”) during a power loss test performed at 1000 rpm on FZG load stage K9.

The thermal equilibrium of a gearbox is reached when the operating temperature stabilizes i.e. when the power dissipated inside the gearbox is equal to the heat evacuated from gearbox to the surrounding environment. The equilibrium temperature is dependent of the gearbox characteristics and of the lubricant properties [43–48]. The higher the power losses the higher will be the equilibrium temperature of the gearbox. A lower equilibrium temperature means higher system efficiency, lower friction coefficient, smaller oil oxidation and longer oil life [43], besides influencing also the protection against wear and failures like pitting, micropitting and scuffing [49].

The lubricant temperature has two opposite effects, when it increases promotes higher chemical activity and better tribological layer formation, and, at the same time leads to lower viscosity and thinner oil film thickness [49]. The heat evacuation from the gearbox is done by conduction, convection and radiation [44–46].

The equilibrium temperatures of different lubricants, materials or surface coatings obtained in power loss tests allow a direct comparison of efficiency, because lower equilibrium temperature means lower power dissipation.

3.3 Energetic balance model of a gearbox

Eq. 3.1 establishes an approximated model for the energetic behaviour of the test gearbox. Eq. 3.1 depends on 5 unknown variables: the oil stabilized temperature (T_{oil}), the gearbox wall temperature (T_w), the room temperature (T_{room}), and the friction coefficient between gear teeth (μ_m). This equation allows the determination of the oil temperature in permanent conditions (equilibrium temperature) for any combination of the operating conditions imposed to the gearbox. Figure 3.2 shows a

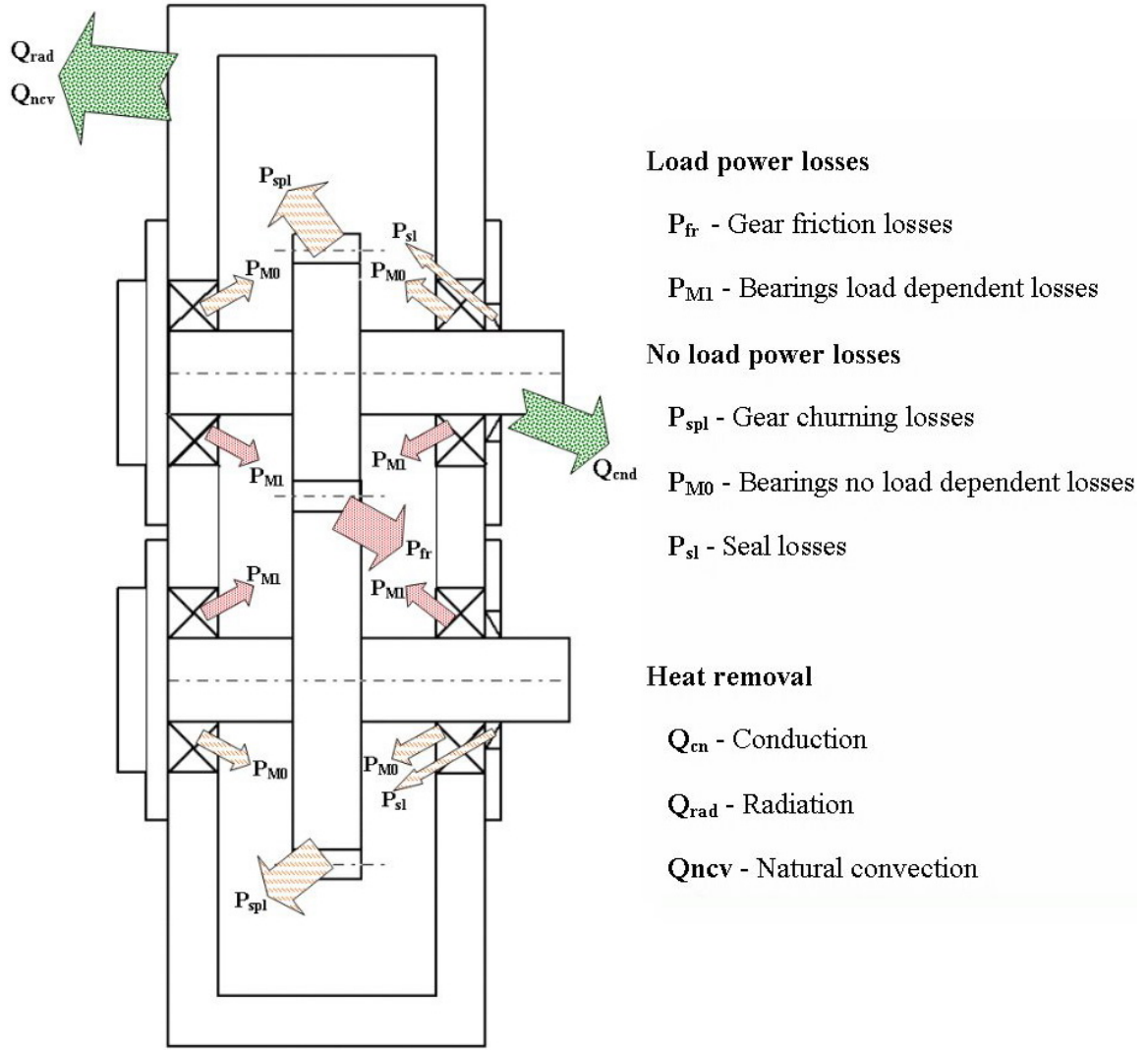


Figure 3.2: Schematic view of FZG gearbox and the different mechanisms of power dissipation and heat evacuation.

schematic view of FZG gearbox's power dissipation and heat evacuation mechanisms.

$$P_{fr} + P_{M1} + P_{spl} + P_{M0} + P_{sl} = Q_{rad} + Q_{cnv} + Q_{cn} \quad (3.1)$$

The main mechanisms of power dissipation inside a gearbox are the churning losses and the frictional losses, in which the lubricant has capital influence.

Some of the most important works related to the thermal equilibrium of gearboxes were performed by Hohn et al. [44] and Winter et al. [45], being the work performed by Changenet et al. [46,47], Luke et al. [50] and Terekhov [51] also very important for the evaluation of churning losses. The bearings and seals power losses are reported in several works [44, 48].

The churning losses are related with the moving parts immersed on the lubricant bath, and are generated by components like gears (P_{spl}), roller bearings (P_{M0}), shafts, seals (P_{sl}) and other moving components inside a gearbox. The gear churning losses are dependent of gear geometry, immersion depth, rotating speed and gears immersed

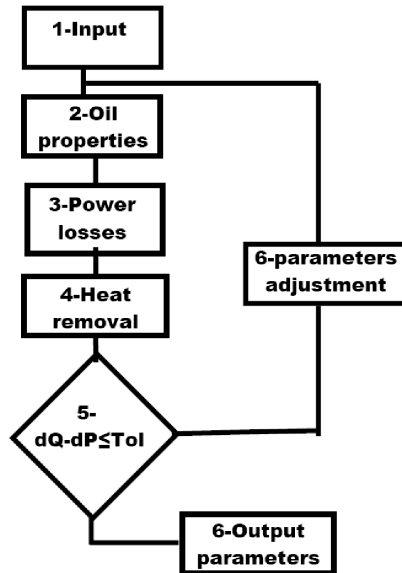


Figure 3.3: Algorithm for the energetic balance of gearboxes.

area as well as lubricant viscosity and density. Other influencing parameters are the gearbox geometry and the fluid flow inertial, viscous and gravitational forces [46,47].

The friction power losses result from the contact between bodies with relative movement, being its main source the gears (P_{fr}) and the roller bearings (P_{M1}), in which the lubricant has also capital influence. The gear friction losses depend on the gear geometry, the number of teeth, the operating conditions and the friction coefficient between the contacting tooth [44], while the rolling bearing friction losses depend on the applied load, type of bearing, bearing diameter and friction coefficient in bearing contact [48].

A presentation of the energetic model for FZG gearbox is displayed in **Paper C**, **Paper D** and **Paper F**.

3.3.1 Model structure

The algorithm developed for the energetic balance of the gearbox is defined in Figure 3.3. This model is based on optimization techniques using the least squares method implemented in Matlab[®] and it can be used to optimize several variables. The optimization function is Eq. 3.1 displayed above and the variables to optimize can be any among the ones present in the model.

The input module defines the gears, bearing, seals, gearbox case characteristics and the operating conditions. The oil properties module determines the viscosity and density of the oil for the operating temperature. The power losses and heat removal are then compared and the parameters are optimized until a solution is obtained.

The main application for the model was the determination of a correction factor for the friction coefficient, being the experimental equilibrium temperatures used as input and the correction factor as parameter to be optimized.

The model was also used to determine the conduction factor (f_{cn} , see **Paper C**) [33,39,45], being only used for that purpose the experimental results obtained

on no-load tests. The no-load test were also used for the validation of the churning losses (or no-load power losses) part of the model. In both cases, the experimental temperatures was used as input.

Other application of the model was the prediction of the stabilization temperature of the gearbox, being an example of application presented in section 6.4.4.

Optimization of the friction coefficient

One of the main influences of using a different lubricant or a different gear material in a tooth contact is on the friction coefficient. Hohn et al. [44] presented a formula for the average friction coefficient along the contact line, displayed in Eq. 3.2. This formula already contemplate a lubricant factor X_L , that assumes the value $X_L = 1$ for additive free mineral oils. In this work all the lubricants had different base oils and different additivation, thus it was expected a different X_L parameter value for each one.

$$\mu_m = 0.048 \cdot \left(\frac{F_{bt}/b}{v_{\Sigma c} \cdot \rho_c} \right)^{0.2} \cdot \eta_{oil}^{-0.05} \cdot Ra^{0.25} \cdot X_L \quad (3.2)$$

For each combination of material (or material and surface coating) - lubricant tested the lubricant factor X_L was optimized in order to obtain the best correlation with the experimental results. The expression used for X_L parameter was dependent of all variables involved in Eq. 3.2, that are the tooth normal force in the transverse section F_{bt} , the sum velocity at pitch point $v_{\Sigma c}$ and the oil viscosity η_{oil} . The results showed that in all cases tested the X_L parameter that presented the best correlation was only dependent on load (F_{bt}), having the other variables an insignificant weight. The X_L parameter used is displayed in equation 3.3.

$$X_L = \frac{1}{(F_{bt}/b)^{b1}} \quad (3.3)$$

When exponent $b1$ increases, the influence of load on the friction coefficient becomes smaller and the friction coefficient decreases ($(F_{bt}/b)^{0.2-b1}$).

3.4 Discussion

The power loss tests proved to be a very interesting type of procedure to compare and evaluate the energetic efficiency of lubricants, materials and coatings.

These test procedures also allow to compare and evaluate the wear behaviour of the combinations lubricant/material or lubricant/surface coating when combined with post analysis techniques of the lubricant.

Another interesting characteristic of this test procedure is that it was performed at a wide range of operating conditions, from very low loads to considerably high loads, being more representative of gears daily range of operation than the typical failure tests (scuffing, pitting, ...). This test also provided an idea of the behaviour of the combination material / lubricant for very different contact pressures and rotating speeds.

3 Gearbox power loss and a thermal equilibrium model

The thermal equilibrium model developed showed to be a very usefully tool to help understanding the behaviour of the FZG gearbox, i.e. the influence of the bearings or seals in the total power losses, or to understand better the variation of the churning and friction losses and their influence in the total power loss. This kind of knowledge allows to have a better idea of the impact of changing the lubricant type, the lubricant viscosity, changing the gears geometry etc.

The numerical model is quite flexible, allowing to determine a correction factor for the friction coefficient formula for a specific lubricant, based on experimental power loss tests. If the friction coefficient for a lubricant is known, the model allows to determine the equilibrium temperature for different operating conditions.

4 Gear Materials

4.1 Introduction

This chapter presents the results of a systematic experimental evaluation of Austempered Ductile Iron (ADI) as a gear material, and whenever possible comparing it to carburizing steel, concerning two main aspects: power loss and contact fatigue resistance (pitting and micropitting).

The ADI material used in this work has been developed by H. Santos [19] and several works have been published by Magalhães et al. [16–18, 52–54], although the fatigue characterisation in gears had not been done yet. Other very important issue presented in this work is the power losses promoted by ADI material [40].

The ductile iron used in this work has the following chemical composition (in weight percentage): 3.38 % C, 2.43 % Si, 0.55 % Mn, 1.11 % Cu, 0.015 % P, 0.020 % S [16, 17, 40, 52–54]. All gear tests were performed on the FZG test rig using type C gears (presented on section 2.2).

The extended results of this evaluation are presented in **Paper E** [40] and **Paper F** [41]. The evaluation of micropitting and power losses were done considering two completely different lubricant products, a mineral gear oil and a biodegradable low-toxicity ester based oil.

The ADI material has an interesting combination of mechanical properties [18] and the replacement of some conventional steel parts by ADI's might result in several advantages which promote the acceptance and use of these materials, namely in the automotive industry. The ADI's are a material cheaper than steel; ADI's are casting materials, thus products can be moulded, allowing significant cost reduction of the manufacturing process when compared to conventional steel machining [13]; the ADI's heat-treatments are also low-energy consumers (austempering is done at about 300°C) when compared to steel conventional heat-treatments [13]; ADI's have lower density than steel (10% lighter than steel); ADI's present high vibration absorption (according to Harding [14] more than 6 dB in gearboxes); ADI's also show very high resistance to wear and scuffing [52].

The ADI used in the present work was austempered at 300 °C during approximately 4 hours. The heat treatment procedure is resumed in Figure 4.1 [40]. The temperature of 300 °C was choose to promote the best equilibrium between the mechanical resistance (higher for lower austempering temperature) and ductility (higher for higher austempering temperature).

The mechanical properties measured for the ADI material are presented in Table 4.1 and compared with those of DIN 20MnCr5 carburizing steel, a material widely used for gear manufacturing.

The ADI distribution of graphite nodules, as well as the microstructure are presented in Figure 4.2. The graphite nodules have a uniform distribution and size, and

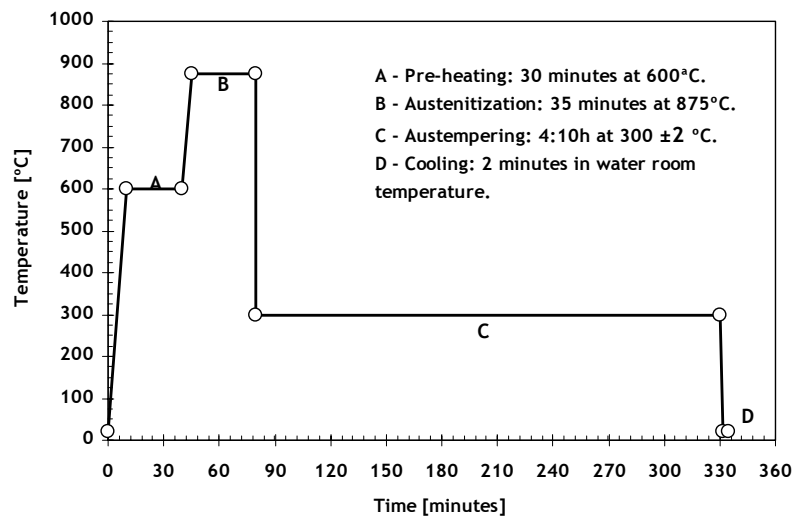


Figure 4.1: Procedure of ADI austempering heat treatment.

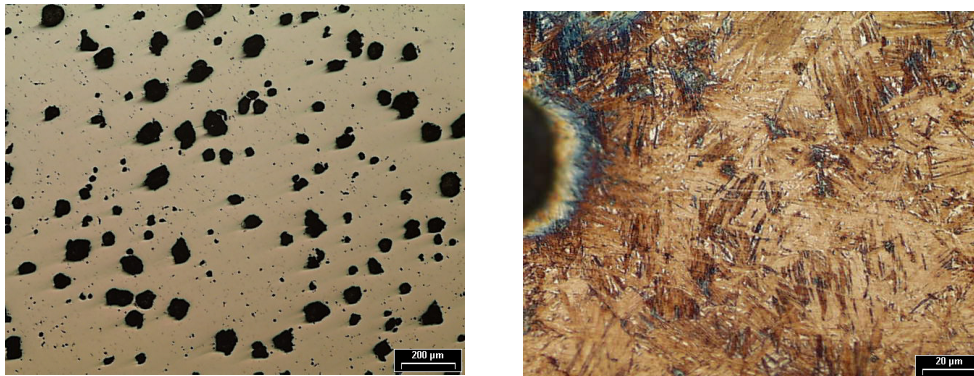


Figure 4.2: Graphite nodules on the surface (left) and a microstructure (right) of ADI material.

the ADI microstructure was composed of austenite and Ausferrite (acicular ferrite and carbon stabilized austenite).

4.2 Scuffing protection

Magalhães et al. [52] performed scuffing tests with ADI gears austempered at different temperature using an ISO VG 68 additive free mineral lubricant. The ADI gears had a geometry of type A, but with a width of $b = 16\text{mm}$ in order to obtain a contact pressure equal to the obtained with $b = 20\text{mm}$ steel gears. The FZG scuffing load stage on those tests was $K_{FZG} = 11$ or $K_{FZG} = 12$ depending on the austempering temperature, while standard steel gears ($b = 20\text{mm}$) lubricated with a similar lubricant reached scuffing on FZG load stage $K_{FZG} = 4$ [55].

Those impressive results shows that ADI material has a very high scuffing load capacity, mainly due to the graphite nodules present in the material that act as a solid lubricant and eventually as an additive for oil. Those results also show that the ADI material is prone to work well with lubricants with low additivation [52].

Properties	Unit	ADI	20MnCr5
Modulus of elasticity	103 N/mm ²	170	210
Density	g/cm ³	7.06	7.85
Poisson ratio	/	0.25	0.3
Surface hardness	HRC	42	58-62
Tensile strength	N/mm ²	1280	1300
Yield strength 0.2%	N/mm ²	1063	550
Elongation	%	6	8

Table 4.1: Mechanical properties of Austempered Ductil Iron.

4.3 Pitting

This paragraph presents the results obtained in the pitting gear tests, performed in the FZG test rig. The test and test procedure were presented on section 2.2. Figure 4.3 shows the results of pitting tests, as well as the cases where micropitting occurred before pitting. In these cases, the test pursued up to the pitting failure or up to 20 million cycles.

The ADI gears didn't had pitting failures for contact pressures below 1.2 GPa. In some cases micropitting was observed in the teeth surface during the test, having those tests a lower pitting life (10 to 25%) than the test where micropitting wasn't observed. Although in a pitting test performed at a contact pressure of 1.19 GPa micropitting was detected and a pitting failure did not occurred.

The trend line that best correlates the experimental results is displayed in Figure 4.3 (correlation coefficient $R^2 \geq 98\%$).

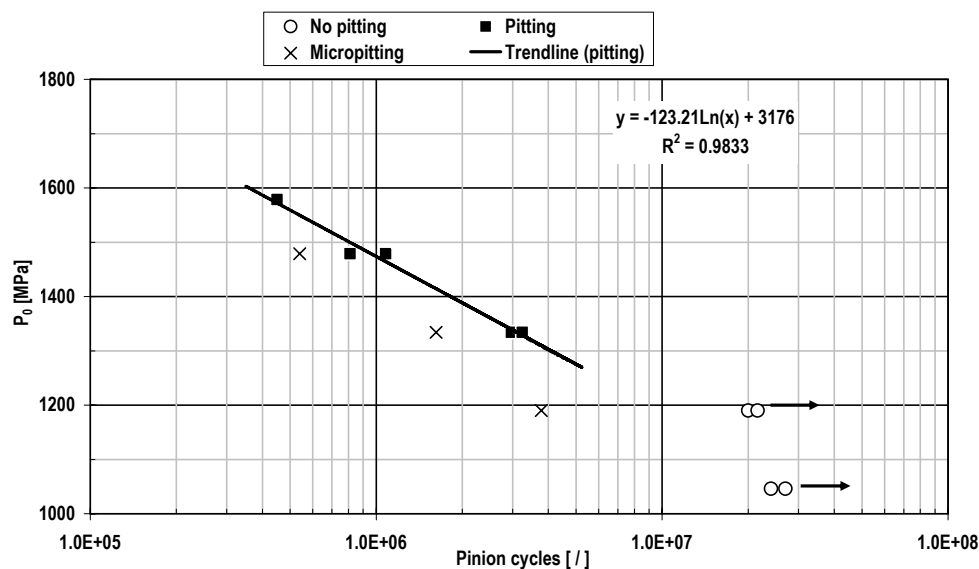


Figure 4.3: Gear pitting tests. Contact pressure v.s. number of cycles

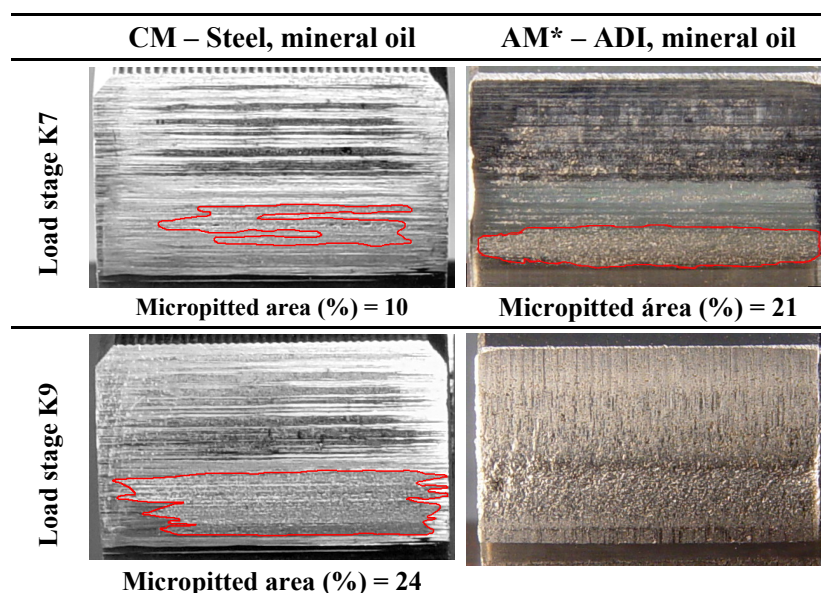


Figure 4.4: Pictures of ADI and steel (CM, AM*) pinion tooth flanks after standard load stages of gear micropitting tests.

4.4 Micropitting protection

To study the micropitting protection of ADI material, several gear micropitting tests were performed and compared with those of carburized steel gears, using the same lubricants.

The micropitting tests of ADI gears performed at the standard load stages according to DGMK-FZG micropitting test [30] revealed that the ADI gears could not be submitted to a load stage as high as carburized steel gears, even though for the same load stage ADI gears had lower contact pressure due to its lower Young modulus (see Table 2.3).

Only one ADI gear test was performed using these operating conditions with mineral oil. The mass loss measurements after load stage K7 was already twice larger than that measured for carburized steel gears and after load stage K9, the tooth surface of ADI gears was completely damaged, having a mass loss over 1.5 g. Figure 4.4 displays pictures of gear tooth flanks after each load stage of the standard procedure (i.e. after load stage K7 and K9) both for the ADI and the carburized steel gears. The micropitting areas were surrounded by a red line for easier identification and, as can be observed, the micropitting area measured on the ADI gear after load stage K7 is twice larger than that measured on carburized gear.

The standard DGMK operating conditions allowed to make a direct comparison with carburized steel gears, but won't allow the comparison of lubricants behaviour using ADI gears, neither the comparison of different ADI's. Thus the operating conditions were modified, decreasing the load applied on each load stage. In section 2.2 the new operating conditions were reported.

In the updated operating conditions (load stage K5 and K7 were used) ADI gears exhibit micropitting areas similar to those obtained with carburized steel gears on standard operating conditions, being an indication of the limit operating conditions

	AE	AM
K3+K5	20	35
K7	132	155

Table 4.2: ADI gears mass loss in micropitting modified test for ester (AE) and mineral (AM) oil

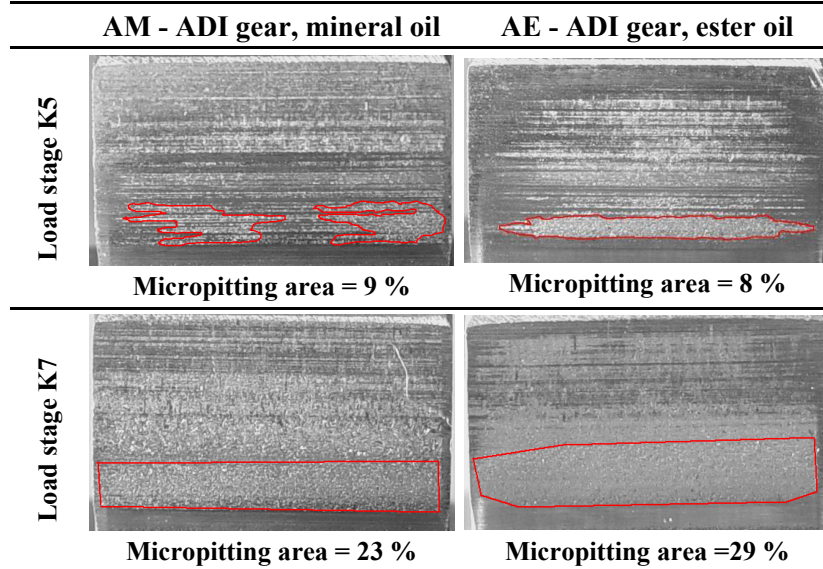


Figure 4.5: Pictures of ADI (AM, AE) pinion tooth flanks after modified micropitting tests.

for ADI gears and showing that the modified operating conditions are adequate for the lubricant micropitting performance evaluation with ADI gears. Figure 4.5 shows pictures of ADI gear tooth lubricated with two different lubricants during micropitting tests, both having similar micropitting areas than carburized steel on standard micropitting test, although with higher mass loss.

The mass loss during the micropitting tests performed with ADI gears are a result of micropitting (below pitch line) and also from mild wear above the pitch line. This is observed in the flank photographs and also in the roughness measurements that displayed a decrease of R_{z-D} and R_{VK} roughness parameters during the test. This helps to explain the reason why the ADI gear lubricated with mineral oil (AM) has lower micropitting area, but had 17% higher mass loss than the gear lubricated with ester oil (AE), as presented in Table 4.2. Figure 4.5 shows that AM gear has the tooth surface after load stage K7 more damaged than AE gear.

A further discussion on these results is presented in Chapter 6 during the presentation of lubricants results.

4.5 Gear power loss

Power loss tests were performed to evaluate the influence of ADI material, combined with a mineral and an ester lubricant, on the energetic efficiency of gears. The power

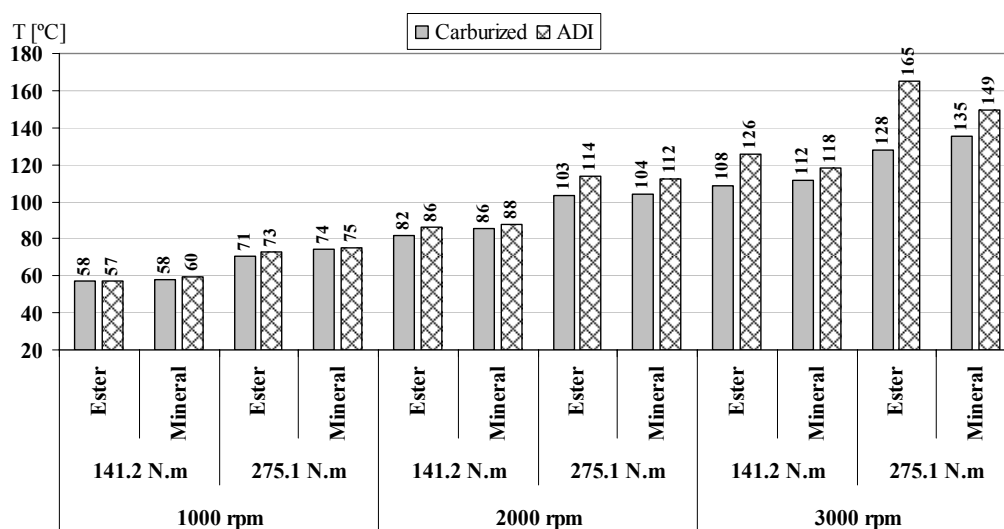


Figure 4.6: Equilibrium temperature in power loss tests: ADI v.s. carburized steel.

loss tests performed were described on section 2.2 and all the results are reported on **Paper E** and **Paper F** [40, 41]. Power loss tests at the same operating conditions were also performed with carburized steel gears, allowing a direct comparison between the two materials.

The main result in power loss tests was the equilibrium (or stabilization) temperature reached for each set of operating conditions. The lower the stabilization temperature the lower were the power losses inside the gearbox. Figure 4.6 shows the equilibrium temperature attained on the power loss tests for the two materials and both lubricants.

The ADI gears, in general, displayed higher stabilization temperatures than steel, between 1 to 4 °C, being the differences larger for the most severe operating conditions. An abnormal equilibrium temperature was obtained on the test with ADI gear and ester lubricant at the highest input power test, where the difference reached 18 °C, although no sign of failure was observed.

For the lowest tests at lowest input power (1000 and 2000 rpm), the ester oil presented slightly best results with both materials. For the highest input power (3000 rpm), the ADI gears lubricated with mineral lubricant displayed lower stabilized temperature, though for carburized steel gears the ester lubricants always promoted the lowest operating temperature.

The lubricant analysis of ADI gear tests with ester lubricant displayed values of *ISUC* and *CPUC* lower than the measured for mineral lubricant on the two first samples (1000 and 2000 rpm). On the third sample, as expected due to the abnormal stabilized temperature obtained, the ester gear lubricated with ester lubricant already displayed highest values of *ISUC* and *CPUC* indexes.

The mass loss of ADI gears was: 73 mg for the gear lubricated with ester oil and 150 mg for the gear lubricated with mineral oil. This result shows that beside having an abnormal increase of temperature in the last load stage, the ester lubricant promoted lower mass loss than the mineral lubricant.

The mass loss and oil analysis of ADI gears are not directly comparable with

	Mineral	Ester
steel	0.055	0.076
ADI	0.016	0.037

Table 4.3: Lubricant factor exponent b_1 of X_L parameter ($n_{wheel} \leq 2000$ rpm).

carburized steel gears, once the test procedure for carburized gears include the load stage K9. So, the carburized gears performed an extra load stage at three input speeds and that load stage was the most severe (for more details please consult **Paper F**).

4.5.1 Friction coefficient

The influence of ADI gears, in combination with the two lubricants, on the friction coefficient was accessed inputting the results obtained in the power loss tests (presented above) in the energetic model of the FZG gearbox presented in Chapter 3. The model will allow the determination of a correction factor for the friction coefficient for each combination tested within the range of operating conditions tested. The friction coefficient for carburized gears was also obtained.

The results of power loss tests performed at 3000 rpm were not included on the input of the energetic balance of the FZG gearbox, because the ADI gear had temperatures abnormally high and some surface damage occurred.

Using the energetic balance model, the exponents b_1 of the friction correction factor of Eq. 3.3, $X_L = 1/(F_{bt}/b)^{b_1}$, were determined. The values obtained are given in Table 4.3. The larger the exponent b_1 , the smaller will be the friction coefficient.

As expected from gear power loss tests results, the ADI gears have a friction coefficient higher than that of carburized steel gears. Figure 4.7 displays the friction coefficient determined numerically with the correction factor presented in Table 4.3 for an oil temperature of 90°C and a input speed of 2000 rpm.

The ADI gears have a friction coefficient between 14 to 30% higher than carburized steel gears lubricated with the same oil. The ADI gears even so allow a considerable friction reduction in comparison to a mineral additive free lubricant ($X_{L=1}$) with carburized gears.

ADI and carburized steel gears lubricated with ester oil had a friction coefficient 6 to 13% lower than when lubricated with mineral oil.

4.6 Discussion

The scuffing behaviour of ADI gears was outstanding. Using the same lubricant than carburized steel gears and having lower width (in order to have the same maximum contact pressure), the ADI gears supported more 7 FZG load stages than carburized steel gears. This characteristic makes the ADI material recommendable for applications with the occurrence of starvation or frequent start and stop operation.

The SN curve for ADI was plotted using real components, gears, and it was observed that no pitting failure occurred for contact pressures up to 1.2 GPa. It was also observed that in the tests where micropitting occurred the number of cycles necessary

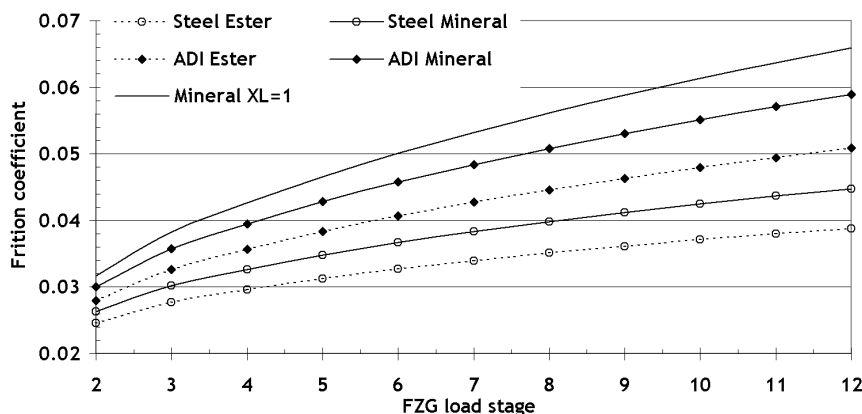


Figure 4.7: Numerical friction coefficient for ADI and carburized steel gears (Toil = 90 °C; 2000 rpm).

to reach pitting failure decreased around 10 to 25 % compared to the tests where micropitting didn't occur.

In what concerns to micropitting protection, the ADI gears have a operating limit considerably lower than the carburized steel gears. When the standard DGMK micropitting tests procedure was performed with ADI gears the teeth surface was completely damaged and the mass loss was over 1.5 g. So, in order to evaluate and compare lubricants with ADI gears the operating conditions couldn't be so severe.

In the modified gear micropitting tests, the ADI gear combined with ester lubricant (AE) presented 15 % lower mass loss than combined with mineral oil (AM), although presenting 6 % higher micropitting area. The oil analysis results show that the wear particles concentration index (CPUC) and the large particles index (DI) for AE gear were 15 % lower than for AM gear, confirming the lowest mass loss. The visual inspection of the tooth flanks shows that the degradation of AM gear was more severe than that of AE gear, being also confirmed by the roughness measurements.

In power loss tests ADI gears always presented higher stabilization temperature than carburized steel gears, although on the tests at 1000 rpm and 2000 rpm the stabilization temperature difference was very small. In the tests performed at higher speed and load (higher input power) the ADI gears displayed considerably higher stabilization temperatures than carburized steel, being this behaviour observed for both lubricants.

The application of an energetic model allowed the definition of a friction coefficient expression for each combination of material-lubricant. The friction coefficient is always higher for ADI whichever the lubricant. The ester lubricant promoted lower friction coefficient for both ADI and carburized steel gears. These results are coherent with the lubricant equilibrium temperatures observed during gear power loss tests. In what concerns to wear, ADI gears lubricated with ester oil generated significantly smaller mass loss (50% less) than when lubricated with mineral oil and the ferrometric wear indexes confirm those results.

ADI gears have some very interesting advantages over carburized steel gears, mainly the lower cost, the lower weight and higher vibration absorption, the higher resistance to scuffing if non additivated lubricants are used, but have lower fatigue resistance

and must operate at lower contact pressures, as demonstrated by the micropitting tests.

5 Surface coatings

5.1 Introduction

This chapter will describe the work performed to provide tribological information about the applicability of two multi-layer composite surface coatings to gear applications. The main objectives of this work were the evaluation of gear power losses and gear scuffing load capacity of coated gears, as well as the determination of the corresponding friction coefficient between gear tooth. In an earlier phase several screening tests were performed to assess the coatings tribological performance, like adhesion to the substrate, the applicability to heavy loaded contacts and the wear resistance. This work was presented in **Paper A** [32], **Paper D** [33] and **Paper G** [34].

DLC (diamond-like carbon) coatings are very hard and have a low friction coefficient but tend to be brittle and have poor adhesion, being unsuitable for highly loaded applications. Coatings made of amorphous hydrogenated carbon films, containing a small amount of metal (Me-C:H), tend to be less brittle but are much softer and can only be used at moderately high loads [6, 8]. To provide a better wear protection it is interesting that the coating behaves like a true solid lubricant [6] like graphite or MoS₂. The MoS₂ coatings can be improved with the co-deposition of other metals such as Ti [7] or Cr [9]. In the case of graphite it can be co-deposited with Cr [56].

Two multi-layer composite surface coatings were considered, both deposited by DC magnetron sputtering using a standard CFUBMSIP [57, 58] Teer Coatings PVD system, with four targets. The C/Cr surface coating [34, 56, 59] has a structure based on graphite, with a friction coefficient similar to that of graphite but with a much higher hardness and wear resistance. It was deposited using three carbon targets and one chromium target, being the typical thickness around 1.7 μm and the hardness around 2200 HV. The C/Cr coating critical load on standard scratch tests was 80 N and a friction coefficient of 0.06 was measured on pin-on-disc tests with a load of 140 N, being the specific wear rate in these conditions very low and almost constant [34].

The MoS₂/Ti coating used was harder, more resistant and less sensitive to atmospheric water vapour than MoS₂ or common DLC coatings and has a friction coefficient similar to MoS₂. The higher hardness combined with low friction and good adhesion to the substrate leads to low wear rates and to high load bearing capacity [8]. The MoS₂/Ti surface coating [4–8, 33, 41, 60, 61] has a deposition procedure similar to C/Cr, although with three MoS₂ targets and one Ti target, being the coating thickness around 1.2 μm and a dynamic hardness of near 12 GPa [5]. On standard scratch tests no failures occurred for loads up to 100 N, and on pin-on-disc tests a friction coefficient as low as 0.04 was found [32] being also the wear rate very low on reciprocating wear tests [32].

5.2 Scuffing protection

Scuffing tests were performed in the FZG test machine using type C gears to evaluate the scuffing load capacity of the C/Cr and MoS₂/Ti surface coatings. The test procedure and operating conditions were presented in section 2.2.

The tests were performed with a mineral additive free ISO VG 100 lubricant. The main reason for choosing an additive free oil was the expected high scuffing load capacity of the surface coatings, that if combined with a lubricant that also had high scuffing load capacity, will not reach scuffing failure within the load capacity of the FZG test rig. Thus not allowing the comparison of the surface coatings.

Four different gears sets were tested. One uncoated gear, two MoS₂/Ti coated gears and one C/Cr coated gear:

- NC - Uncoated gear ($R_a = 2.4 \mu\text{m}$);
- MST - MoS₂/Ti coated gear ($R_a = 2.4 \mu\text{m}$);
- MST* - MoS₂/Ti coated super-finished gear ($R_a = 0.4 \mu\text{m}$);
- CCR - C/Cr coated gear ($R_a = 2.4 \mu\text{m}$).

The scuffing test procedure was performed at two different speeds, 1500 rpm and 3000 rpm and the hertzian contact pressure can be as high as 2.08 GPa.

The influence of surface coatings on the scuffing load capacity is displayed in Figure 5.1. At 1500 rpm, the scuffing load capacity was increased 1 load stage using the C/Cr surface coating (CCR), at least 2 load stages using the MoS₂/Ti surface coating (MST) and at least by 3 load stages in the case of MoS₂/Ti coating with very low surface roughness (MST*). The transmitted power at which scuffing occurred increased 19 % for the CCR gear and at least 40 % for the MST and MST* gears. At 3000 rpm, the scuffing load capacity had an even larger increase due to the application of surface coatings. The scuffing load capacity increased 5 load stages for the gears CCR and MST, and at least 6 load stages for the low surface roughness coated gear MST*. At 3000 rpm the increase of transmitted power, at scuffing conditions, increased 190 %, which is an outstanding result.

5.2.1 Friction coefficient in scuffing conditions

The application of an energetic scuffing criterion [32,62] to the scuffing test results allowed the determination of a friction coefficient factor to include the influence of the surface coating on the friction coefficient at near scuffing conditions. The Dyson criterion [62] defined as the product of the friction coefficient (μ) by the normal force (F_n) and by the sliding speed (V_S), that is $FPI = \mu \cdot F_n \cdot V_S$, was slightly modified and instead of the normal force, it was considered the contact pressure (also mentioned by Dyson), resulting in a criterion that is the friction power intensity per unit of area, i.e. $FPI_M = FPI = \mu \cdot p_H \cdot V_S$.

This scuffing criterion postulates that scuffing occurs when a limit constant value of the friction power intensity is reached, that in this modified criterion will be when the friction power intensity per unit of area is reached:

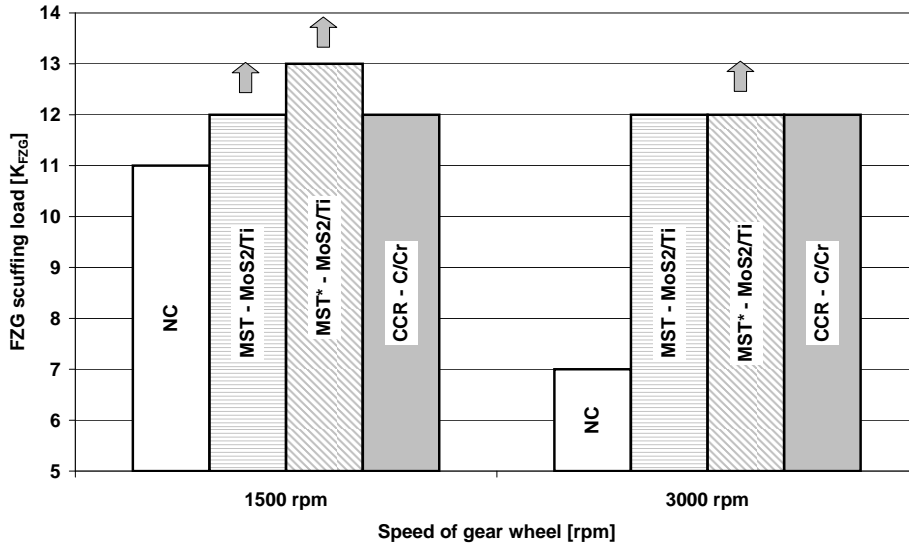


Figure 5.1: Scuffing load stage (or maximum load stage) of uncoated and surface coated gears on FZG scuffing tests with additive free ISO VG 100 lubricant.

$$\mu \cdot p_H \cdot V_S = C^{te} \quad (5.1)$$

On all the tested gears the scuffing failure occurred at the pinion root - wheel tip contact point, that corresponds to the maximum value of the product $\mu \cdot p_H \cdot V_S$.

The application of the scuffing criterion was performed using the friction coefficient formula proposed by Hohn et al. [44] presented in Eq. 3.2, where, beside the lubricant parameter (X_L) a material parameter (X_{SC}) was also included. The lubricant parameter has the value $X_L = 1$ for additive free lubricants, which was the case. The friction coefficient equation becomes:

$$\mu_M = 0.048 \cdot \left(\frac{F_{bt}/b}{v_{\Sigma c} \cdot \rho_c} \right)^{0.2} \cdot \eta_{oil}^{-0.05} \cdot Ra^{0.25} \cdot X_L \cdot X_{SC}, \quad (5.2)$$

being the X_{SC} parameter equal to 1 for an uncoated steel gear.

The application of this criterion is based on several assumptions:

- Surface coatings affect the friction coefficient between the gear teeth, and consequently also affect gear scuffing.
- The Limiting Gear Scuffing Constant ($\mu \cdot p_H \cdot V_S$) is a lubricant characteristic, independent of the surface coating used and independent of the coating type;
- The Limiting Gear Scuffing Constant ($\mu \cdot p_H \cdot V_S$) is a lubricant characteristic influenced by the gear operating speed.

To apply the scuffing criterion to the gear tests where scuffing failure did not occurred, it was assumed that the scuffing failure would occur in the following load stage. Thus, for the MST gear at 1500 rpm the scuffing load stage was $K_{FZG} = 13$ (this gear didn't scuff on load stage K12); for the MST* gear at 1500 rpm and at 3000 rpm the scuffing load stage was $K_{FZG} = 14$ (this gear didn't scuff on load stage K13).

The limiting gear scuffing constant for uncoated gears was then determined for both rotating speeds and the following values were determined: $C_{FPI}^{1500} = 0.415 \text{ GPa} \cdot \text{m} \cdot \text{s}^{-1}$ and $C_{FPI}^{3000} = 0.385 \text{ GPa} \cdot \text{m} \cdot \text{s}^{-1}$.

Knowing these two constants and applying the FPI criterion to the gear tests performed with coated gears, the X_{SC} parameters might be determined using Eq. 5.2 and Eq. 5.3. The X_{SC} determined take into account the type of coating, the roughness and the operating conditions at the scuffing stage.

$$\mu_M^{coated} \cdot p_H^{coated} \cdot V_S^{coated} = C_{FPI}^{1500} \quad (5.3a)$$

$$\mu_M^{coated} \cdot p_H^{coated} \cdot V_S^{coated} = C_{FPI}^{3000} \quad (5.3b)$$

At 1500 rpm the X_{SC} parameter had the values 0.89 and 0.79 for the C/Cr and MoS₂/Ti coated gears, respectively. At 3000 rpm the X_{SC} parameter had the value of 0.47 for both surface coatings.

These results show that the surface coating has a very important influence on the friction coefficient in near scuffing conditions and also that the influence of surface coatings increase with the increasing rotating speed.

Figure 5.2 displays the friction coefficient determined according to Eq. 5.2, using the X_{SC} parameter determined. the application of surface coating improved the friction coefficient between 8 % to 15 % at 1500 rpm and attained 21 % if MoS₂ was applied in a low roughness gears. At 3000 rpm the improvement promoted by the surface coatings in the friction coefficient was above 40 % and if MoS₂ was applied to a low roughness gear the improvement attain almost 50 %.

The scuffing tests performed showed that the surface coatings promoted a large increase on the scuffing load carrying capacity of the FZG type C gears. The simplified analysis of the friction coefficient between gear teeth in scuffing conditions showed also the huge influence that surface coatings promoted on the friction coefficient. The excellent finishing of the gear flanks had also a similar effect on the scuffing load capacity of gears.

5.3 Power loss

Paper A and **Paper G** present results of efficiency tests performed on a gearbox test rig using a transfer gearbox. This gearbox is used in a commercial diesel vehicle after the main gearbox, allowing it to have a lower gear ratio and also an auxiliary power output.

The efficiency tests were performed using three gearboxes, one with uncoated gears, another with MoS₂/Ti coated gears and a third with C/Cr coated gears. These tests were performed with a mineral based industrial gear oil, whose main properties are displayed in Table 6.1 with the reference M1 (see section 6.1.1). Further details are presented in **Paper A** and **Paper G**.

The results of the efficiency tests, presented in Figure 5.3, showed that the C/Cr surface coating promote a improvement in the gearbox efficiency of about 0.1 to 0.2 %, while the MoS₂/Ti surface coating promoted a gearbox efficiency improvement around 0.5 % in comparison to uncoated steel gears. The observation of tooth flanks

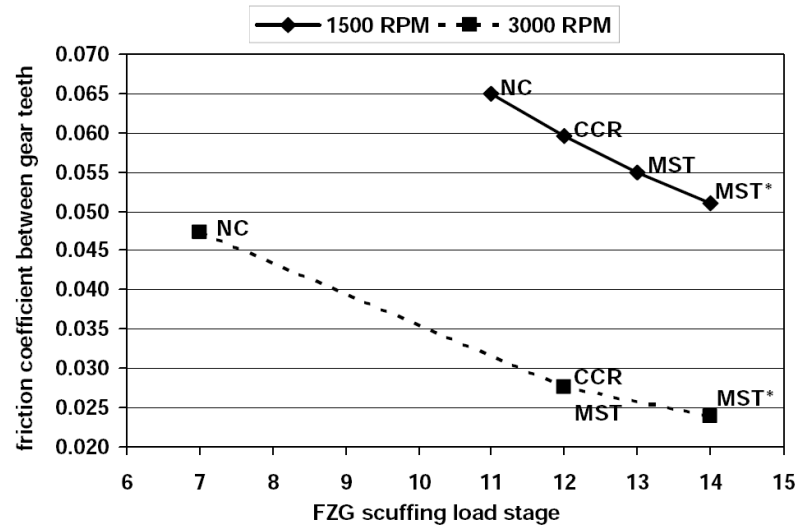


Figure 5.2: Friction coefficient between gear tooth, in scuffing conditions, at 1500 rpm and 3000 rpm.

also shows that the wear behaviour was better for the MoS₂/Ti surface coating than for the C/Cr surface coating.

These results combined with the scuffing results presented above (section 5.2) showed that the MoS₂/Ti surface coating has better properties for gear applications than C/Cr surface coatings. So further power loss tests were performed on the FZG test rig with MoS₂/Ti coated gears in order to evaluate its efficiency or power loss behaviour in a wider range of operating conditions and also to determine the influence of the coating on the friction coefficient.

Power loss tests were performed on the FZG test rig using MoS₂/Ti surface coated type C gears, being the tests performed according to the procedure presented in section 2.2. These results were presented in **Paper F**.

Two industrial gear lubricants were used, one was a non-toxic biodegradable ester based oil (E1 in Table 6.1) and the other was a mineral based oil (M1 in Table 6.1). Figure 5.4 shows the difference between the equilibrium oil bath temperature and the room temperature ($\Delta T = T_{oil} - T_{room}$) on the power loss tests for the uncoated gears and for the MoS₂/Ti coated gears, both lubricated with ester oil. The coated gear displays lower ΔT values than the uncoated steel gear, indicating that the surface coating promotes lower power losses. At 3000 rpm this tendency is not so clear.

Figure 5.5 also displays the comparison of ΔT between uncoated and MoS₂/Ti coated gears, but in this case using mineral lubricant. The MoS₂/Ti coated gear displays similar or slight smaller values of ΔT for the lowest input speed, although for an input speed of 2000 rpm and high torque the coated gear displayed larger values of ΔT . The coated gear test ended after load stage K9 at 2000 rpm because a spall was found in a teeth surface. So, the MoS₂/Ti surface coating doesn't display any power loss advantage over uncoated gears when mineral oil was used, although not all the tests of MoS₂/Ti coated gear were performed with mineral oil. In the test at 3000 rpm / 453 Nm the oil bath temperature reached the limit value of 180 °C after 133 minutes of test and was stopped.

The total mass loss (pinion plus wheel) for the four power loss tests performed is

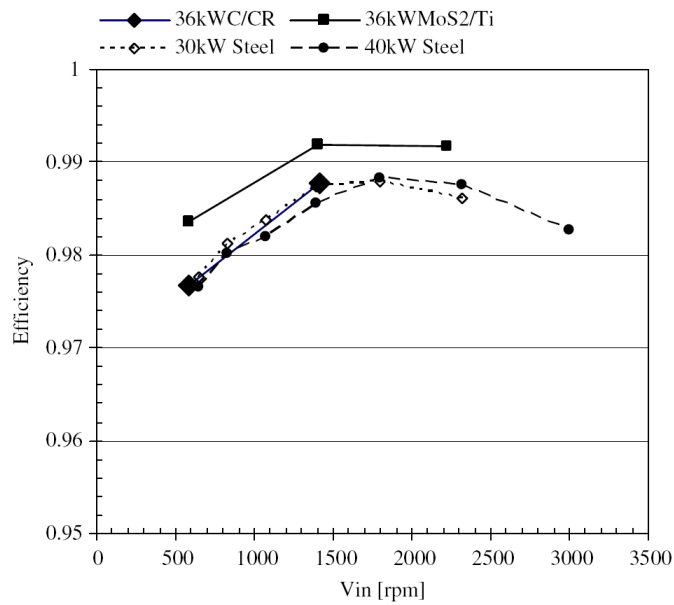


Figure 5.3: Efficiency of transfer gearbox with uncoated, C/Cr and MoS₂/Ti coated gears.

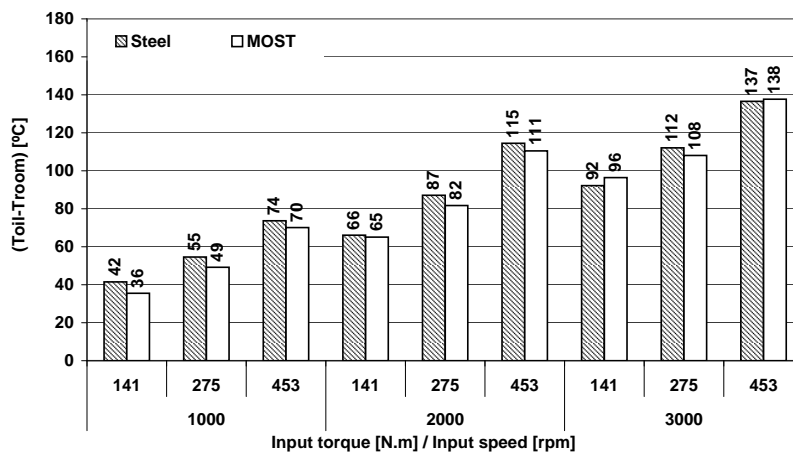


Figure 5.4: Equilibrium temperature (ΔT) on power loss tests of uncoated and MoS₂/Ti coated gears lubricated with ester lubricant in FZG test rig.

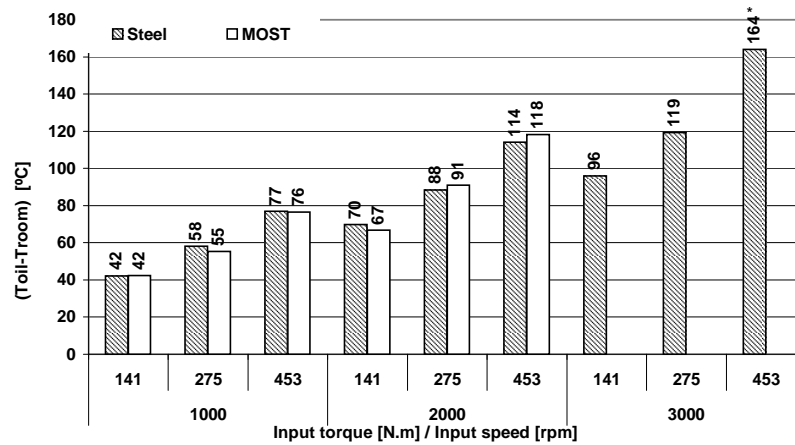


Figure 5.5: Equilibrium temperature (ΔT) on power loss tests of uncoated and MoS₂/Ti coated gears lubricated with mineral oil. * - test reached the limit temperature after 133 minutes and was stopped.

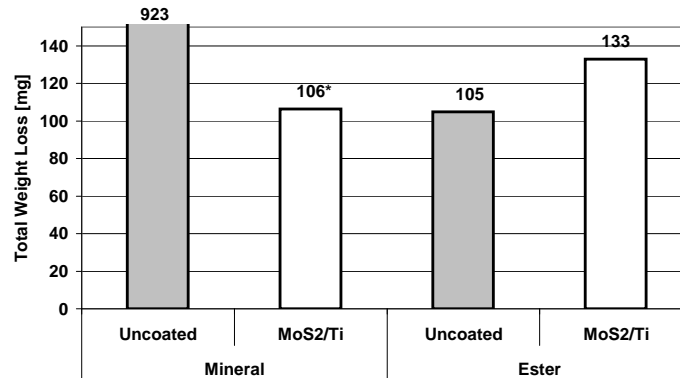


Figure 5.6: Total weigh loss after the power loss tests. * - not performed the tests at 3000 rpm.

displayed in Figure 5.6. The mass loss of power loss tests lubricated with mineral lubricant was quite high, specially for the uncoated gear where a scuffing failure was noticed, due to the very high temperature of the last load stage (3000 rpm / 453 Nm). The MoS₂/Ti coated gear lubricated with mineral lubricant did not perform part of the power loss test (the tests at 3000 rpm), despite displaying a weight similar to the obtained with ester lubricant. In the power loss tests performed with ester lubricant, the uncoated gear displayed $\simeq 20\%$ lower mass loss than the MoS₂/Ti coated gear.

5.3.1 Friction coefficient

The influence of MoS₂/Ti surface coating combined with the two lubricants tested was assessed, using the results obtained in the power loss tests in combination with the energetic model of the FZG gearbox presented in section 3.3. The energetic model of the gearbox allowed the determination of a friction correction factor by optimisation of the numerical and the experimental results presented above. The influence of the surface coating on the friction coefficient was reflected on the load, thus the X_L parameter was only dependent of load, as represented in Eq. 3.3, $X_L = 1/(F_{bt}/b)^{b1}$.

	Ester	Mineral
Carburized steel	0.076	0.055
MoS ₂ /Ti	0.084	0.047
ADI	0.037	0.016

Table 5.1: Lubricant factor exponent b_1 for uncoated, ADI and MoS₂/Ti coated gears lubricated with both mineral and ester lubricant ($n_{wheel} \leq 2000$ rpm and $T_{wheel} \leq 275$ Nm).

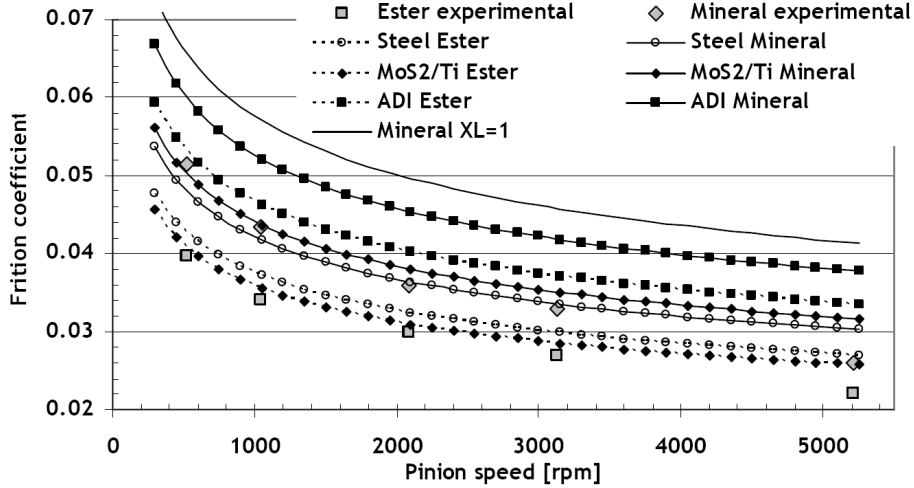


Figure 5.7: Friction coefficient measurements (Hohn et al.) and numerical results considering the XL parameters mentioned in Table 5.1 ($T_{oil}=90$ °C , $p_H=1.1$ GPa).

This correction factor will include the effect of the lubricant added to the effect of the surface coating. The determined values for the b_1 exponent are displayed in Table 5.1. The larger the value of the exponent b_1 the larger is the decrease of friction coefficient promoted by the combination material/lubricant. The correction factor was also obtained for carburized gears.

The results of power loss tests performed at 3000 rpm were not included in the input of the energetic balance of the gearbox, neither the tests at 453 Nm, because this speed was not tested on the power loss test of MoS₂/Ti coated gear lubricated with mineral lubricant and the highest torque was not performed in ADI test (see **Paper F**).

Table 5.1 shows that the MoS₂/Ti coated gear lubricated with ester oil displays lower friction coefficient than the uncoated gear, while the opposite happens when mineral oil was used, as expected from equilibrium temperatures represented in Figure 5.4 and Figure 5.5.

The determined friction coefficients were also in agreement with the experimental measurements of the friction coefficient performed by Hohn et al. [43] with carburized gears, as represented in Figure 5.7. Figure 5.8 represents the friction coefficient determined numerically is plotted against the FZG load stage (proportional to the load parameter F_{bt}/b), for the lubricant / material / surface coating tested.

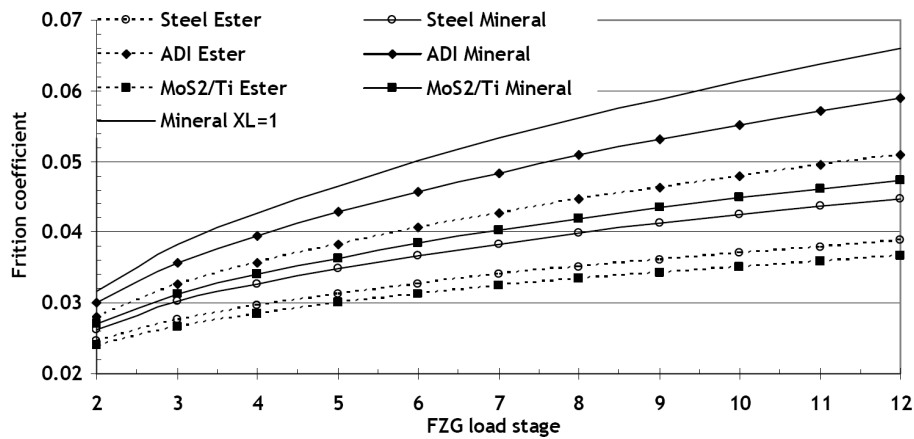


Figure 5.8: Numerical results for the friction coefficient considering the XL parameters mentioned in Table 5.1 (Toil=90 °C , pinion speed = 2000 rpm).

5.4 Discussion

Both the C/Cr and MoS₂/Ti surface coatings proved to have an excellent adhesion to the surface even at high contact pressures and high sliding speeds, very high hardness, exhibiting also very low friction coefficient in tests like pin-on-disk and reciprocating wear tests.

The MoS₂/Ti and C/Cr surface coatings provided a very significant increase of the scuffing load capacity of FZG type C gears, mainly at high speeds. In the case of MoS₂/Ti coating, this higher scuffing load capacity was even increased using super-finished tooth flanks with a surface roughness of Ra = 0.3 μm. The analysis of gear scuffing results, using the modified FPI scuffing criterion ($\mu \cdot p_H \cdot V_S = cte$), showed that surface coatings reduced the friction coefficient between gear teeth between 8 % and 41 %, in near scuffing conditions, depending on the operating speed and coating type.

The coated gears improved the efficiency of a gearbox, particularly at low speed / high torque conditions when the friction power losses between gear teeth were more important. MoS₂/Ti coated gears increased the transfer gearbox's efficiency by 0.5 % and the C/Cr coated gears improved the efficiency by 0.1 to 0.2 %.

The power loss tests performed in the FZG test rig showed that the MoS₂/Ti surface coating promoted lower friction coefficient than uncoated steel gears, although only if lubricated with ester oil. When mineral oil was used, no improvement was detected. In the FZG gear power loss test the MoS₂/Ti coated gear displayed higher mass loss than the uncoated gear.

The properties exhibited both by the MoS₂/Ti and C/Cr coatings are of great interest, particularly in severe applications involving high contact pressures and high sliding, with frequent start-up or inefficient lubrication.

6 Influence of lubricants in gears behaviour

6.1 Introduction

This chapter presents the systematic evaluation of the influence of biodegradable lubricants on the tribological properties of gears, mainly in what concerns to scuffing, micropitting protection and power loss behaviour.

6.1.1 Lubricants properties

Three industrial gear lubricants were tested and compared: a reference ISO VG 150 mineral oil, containing an additive package to improve micropitting resistance, and two ISO VG 100 ester lubricants based on harvestable materials, both being biodegradable and containing a low toxicity additivation. The three oils were formulated as CLP gear oils according to DIN 51517, and their main properties are represented in Table 6.1.

The reference gear lubricant is based on a paraffinic mineral oil with significant residual sulphur content. It contains an ashless antiwear additive package based on phosphorous and sulphur chemistry and metal-organic corrosion preventives. The additive content of this lubricant is considerably higher than the one of the ester based lubricants. In contrast, the other two fluids use an ester base, being one fully saturated (E1), and other highly saturated (E2). The absence of unsaturated bonds in these base fluids leads to excellent thermal and oxidative stability. To combine the desired low toxicity with superior gear performance, environmentally compatible, highly efficient additives were added to the ester lubricants and in the case of E1 lubricant metal-organic compounds had been completely avoided.

The three lubricants have similar viscosity's around 100 °C , although the ester lubricants have a considerably higher viscosity index and on the other side have a considerably lower piezoviscosity parameter [63]. Those two physical properties have similar contributions on the film formation, a higher viscosity increases film thickness and a higher piezoviscosity will also increase the film thickness.

Standardised and internationally recognised test methods are available for determining the biodegradability (OECD 301B) and environmental toxicity (OECD 201, OECD 202) of lubricants and their components. The mineral oil did not match the minimum requirements of 60% biodegradability in 28 days, while the ester based oils exceeded the minimum requirements of 60% biodegradability in 28 days (according to OECD 301B). All the three lubricants passed OECD 201 and OECD 202 toxicity tests, as represented in Table 6.1.

Parameter	Method	Desig.	Units	Lubricating Oils		
				Paraffinic mineral oil	Fully saturated ester	Highly saturated ester
Base oil	DIN 51451			M1	E1	E2
Oil reference						
Chemical Content						
Zinc	ASTM D 4927	Zn	ppm	-	-	-
Calcium	ASTM D-4927	Ca	ppm	40	-	-
Phosphorus	ASTM D-4927	P	ppm	175	146	300
Sulphur	ASTM D-4927	S	ppm	15040	180	5500
Physical properties						
Density @ 15 °C	DIN 51757	ρ_{15}	g/cm ³	0.894	0.928	0.962
Kinematic Viscosity						
40 °C	DIN 51562	ν_{40}	cSt	153.6	98.4	116.6
100 °C	DIN 51562	ν_{100}	cSt	14.4	13.3	16.9
Viscosity Index	ISO 2909	VI		96	152	162
Pour point	ISO 3106		°C	-27	-42	<-30
Piezoviscosity [63]	$\alpha(p, T) = (a_1 + a_2 * T + (b_1 + b_2 * T) * p)^{-1}$					
		a1	bar	367	477	
		a2	bar/°C	2.96	6.18	
		b1		9.98x10-3	3.93x10-3	
		b2	1/°C	2.07x10-4	-4.01x10-4	
Wear properties						
KVA						
weld load	DIN 51350-2		N	2200	2200	-
wear scar (1h/300N)	DIN 51350-3		mm	0.32	0.35	-
Brugger	DIN 51347-2		N/mm ²	68	37	-
FZG rating	DIN 51354	K_{FZG}		>12	>12	>12
Biodegradability and toxicity properties						
Biodegradability	OECD, 301 F		%	<60	≥60	≥60
Aquatic toxicity						
Daphnia	OECD, 202	EL₅₀	mg/l	>1000	>100	>100
Algae	OECD, 201	EL₅₀	mg/l	>100	>100	>100

Table 6.1: Main properties of the tested lubricants.

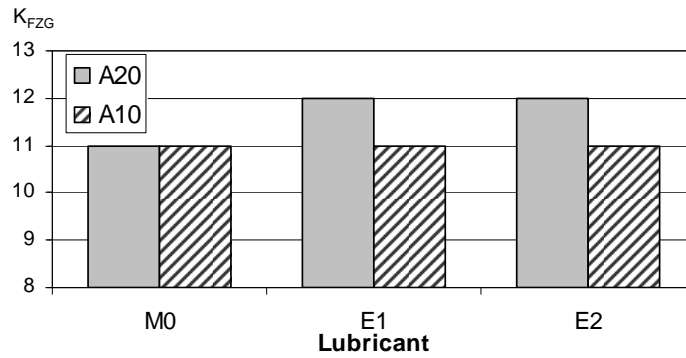


Figure 6.1: Scuffing load stage.

6.2 Scuffing

This section shows the results of the gear scuffing tests performed with the lubricants just presented. Such results are presented in detail in **Paper H** [64].

The load carrying capacity of gears against scuffing was evaluated using the FZG gear test rig, which is a well known back-to-back spur gear test rig with power circulation (please see section 2.2).

The test gears used in these scuffing tests were FZG type A gears, although they have a lower manufacturing accuracy grade than the proposed in standard DIN ISO 14635-1 [26]. The gears were manufactured in standard carburizing steel (DIN 20 MnCr 5).

Two test procedures were performed, A20/16.6/90 and A10/16.6/90 (see section 2.2 for further details), being both performed at 3000 rpm (16.6 m/s). Those tests were more severe than the standard scuffing test A20/8.3/90 (according to ISO14635-1 [26]) because the speed is twice larger, once it was expected that those lubricants had high load carrying capacity. The A10/16.6/90 test was even more severe once it is performed with 10 mm wide gears, increasing the contact pressure in 41.4 %.

The scuffing load stages for A20/16.6/90 and A10/16.6/90 tests are presented in Figure 6.1. In the tests A20/16.6/90 the ester oils reached scuffing failure during load stage K12 ($p_H = 2.0GPa$), one load stage more than the mineral oil that reached scuffing failure on load stage K11 ($p_H = 1.8GPa$). On the test A10/16.6/90 all the oils reached scuffing failure on load stage K11 ($p_H = 2.5GPa$).

Both ester oils had the same load carrying capacity on A20 and A10 tests, although the scuffing failure took place at considerably different oil temperatures. Table 6.2 displays the maximum oil bath temperature on the load stage where scuffing occurred. The E1 lubricant displayed the higher oil bath temperature at scuffing conditions in both A20 and A10 tests.

Table 6.2 also shows the mass loss after the scuffing test, as well as the calculated viscosity of the lubricants at the maximum temperature registered during the scuffing load stage.

In scuffing conditions both the mass loss and the maximum temperature must be compared carefully because the scuffing failure implies metal to metal contact and the gears could operate during a variable time after the scuffing failure took place until the FZG test rig stops due to high vibrations detection or up to the end of the

Test type Lubricant	A20/16.6/90			A10/16.6/90		
	M1	E1	E2	M1	E1	E2
k_{FZG}	11*	12	12	11	11	11
Weight Loss [mg]	414*	81	1 888	1049	181	75
Max. Oil Temperature [°C]	155,5	174,7	156,4	144,3	164,2	131,7
Contact pressure at scuffing [GPa]	1,80	1,96	1,96	2,54	2,54	2,54
Oil viscosity at scuffing [cSt]	4,50	4,16	6,12	5,41	4,76	9,03

Table 6.2: Resume of scuffing tests results (* - load stage K12 performed after scuffing)

stage time. Anyway the higher the mass loss and the higher the surface roughness the higher will be the severity of the scuffing failure.

The evolution of maximum temperature measured during the load stages of test A20/16.6/90 show that E2 oil displays higher maximum temperatures up to load stage K10 (reaching 156 °C), probably due to the highest viscosity and also to the highest specific weight. Although, oil E2 displays the smaller maximum temperature on the next two stages and besides it remains constant from load stage K10 up to load stage K12, being probably due to some chemical reaction at those temperatures.

The maximum temperatures for each load stage on test A10/16.6/90 were smaller than on the test A20/16.6/90, fact due to the smaller width of the teeth that implies a smaller churning power loss. The difference between lubricants maximum temperature up to load stage k9 was smaller on A10/16.6/90 test than on A20/16.6/90, presenting from that stage on the same relative position than on A20 test with E1 oil exhibiting the highest temperature followed by M1 oil.

6.2.1 Critical lubricant temperature scuffing criterion

The use of a scuffing criterion allows the prediction of scuffing failure if a lubricant is used at specified operating conditions. Figure 6.2 displays schematically the type A gear and the evolution of sliding speed and normal force along pinion tooth.

Castro et al. [65] proposed a scuffing criterion for FZG gears, based on the concept of *Critical Lubricant Temperature* (T_{CR}) that is the maximum oil bath temperature for which a scuffing failure can occur, whatever the load and the speed. The criterion establishes:

$$T_{CR} - T_0 \leq \frac{\mu \cdot P_0 \cdot V_S \cdot T}{C} \quad (6.1)$$

In Eq. 6.1 T_0 represents the oil bath temperature, C is a constant dependent of oil type and gear material, P_0 is the contact pressure, V_S is the sliding speed and T is the distance from the contact point considered to the pitch point on the meshing line.

The most severe contact conditions between type A gears occur at the pinion tip / wheel root contact point (B), once at that point the sliding speed is maximum and the distance to the pitch point (I) is also maximum. The scuffing failures always took place at this point for type A gears.

The right side of Eq. 6.1 was determined in scuffing conditions and plotted versus of the oil bath temperature for the two scuffing tests performed (A20 and A10) with

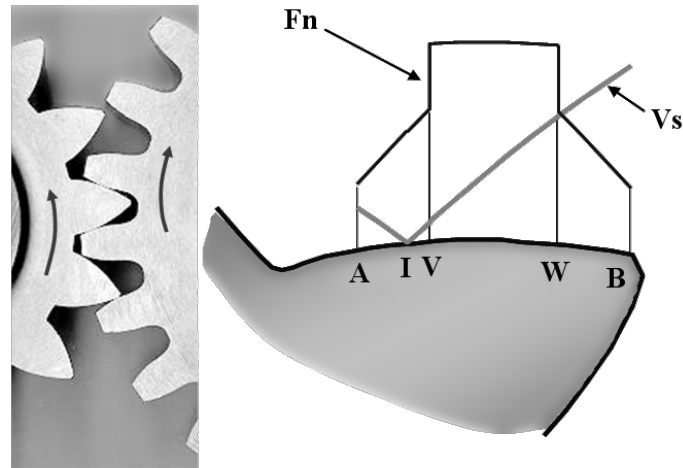


Figure 6.2: FZG type A gear geometry, reference points (A, I, V, W, B), normal force (F_n) and sliding speed (V_s) along pinion tooth.

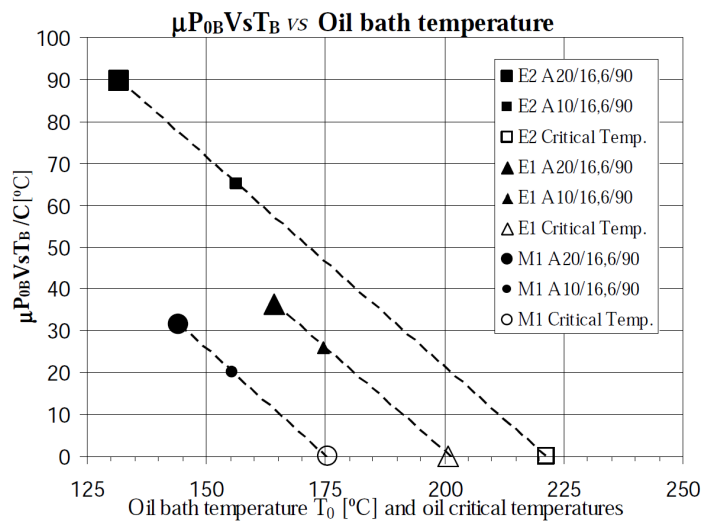


Figure 6.3: Representation of scuffing criteria as function of oil bath temperature for pinion tip - wheel root contact point.

each lubricant, then the critical scuffing temperature could be directly assessed as the interception of the line that connects the two points of each lubricant with the xx axis, as represented in Figure 6.3.

The critical lubricant temperature for each lubricant is displayed in Table 6.3, and as expected, the lubricant with the lowest critical temperature was the M1 oil (176 $^\circ C$) and the one with the highest was the E2 (221 $^\circ C$).

6.3 Micropitting

This section will present the influence of the lubricants in gear micropitting. This results were reported in **Paper B** [66].

The micropitting tests were performed in the FZG gear test rig, (please see section 2.2), using type C gears (see section 2.2.4). Two lubricants were tested, a mineral

Lubricant	M1	E1	E2
TCR [°C]	176	201	221

Table 6.3: Critical lubricant temperatures (TCR) determined for each lubricant.

	Test reference	Lubricant	Ra
Standard gear	-	-	0.5 μm
20MnCr5	CM	M1	1.0 μm
carburized	CE	E1	1.1 μm

Table 6.4: Test reference, lubricant and surface roughness of gear micropitting tests.

based oil M1 and a biodegradable ester E1, being both described in section 6.1.1.

The test procedure used is based on the DGMK-FZG micropitting short procedure test [30] and in the FVA-FZG micropitting test [29] and is described in section 2.2.4. In these micropitting tests the last load stage was repeated with the objective of more clearly distinguish both lubricants.

The test reference of each micropitting test is displayed in Table 6.4, as well as the lubricant used and the initial surface roughness (after manufacturing) of the tooth flanks. According to ISO 1328, the quality grade of the test gears used (grade 9) was inferior to that specified by the standard procedures (grade 5), and this lower quality was also reflected in the higher surface roughness of the teeth flanks, as shown in Table 6.4.

The pinion performs 1.5 times more cycles than the wheel, thus it is prone to micropitting failure and the post test analysis are focused on it, except the mass loss and the oil analysis that are referred to both pinion and wheel. The micropitting evaluation was performed by the mass loss of the gear, by visual inspection, by surface roughness measurements and by oil analysis.

6.3.1 Visual inspection

The in situ assessment of micropitting by visual inspection is a very difficult task [35]. The visual assessment needs high intensity light to distinguish the grey stained areas that micropitting resembles. To overcome this difficulty the gears were dismantled after each load stage for photography. Table 6.4 shows photographs of pinion tooth flanks after each load stage. To allow an easier reading of micropitting area, it was surrounded by a red line.

As represented in Figure 6.4 the micropitting appears on load stage K7 in both tests, being the affected area similar. On load stage K9 the micropitting area increased significantly, doubling the area measured in load stage K7. The repetition of load stage K9 didn't increased in a substantial form the micropitting area, although it become wider. The micropitting area of the gear lubricated with ester oil is slightly larger than in the gear lubricated with mineral lubricant.

Above the pitch line smooth wear is observed, once the grinding marks start to disappear. After the repetition of the load stage K9, some adhesion marks in the radial direction appeared.

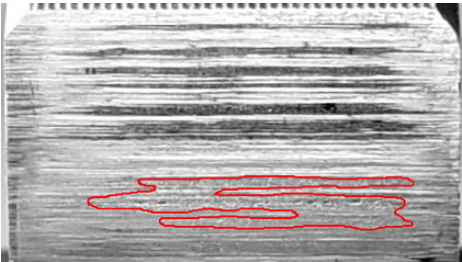
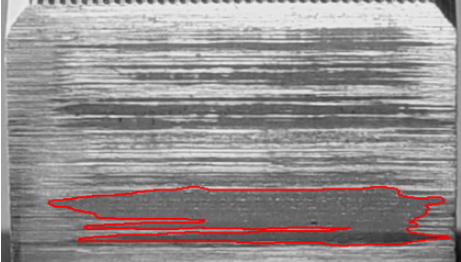
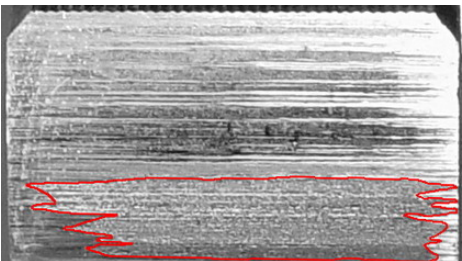
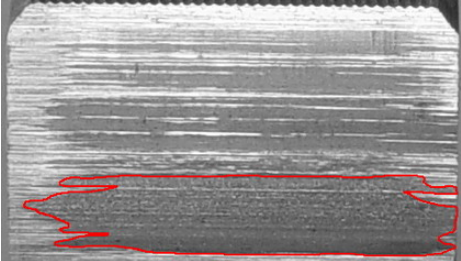
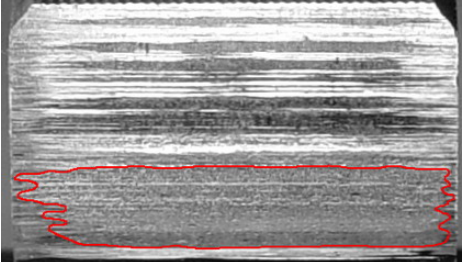
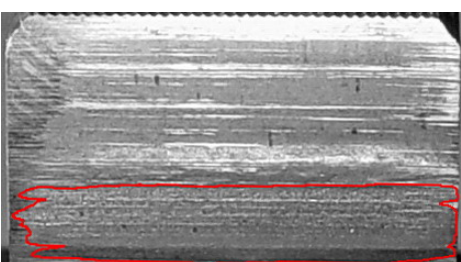
Stage	CM	CE
K7		
	Micropitting area=10%	Micropitting area=13%
K9-1		
	Micropitting area=24%	Micropitting area=26%
K9-2		
	Micropitting area=28%	Micropitting area=28%

Figure 6.4: Pictures of pinion teeth flanks and micropitting area.

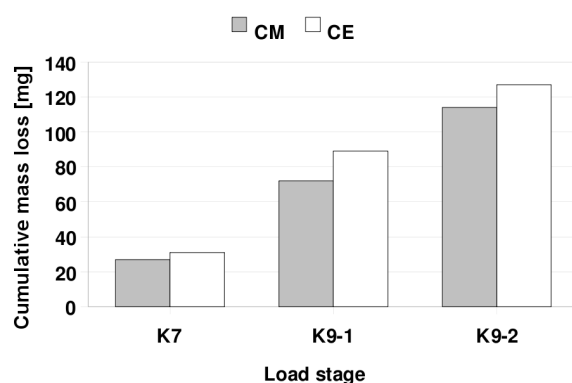


Figure 6.5: Mass loss during micropitting tests for M1 and E1 lubricants.

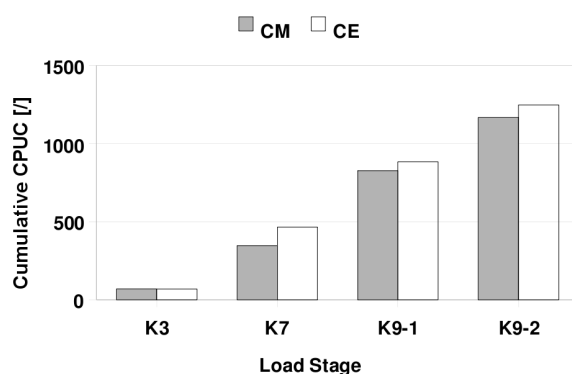


Figure 6.6: CPUC wear index during micropitting tests.

6.3.2 Mass loss and oil analysis

Figure 6.5 displays the cumulative gear mass loss during the micropitting test. The mass loss was slightly larger on the gear lubricated with ester oil, although the difference decreased after the repetition of load stage K9.

The ferrometry measurements of the lubricant samples indicate that the ester lubricant promotes larger wear than the mineral oil, as shown in Figure 6.6, in accordance with the mass loss measurements. Although the largest difference between the two lubricants is observed after load stage K7, becoming smaller from then on. The ester oil wear particles generation remains almost constant from load stage k7 onwards, even after the load stage K9 repetition, while with mineral lubricant the wear particles generation exhibits a progressive increase, this difference is probably due to the additive package, in particular to the high sulphur content of the mineral lubricant that promotes the formation of a protective layer of the surface being more effective in the first stages.

The analytical ferrography performed to the oil samples collected during the micropitting tests showed similar evolution along the load stages for both lubricants (the ferrograms are displayed in **Paper B**).

After the first load stage (K3) both ferrograms showed large wear particles typical of the running-in process. After the load stage K7 the total number of particles increased substantially, although the number of large particles did not. However from load stage K7 onwards the typical micropitting wear particles, small, thin and

		CM		CE	
		Rmax [μm]	Rz-D [μm]	Rmax [μm]	Rz-D [μm]
	new	5.8	4.9	6.6	5.4
below	K7	12.3	7.1	7.7	4.8
pitch	K9-1	8.2	5.5	7.3	4.2
line	K9-2	7.9	5.5	5.4	3.7
above	K7	5.9	3.4	4.1	2.9
pitch	K9-1	4.7	3.2	4.3	2.8
line	K9-2	4.3	2.8	4.5	2.9

Table 6.5: Roughness parameters in gear micropitting tests

with straight borders appeared in large number. After load stage K9 the ferrograms showed a global increase in the size of the wear particles, specially the micropitting fatigue particles.

6.3.3 Surface roughness and surface analysis

At the end of each load stage surface roughness measurements were performed in order to evaluate the roughness evolution, both below and above the pitch line. The roughness profiles obtained below the pitch line are characteristic of the micropitting zone, while the roughness profiles obtained above the pitch line are characteristic of the wear zone, once the micropitting failure appears mainly below the pitch line.

The surface roughness measurements were performed in the radial direction in several tooth flanks, below and above the pitch line and in different locations. An assessment length of 1.5 mm and a cut-off of 0.25 μm were used. Table 6.5 displays the Rmax and R_{z-D} roughness parameters for the two tested gears (CM and CE) and for the two measured areas, below and above the micropitting area. In both CM and CE tests, the roughness measurements above the pitch line didn't show any evidence of micropitting cavities, as shown in Table 6.5, once the Rmax values are all smaller than 6 μm .

The roughness parameters measured for CE pinion presented smaller values than the measured for CM pinion, both above and below the pitch line. Indicating a faster running-in and also a higher wear, also confirmed by the mass loss measurements. Below the pitch line, the Rmax parameter reached 12 μm for CM pinion, while the CE pinion presented a maximum Rmax value of 7.7 μm . The maximum value of Rmax was attained after load stage K7 for both tests, decreasing in the subsequent stages also for both tests.

Figure 6.7 displays the R_K roughness parameters of the measurements performed below the pitch line. In the micropitting test performed with mineral lubricant (CM) the R_{VK} parameter after the first stage (K7) was considerably larger than the measured for CE test, indicating a larger depth of the micropitting cavities. The same effect was observed on the other two load stages performed. The decrease of the sum of the three R_K parameters (R_{PK} , R_K and R_{VK}) with the progression of the micropitting test was due to the wear of the surface. This effect is more intense on the gear lubricated with ester oil.

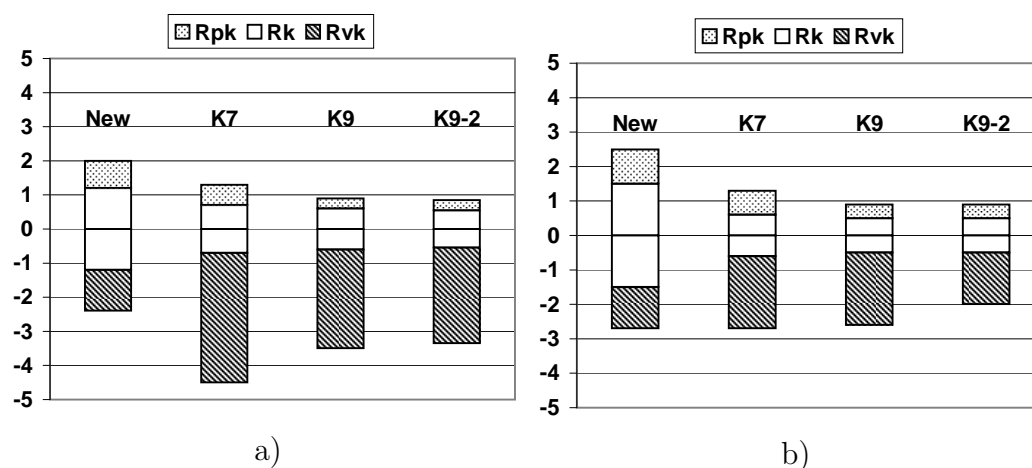


Figure 6.7: Rpk, Rk and Rvk roughness parameters [μm] of the measurements performed below the pitch line during: a) CM micropitting test; b) CE micropitting test.

The topography is a very useful method that guarantee a very accurate image of the surface, allowing a visual observation and measurement of the micropits and after some numerical treatment, also allows the determination of the percentage area affected by micropitting. The only inconvenient is that it is a high time consuming method.

As an example, Figure 6.8 displays in detail a micropitting cavity observed in the topography of CM pinion, whose dimensions are: width= $100 \mu\text{m}$, large: $40 \mu\text{m}$ and depth= $15 \mu\text{m}$.

Figure 6.9 displays two topographies performed to both CM and CE pinion, in Figure 6.9a and in Figure 6.9c, respectively. Figure 6.9 also shows the analysis of those topographies in order to measure their micropitting area, being represented in Figure 6.9b and in Figure 6.9d the micropits with deeper larger than $6 \mu\text{m}$ for CM and CE pinions, respectively. The CM pinion micropitting area was higher (1.5 %) than CE micropitting area (0.7 %), besides the micropitting cavities are more widespread on the surface and the micropits were deeper on the CM topography.

6.4 Power losses

This section presents a comparative study about the energetic efficiency of a mineral lubricant (M1) and a biodegradable ester (E1). This work was reported in **Paper C** [39].

The tests were performed in the FZG test rig using type C gears. The power loss tests procedure was described in section 2.2.6.

Basically, each lubricant is submitted to a set of gear power loss tests performed at a wide range of speed and torque. Each pair of speed-torque operating conditions is run with the oil temperature set free until the oil temperature stabilizes. The oil bath equilibrium temperature occurs when the sum of the power losses inside the FZG gearbox is equal to the sum of the heat evacuation from the gearbox [39, 41, 42, 44–47, 50, 67]. This test method allow a direct comparison of lubricants, since the room temperatures and the operating conditions were similar, the lubricant that

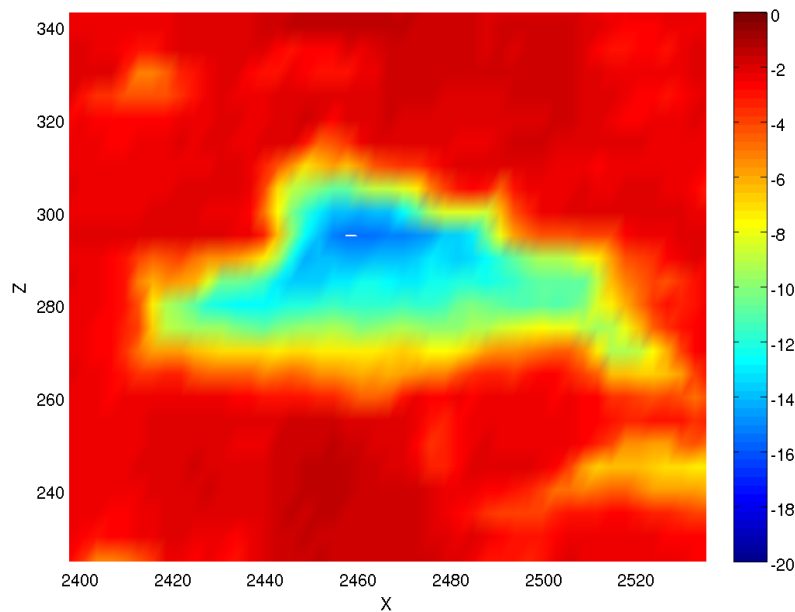


Figure 6.8: Magnification of a micropit observed in the topography of CM pinion. All units in μm .

displays the lower equilibrium temperature will be the one with lower power losses. Among the load stages, some are performed at very low torque in order to evaluate the churning losses. Besides the thermal behaviour, the wear behaviour and the lubricants degradation were also analysed.

The experimental results of the power loss test were correlated with the numerical model of the energetic balance of the FZG gearbox presented in section 3.3. This correlation allows the optimisation of the friction coefficient formula for each lubricant tested based on the experimental results. So, one of the most important results is to have an expression for the friction coefficient that was optimised as function of the lubricant real behaviour in power loss tests.

Using the optimised friction coefficient formula for each lubricant a prediction of the lubricant behaviour was performed for different operating conditions and compared with experimental power loss test results that were reported in **Paper I** [42].

6.4.1 Equilibrium oil bath temperature

Figure 6.10 displays an example of the evolution of oil bath temperature of mineral (M1) and ester (E1) oils during the power loss tests performed at 3000 rpm. This figure shows that the ester oil has a smaller increase rate of temperature along test time, as well as a smaller equilibrium temperature.

The equilibrium temperature of each test was recorded and is shown in Figure 6.11 for all the power loss tests performed, in function of the input speed and torque for both oils. These results were published in **Paper C**.

For the no load (5 Nm) operating conditions, the ester biodegradable lubricants displayed smaller equilibrium temperatures up to the test at 3000 rpm, on which the mineral lubricant displayed a smaller equilibrium temperature. These differences are explained by the viscosity of the lubricants, once the mineral lubricant has higher

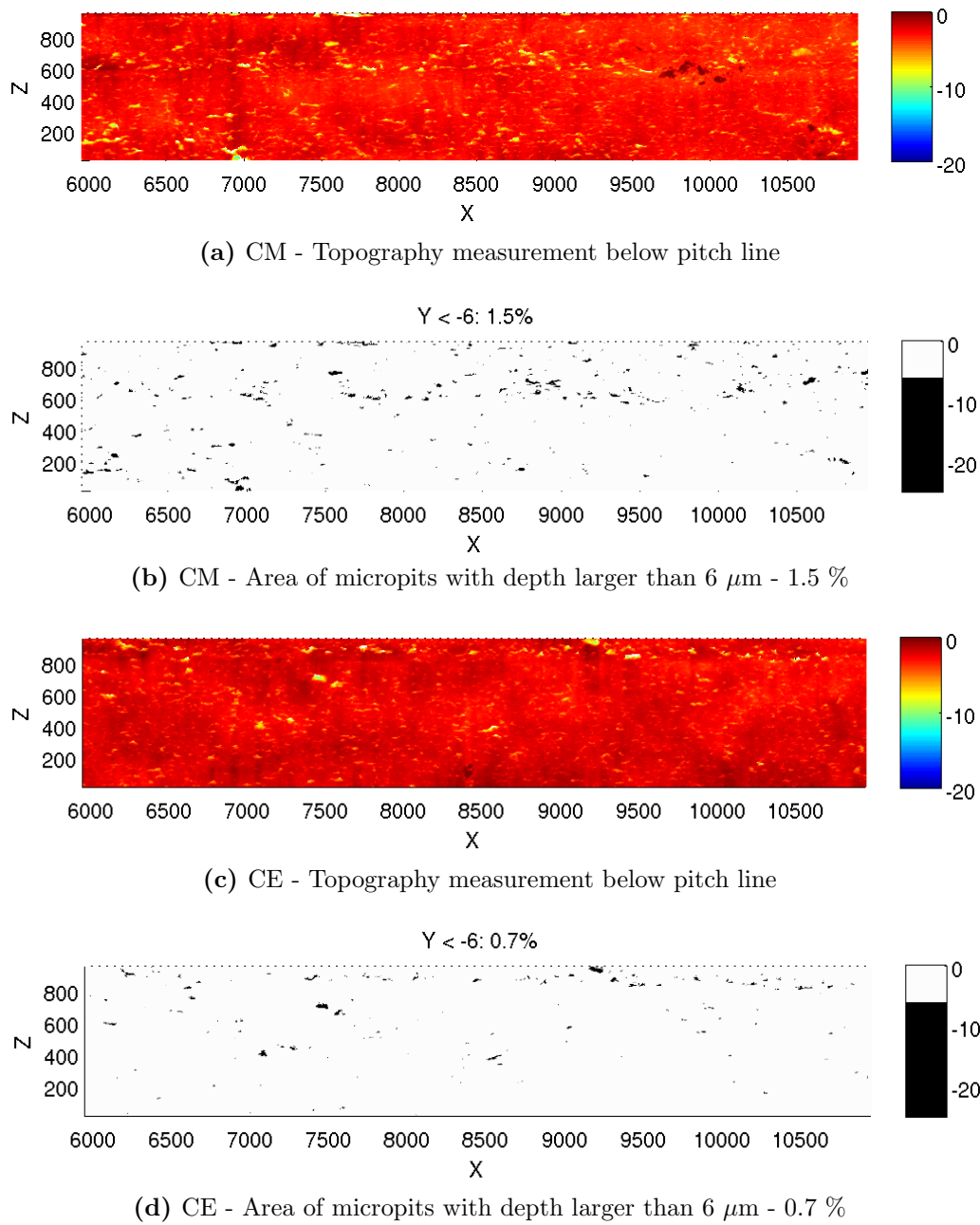


Figure 6.9: Topography after CM and CE micropitting tests performed below the pitch line of a pinion tooth and analysis of the micropitting area with depth larger than $6 \mu\text{m}$ (at black). All units in μm .

viscosity at lower temperatures, as represented in Figure 6.12, but for a temperature near 80 °C all lubricants have similar viscosity. So, the higher stabilisation temperature of the ester lubricants at 3000 rpm, that is around 80 °C, is explained due to the higher density of the ester oils that increased the oil churning losses. Above 100°C the mineral oil has lower viscosity than the ester lubricants, as represented in Figure 6.12, thus generates lower churning losses.

For higher input torque the mineral oil always displayed higher equilibrium temperature than the ester oil. The difference in equilibrium temperature between the two oils ranges from 2 to 15 °C, and the maximum difference was observed in load stage k9 (wheel torque of 453 Nm), where the mineral oil (M1) reached the maximum temperature of 180 °C after 112 minutes while the ester oil (E1) only reached an oil bath temperature of 156 °C after 240 minutes (see Figure 6.10).

These results indicate that the friction losses promoted by the ester oils are smaller than those generated by the mineral lubricant and are responsible for the lowest equilibrium temperatures observed. The increasing difference in equilibrium temperature between ester and mineral oil with the increasing torque suggests that the ester oil friction losses are less dependent of load than the mineral oil.

6.4.2 Wear behaviour and oil degradation

During each power loss test three samples of lubricant were collected for Direct Reading Ferrometry (DRIII) to evaluate the wear behaviour of the lubricants. Section 2.4.3 describes the DRIII procedure and analysis. The samples were collected after the tests at 1000, 2000 and 3000 rpm, as represented in Table 2.5. The last sample collected was used for DRIII analysis and also for viscosity measurement, thus allowing to know the viscosity variation after the 42 hours of the power loss test. An elemental analysis by RFA [68] was also performed before and after the power loss test, to know the amount of Iron present in the oil samples.

Figure 6.13 displays the evolution of CPUC and ISUC wear indexes during the power loss tests for both oils. The figure shows that the ester oil presents smaller values of both CPUC and ISUC indexes, specially after first oil sample (collected after the no-load tests), indicating that the ester oil generated less wear particles and of smaller size.

Table 6.6 represents the viscosity [69] measurements at 40 °C and 100 °C, the viscosity index and the Iron content [68] for M1 and E1 oils, in a fresh oil sample and in a sample after the power loss test (i.e. after 42 hours of service). The lubricants didn't present any sign of degradation by oxidation, once the viscosity modification was very small. The Iron content measured by RFA confirms the ferrometry results indicating a much larger value for the oil sample of mineral lubricant (M1).

6.4.3 Optimized friction coefficient between gear tooth

The experimental results presented in the last paragraph were used together with the energetic model of the FZG gearbox presented in section 3.3. Such combination allows among other things the optimization of the friction coefficient formula for each lubricant based on the experimental results. Such optimization consist in finding a lubricant factor X_L that modifies the original friction coefficient formula proposed by

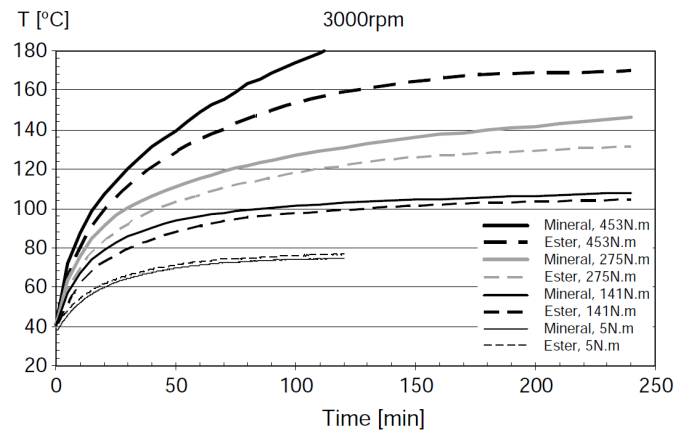


Figure 6.10: Oil bath temperature evolution for M1 and E1 oils at 3000 rpm for the 4 load conditions tested.

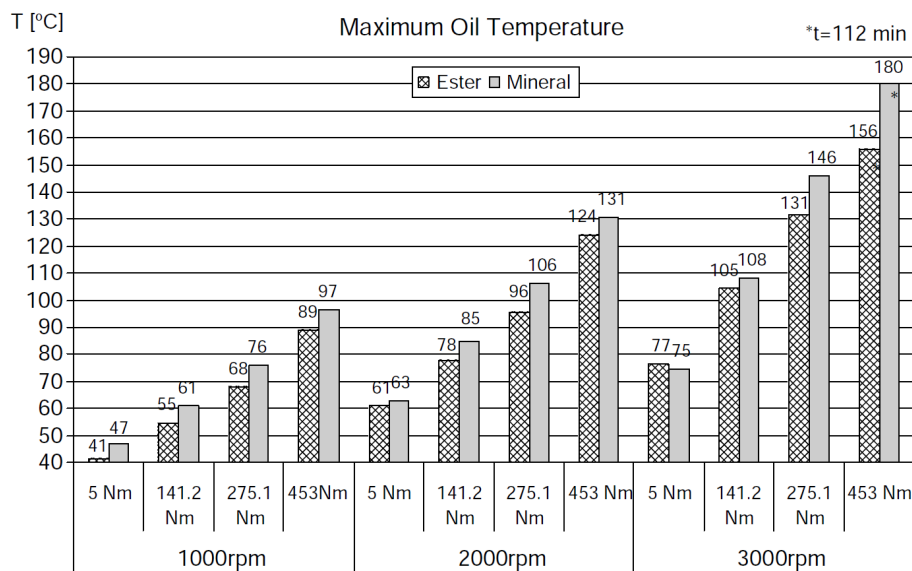


Figure 6.11: Oil bath equilibrium temperature.

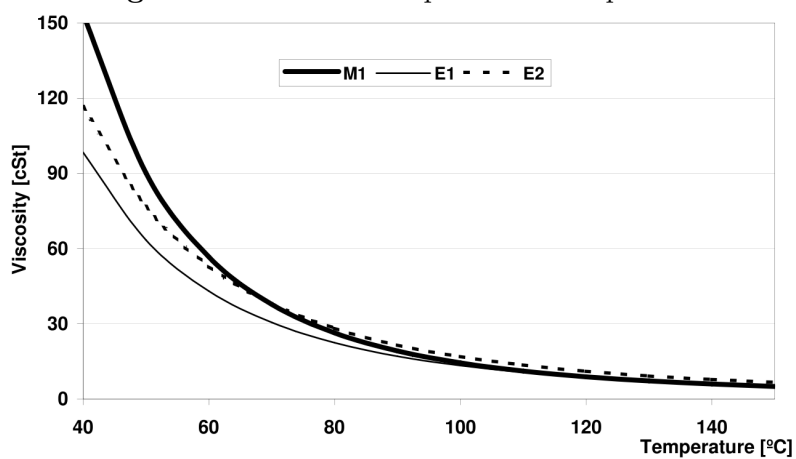


Figure 6.12: Variation of lubricants viscosity with temperature.

Oil	Properties	Fresh oil	Used oil	Variation (%)
Mineral (M1)	μ_{40} [cSt]	144.5	145.8	0.9
	μ_{100} [cSt]	14.0	14.1	0.7
	VI [/]	92	94	+3
	Fe [ppm]	0	18	-
Ester (E1)	μ_{40} [cSt]	99.4	100.2	+0.8
	μ_{100} [cSt]	14.6	14.6	0
	VI [/]	150	150	0
	Fe [ppm]	0	5	-

Table 6.6: Viscosity properties and Iron content measured before and after the power loss test for both lubricants.

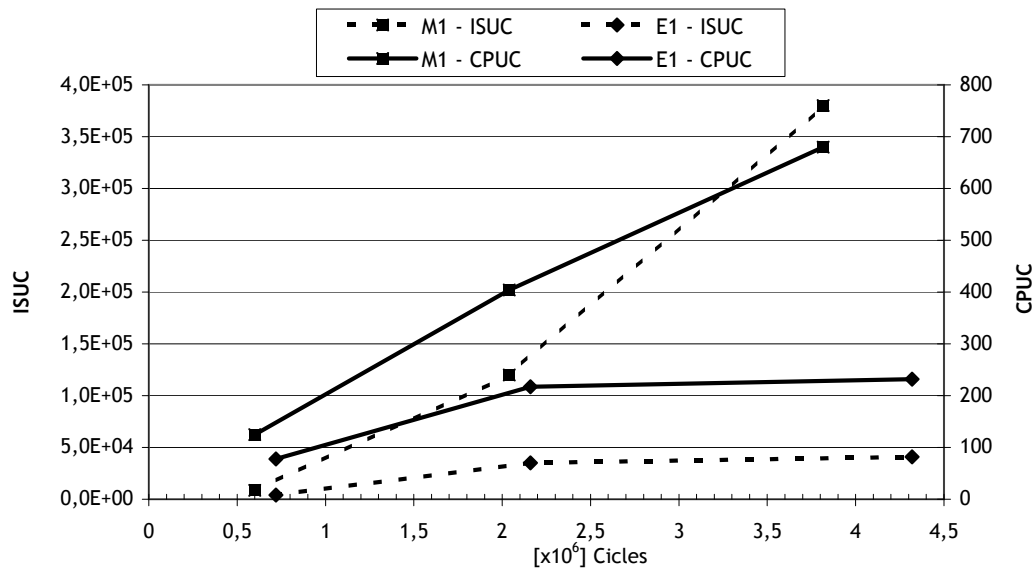


Figure 6.13: CPUC and ISUC evolution during power loss tests for M1 and E1 oils.

Hohn et al. [44] (see Eq. 3.2) in order to reflect the influence of lubricant base oil and additives in the friction behaviour.

As discussed in **Paper C** and in section 3.3 the lubricants tested in this work promote a reduction of the friction coefficient, and this reduction is due to a smaller dependence of friction with load than a mineral additive free lubricant. This fact was observed in experimental results and confirmed in the numerical analysis, once the optimization of the friction coefficient show very low dependence of other variables than load (see **Paper C**).

The X_L lubricant factor is:

$$X_L = \frac{1}{(F_{bt}/b)^{b1}} \quad (6.2)$$

So, introducing the experimental results of power loss tests in the numerical model to optimize the lubricant factor a value for the exponent $b1$ is obtained for each oil tested. Table 6.7 displays the exponent value and as expected, the exponent of load for ester oil E1 is larger than for mineral oil M1, thus evidencing a smaller increase of friction when the load increases.

Oil	$b1$
Mineral - M1	0.0651
Ester - E1	0.1055

Table 6.7: Optimized lubricant factor exponent $b1$ for oils M1 and E1. ($1000 \leq n_{wheel} \leq 3000$ rpm and $5 \leq T_{wheel} \leq 323$ Nm)

The $b1$ values presented in Table 6.7 are larger than those presented in Table 5.1, because the operating conditions now used and considered in the numerical model, included the input speed of 3000 rpm and, specially, because includes load stages at higher torque (323 Nm). As already referred, the main influence of materials, lubricants and surface coatings in the friction coefficient, for the operating conditions used, was in the load exponent. So, by considering higher torque load stages, the load exponent ($b1$) increases. The load exponent $b1$, had a larger increase for E1 oil than for M1 oil, indicating, as expected, that the E1 oil displays lower increase of the friction coefficient with the increase of load than the M1 oil.

6.4.4 Prediction of lubricant behaviour for different operating conditions using the energetic model

A good way to prove the validity of the model developed (see section 3.3) consists in predicting the oil bath equilibrium temperature of the FZG gearbox for operating conditions different of those used in the optimisation of the friction coefficient, and compare those predictions with experimental results.

Using the optimized friction coefficient presented in last section (6.4.3) in the model, together with different operating conditions, such as those presented in **Paper I**, the equilibrium temperature can be predicted for such conditions.

Figure 6.14 and Figure 6.15 display the comparison of the experimentally measured oil bath equilibrium temperature and the temperatures predicted by the model, for the mineral (M1) and ester (E1) oils, respectively.

As shown, the prediction was quite accurate, being the correlation factor equal to 0.997 for the mineral lubricant M1 and equal to 0.979 for the ester lubricant E1 (on the E1 power loss test a scuffing failure occurred, being the reason for the abnormal equilibrium temperature occurred at some stages).

The numerical model also allows the differentiation of the sources of power losses, i.e. for a given operating condition it allows to estimate the amount of energy dissipated by friction inside tooth contact, by gear churning, by the bearings and also by the seals. This overview is very important when, for example, optimizing the operating regime of an industrial gearbox, once it helps understanding which are the main sources of power loss and at what level is it possible to improve the overall efficiency. This kind of analysis can also be of interest to evaluate the impact of any modification, such as operating temperature or the load regime.

As example, Figure 6.16 presents the distribution of power losses at 2000 rpm, load stage K5 (wheel torque of 105 Nm) and at load stage K9 (wheel torque of 323 Nm) for oils M1 and E1 (using the temperatures predicted by the model). In Figure 6.16 the vales inside the chart represent the amount of power losses in Watt for each variable considered. The variables represented are: Pt - total power loss; Pfr - gear friction losses; Pspl - gear churning losses; $P_{M0}+P_{M1}$ - bearing losses; Psl - seal losses.

The load stage K5 is particularly interesting, because it represents a situation where the gear churning losses, the gear friction losses and the bearing losses are similar. The mineral lubricant at this load stage has lower churning losses than the ester, although it displays higher gear friction losses, resulting in a slightly higher total power losses.

At load stage k5 the friction losses represent between 35 to 40 % of the total power losses (Pt), the gear churning losses represent around 30 %, the bearing losses represent around 20 % and the seal losses represent less than 10 %. With the increase of load, load stage k9, these proportions change completely, and the gear friction losses become the most important source of power losses, becoming higher than 70 %.

Other interesting observation of Figure 6.16 is that the value of bearing power losses distribution decreases from load stage k5 to load stage k9. This happens because the oil bath temperature at load stage k9 is much higher than in load stage k5, thus the bearing churning losses decrease in a large amount than the bearing friction losses increase, resulting in a total bearing losses ($P_{M0}+P_{M1}$) smaller than in load stage k5.

6.5 Discussion

6.5.1 Scuffing

The lubricants used in this work, a mineral reference oil M1 and the ester biodegradable oils E1 and E2 were expected to have a high scuffing load capacity in standard scuffing test ISO 14635-1 [26], passing load stage 12 ($K_{FZG} > 12$). In this work a deeper study of the scuffing capacity was performed to allow a better comprehension of the scuffing capacity and to distinguish the ester oils between them and from the mineral oil.

On the first scuffing test performed, A20/16.6/90, the M1 oil reached scuffing failure at load stage K11 ($p_H=1.8$ GPa) and the E1 and E2 oils reached scuffing on

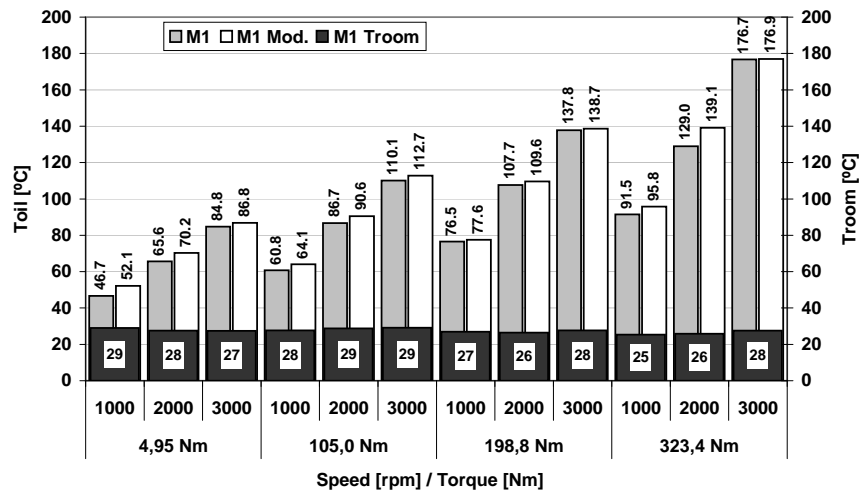


Figure 6.14: Comparison of model and experimental oil bath temperatures for oil M1.

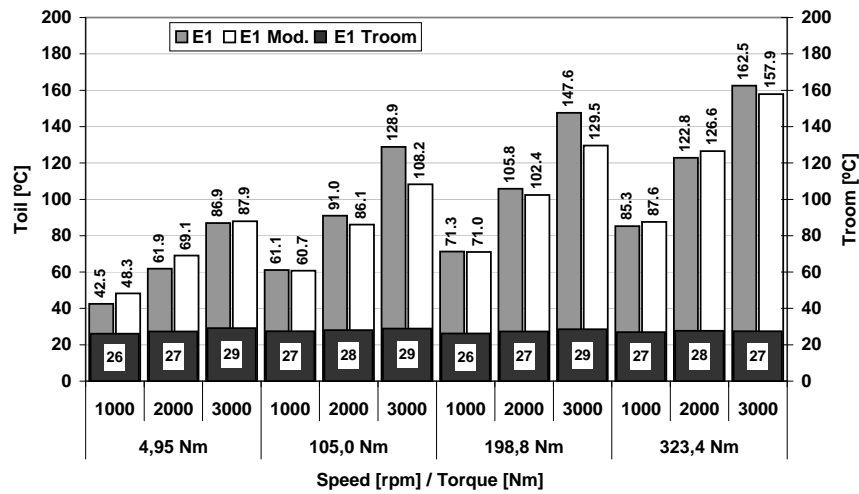


Figure 6.15: Comparison of model and experimental oil bath temperatures for oil E1.

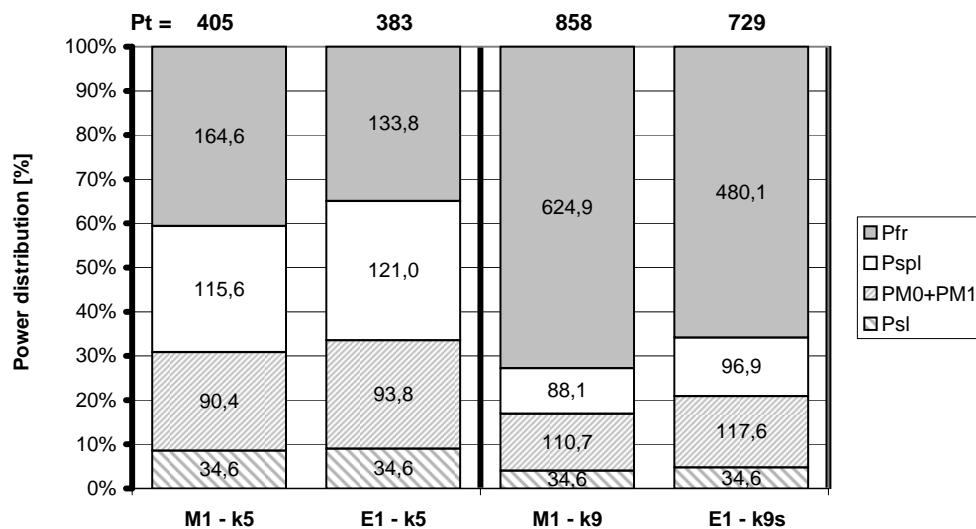


Figure 6.16: Distribution of power losses as function of load stage for oils M1 and E1. The values inside chart represent the power losses in Watts.

load stage K12 ($p_H=2.0$ GPa). The scuffing temperatures (maximum temperature reached at scuffing load stage) were 156 °C for M1 and E2 oils and 174 °C for E1 lubricants. This test allow to distinguish the ester oils E1 and E2 from M1 mineral oil, showing an higher scuffing load capacity for the ester oils, although this difference is inside the error margin of the scuffing test. This test also showed that the E1 ester oil supports a lower film thickness than M1 and E2 oils, once it reaches scuffing failure at higher oil bath temperature.

In the test A10/16.6/90, the three oils exhibit the same load carrying capacity, reaching scuffing failure on load stage K11 ($p_H=2.54$ GPa), displaying maximum oil bath temperatures of 144, 164 and 132 °C for oils M1, E1 and E2, respectively. This scuffing test procedure was more severe than the previous, but it did not put in evidence any difference in load carrying capacity, although it showed the same tendency in the maximum temperatures attained in scuffing load stage, where the E1 lubricant, once again, exhibited the higher temperature, thus the lower viscosity and the lower film thickness.

In what concerns to mass loss after scuffing, E1 oil displayed the lowest mass loss, on both tests performed.

The critical lubricant temperature (T_{CR}) of the scuffing criterion proposed by Castro et al. was determined for all lubricants, providing the following values: 176 °C , 201 °C and 221 °C for oils M1, E1 and E2, respectively.

So, in what concerns scuffing load capacity, the ester oils proved to have excellent properties.

6.5.2 Micropitting

The micropitting behaviour of lubricants has an increasing importance with the use of high strength, high hardness and high ductility materials, that allow the increase of the power density as well as the contact pressure between gear tooth. This increase of contact pressure makes micropitting a fatigue failure to be taken into account.

The mineral oil, M1, has an additive package to improve micropitting performance, so beside being a good reference for comparison with biodegradable ester E1, is also a good reference for micropitting performance.

In what concerns to micropitting affected area, the gear lubricated with ester oil displayed higher micropitting affected area, specially after the first stage, although that difference decreases after load stage K9 and becomes null with the repetition of load stage K9. This result is also confirmed by ferrography, by ferrometry measurements and also by mass loss measurements.

So, in the running-in, load stage K3, and in load stage K7 the test performed with ester oil exhibit slightly higher mass loss and slightly higher micropitting area, probably due to the additivation package of the mineral lubricant that has high content in Sulphur, Phosphor and Calcium, promoting the formation of protective layers since the beginning of the micropitting test.

The ferrometry and ferrography analysis of oil samples after load stage K3 suggests that the running-in process is faster with ester oil, once the amount of small particles was larger than for mineral oil and Figure 6.7 also suggests a faster reduction of surface roughness with the progression of test, besides showing that the ester lubricated gear had small depth micropits.

The observation of the topographies performed on the micropitting area (zone below the pitch line) after the micropitting test, displayed in Figure 6.9, shows that CE topography presents an image with smaller area affected by micropitting and also with micropits less widespread on the surface. This observation might seem contradictory, although the amount and depth of micropits could be considerably different and still displaying the typical micropitting grey shaded colour. So beside having the same micropitting area, evaluated by visual inspection, the CE pinion has less density of micropits and with smaller depth.

The tests performed showed that in general the micropitting performance of the ester oil E1 is similar to the obtained with mineral lubricant M1, despite presenting slightly higher mass loss.

6.5.3 Power loss

The efficiency of mechanical systems is of capital importance nowadays, being its reduction extremely important for both the energetic bill and also for the environment. The environment compatibility is usually viewed by the biodegradability and toxicity issues, although the lubricants performance is also very important on the overall environment compatibility, once low power consumption, low wear, higher life time, higher efficiency promote a lower impact on the environment.

The power loss tests performed show that the ester oil E1 exhibits lower oil bath equilibrium temperatures than the mineral lubricant M1, for the same operating conditions and such difference increases when the severity of the operating conditions also increase (higher input torque).

The no-load tests showed that the churning losses were not very different in absolute value, although were higher for mineral lubricant if the operating temperature was low and were higher for the ester lubricant if the operating temperature was high. This transition temperature was around 60 to 70 °C for the lubricants M1 and E1.

For the tests performed at high torque, the highest the torque, the highest was the difference between the ester lubricant E1 and the mineral lubricant M1, indicating lower energetic dissipation and lower friction for high contact pressures.

In what concerns to wear behaviour, the ester oil E1 displayed lower amount of wear particles and of smaller size, as confirmed by the lowest wear indexes CPUC and ISUC and by the lowest iron content in the lubricant sample (measured by RFA). The most severe operating conditions promoted equilibrium temperatures quite high, being in several cases above 100 °C, that for a mineral oil is above recommendations, although it was not detected any significant variation in the oil viscosity of both M1 and E1.

The energetic model developed for the FZG gearbox simulates quite well its behaviour. It allowed the optimisation of the friction coefficient between gear tooth for both lubricants tested, M1 and E1, based on the experimental results obtained in the gear power loss tests. The correction proposed for the friction coefficient was based on the optimization of the load exponent. The b_1 load exponent has the value of 0.651 for the M1 oil and has the value of 0.1055 for the E1 oil (see Eq. 3.2), being the highest value the one that grants the lower friction coefficient. For the highest loads the friction coefficient reduction promoted by the E1 oil in comparison to M1 oil might exceed 20 %.

The energetic model also worked very well on the prediction of the equilibrium temperature of the FZG gearbox for other operating conditions. It also proved to be very interesting to analyse the distribution of the power losses in function of its source, allowing a much better comprehension of the relative influence of each gearbox component, like bearings, gears and seals.

On **Paper I**, power loss tests were also performed with E2 and E3 biodegradable ester oils, beside M1 and E1 oils, and both present similar or even better energetic behaviour than E1 oil.

These results clearly indicate that biodegradable low toxicity ester formulation have significant advantages in what concern to power dissipation inside gearboxes, when compared to highly doped mineral oils. The results show that it is possible and desirable the esters widespread use, because beside the better power losses also present better wear behaviour, the possibility of working at higher temperatures and also having lower oxidation, thus long oil life.

7 Conclusions and future work

7.1 Conclusions

The use of ADI material in gears proved to be a valid solution, although it has some limitations. The main conclusions about its use on gears were:

- 1.1 In terms of power loss, ADI and carburized steel gears presented similar values of the equilibrium temperature for an input power up to 50 kW. For an input power above that value carburized gears displayed lower equilibrium temperature than ADI.
- 1.2 ADI gears had lower mass loss and lower equilibrium temperatures when lubricated with bio-oil, instead of mineral lubricant, for input speeds up to 2000 rpm.
- 1.3 Whatever the lubricant, ADI gears always had a higher friction coefficient than carburized gears.
- 1.4 The S/N curve determined for the ADI gears austempered at 300 °C showed that the pitting life was infinite for contact pressures below 1.2 GPa.
- 1.5 The ADI gears had a lower micropitting resistance than carburizing gears, and a special micropitting test procedure was developed to compare the micropitting performance of lubricants with ADI gears.
- 1.6 The micropitting behaviour of ADI gears lubricated with mineral and ester oils was very similar, although gears lubricated with ester oil showed a smaller mass loss.
- 1.7 The ADI material proved to be a good material for gear applications, although the gear design must be performed specifically for ADI gears, once the contact pressure could not be so high as with conventional carburizing steel, but in compensation ADI has lower weight, promotes lower noise and lower production costs. ADI could also be used with biodegradable ester oils with advantage in comparison to mineral oils.

Both MoS₂/Ti and C/Cr coatings proved to have very good tribological performance in several screening tests, such as POD, scratch tests, Daimler test etc. The main conclusions about the applicability of these surface coating on gears are:

- 2.1 MoS₂/Ti and C/Cr surface coatings provided an impressive increase of the scuffing load capacity of FZG type C gears, up to 5 load stages. It was also observed that improving the surface roughness of the coated gears, resulted in an additional increment of the scuffing load capacity.

7 Conclusions and future work

- 2.2 The analysis of gear scuffing results using the modified FPI scuffing criterion showed that, in scuffing conditions, surface coatings reduced the friction coefficient between 8 % and 41 %.
- 2.3 The FZG power loss tests performed with MoS₂/Ti coated gears showed that the oil bath operating temperature had a significant decrease when compared to uncoated gears, due to the lower friction coefficient provided by the coating.
- 2.4 The combination of MoS₂/Ti surface coating with biodegradable ester presented the best power loss results in FZG power loss tests.
- 2.5 MoS₂/Ti-coated gears generated a larger wear than uncoated gears, in FGZ power loss tests, due to coating wear.
- 2.6 The efficiency of a transfer gearbox improves by 0.5 % if MoS₂/Ti coated gears are used, being this difference specially noticed at high torque - low speed regime. The C/Cr surface coating displayed a narrow increase of efficiency.
- 2.7 The surface coatings tested, especially MoS₂/Ti, have characteristics of great interest, particularly in severe applications involving high contact pressures and high sliding with frequent start-up or deficient lubrication. May as well be used as tribo-reactive materials for substituting non-biodegradable and toxic additives in environmental friendly lubricants.

The evaluation of the applicability of biodegradable non-toxic lubricants to gears was studied in what concerns to scuffing protection, micropitting protection, power loss and lubricant degradation in service. The biodegradable ester oils tested (ISO VG 100) have a lower viscosity grade than the reference mineral oil (ISO VG 150).

In what concerns to scuffing protection the main conclusions are:

- 3.1 The ester bio-lubricants, tested for wear preventive properties in the four ball machine, exhibited similar or better wear protection than the mineral reference oil. The best result was obtained with E2 oil.
- 3.2 The gear scuffing load carrying capacity, evaluated in the FZG test rig, showed that the ester biodegradable lubricant have higher load carrying capacity than the reference mineral oil.
- 3.3 The ester based biodegradable gear oils, E1 and E2, showed a very good anti-wear and anti-scuffing performance, thus making them a valid solution for replacing mineral lubricants in what concerns to load carrying capacity.

In what concerns to micropitting protection the main conclusions are:

- 4.1 The micropitting evolution during the test procedure was similar for both ester and mineral oils.
- 4.2 The biodegradable ester lubricant compared with the mineral lubricant presented similar protection properties against micropitting.
- 4.3 The ester oil displayed a higher mass loss than the mineral lubricant.

4.4 The biodegradable and non-toxic ester oil proved to be a valid solution for substituting environment harmful lubricants on gear lubrication in what concerns to micropitting protection.

In what concerns to the power loss behaviour of biodegradable ester oils, the main conclusions are:

5.1 The churning losses were similar for both mineral and ester oils.

5.2 The ester based oils presented a smaller oil bath equilibrium temperature than mineral oil and the difference increases for higher input torques.

5.3 The mass loss measured during power loss tests was smaller for the gears lubricated with ester oils. This was confirmed by direct measurements and also by oil analysis.

5.4 The variation of ester oils viscosity was very small during the power loss tests, while the mineral oil displayed a decrease of 25 % of its viscosity index.

5.5 The ester oils promote a significant decrease of friction coefficient between gear tooth, reaching 27 %, that might represent an overwall decrease of the power losses of 0.25 % when compared to the reference mineral oil.

5.6 The gear power loss results clearly indicate that it is possible to formulate biodegradable low toxicity gear oils that have a better performance than highly doped mineral lubricants, in what concerns to gear power losses, tooth flank wear and oil degradation.

The energetic balance model developed for the FZG gearbox simulates quite well the power dissipation vs. heat evacuation behaviour. This numerical model developed allows the correction of the friction coefficient between gear teeth, through the XL parameter that is based in the real behaviour of each lubricant during power loss tests and allowed to determine that value for each lubricant. The model also allows to estimate, with good precision, the equilibrium temperature for given operating conditions. Other interesting feature of this model is to allow a better understanding and evaluation of the power loss in each gearbox component (gears, bearings and seals), in terms of churning and friction losses, whatever the operating condition (torque, speed and temperature).

7.2 Future work

This work left several indications about potential investigations for the future:

- a) Develop a transient thermal model of the gearbox, evaluating the evolution of temperature with time. Such model will also allow to determine the friction coefficient with a smaller number of gear power loss tests.
- b) Measure the power loss directly. This was a very interesting development of the test rig and it was the best way to validate the model and to refine it.
- c) Include the windage power losses in the model.
- d) Improve the power loss model of roller bearings. For that purpose it is necessary to perform power loss test with a roller bearing alone. Analyse the correlation between the friction coefficient of roller bearings and gears.
- e) Perform the micropitting tests on surface coated gears.
- f) Develop a micropitting damage model (in development).
- g) Develop lower cost biodegradable low toxicity gear oils.
- h) Develop ADI gears with improved tooth flank geometry for minimization of power losses (in development).

Bibliography

- [1] M. Weck, O. Hurasky-Schonwerth, and C. Bugiel, "Service behaviour of pvd-coated gearing lubricated with biodegradable synthetic ester oils," *VDI-Berichte*, no. Nr1665, 2002.
- [2] F. Joachim, N. Kurz, and B. Glatthaar, "Influence of coatings and surface improvements on the lifetime of gears," *VDI Berichte*, vol. 2, no. 1665, pp. 565–582, 2002.
- [3] R. Amaro, R. Martins, J. Seabra, and A. Brito, "Most low friction coatings for gears application," in *GEARS 2003 - Gears and transmissions workshop* (P. T. de Castro, L. Ferreira, J. Seabra, and J. Almacinha, eds.), 2003.
- [4] N. Renevier, V. Fox, N. Lobiondo, D. Teer, and J. Hampshire, "Performance of mos2/metal composite coatings used for dry machining and other applications," *Surface and coatings technology*, vol. 123, no. 1, pp. 84–91, 2000.
- [5] N. Renevier, V. Fox, D. Teer, and J. Hampshire, "Coating characteristics and tribological properties of sputter-deposited mos2/metal composite coatings deposited by closed field unbalanced magnetron sputter ion plating," *Surface and coatings technology*, vol. 127, no. 1, pp. 24–27, 2000.
- [6] N. Renevier, V. Fox, D. Teer, and J. Hampshire, "Hard lubricating coatings for cutting and forming tools and mechanical components," *Surface and coatings technology*, vol. 125, pp. 347–353, 2000.
- [7] N. Renevier, V. Fox, D. Teer, and J. Hampshire, "Performance of low friction mos2-titanium composite coatings used in forming applications," *Materials and design*, no. 21, pp. 337–343, 2000.
- [8] N. Renevier, J. Hampshire, V. Fox, J. Witts, T. Allen, and D. Teer, "Advantages of using self-lubricating, hard, wear-resistant mos2-based coatings," *Surface and coatings technology*, vol. 142-144, pp. 67–77, 2001.
- [9] Y. Su and W. Kao, "Tribological behaviour and wear mechanisms of mos2-cr coatings against various conterbodies," *Tribology International*, vol. 36, pp. 11–23, 2003.
- [10] V. Rigato, G. Maggioni, A. Patelli, D. Boscarino, N. Renevier, and D. Teer, "Properties of sputter-deposited mos2/metal composite coatings deposited by closed field unbalanced magnetron sputter ion plating," *Surface and coatings technology*, vol. 131, no. 13, pp. 206–210, 2000.

- [11] K. Holmberg, A. Mathews, and H. Roncainem, “Friction and wear mechanisms of coated surfaces,” *Finish Journal Tribology*, 1998.
- [12] N. Cardoso, R. Martins, J. Seabra, A. Igartua, X. Fdez-Perez, and R. Luther, “Micropitting performance of nitriding steel gears lubricated with mineral and ester oils,” *Tribology International (submitted)*, 2008.
- [13] J. D. Mullins, *Ductil Iron Data for Design Engineers*. SOREMETAL, Rio Tinto Iron and Titanium inc., 1990.
- [14] R. Harding, “The use of austempered ductile iron for gears,” 1986.
- [15] P. Salonen, “Improved noise damping and reduced weight in truck componentes with kymenite adi,” 1997.
- [16] L. Magalhães, *Caracterização Tribológica de um Ferro Nodular Austemperado em Ensaio Disco-Disco e de Engrenagens FZG*. PhD thesis, Universidade do Porto, 2003.
- [17] L. Magalhães and J. Seabra, “Artificial indentations for the study of contact fatigue of austempered ductile iron (adi) discs,” *WEAR*, vol. 258, no. 11-12, pp. 1755–1763, 2005.
- [18] L. Magalhães and J. Seabra, “Contact properties of cu-mn austempered ductile iron gears. experimental evaluation using the fzg test rig.,” in *Proceedings of the International Conference on Gears*, vol. 2, (Garching, Germany), pp. 1145–1163, VDI - Berichte 1904, 2005.
- [19] A. Santos, H. Pinto and T. V., “Cu-mn adi: a low cost high performance material,” in *58th World Foundry Congress Poland*, (Poland), 1991.
- [20] B. Rostro, “Everything old,” *Tribology and Lubrication Technology*, vol. 63, pp. 26–37, Dec 2007.
- [21] T. Mang and W. Dresel, eds., *Lubricants and Lubrication*. Wiley-VCH, 2007.
- [22] D. Horner, “Recent trends in environmentally friendly lubricants,” *Journal of Synthetic Lubrication*, vol. 18, no. 4, pp. 327–347, 2002.
- [23] R. Martins, J. Seabra, C. Seyfert, R. Luther, A. Igartua, and A. Brito, “Power loss in fzg gears lubricated with industrial gear oils: biodegradable ester vs. mineral oil,” in *Proceedings of the 31th “Leeds-Lyon Symposium” on Tribology*, (Leeds, UK), 2004.
- [24] L. Honary, “Biodegradable/biobased lubricants and greases,” *Machinery Lubrication Magazine*, no. 200109, 2001.
- [25] H. Winter and K. Michaelis, “Fzg gear test rig - description and possibilities,” In: *Coordinate European Council Second International Symposium on The performance Evaluation of Automotive Fuels and Lubricants*, pp. 29–42, 1985.

- [26] ISO-14635-1, “Fzg test procedures - part 1: Fzg test method a/8,3/90 for relative scuffing load-carrying capacity of oils,” 2000.
- [27] ISO-14635-2, “Fzg test procedures - part 2: Fzg step load test a10/16, 6r/120 for relative scuffing load-carrying capacity of high ep oils,” 2004.
- [28] ISO-14635-3, “Fzg test procedures - part 3: Fzg test method a/2,8/50 for relative scuffing load-carrying capacity and wear characteristics of semifluid gear,” 2005.
- [29] F. A. E. FVA, “Fva research project nr. 54/i-iv,” 1993.
- [30] I. sheet DGMK, “Short test procedure for the investigation of the micropitting load capacity of gear lubricants,” 2002.
- [31] H. Winter and K. Michaelis, “Scoring tests of aircraft transmission lubricants at high temperatures,” *Journal of synthetic lubrication*, vol. 3, no. 2, 1986.
- [32] R. Martins, R. Amaro, and J. Seabra, “Influence of low friction coatings on the scuffing load capacity and efficiency of gears,” *Tribology International*, vol. 41, pp. 234–243, Apr 2008.
- [33] R. C. Martins, P. S. Moura, and J. O. Seabra, “Mos2/ti low-friction coating for gears,” *Tribology International*, vol. 39, no. 12, pp. 1686–1697, 2006.
- [34] R. I. Amaro, R. C. Martins, F. O. Seabra, S. Yang, D. G. Teer, and N. M. Renevier, “Carbon/chromium low friction surface coating for gears application,” *Industrial Lubrication and Tribology*, vol. 57, no. 6, pp. 233–242, 2005.
- [35] H. Winter and P. Oster, “Influence of the lubricant on pitting and micro pitting (grey staining, frosted areas) resistance of case carburized gears and test procedures,” *AGMA*, 1987.
- [36] L. Mummery, *Surface Texture Analysis: The Handbook*. Hommelwerke GmbH, 1990.
- [37] T. Hunt, *Handbook of Wear Debris Analysis and Particle Detection in Liquids*. 1993.
- [38] J. Denis, J. Briant, and J.-C. Hipeaux, *Physico-Chimie des Lubrifiants - Analyses et Essais*. Éditions Technip, 1997.
- [39] R. Martins, J. Seabra, A. Brito, C. Seyfert, R. Luther, and A. Igartua, “Friction coefficient in fzg gears lubricated with industrial gear oils: Biodegradable ester vs. mineral oil,” *Tribology International*, vol. 39, no. 6, pp. 512–521, 2006.
- [40] R. Martins, J. Seabra, and L. Magalhães, “Austempered ducil iron (adi) gears: Power loss, pitting and micropitting,” *WEAR*, vol. 264/9-10, pp. 838–849, 2008.
- [41] R. Martins, P. Moura, and J. Seabra, “Power loss in fzg gears: Mineral oil vs. biodegradable ester and carburized steel vs. austempered ductile iron vs. mos2-ti coated steel,” *VDI Berichte*, no. 1904 II, pp. 1467–1486, 2005.

- [42] R. Martins, N. Cardoso, and J. Seabra, “Gear power loss performance of biodegradable low-toxicity ester based oils,” *IMEch Part J. (to be published)*.
- [43] B.-R. Höhn, K. Michaelis, and A. Doleschel, *Frictional behavior of synthetic gear lubricants*, pp. 759–768. Tribology series ; 39, Amsterdam ; New York: Elsevier, 2001.
- [44] B.-R. Höhn, K. Michaelis, and T. Vollmer, “Thermal rating of gear drives: Balance between power loss and heat dissipation,” *AGMA Technical Paper*, 1996.
- [45] H. Winter and K. Michaelis, “Investigations on the thermal balance of gear drives,” in *Fifth World Congress on Theory of Machines and Mechanisms*, American Society of Mechanical Engineers, 1979.
- [46] C. Changenet and M. Pasquier, “Power losses and heat exchange in reduction gears: Numerical and experimental results,” *VDI Berichte*, vol. 2, no. 1665, pp. 603–613, 2002.
- [47] C. Changenet and P. Velez, “A model for the prediction of churning losses in geared transmissions - preliminary results,” *Journal of Mechanical Design*, vol. 1, pp. 128–133, Jan 2007.
- [48] P. Eschmann, L. Hasbargen, U. Weigand, J. Brndlein, and F. K. G. S. KGaA., *Ball and roller bearings - Theory, design and applications*. 1985.
- [49] B. R. Hohn and K. Michaelis, “Influence of oil temperature on gear failures,” *Tribology International*, vol. 37, no. 2, pp. 103–109, 2004.
- [50] P. Luke and A. Oliver, “A study of churning losses in dip-lubricated spur gears,” *Journal of Institution of Mechanical Engineers*, vol. 213, no. Part G, 1999.
- [51] A. S. Terekhov, “Basic problem of heat calculation of gear reducers,” International Conference on Motion and Power Transmissions, pp. 490–495, Proceeding of Japanese Society of Mechanical Engeners, November 1991.
- [52] J. Magalhães, L. Seabra, “Wear and scuffing of austempered ductile iron gears,” *WEAR*, vol. 215, no. 1-2, pp. 237–246, 1998.
- [53] L. Magalhães, J. Seabra, and C. Sá, “Contact fatigue behaviour of artificially indented adi discs,” in *29th Leeds-Lyon Symposium on Tribology* (D. Dowson, A. Lubrecht, G. Dalmaz, and M. Priest, eds.), vol. 258, (Lyon, France), pp. 469–482, Elsevier, 2000.
- [54] L. Magalhães, J. Seabra, and C. Sá, “Experimental observations of contact fatigue crack mechanisms for austempered ductile iron (adi) discs,” *WEAR*, vol. 246, no. 1-2, pp. 134–148, 2000.
- [55] J. Castro and J. Seabra, “Scuffing and lubricant film breakdown in fzg gears part i. analytical and experimental approach,” *Wear*, vol. 215, no. 1-2, pp. 104–113, 1998.

- [56] S. Yang, X. Li, N. Renevier, and D. Teer, "Tribological properties and wear mechanism of sputtered c/cr coating," *Surface and coatings technology*, vol. 142-144, pp. 85–93, 2001.
- [57] D. Teer, "Uk patent n. gb 2258343b, u.s.a. patent n. 5556519, eu patent n. 0521045," 1996.
- [58] D. Teer, J. Hampshire, and V. Bellido, "Eu patent n. 969249879," 1996.
- [59] S. Yang, D. Camino, N. Renevier, A. Jones, and D. Teer, "Deposition and tribological behavior of sputtered carbon hard coatings," *Surface and coatings technology*, vol. 124, no. 2-3, pp. 110–116, 2000.
- [60] D. Teer, "New solid lubricant coatings," *WEAR*, vol. 251, no. 1-12, pp. 1068–1074, 2001.
- [61] R. I. Amaro, R. C. Martins, J. O. Seabra, N. M. Renevier, and D. G. Teer, "Molybdenum disulphide/titanium low friction coating for gears application," *Tribology International*, vol. 38, no. 4, pp. 423–434, 2005.
- [62] A. Dyson, "Scuffing - a review," *Tribology International*, vol. 8, no. 2, pp. 77–87, 1975.
- [63] J. W. Gold, A. Schmidt, H. Dicke, H. Loos, and C. Aßmann, "Viscosity-pressure-temperature behaviour of mineral and synthetic oils," *Journal of Synthetic Lubrication*, vol. 18, no. 1, p. 51, 2001.
- [64] R. Martins, J. Seabra, and N. Cardoso, "Influence of lubricant type in gear scuffing," *Industrial Lubrication and Tribology (to be published)*, no. 6, 2008.
- [65] J. Castro and J. Seabra, "Power dissipation - temperature scuffing criterion for fzg gears," in *International Conference on Gears*, pp. 1165–1184, VDI-Berichte 1904.2, 2005.
- [66] R. Martins and J. Seabra, "Micropitting performance of mineral and biodegradable ester gear oils," *Industrial Lubrication and Tribology (to be published)*, no. 6, 2008.
- [67] K. Michaelis and B. R. Hohn, "Influence of lubricants on power loss of cylindrical gears," *S T L E Tribology Transactions*, vol. 37, no. 1, pp. 161–167, 1994.
- [68] DIN-51396-part2, "Testing of lubricants - determination of wear elements - part 2: Analysis by wavelength dispersive x-ray spectrometry (xrs)," 06 1998.
- [69] IP-212/92, "Determination of viscosity of bitumen emulsions - engler method," 1992.

A Appended Papers

Role of authors in the papers

Paper A

Authors: R. Martins, R. Amaro, and J. Seabra
Title: Influence of low friction coatings on the scuffing load capacity and efficiency of gears
Journal: Tribology International, vol. 41, pp. 234-243, Apr 2008

R. Amaro: Performed the FZG tests.
R. Martins: Performed the transfer gearbox tests, made the friction analysis and wrote the paper.
J. Seabra: Made the teste planing, supervised the work within the R&D of projects and revised the manuscript.

Paper B

Authors: R. Martins and J. Seabra
Title: Micropitting performance of mineral and biodegradable ester gear oils
Journal: Industrial Lubrication and Tribology, 2008(6) (to be published)

R. Martins: Made the test planing, performed experiments, analysed the results and wrote the paper.
J. Seabra: Supervised the work within the R&D projects and revised the manuscript.

Paper C

- Authors: R. Martins, J. Seabra, A. Brito, C. Seyfert, R. Luther, and A. Igartua
- Title: Friction coefficient in fzg gears lubricated with industrial gear oils: Biodegradable ester vs. mineral oil
- Journal: Tribology International, vol. 39, no. 6, pp. 512-521, 2006
- A. Brito: Provided the FZG gears.
- Ch. Seyfert and R. Luther: Developed and provided the biodegradable ester oil and performed the RFA analysis.
- A. Igartua: Performed the biodegradability and toxicity tests to the oils.
- R. Martins: Made the test planning, performed experiments, developed the numerical model, analysed the results and wrote the paper.**
- J. Seabra: Supervised the work within the R&D projects and revised the manuscript.

Paper D

- Authors: R. C. Martins, P. S. Moura, and J. O. Seabra
- Title: MoS₂/Ti low-friction coating for gears
- Journal: Tribology International, vol. 39, no. 12, pp. 1686-1697, 2006
- P. Moura: Performed the experiments.
- R. Martins: Made the test planning, performed the analysis and wrote the paper.**
- J. Seabra: Supervised the work within the R&D projects and revised the manuscript.

Paper E

- Authors: R. Martins, J. Seabra, and L. Magalhães
- Title: Austempered Ductile Iron (ADI) Gears: Power Loss, Pitting and Micropitting
- Journal: WEAR, Vol.264 no. 9-10, pp. 838-849, 2008
- L. Magalhães: Defined the material composition and heat treatment.
- R. Martins: Made the test planing, performed the heat treatment, performed experiments and wrote the paper.**
- J. Seabra: Supervised the work within the R&D projects and revised the manuscript.

Paper F

Authors: R. Martins, P. Moura, and J. Seabra
Title: Power loss in FZG gears: Mineral oil vs. biodegradable ester and carburized steel vs. austempered ductile iron vs. MoS₂-Ti coated steel
Journal: VDI Berichte, no. 1904 II, pp. 1467-1486, 2005

P. Moura: Performed the experiments
R. Martins: Made the test planning, performed the analysis and wrote the paper.
J. Seabra: Supervised the work within the R&D projects and revised the manuscript.

Paper G

Authors: R. Amaro, R. Martins, F. Seabra, S. Yang, D. G. Teer, and N. M. Renevier
Title: Carbon/chromium low friction surface coating for gears application
Journal: Industrial Lubrication and Tribology, vol. 57, no. 6, pp. 233-242, 2005

S. Yang, D.G. Teer and N. Renevier: Developed the surface coating and performed the screening tests.
R. Amaro: Performed the FZG tests.
R. Martins: Performed the transfer gearbox tests and wrote the paper.
J. Seabra: Made the test planning, supervised the work within the R&D projects and revised the manuscript.

Paper H

Authors: R. Martins, N. Cardoso, and J. Seabra
Title: Influence of lubricant type in gear scuffing
Journal: Industrial Lubrication and Tribology, 2008(6) (to be published)

N. Cardoso: Performed the experiments and analysis.
R. Martins: Made the test planning and wrote the paper.
J. Seabra: Supervised the work within the R&D projects and revised the manuscript.

Paper I

Authors: R. Martins, N. Cardoso, and J. Seabra
Title: Gear power loss performance of biodegradable low-toxicity ester based oils
Journal: IMEch Part J. (to be published)

N. Cardoso: Performed the experiments.
R. Martins: Made the test planning, analysed the results and wrote the paper.
J. Seabra: Supervised the work within the R&D projects and revised the manuscript.

A.1 Paper A

R. Martins, R. Amaro, and J. Seabra, “Influence of low friction coatings on the scuffing load capacity and efficiency of gears ”, Tribology International, vol. 41, pp. 234-243, Apr 2008.

Influence of low friction coatings on the scuffing load capacity and efficiency of gears

R. Martins^{a,*}, R. Amaro^{a,1}, J. Seabra^b

^aINEGI, Instituto de Engenharia Mecânica e Gestão Industrial, Porto, Portugal

^bFEUP, Faculdade de Engenharia da Universidade do Porto, Portugal

Received 2 March 2005; received in revised form 2 May 2005; accepted 10 May 2007

Available online 14 September 2007

Abstract

The influence of multilayer composite surface coatings on gear scuffing load carrying capacity, gear friction coefficient and gearbox efficiency is discussed in this work.

The deposition procedures of molybdenum disulphide/titanium (MoS₂/Ti) and carbon/chromium (C/Cr) composite coatings are described.

Tests reported in the literature, such as Rockwell indentations, ball cratering, pin-on-disc and reciprocating wear, confirm the excellent adhesion to the substrate and the tribological performance of these coatings, suggesting they can be applied with success in heavy loaded rolling-sliding contacts, such as those found in gears.

FZG gear scuffing tests were performed in order to evaluate the coatings anti-scuffing performance, which both improved very significantly in comparison to uncoated gears. These results in conjunction with the friction power intensity (FPI) scuffing criterion allowed the determination of a friction coefficient factor X_{SC} to include the coating influence on the friction coefficient expression.

The composite coatings were also applied to the gears of a transfer gearbox and its efficiency was measured and compared at different input speeds and torques with the uncoated carburized steel gears. Significant efficiency improvement was found with the MoS₂/Ti coating.

© 2007 Elsevier Ltd. All rights reserved.

Keywords: Surface coatings; Gear efficiency; Scuffing load capacity; Gears

1. Introduction

Surface coating technology has been significantly improved in the last decades, allowing higher load capacity and higher protection against surface failures in situations where lubrication was inefficient. The application of low friction surface coatings to power transmission equipments can improve their efficiency and might represent a significant reduction of energy consumption. In the near future, surface coatings will probably contribute to the reduction/elimination of non-biodegradable and toxic lubricant additives and promote the use of environment friendly lubricants.

Diamond-like carbon (DLC) coatings are very hard and have a low friction coefficient against a variety of materials, but they tend to be brittle and have poor adhesion, being unsuitable for highly loaded applications. Coatings of amorphous hydrogenated carbon films containing a small amount of metal (Me-C:H) tend to be less brittle but are much softer and can be used at moderately high loads [1,2]. There are several types of coatings that can be used in gears, for instance, tungsten carbide/carbon (WC/C) [3], boron carbide/carbon (B₄C) [3,4] or molybdenum disulphide/titanium (MoS₂/Ti) [1,2,4–9], carbon/chromium (C/Cr) [10–12] among others [13]. In order to provide a better wear protection it is interesting that the coating behaves like a true solid lubricant [2] like graphite or MoS₂ [14]. The MoS₂ coatings can be improved with the co-deposition of other metals such as Ti [5] or Cr [13].

*Corresponding author.

E-mail address: rcm@fe.up.pt (R. Martins).

¹Present address: RENAULT-CACIA, Aveiro, Portugal.

The MoS₂/Ti coating [1,2,4–8] used in this work is harder, more resistant and less sensitive to atmospheric water vapour than MoS₂ or common DLC coatings and has a friction coefficient similar to that of MoS₂. The higher hardness combined with low friction and good adhesion to the substrate leads to low wear rates and to high load bearing capacity [1]. The C/Cr coating, also used in this work, has a structure based on graphite, with a friction coefficient similar to that of graphite but with a much higher hardness and wear resistance [11,15].

In standard FZG scuffing tests Joachim et al. [4] obtained an improvement in scuffing resistance of two FZG load stages when comparing uncoated gears with WC/C or B₄C coated gears. They also obtained an improvement in scuffing resistance (one FZG load stage) comparing standard and super-finished uncoated FZG gears. Weck et al. [3] obtained an improvement in scuffing resistance (one FZG load stage) in standard FZG scuffing tests between uncoated and WC/C coated gears. Both Joachim [4] and Weck [3] noticed a considerable decrease in the wear of the teeth flanks.

The contribution of MoS₂/Ti and C/Cr composite surface coatings to a better protection against gear scuffing failures and higher gear efficiency is discussed in this work. The influence of these surface coatings on the friction coefficient between gear teeth is also analysed.

2. Coatings deposition procedure, physical and tribological performance

2.1. MoS₂/Ti coating

The MoS₂/Ti composite coating [1,2,5,6] was deposited by DC Magnetron Sputtering using a standard closed field unbalanced magnetron sputter ion plating (CFUBMSIP) [16] Teer Coatings PVD system, with four targets (one Ti and three MoS₂ targets). The coating procedure started with an ion cleaning, followed by a 70 nm Ti layer, a 200 nm MoS₂/Ti multilayer, a 900 nm MoS₂/Ti (non-multilayer) and a last 50 nm layer of MoS₂ for colouration. Further details about the coating deposition may be found in Refs. [1,2,5,6,17].

A 1.2 μm thick [1] MoS₂/Ti coating was deposited on M42 steel, polished to 1200 grain size with SiC paper, and several tribological tests were performed to evaluate its performance.

Rockwell C indentations (Daimler–Benz test [18]) were performed to assess, qualitatively, the adhesion of the

coating to the substrate, which showed a very small amount of plastic deformation. On the standard scratch test (Rockwell C diamond with 0.2 mm tip radius) at 0.17 mm/s, no coating failure occurred for loads up to 100 N. The dynamic hardness measurement test indicated that the MoS₂/Ti coating had a plastic hardness of approximately 12 GPa [17].

Pin-on-disc (POD) tests, performed at 200 mm/s and 50% humidity, with a 5 mm diameter uncoated WC-6%Co ball for 1 h, showed low wear and low friction coefficient. The friction coefficient increased as the load decreased, being rather small (0.04–0.045) at the highest load (80 N) and reaching the value of 0.1 for a 10 N load [17]. Coating wear was evaluated as the percentage of coating thickness reduction, measured by the ball cratering technique (for further details see Refs. [11,17]) on the disc track, as presented in Fig. 1 [7]. Its value was 10% for a load of 10 N, reaching 24% for a load of 80 N [7].

The reciprocating wear test was performed at room temperature and 50% humidity, under a 100 N load and a 2.5 mm/s sliding speed, using a 5 mm diameter uncoated WC-6%Co ball. After 10,000 cycles the coating was not worn away and the specific wear rate was $3.1 \times 10^{-17} \text{ m}^3/\text{mN}$ with a friction coefficient of 0.04 [17].

2.2. C/Cr coating

The C/Cr composite coatings [11,12,15] were deposited by the same procedure as MoS₂/Ti, although with one Cr and three C targets. Further details about the coating deposition may be found in Refs. [11,12].

A 1.7 μm thick [10] C/Cr coating was deposited on M42 steel, polished to 1200 grain size with SiC paper, and several tests were performed in order to evaluate its performance.

A critical load of 80 N and a hardness of 2200 HV were measured in the scratch test, and no cracks, chips or flakes outside the track were observed, indicating excellent coating adhesion to the substrate. The Rockwell C indentation (Daimler–Benz test) also indicated a very good adhesion to the substrate. POD tests, performed on the C/Cr composite coating at 200 mm/s for 1 h, using a 5 mm diameter uncoated WC-6%Co ball, indicated that the friction coefficient decreases from 0.1 for a load of 20 N to 0.06 for a load of 140 N, while the bearing load capacity increases from 2.1 to 3.4 GPa for the same load variation. In this load range the specific wear rate was almost constant at $2.2 \times 10^{-17} \text{ m}^3/\text{Nm}$ [10].

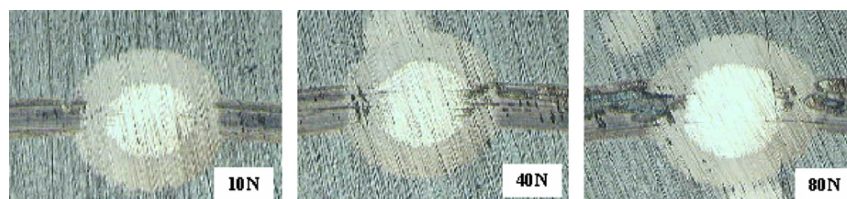


Fig. 1. Ball craters in worn tracks of MoS₂/Ti coating using loads of 10, 40 and 80 N on the pin [7].

Fig. 2 [10] shows the ball craters used to calculate, from optical measurements, the remaining coating thickness on the disc wear track, allowing the determination of the specific wear rate [12].

3. FZG gear tests

3.1. Test rig and FZG type C gears

The gear tests were performed on a FZG machine, a “back-to-back” gear test rig with recirculating power, used for micropitting [19], pitting [20] and scuffing [21] gear tests, as well as gear oil testing. FZG type C gears [21] were used, lubricated with an ISO VG 100 mineral oil without extreme-pressure (EP) and anti-wear (AW) additives, that was kept at a constant temperature of 90 °C. The geometry and material of the gear and the physical properties of the lubricant are presented in Table 1.

Four different gears sets were tested. One uncoated gear, two MoS₂/Ti coated gears and one C/Cr coated gear:

1. NC—uncoated gear ($R_a = 2.4 \mu\text{m}$);
2. MST—MoS₂/Ti coated gear ($R_a = 2.4 \mu\text{m}$);
3. MST*—MoS₂/Ti coated super-finished gear ($R_a = 0.4 \mu\text{m}$);
4. CCR—C/Cr coated gear ($R_a = 2.4 \mu\text{m}$).

3.2. Gear testing conditions

Before each test the gears were run-in for 4 h in FZG load stage 6 (wheel torque $T_{\text{wheel}} = 203 \text{ N m}$) at 1500 rpm with the purpose of softening the surface roughness of the

teeth flanks, mainly for the high surface roughness gears (NC, MST and CCR).

The test procedure was performed at two different speeds, 1500 and 3000 rpm. After run-in, all tests started on FZG load stage 7 ($T_{\text{wheel}} = 275 \text{ N m}$) and the torque was increased step by step up to FZG load stage 13 ($T_{\text{wheel}} = 940 \text{ N m}$) or until any type of surface failure of the teeth flanks was observed. The duration of each load stage was 15 min, during which both the speed and the lubricant temperature were kept constant. At the end of each load stage the teeth flanks were visually inspected looking for surface failures, in particular scuffing and excessive wear.

The tribological operating conditions of the contact between the teeth flanks were extremely severe, as the torque increased from load stages 7 to 13. Increase in the torque by one FZG load stage corresponds, approximately, to increase in the maximum Hertzian contact pressure between gear teeth by 0.19 GPa. At the wheel tip/pinion root contact point, the maximum Hertzian pressure increased from 1.13 to 2.08 GPa, while the lubricant film thickness, although remaining almost constant with load, was very thin, 0.15 and 0.20 μm , at 1500 and 3000 rpm, respectively.

At the end of each test the gear was dismantled and the teeth were visually inspected for scuffing, wear and other surface failures assessment.

3.3. Gear tests results

Fig. 3 shows the influence of the surface coatings on the gear scuffing load stage. At 1500 rpm the uncoated gear

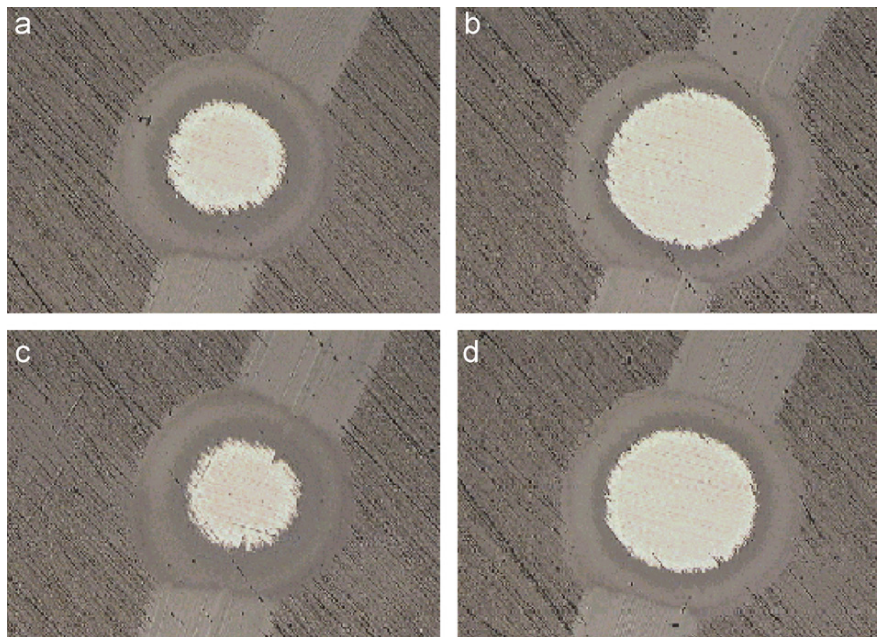


Fig. 2. Ball craters in worn tracks of carbon/chromium using loads of 80, 100, 120 and 140 N on the pin [10].

Table 1
Characteristics of the FZG type C gears and lubricant physical properties

Parameters [units]	Designation	Pinion	Wheel
Number of teeth [-]	z	16	24
Tooth width [mm]	b	14	14
Module [mm]	m	4.5	4.5
Pressure angle [°]	α	20	20
Profile shift factor [-]	x	0.182	0.171
Tip circle [mm]	d_a	82.45	118.35
Centre distance [mm]	a_w	91.5	91.5
Working pressure angle [°]	α_w	22.5	22.5
Contact ratio [-]	ϵ	1.47	1.47
Material	–	DIN 20MnCr5	DIN 20MnCr5
Heat treatment		Case hardened, quenching and annealing	
Surface hardness	HRC	58–62	58–62
Surface roughness in teeth flanks (NC, CCR and MST) [μm]	Ra	2.388	2.396
Surface roughness in teeth flanks (MST*) [μm]	Ra	0.405	0.420
Oil type		ISO VG 100 mineral oil, additive free	
Cinematic viscosity at 40 °C [mm^2/s]	ν_0	100.0	
Cinematic viscosity at 100 °C [mm^2/s]	ν_1	11.1	
Specific gravity at 15 °C [-]	Sp Gr	0.891	
Viscosity index [-]	VI	95	
Oil operating temperature [°C]	T	90 ± 2	

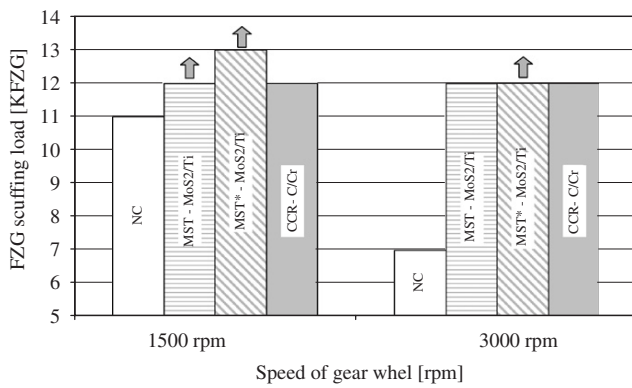


Fig. 3. Scuffing (or maximum) load stage at 1500 and 3000 rpm gear tests (FZG type C gears lubricated with additive free ISO VG 100 mineral oil at 90 °C).

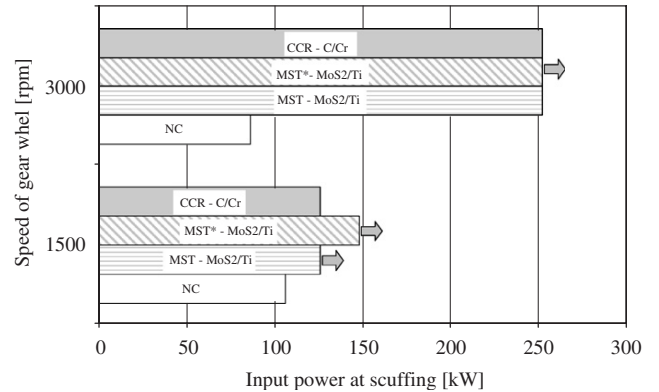


Fig. 4. Power transmitted by the FZG type C gear at the scuffing load stage or at the end of the test (additive free ISO VG 100 mineral oil at 90 °C).

reached scuffing in load stage $K_{FZG}^{NC} = 11$ ($T_{wheel} = 675 \text{ N m}$), the CCR in load stage $K_{FZG}^{CCR} = 12$, while both MoS₂/Ti coated gears did not reach scuffing: $K_{FZG}^{MST} > 12$ and $K_{FZG}^{MST^*} > 13$. Thus, the scuffing load capacity increased 1 load stage due to the C/Cr coating, at least 2 load stages due to the MoS₂/Ti coating and at least 3 load stages due to the MoS₂/Ti coating when applied to super-finished gears. At 3000 rpm the uncoated gear reached scuffing in load stage $K_{FZG}^{NC} = 7$, the C/Cr and the MoS₂/Ti coated gears in load stage $K_{FZG}^{CCR} = K_{FZG}^{MST} = 12$, while the MoS₂/Ti coated super-finished gear overcome load stage $K_{FZG}^{MST^*} > 12$. So, at 3000 rpm the C/Cr (CCR gear) and MoS₂/Ti (MST gear) coatings improved the scuffing resistance by 5 FZG load stages, which is a very significant result.

These differences in scuffing load stage also represent a significant difference in transmitted power by the FZG type

C gear, as shown in Fig. 4. At 1500 rpm the C/Cr coated gear (CCR) transmitted 19% more power than the uncoated gear (NC), while the MoS₂/Ti coated gears (MST and MST*) transmitted at least 40% more power than the uncoated one. At 3000 rpm any coated gear transmitted, at least, 190% more power than the uncoated gear (NC). At this speed the super-finished gear (MST*) transmitted at least 17% more power than the other coated gears with higher surface roughness.

4. Scuffing criterion

4.1. Friction power intensity (FPI) criterion

The FPI [22] is an energetic scuffing criterion, defined by the product of the friction coefficient μ by the normal force

F_n and by the sliding speed V_S , that is $FPI \Leftrightarrow \mu F_n V_S$. Dyson [22] also mentioned a criterion based on tangential stresses and sliding speed. So, for the same point of the gear meshing line (e.g. pinion root—wheel tip) and for the same gear geometry, the product of the friction coefficient μ with the maximum Hertzian pressure p_H and the sliding speed V_S , $\mu p_H V_S$, might be used instead, defining the FPI per unit of area.

For a given lubricant and gear geometry, the criterion postulates that scuffing occurs when a limiting constant value is reached, at any point of the gear meshing line, that is,

$$\mu p_H V_S = C^{te} \quad (1)$$

The FZG scuffing test results were analysed according to this modified FPI criteria.

Fig. 5 shows the variation of the maximum Hertzian pressure and of the sliding speed along the meshing line of the FZG type C gear, and the corresponding $\mu p_H V_S$ product, considering the friction coefficient between gear teeth proposed by Höhn et al. [23]. The values shown were obtained for FZG load stage 10 ($T_{\text{wheel}} = 560 \text{ Nm}$) and a wheel speed of 750 rpm, corresponding to an input power of 43.9 kW.

This figure clearly shows that the $\mu p_H V_S$ product reached its maximum value at the beginning of the gear meshing line (point A), that is, at the pinion root/wheel tip contact point. Thus, scuffing always occurred at point A of the meshing line, as experimentally observed in all tests performed.

The application of the energetic scuffing criterion to the gear scuffing tests was based on the following assumptions:

- The tests were all performed using the same additive free lubricant oil;
- The tests were all performed using the same gear geometry and gear material;

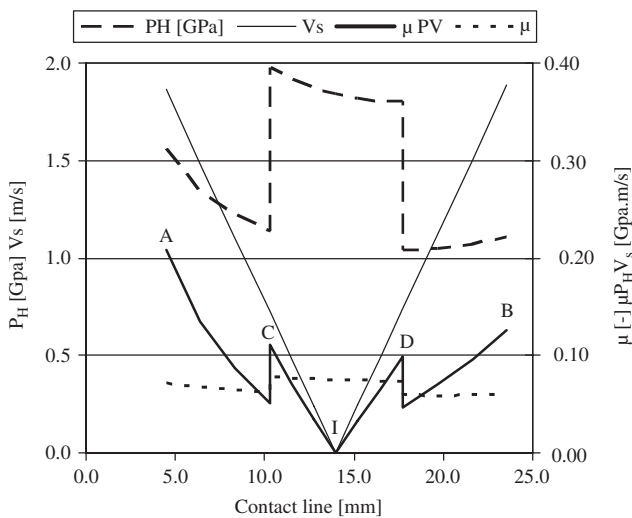


Fig. 5. Variation of the maximum Hertzian pressure, sliding speed, friction coefficient and $\mu p_H V_S$ value along the gear meshing line ($K_{FZG} = 10$, $n = 750 \text{ rpm}$).

- The limiting gear scuffing constant ($\mu p_H V_S = C_{FPI}$) is a lubricant characteristic, independent of the surface coating used and independent of the coating type;
- The limiting gear scuffing constant ($\mu p_H V_S = C_{FPI}$) is a lubricant characteristic influenced by the gear operating speed;
- Surface coatings affect the friction coefficient between the gear teeth, and consequently also affect gear scuffing.

4.2. Friction coefficient between gear teeth

The friction coefficient for the contact between gear teeth of carburized steel gears, proposed by Höhn et al. [23], is defined as

$$\mu_{\text{Michaelis}} = \mu_M = 0.048 \left(\frac{F_{bt}/b}{v_{\Sigma C} \rho_C} \right)^{0.2} \times \eta_{\text{oil}}^{-0.05} Ra^{0.25} X_L X_{SC} \quad (2)$$

where F_{bt} stands for the tooth normal force on the transverse section, b is the gear width, $v_{\Sigma C}$ the sum velocity at pitch point, ρ_C the equivalent curvature radius at pitch point, η_{oil} the oil dynamic viscosity, and Ra the composite surface roughness of the teeth contacting flanks.

The influence of lubricant type and lubricant additives on the friction coefficient is represented by the parameter X_L . Typically, $X_L = 1$ for additive free mineral oils. The X_{SC} parameter was added to the original Höhn expression in order to take into account the influence of the surface coating. For the uncoated gear the X_{SC} parameter is 1.

4.3. Correlation between the experimental results and the gear scuffing criterion

In order to apply the scuffing criterion to the experimental scuffing results, the following hypotheses were considered:

- The scuffing load stage for the MST gear at 1500 rpm is $K_{FZG} = 13$ (this gear did not scuff on load stage 12).
- The scuffing load stage for the MST* gear at 1500 rpm and at 3000 rpm is $K_{FZG} = 14$ (this gear did not scuff in any of the tests).

Since X_{SC} parameter was known for the uncoated gear ($X_{SC}^{NC} = 1$), the limiting gear scuffing constant, according to the modified FPI criterion, could be determined for both rotating speeds. The following values were determined: $C_{FPI}^{1500} = 0.415 \text{ GPa m/s}$ and $C_{FPI}^{3000} = 0.385 \text{ GPa m/s}$. Knowing these two constants and applying the FPI criteria to the gear tests performed with coated gears, the corresponding X_{SC} parameters might be determined, taking into account the coating composition, the teeth flanks surface roughness and the operating conditions (torque, speed and oil temperature) at the scuffing stage,

that is

$$\mu_M^{NC} p_H^{NC} V_S = \mu_M^{coated} p_H^{coated} V_S, \quad (3)$$

and so

$$\mu_M^{coated} = \mu_M^{NC} \frac{p_H^{NC}}{p_H^{coated}}. \quad (4)$$

Eq. (4) combined with Höhn's expression (2) for the friction coefficient gives the X_{SC} parameter corresponding to each surface coating. The results obtained are displayed in Figs. 6 and 7 for the operating speeds of 1500 and 3000 rpm, respectively.

At 1500 rpm (see Fig. 6) X_{SC} parameter for the C/Cr and MoS₂/Ti coated gears was 0.89 and 0.79, respectively. At 3000 rpm (see Fig. 7) X_{SC} parameter was the same for both surface coatings and was equal to 0.47. These results show that surface coatings had a significant influence on the friction coefficient and that influence increased when the operating speed also increased.

These X_{SC} values can also be used to compare the friction coefficient in scuffing conditions between uncoated and coated gears. Fig. 8 shows the relation between the friction coefficient and the FZG scuffing load stage taking into account the influence of the surface coatings.

At 1500 rpm (see Fig. 8), the friction coefficient between gear teeth when scuffing occurred (FZG load stage 11) was 0.065 for the uncoated gears. For CCR the friction coefficient at scuffing conditions was reduced to 0.060 (less 8%) and consequently the FZG scuffing load stage was now 12. In the case of MoS₂/Ti coated gears (MST) the friction coefficient reduced to 0.055 (less 15%) and consequently the FZG scuffing load stage was 13. Finally, for the MoS₂/Ti coated super-finished gears (MST*) the friction coefficient had an additional reduction to 0.051 (less 21%), due to the lower surface roughness of teeth flanks, and consequently the FZG scuffing load stage was 14.

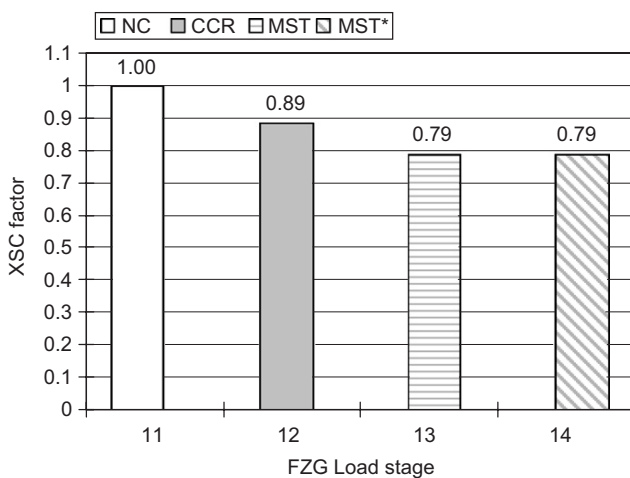


Fig. 6. Surface coating factor X_{SC} in scuffing conditions at 1500 rpm.

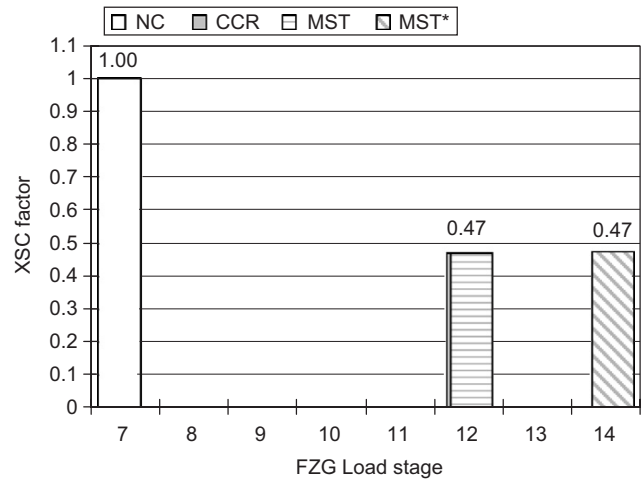


Fig. 7. Surface coating factor X_{SC} in scuffing conditions at 3000 rpm.

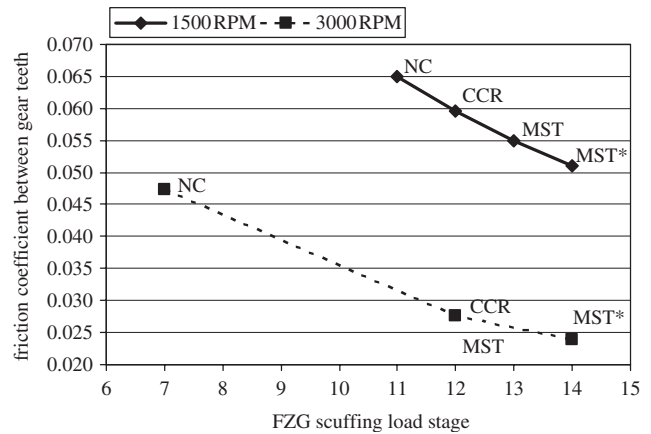


Fig. 8. Friction coefficient between gear teeth in scuffing conditions at 1500 and 3000 rpm.

At 3000 rpm (see Fig. 8) a similar situation was observed. The friction coefficient between the gear teeth when scuffing occurred (FZG scuffing load stage 7) was 0.047 for the uncoated gears. In the case of the C/Cr and of the MoS₂/Ti coated gears (CCR and MST) the friction coefficient at scuffing conditions was reduced to 0.028 (less 41%) and consequently the FZG scuffing load stage is now 12. Finally, for the MoS₂/Ti coated super-finished gears (MST*) the friction coefficient had an additional reduction to 0.024 (less 49%), due to the lower surface roughness of the teeth flanks, and consequently the FZG scuffing load stage was 14.

This simplified analysis of the friction coefficient between gear teeth in scuffing conditions, showed the huge influence that surface coatings promoted on the friction coefficient and, consequently, on the scuffing load carrying capacity of the FZG type C gears. In a minor scale, the super-finishing of the gear flanks had a similar effect on the scuffing load capacity of gears.

5. Efficiency tests with a transfer gearbox

5.1. Transfer gearbox

Fig. 9 shows a cross-section of a two-speed transfer gearbox used in four-wheel drive light trucks. The transfer gearbox is mounted after the conventional gearbox of the vehicle, allowing it to have two drive axles and an auxiliary power output.

This transfer gearbox used 5 gears mounted in three shafts employing keys and splined shafts. The gears mounted on the input and output shafts were supported by needle roller bearings. The gears were manufactured with DIN 15CrNi6 steel. After machining, the gears were case hardened, quenched in oil and annealed. The geometric characteristics of the gears are given in Table 2.

The reference lubricant for this transfer gearbox was a mineral based industrial gear oil with viscosity grade ISO VG 150, containing EP and AW additives. The transfer gearbox was filled up with 2.851 of lubricant oil, as recommended by the gearbox manufacturer. The most significant properties of the lubricant are displayed in Table 2.

5.2. Gearbox efficiency tests

The transfer gearbox tests were performed in a back-to-back test rig with recirculating power, where the driving electrical motor only supplied the power needed to overcome inertia, frictional and churning losses and to reach and maintain the desired operating speed, resulting in a significant reduction of energy consumption. A hydraulic cylinder displaced a helical gear pinion over a shaft and, consequently, the closed kinematic system twisted, applying the desired torque.

Two different gearboxes, one with C/Cr coated gears and another with MoS₂/Ti coated gears, were tested in a

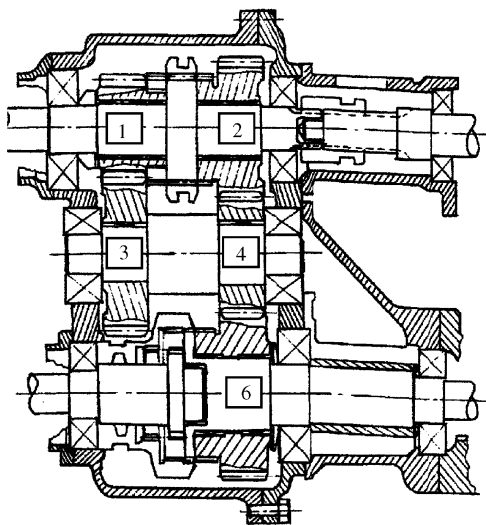


Fig. 9. Cross-section of the two speeds transfer gearbox.

Table 2

Geometric characteristics of the transfer gearbox gears and lubricant physical properties

Parameter [units]	Design	Gear wheel no				
		1	3	2	4	6
Module [mm]	m	4	4	3.5	3.5	3.5
Number of teeth [-]	Z	17	28	27	23	32
Profile shift factor [-]	x	0.051	-0.24	0.161	0.415	0.381
Width [mm]	b	35	33.5	35	35	35
Pressure angle [°]	α	20	20	20	20	20
Helix angle [°]	β	20	20	20	20	20
Max. addendum diameter [mm]	da_{max}	80.7	125.2	108.4	95.3	128.6
Oil type	ISO VG 150 mineral oil					
Cinematic viscosity at 40 °C [mm ² /s]	ν_0	150				
Cinematic viscosity at 100 °C [mm ² /s]	ν_1	14.5				
Specific gravity at 15 °C [-]	Sp Gr	0.896				
Viscosity index [-]	VI	95				
FZG rating	K_{FZG}	12>				

Table 3

Operating conditions in the transfer gearbox efficiency tests with coated gears

Parameter	Design Stages					
Vehicle speed [km/h]	V	5.7	13.6	21.5	29.4	37.4
Input speed to transfer gearbox [rpm]	n	573	1376	2178	2981	3784
$P \cong 36$ kW Input torque [Nm]	T_{in}	600	250	160	120	90

wide range of operating conditions (input torque and speed) in order to measure their efficiency. The run-in of each gearbox lasted approximately half million cycles, applying increasing input power, from 7.5 to 41 kW. After run-in the lubricant oil was replaced.

Each efficiency test was performed at constant speed and torque, during which the oil temperature was free and continuously measured. The initial oil temperature was 40 °C and the test was stopped if the lubricant temperature exceeded 120 °C. The test duration was 120 min and the final oil temperature depends on the operating conditions (torque and speed). Table 3 shows the test programme where the operating conditions are defined as well as the corresponding speed of the vehicle using this transfer gearbox.

5.3. Efficiency of the transfer gearbox

The efficiency results for the C/Cr and MoS₂/Ti coated gearboxes tested are presented in Fig. 10 and are compared with previous data obtained with the same gearbox using uncoated gears [7]. In all cases the operating conditions were very similar and the oil temperature was in the range 60–70 °C.

For an input power of 36 kW (see Fig. 10) the maximum efficiency was obtained for an input speed between 1400 and 2200 rpm, both for coated and uncoated gears. The efficiency of the MoS₂/Ti coated gearbox was 0.5% above that of the C/Cr and uncoated gears. The efficiency improvement promoted by the C/Cr coating, when compared with uncoated steel, was small, presenting approximately the same efficiency at 36 kW that the uncoated gears have at 30 kW. In this case (36 kW) the maximum variation of efficiency with speed was around 1%.

Fig. 11 shows the active flanks of pinion no 4 (see Fig. 9) of all three gearboxes, MoS₂/Ti and C/Cr coated and uncoated. The analysis of those surfaces showed that they were in perfect state, exhibiting small mild wear, although the C/Cr coating presented higher wear than MoS₂/Ti coating, especially below the pitch line.

6. Discussion

6.1. FZG gear scuffing tests

The FZG gear scuffing tests showed that both coatings promote a significant improvement of the scuffing load carrying capacity. At 1500 rpm the C/Cr coated gear reached one more FZG load stage than the uncoated gear, representing an increase of 19% on the transmitted torque. At the same speed, the MoS₂/Ti coated gear (MST gear) did not reach scuffing in load stage 12, meaning that it improved the scuffing load capacity at least by two FZG load stages (40% increase on applied torque), and the MST* gear promoted at least an improvement of three FZG load stages in the scuffing load capacity,

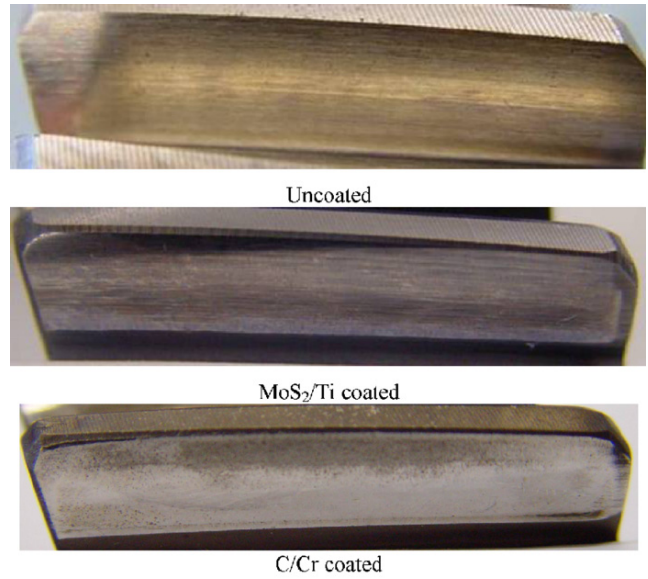


Fig. 11. Teeth flanks of gearbox pinion no 4 after testing.

representing a more than 62% improvement in transmitted torque.

At 3000 rpm the influence of the surface coatings on the scuffing load failure was even greater. The CCR and MST gears reached scuffing in FZG load stage 12, representing 5 more FZG load stages more than the uncoated gear, and a transmitted torque 190% higher. The MST* gear did not reach scuffing, improving the FZG scuffing stage by at least six load stages.

These improvements in scuffing load carrying capacity are directly related to the reduction in the friction coefficient between the contacting teeth flanks promoted by the low friction composite coatings, which generate lower contact temperatures and thus a higher scuffing load capacity. The teeth flank roughness also plays an important role, as proved by the MST* gear that showed an increase of at least one FZG load stage on the scuffing resistance in relation to the gear with higher surface roughness.

6.2. Friction power intensity scuffing criterion

The modified FPI scuffing criterion allowed the proposal of an additional parameter X_{SC} to the friction coefficient equation, in order to take into account the influence of the surface coatings. For the moment, the X_{SC} factors determined are only valid for the operating conditions considered and for the coatings used. Further tests and analysis are needed to arrive at a more general factor for each surface coating. The X_{SC} parameter also allowed the evaluation of the friction coefficient reduction promoted by the surface coatings applied to the FZG type C gears. At 1500 rpm, the friction reduction promoted by the coatings attains 8% for CCR gear, 15% for MST gear and 21% for

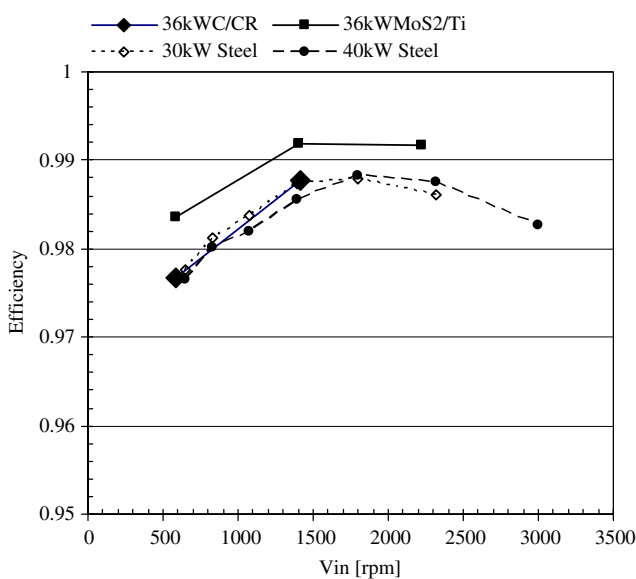


Fig. 10. Efficiency of the transfer gearbox at constant input power (36 kW). Influence of the MoS₂/Ti and C/Cr surface coatings.

MST* gear, while at 3000 rpm the reduction is 41% for CCR and MST gears and 49% for the MST* gear, when compared with the uncoated steel gears (see Fig. 8). The friction coefficients determined were consistent with similar results obtained in POD and reciprocating wear tests.

6.3. Gearbox tests

The efficiency measurements made during the transfer gearbox tests, with uncoated and coated gears, confirmed the influence of the surface coatings on the reduction of the friction coefficient between gear teeth and, consequently, the reduction of the friction power loss inside the gearbox and the improvement of gearbox efficiency. At constant input power, such influence was more effective at low operating speed and high torque, when the lubricant film thickness between the gear teeth is smaller and the contact pressure is higher, and the friction power loss became more important than the churning power loss. Under these conditions, surface coatings played an important role in improving gearbox efficiency.

As observed in the FZG gear scuffing tests, the MoS₂/Ti coating seems to have a better performance than the C/Cr coating. The improvement provided by the two surface coatings in gearbox efficiency is around 0.5% for the MoS₂/Ti coating and 0.1% for the C/Cr coating. The wear of the teeth flanks also confirms the better performance of the MoS₂/Ti coating.

7. Conclusions

Both MoS₂/Ti and C/Cr coatings have very good tribological performance, confirmed by the results obtained in several different tests, such as, POD, FZG scuffing tests and transfer gearbox efficiency tests.

The main conclusions of this study are:

1. MoS₂/Ti and C/Cr surface coatings provided a very significant increase of the scuffing load capacity of FZG type C gears, mainly at high speeds. In the case of MoS₂/Ti coating, this higher scuffing load capacity was even increased using super-finished gear teeth flanks with low surface roughness ($R_a = 0.3 \mu\text{m}$).
2. The analysis of gear scuffing results using the modified FPI scuffing criterion ($\mu p_H V_S = c^{te}$), showed that surface coatings reduced the friction coefficient between gear teeth between 8% and 41%, depending on the operating speed and coating type.
3. Coated gears improved the efficiency of a gearbox, particularly at low speed–high torque conditions when the friction power losses between gear teeth were more important. MoS₂/Ti coated gears increased the transfer gearbox's efficiency by 0.5%.

These characteristics show that both the MoS₂/Ti and C/Cr coatings are of great interest, particularly in severe

applications involving high contact pressures and high sliding with frequent start-up or deficient lubrication, as well as acting as tribo-reactive materials and substituting non-biodegradable and toxic additives in environmental friendly lubricants.

Acknowledgements

The authors would like to thank the European Commission for the financial support given to this study through the project “Reduction of fluid lubricant use in heavily loaded motion transmission systems through the application of self-lubricating coatings.” Project no BE-S2-5389, Contract no BRST-CT97-5363, 1998–2000.

References

- [1] Renevier N, et al. Advantages of using self-lubricating, hard, wear-resistant MoS₂-based coatings. *Surf Coatings Technol* 2001; 142–144:67–77.
- [2] Renevier N, et al. Hard lubricating coatings for cutting and forming tools and mechanical components. *Surf Coatings Technol* 2000; 125(1–3):347–53.
- [3] Weck M, Hurasky-Schonwerth O, Bugiel C. Service behaviour of PVD-coated gearing lubricated with biodegradable synthetic ester oils. *VDI-Ber* 2002;1665.
- [4] Joachim F, Kurz N, Glatthaar B. Influence of coatings and surface improvements on the lifetime of gears. *VDI Ber* 2002;2(1665):565–82.
- [5] Renevier N, et al. Performance of MoS₂/metal composite coatings used for dry machining and other applications. *Surf Coatings Technol* 2000;123(1):84–91.
- [6] Renevier N, et al. Performance of low friction MoS₂-titanium composite coatings used in forming applications. *Mater Des* 2000(21):337–43.
- [7] Amaro R, et al. MoST low friction coating for gears application. In: *Proceedings of GEARS 2003—gears and transmissions workshop*, 2003, FEUP-Porto-Portugal.
- [8] Amaro R, et al. Molybdenum disulfide/titanium low friction coating for gears application. *Tribol Int* 2004;38–4:423–34.
- [9] Teer D. New solid lubricant coatings. *Wear* 2001;251(1–12):1068–74.
- [10] Amaro R, et al. Carbon/chromium low friction surface coating for gears application. *Ind Lubr Tribol* 2005;57(6).
- [11] Yang S, et al. Deposition and tribological behavior of sputtered carbon hard coatings. *Surf Coatings Technol* 2000;124(2–3):110–6.
- [12] Yang S, et al. Tribological properties and wear mechanism of sputtered C/Cr coating. *Surf Coatings Technol* 2001;142–144:85–93.
- [13] Su Y, Kao W. Tribological behaviour and wear mechanisms of MoS₂-Cr coatings against various counterbodies. *Tribol Int* 2003;36:11–23.
- [14] Holmeberg K, Mathews A, Roncainem H. Friction and wear mechanisms of coated surfaces. *Fin J Tribol* 1998.
- [15] Field SK, Jarratt M, Teer D. Tribological properties of graphite-like and diamond-like carbon coatings. *Tribol Int* 2004(37):949–56.
- [16] Teer D, UK patent no GB 2258343B, USA patent no 5556519, EU patent no 0521045, 1996.
- [17] Renevier N, et al. Coating characteristics and tribological properties of sputter-deposited MoS₂/metal composite coatings deposited by closed field unbalanced magnetron sputter ion plating. *Surf Coatings Technol* 2000;127(1):24–7.
- [18] Daimler-Benz adhesion test. In: *Verein Deutscher Ingenieure (VDI)-Richtlinie 3198*, 1997. p. 7.
- [19] Forschungsvereinigung Antriebstechnik E.V. FVA research project nr 54/I-IV, 1993.
- [20] Forschungsvereinigung Antriebstechnik E.V. Pitting test. FVA-information sheet no 2/IV, 1997.

- [21] Winter H, Michaelis K. FZG gear test rig—description and possibilities. In: Proceedings of the Coordinate European Council second international symposium on the performance evaluation of automotive fuels and lubricants, 1985.
- [22] Dyson A. Scuffing—a review. *Tribol Int* 1975;8(2):77–87.
- [23] Höhn B-R, Michaelis K, Vollmer T. Thermal rating of gear drives: balance between power loss and heat dissipation. AGMA technical paper, 1996.

A.2 Paper B

R. Martins and J. Seabra, “Micropitting performance of mineral and biodegradable ester gear oils”. *Industrial Lubrication and Tribology*, (6) 2008 (to be published)

MICRO-PITTING PERFORMANCE OF MINERAL AND BIODEGRADABLE ESTER GEAR OILS

Ramiro Martins ⁽¹⁾ and Jorge Seabra ⁽²⁾

rcm@fe.up.pt, jseabra@fe.up.pt

⁽¹⁾ – CETRIB, Instituto de Engenharia Mecânica e Gestão Industrial, Rua Dr. Roberto Frias s/n, 4200-465 PORTO, Portugal.

⁽²⁾ – Faculdade de Engenharia, Universidade do Porto,
Rua Dr. Roberto Frias s/n, 4200-465 PORTO, Portugal.

1 INTRODUCTION

Micropitting is a contact fatigue wear phenomenon observed in combined rolling and sliding contacts operating under elastohydrodynamic lubrication (EHL) or mixed EHL/Boundary lubrication conditions. Micropitting can be regarded as a fatigue failure with a net of cracks close to the surface, which typically starts during the first 10^5 to 10^6 stress cycles. The cracks propagate at a shallow angle to the surface forming micro-pits with characteristic depth in the range of 5-10 μ m. The micro-pits coalesce to produce a continuous fractured surface with a dull mate appearance. When the surface cracks propagate deeper into the material, pitting and spalling can be initiated (Lipp, 2003).

Micropitting is known to be influenced by operating conditions such as temperature, load, rolling and sliding speeds, specific lubricant film thickness, lubricant additives and surface material properties (Antoine, 2002; Lipp, 2003; Winter, 1987).

Not considering lubricant chemistry, the key factors for the micropitting surface failure are mixed lubrication and combined rolling and sliding. Thicker EHL films and smoother surfaces can elude micropitting (Lipp, 2003; Winter, 1987).

In the case of gears with parallel axis, pure rolling exists only at the pitch point. Above and below this point there is a combination of rolling and sliding and the sliding speed increases as the contact point moves away from the pitch point. Micropitting may occur almost anywhere on the gear tooth flank. However, the contact condition where sliding and rolling directions are opposite is considered to be the most critical, which always occurs below the pitch diameter both for the driving and the driven gears. Micropitting is also often found at addendum due to high sliding and at local high spots in the surface topography associated with high stresses (Cardis, 2000).

The progression of micropitting may eventually result in pitting or spalling. There are also reported cases (Cardis, 2000) where micropitting progressed up to a point and stops, sometimes described as a form of running-in or stress relief. Although it may appear innocuous, such loss of metal from the gear surface causes loss of gear accuracy, increased vibration, noise and other related problems. The metal particles released into the oil may be too small to be picked up by filters, but large enough to damage tooth and bearing surfaces.

This work presents the results of gear micropitting tests performed with two different lubricants combined with carburizing steel. The micropitting evaluation during the tests was done using accurate mass loss measurements, ferrometric oil analysis, inspection of active teeth flanks and roughness measurements.

2 GEAR OILS

Two industrial gear lubricants were tested and compared: an ISO VG 150 mineral oil, containing an additive package to improve micropitting resistance, and an ISO VG 100 biodegradable fully saturated ester fluid with low toxicity additivation. Both oils are specified as CLP gear oils according to DIN 51517 and their most relevant properties are shown in Table 1, being their kinematic viscosities almost the same at 90 °C.

The mineral gear oil is based on paraffinic base oil with significant residual sulphur content. It contains an ashless anti-wear additive package based on phosphorous and sulphur chemistry and metal-organic corrosion preventives. In contrast, the biodegradable ester product uses a fully saturated ester based on harvestable materials incorporating environmentally compatible and highly efficient additives, being the metal-organic compounds completely avoided. The additive content of the mineral oil is considerably higher than that of the ester oil, mainly in what concerns the sulphur compounds (Martins, 2005; Martins, 2006).

The “ultimate” biodegradability of the lubricants was assessed using a “ready” biodegradability test as published by the OECD and adopted by European Union. The mineral oil didn’t match the minimum requirements of 60% biodegradability in 28 days, as shown in Table 1. Thus, no toxicity tests were performed for this lubricant. The ester based oil exceeded the minimum requirements of 60% biodegradability in 28 days and passed both toxicity tests, OECD 201 “Alga growth inhibition test” and OECD 202 “Daphnia Magna acute immobilization”, as shown in Table 1 (Martins, 2005; Martins, 2006).

<i>Parameter</i>	<i>Method</i>	<i>Desig.</i>	<i>Units</i>	<i>Lubricating Oils</i>	
Base oil	DIN 51451	/	/	paraffinic mineral oil	fully saturated ester
<i>Physical properties</i>					
Density @ 15°C	DIN 51757	ρ_{15}	g/cm ³	0.897	0.925
Kinematic Viscosity @ 40 °C	DIN 51562	v_{40}	cSt	146	99.4
Kinematic Viscosity @ 100 °C	DIN 51562	v_{100}	cSt	14.0	14.6
Viscosity Index	DIN ISO 2909	VI	/	92	152
Pour point	DIN ISO 3106		°C	-21	-42
<i>Wear properties</i>					
KVA weld load	DIN 51350-2	/	N	2200	2200
Kva wear scar (1h/300N)	DIN 51350-3	/	mm	0.32	0.35
Brugger crossed cylinder test	DIN 51347-2	/	N/mm ²	68	37
FZG rating	DIN 513540	K_{FZG}	/	>13	-
<i>Chemical Content</i>					
Zinc	ASTM D-4927	Zn	ppm	-	-
Calcium	ASTM D-4927	Ca	ppm	40	-
Phosphor	ASTM D-4927	P	ppm	175	146
Sulphur	ASTM D-4927	S	ppm	15040	180
<i>Biodegradability and toxicity properties</i>					
Ready biodegradability	OECD, 301 B		%	<60	≥60
Aquatic toxicity with Daphnia	OECD, 202	EL ₅₀	ppm	-	>100
Aquatic toxicity with Alga	OECD, 201	EL ₅₀	Ppm	-	>100

Table 1 – Physical and chemical properties of the lubricants.

3 FZG GEAR MICROPITTING TESTS

3.1 Test rig, gears and material

All the gear tests were performed on the FZG back-to-back spur gear test rig, shown in Figure 1, and the gears used are similar to standard FZG type C gears, having the geometric characteristics presented in Table 2 (Winter, 1985).

The gears were manufactured in DIN 20 MnCr 5 steel, carburized to a depth of 0.8 mm and a surface hardness $58 - 62\text{ HRC}$. It has a very high surface hardness while keeping a very high toughness on the core, being a typical material used for manufacturing highly stressed parts such as gears, crankshafts, ... The physical and mechanical properties (average values) of the gear material are presented in Table 3.

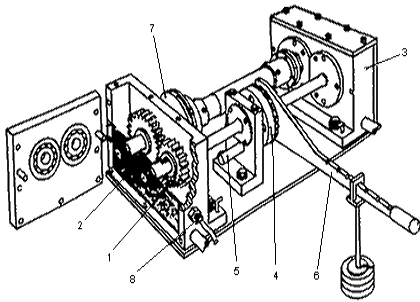


Figure 1 - Schematic view of the FZG Gear Test Rig.

Parameter	[Units]	Pinion	Wheel
Number of teeth	[/]	16	24
Module	[mm]	4.5	
Center distance	[mm]	91.5	
Addendum diameter	[mm]	82.45	118.35
Pressure angle	[°]	20	
Addendum modification	[/]	+0.182	+0.171
Face width	[mm]	14	

Table 2 - Geometry of the test gears.

Properties	Units	Value
Modulus of elasticity	GPa	210
Yield stress	MPa	850
Limit fatigue stress (tooth root)	MPa	430
Limit fatigue stress (hertzian stress)	MPa	1500
Specific heat capacity	J/g.K	0.46
Density	g/cm ³	7.85

Table 3 – Physical properties of carburized 20MnCr5 steel.

3.2 Operating conditions

The gear micropitting tests were based on the DGMK-FZG micropitting short test procedure (abbreviated as GFKT-C/8.3/90) (DGMK Information sheet, 2002), which is a short term test, able to classify candidate lubricants in terms of gear micropitting, analogous to FVA-FZG-micropitting test (Forschungsvereinigung Antriebstechnik E.V, 1993).

The tested gears had a quality grade considered “current” while standard gears have a “fine” quality grade, and this difference was clearly expressed in terms of the average roughness of the teeth flanks. Table 4 shows the test reference, the gear quality and the average roughness of teeth flanks, as well as, the gear quality and the average roughness of type C gear specified on FVA micropitting test procedure (Forschungsvereinigung Antriebstechnik E.V, 1993).

Dip lubrication was used during the gear micropitting tests, using the operating conditions presented in Table 5. The highest load stage on the micropitting test (K9) was run twice, to allow a better assessment of micropitting evolution.

	Gear reference	Lubricant type	Gear quality grade (ISO 1328)	Average roughness of teeth flanks Ra
Standard gear	-	-	5	0.5 μm
20 MnCr 5 carburized	CM CE	Mineral Ester	9 9	1.0 μm 1.1 μm

Table 4 – Test reference, quality grade, average surface roughness and lubricant type on each micropitting test.

Parameter	[Units]	K3 - running in		K7		K9-1 / K9-2	
		pinion	wheel	Pinion	wheel	pinion	wheel
Temperature	[°C]	80		90		90	
Torque	[Nm]	28.8	43.2	132.5	198.8	215.6	323.4
Rot speed	[1/min]	2250	1500	2250	1500	2250	1500
Speed Vt	[m/s]	8.3					
Hertzian Stress	[Mpa]	510		1094		1395	
Power	[kW]	6.8		31.2		50.8	
Duration [h] / cycles	[10 ³]	1/135	1/90	16/2160	16/1440	16/2160	16/1440

Table 5 – Operating conditions of micropitting tests.

The test procedure can be resumed as follow:

1. Load stage K3 (running-in)
2. Collection of a lubricant sample for analysis
3. Load stage K7
4. Collection of a lubricant sample for analysis
5. Dismounting gears, for weight and roughness measurement and surface photography.
6. Mounting gears with fresh lubricant
7. Load stage K9
8. Repeating step 4 and step 5
9. Repeating step 6, step 7 and step 8.

3.3 Results

Micropitting failures appeared first on pinions, since they performed 33% more cycles than gear wheels. Figure 2 displays the gear mass loss measurement after each load stage, during the micropitting test. The mass loss was slightly larger on the gear lubricated with the ester lubricant, although after load stage K9-2 it was slightly smaller.

After each load stage, including running-in FZG load stage 3, a lubricant sample was collected to evaluate lubricant condition. These samples were analyzed by Direct Reading Ferrometry (Hunt, 1993) in order to measure the ferrometric parameters D_L (large wear particles index) and D_S (small wear particles index), which were used to evaluate the concentration of wear particles index - CPUC and the severity of wear particles index - ISUC, defined as $CPUC = \frac{D_L + D_S}{d}$ and $ISUC = \frac{D_L^2 - D_S^2}{d^2}$, where d stands for the oil sample dilution.

The CPUC index grows when the sum of the small and the large particles increase, while the ISUC index grows when the number of particles with a size greater than $5\mu\text{m}$ (D_L) are present

in major number than those with a size smaller than $5\mu\text{m}$ (D_5).

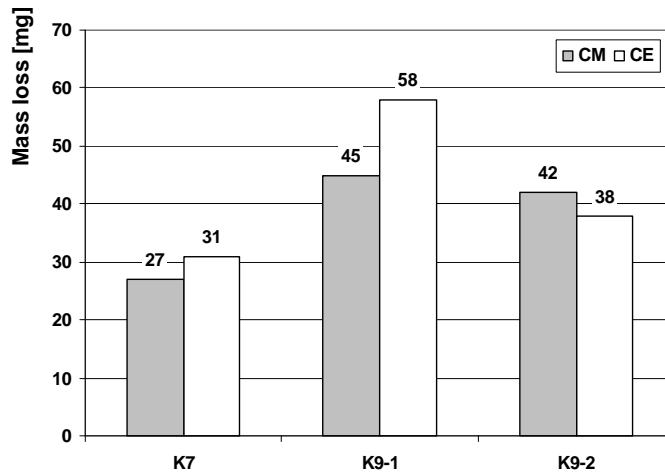


Figure 2 – Mass loss measurements during gear micropitting tests (CM – Mineral gear oil, CE - Ester gear oil).

After load stages K7 and K9 the lubricant was replaced by fresh oil, thus the wear indexes presented refer to the test period and not to all test duration.

Figure 3 and Figure 4 display the CPUC and ISUC ferrometric indexes, respectively, for the lubricant samples collected at the end of each gear micropitting test load stage. The CPUC index shows a significant increase from running-in to load stage K7, as expected, and remains almost stable during the following load stages. At the end of load stage K7, the ester lubricant sample showed larger values of both ferrometric indexes, but from then on both gear oils showed similar values of the ferrometric parameters. The ISUC and CPUC results presented the same tendency.

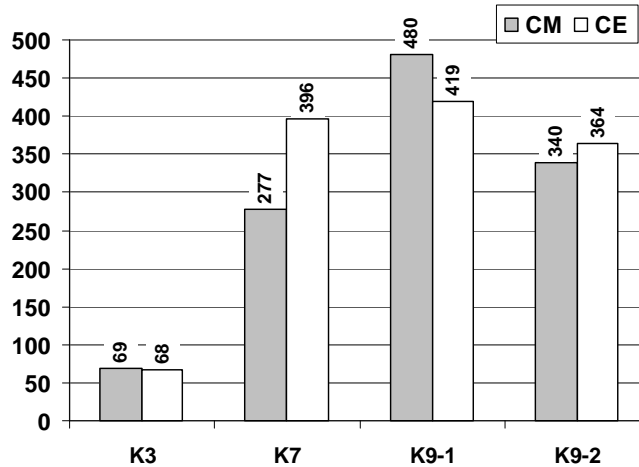


Figure 3 – CPUC index during micropitting test (CM – Mineral gear oil, CE - Ester gear oil).

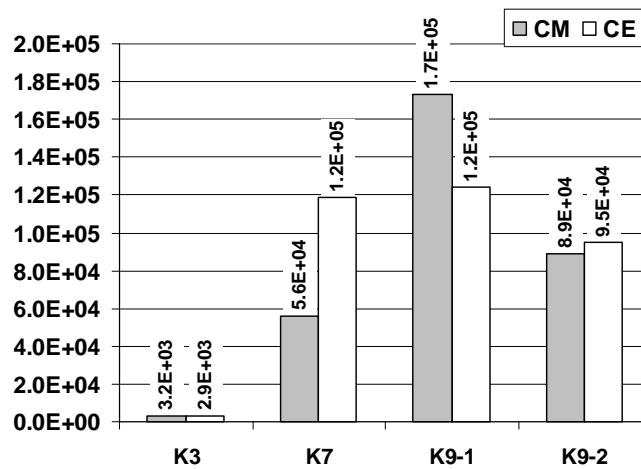


Figure 4 – ISUC index during micropitting test (CM – Mineral gear oil, CE - Ester gear oil).

The ferrograms (Hunt, 1993; Scott, 1975) obtained from each oil sample are shown in Table 6.

The ferrograms corresponding to the gear oil samples collected after load stage K3, contained large size wear particles, typical of the running-in period, and in great number, which were related to the medium-low quality of the teeth surface finishing of the gears used. The ferrograms corresponding to load stage K7 showed a significant increase on the number of wear particles generated inside the contact between the gear teeth (the dilution is now 0.1), but an important decrease on the size of those particles. However, typical micropitting fatigue particles, small and thin with straight borders, increased significantly.

The ferrograms prepared after load stage K9 showed a global increase of the severity and size of the wear particles, mainly of micropitting fatigue particles.

Assessment of micro-pitting failure is a difficult task to perform by visual inspection. It is often reported that with the gears mounted on the shafts, it is almost impossible to detect micropitting (Winter, 1987) and light of high intensity is needed to distinguish the grey stained area that micropitting resembles. To overcome this problem the gears were dismantled after each load stage and a digital camera was used to photograph the teeth. Table 7 shows the micropitting areas on the pinions which were surrounded by a red line for easier reading.

With both gear oils micropitting appeared during load stage K7 and became more severe during load stage K9, almost extending to all area below the pitch line of the pinion. The repetition of load stage K9 (K9-2) didn't change significantly the micropitting area although it got wider, covering completely the teeth width.

Above the pitch line normal mild wear of the teeth flanks also occurred with both gear oils, the grinding marks progressively disappeared and the surfaces got significantly smoother. Apparently, the gear lubricated with the ester oil had a higher wear volume above the pitch line generating a smoother surface than the mineral oil. During the repetition of load stage 9 (K9-2) the surfaces also present small adhesion marks along the radial sliding direction, with both gear oils, which is a typical event when the surfaces got too smooth above the pitch line.

CM – Mineral gear oil	CE – Ester gear oil
-----------------------	---------------------

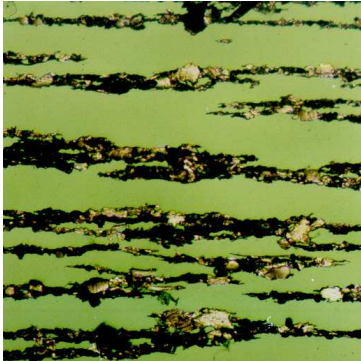
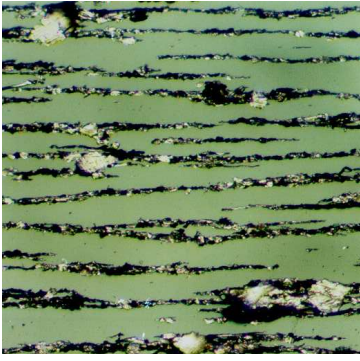
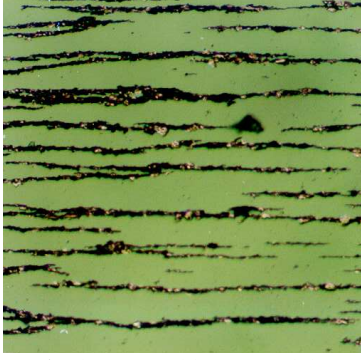
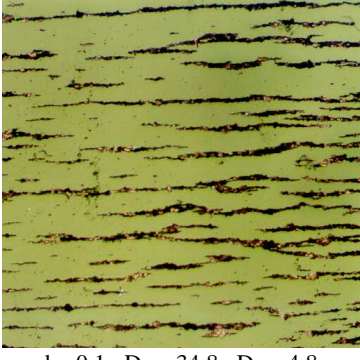
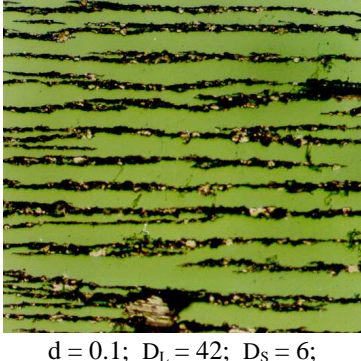
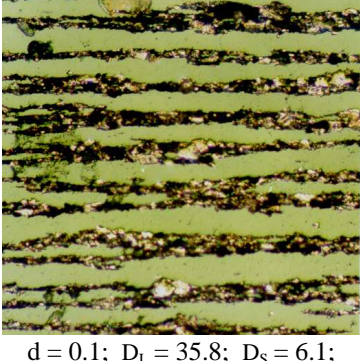
Running in, load stage K3		
	d = 1; D _L = 58; D _S = 11.1; CPUC = 69.1; ISUC = 3.2E3;	d = 1; D _L = 55.4; D _S = 12.6; CPUC = 68; ISUC = 2.9E3;
Load stage K7		
	d = 0.1; D _L = 23.9; D _S = 3.8; CPUC = 277; ISUC = 5.6E4;	d = 0.1; D _L = 34.8; D _S = 4.8; CPUC = 396; ISUC = 1.2E5;
Load stage K9		
	d = 0.1; D _L = 42; D _S = 6; CPUC = 480; ISUC = 1.7E5;	d = 0.1; D _L = 35.8; D _S = 6.1; CPUC = 419; ISUC = 1.2E5;

Table 6 – Ferrogram pictures after each load stage for micro-pitting tests CM and CE. Magnification = 200 x.

The micropitting area doubled its size from load stage K7 to load stage K9 and the repetition of load stage 9 (K9-2) only changed slightly the micropitting area (increasing it with the both lubricants). Micropitting didn't evolve onto other type of surface failure within the other two load stages but the affected area increased.

In general, the inspection of the teeth flanks showed that the gear lubricated with ester gear oil generated a micropitting area slightly higher than the gear lubricated with the mineral lubricant

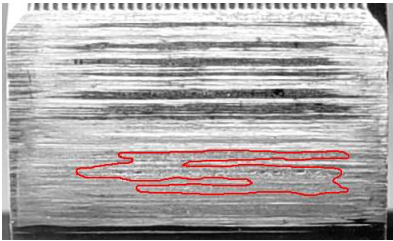
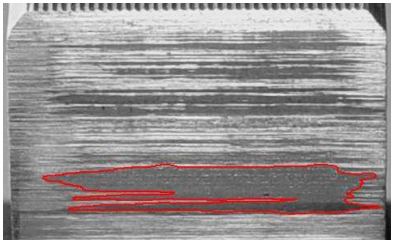
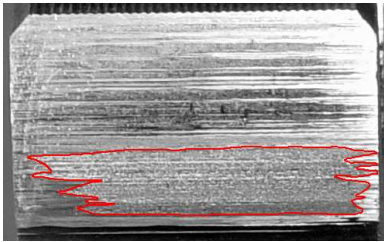
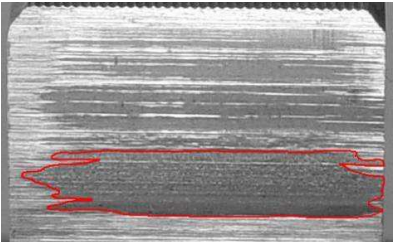
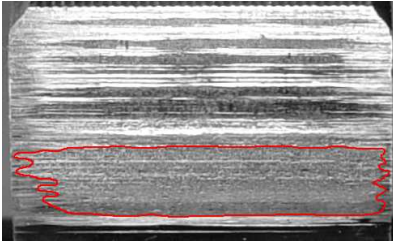
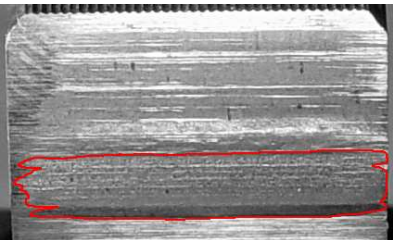
	CM – Mineral gear oil	CE – Ester gear oil
K7 T1 = 132.5 Nm n1 = 2250 rpm P = 31.2 kW	 Micropitted area = 10 %	 Micropitted area = 13 %
K9-1 T1 = 215.6 Nm n1 = 2250 rpm P = 50.8 kW	 Micropitted area = 24 %	 Micropitted area = 26 %
K9-2 T1 = 215.6 Nm n1 = 2250 rpm P = 50.8 kW	 Micropitted area = 28 %	 Micropitted area = 28 %

Table 7 – Pictures of pinion active teeth flank and micropitting area measurements.

Surface roughness measurements were made at the end of each load stage on several teeth flanks, below and above the pitch line and in different locations, as shown in Figure 5. An assessment length of 1.5 mm and a cut-off of 0.25 μ m were used.

The roughness profiles obtained below the pitch line are characteristic of the micropitting zone (designated *micro*) and the roughness profiles obtained above the pitch line are characteristic of the wear zone (designated *wear*). The roughness profiles measured before the tests (designated *original*) are representative of the teeth flanks after grinding.

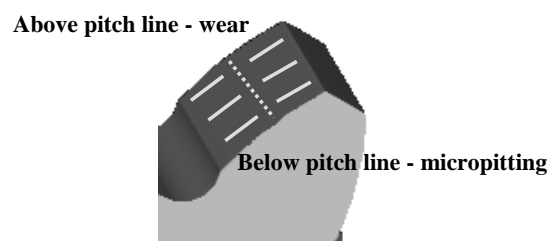


Figure 5 – Roughness measurements points on gear tooth.

The roughness parameters measured during the gear micropitting tests are presented in Table 8 and Table 9, for the gears lubricated with mineral and ester oils, respectively. The values presented are the average of the three measurements performed on two pinion teeth.

Below the pitch line, surface micropitting generated a significant increase of several roughness parameters, such as, R_{max} , R_{z-D} and R_{vk} in the gears lubricated with both oils. The augmentation of the R_{vk} parameter, related to surface roughness valleys, during the gear tests was a clear indication of the presence of micro-pits.

During the gear test with mineral oil the maximum value of R_{max} parameter ($R_{max} = 12.3\mu\text{m}$) was reached on load stage k7. From thereafter the evolution resulted in an increase of the micropitting area (see Table 7) and a slight decrease of R_{max} , R_{z-D} and R_{vk} parameters. In the gear test with ester oil the micropitting failure on load stage k7 was not as severe as with the mineral oil and the roughness parameters decreased slightly in the following load stages.

The value of R_{max} parameter after load stage 7 was $12.3\mu\text{m}$ and $7.7\mu\text{m}$ for the gears lubricated with the mineral and ester oil, respectively, which are similar to the depths of micro pits.

Above the pitch line the average roughness parameters R_{max} , R_{z-D} and R_{vk} decreased during the gear micropitting tests for both lubricants, due to the wear of the teeth flanks. Above pitch line there was no sign sustaining the presence of micropitting.

Mineral gear oil Pinion		R_{max} [μm]	R_{z-D} [μm]	R_a [μm]	R_{vk} [μm]
original		5.8	4.9	0.9	1.2
micro	K7	12.3	7.1	1.2	3.8
	K9-1	8.2	5.5	0.8	2.9
	K9-2	7.9	5.5	0.9	2.8
wear	K7	5.9	3.4	0.6	1.3
	K9-1	4.7	3.2	0.6	1.5
	K9-2	4.3	2.8	0.5	1.2

Table 8 – Roughness parameters on gear micropitting test with mineral oil.

Ester gear oil Pinion		R_{max} [μm]	R_{z-D} [μm]	R_a [μm]	R_{vk} [μm]
original		6.6	5.4	1.1	1.2
micro	K7	7.7	4.8	1.0	2.1
	K9-1	7.3	4.2	0.7	2.1
	K9-2	5.4	3.7	0.7	1.5
wear	K7	4.1	2.9	0.6	1.1
	K9-1	4.3	2.8	0.5	1.3
	K9-2	4.5	2.9	0.5	1.4

Table 9 – Roughness parameters on gear micropitting test with ester oil.

4 DISCUSSION

During the gear micropitting tests the mineral lubricant promoted, in general, a smaller mass loss than the ester lubricant. The total mass loss of the gear lubricated with ester lubricant (CE) was 11% larger than with mineral lubricant (CM), as shown in Table 10.

The evolution of ferrometric indexes CPUC and ISUC for carburized gears, lubricated with mineral and ester gear oils, showed a small increase during the test, till the end of load stage K9. On the repetition of load stage K9 (K9-2) the concentration of wear particles and the severity of wear decreased slightly, as shown in Figure 3. The percentage difference of ferrometric indexes, after each load stage, between the two lubricants (CM and CE gear tests) is shown on Table 11, being clear that both gear oils have a similar behaviour. The correlation between CPUC ferrometry results and mass loss measurements, shown in Figure 6, also indicate that both lubricants have very similar micropitting and wear behaviours.

The analytical ferrography results (ferrograms) of the lubricant samples collected during the gear micropitting tests with mineral (CM) and ester (CE) gear oils showed the presence of very large wear particles after running-in, which were due to the high initial roughness of the teeth flanks and the low manufacturing quality of the gears tested in relation to the GFKT test method. On subsequent load stage (K7) the number of large wear particles decreased substantially, but micropitting particles, characterised by their typical shape, borders and small size, were clearly detected, indicating that a contact fatigue phenomenon was going on. The ferrograms corresponding to the load stage K9 showed a significant increase of the number and size of contact fatigue particles because of the significantly higher contact pressure during this load stage.

The visual inspection of active teeth surface showed that micropitting only appeared below pitch line and normal mild wear occurred above the pitch line. Roughly the micropitting evolution was similar on both tests, although the ester lubricant (CE gear test) after load stage K7 displayed a larger micropitting area, around 30% larger, as showed on Table 12. On load stages K9-1 and K9-2, the micropitting area was similar.

The results obtained clearly show that it is possible to formulate biodegradable non-toxic gear oils with similar micropitting and wear performance of a typical mineral oil containing a special additive package to improve the micropitting resistance of the teeth flanks.

Beside, the biodegradable ester based lubricant generates a very significant reduction of the friction coefficient between the gear teeth, and thus of the gear power loss, as previous results have shown (Martins, 2005; Martins, 2006).

Mass Loss - Mineral Oil ML_{CM} [mg]	Mass Loss - Ester Oil ML_{CE} [mg]	$\frac{ML_{CE} - ML_{CM}}{ML_{CM}}$ [%]
114	127	11.4

Table 10 – Gear mass loss on micropitting tests with mineral and ester lubricants.

FZG load stage	K3	K7	K9-1	K9-2
$\frac{CPUC_{CE} - CPUC_{CM}}{CPUC_{CM}}$ [%]	-2	43	-13	7
$\frac{ISUC_{CE} - ISUC_{CM}}{ISUC_{CM}}$ [%]	-10	113	-28	6

Table 11 – Percentage difference in ferrometric indexes between mineral (CM) and ester (CE) gear oils.

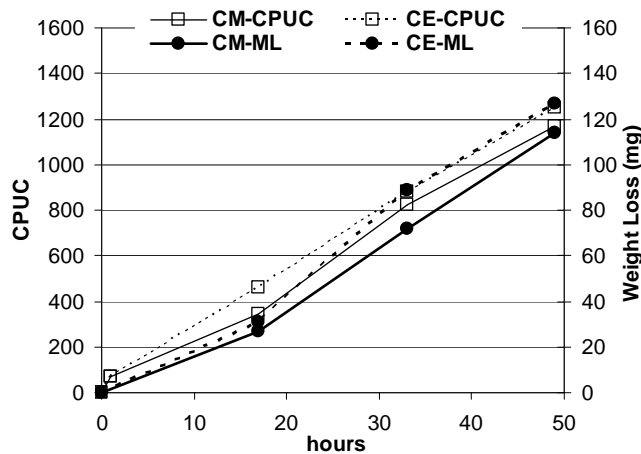


Figure 6 – Cumulative mass loss and cumulative CPUC index during gear micropitting tests with mineral (CM) and ester (CE) gear oils.

FZG load stage	K7	K9-1	K9-2
$\frac{(M_{micropitting} A_{rea})_{CE} - (M_{micropitting} A_{rea})_{CM}}{(M_{micropitting} A_{rea})_{CM}} [\%]$	30	8	0

Table 12 – Percentage difference in micropitting area between the ester (CE) and mineral oil (CM).

5 CONCLUSIONS

1. The biodegradable ester lubricant compared with the mineral lubricant conferred similar protection properties against micropitting failure, despite being slightly worst in terms of mass loss (**11%** higher cumulative mass loss).
2. The micropitting evolution during test procedure was similar for both lubricants.
3. The properties chosen to evaluate tests results are adequate and allow the analysis of surface evolution along test.
4. The mass loss and the direct ferrometry index are very well correlated.
5. The biodegradable ester lubricant has proved to be a valid solution for substituting environment harmful lubricants on gear lubrication.
6. The tests presented in this report are done with specimens (gears) of current quality that are able to preview the overall lubricant behaviour at much lower costs.

ACKNOWLEDGEMENTS

The authors express their gratitude to the European Union for the financial support given to this work through the Project: “EREBIO – Emission reduction from engines and transmissions substituting harmful additives in biolubricants by triboreactive materials” (Proposal n°. GRD2-2001-50119, Contract N° G3RD-CT-2002-00796-EREBIO)

The authors would also like to thank Dr. Rolf Luther from “FUCHS Petrolub AG” in Germany for the support and supply of ester biodegradable lubricant.

REFERENCES

- F. Antoine and J.-M. Besson (2002). "Simplified modellization of gear micropitting." ImechE **216, Part G**.
- A. Cardis and M. Webster (2000). "Gear oil micropitting evaluation." Gear Technology **17**(n° 5).
- DGMK Information sheet (2002). "Short Test Procedure for the investigation of the micropitting load capacity of gear lubricants."
- Forschungsvereinigung Antriebstechnik E.V (1993). "FVA Research Project Nr. 54/I-IV."
- T. Hunt (1993). Handbook of Wear Debris Analysis and Particle Detection in Liquids.
- K. Lipp and G. Hoffmann (2003). "Design for rolling contact fatigue." International Journal of Powder Metallurgy **n°39**.
- R. Martins, P. Moura, et al. (2005). "Power loss in FZG gears: Mineral oil vs. biodegradable ester and carburized steel vs. austempered ductile iron vs. MoS₂-Ti coated steel." VDI Berichte(1904 II): 1467-1486.
- R. Martins, J. Seabra, et al. (2006). "Friction coefficient in FZG gears lubricated with industrial gear oils: Biodegradable ester vs. mineral oil." Tribology International **39**(6): 512-521.
- D. Scott, W. Seifert, et al. (1975). "Ferrography—an advanced design aid for the 80's." WEAR (34): 251-260.
- H. Winter and K. Michaelis (1985). "FZG gear test rig - Description and possibilities." In: Coordinate European Council Second International Symposium on The performance Evaluation of Automotive Fuels and Lubricants.
- H. Winter and P. Oster (1987). "Influence of the Lubricant on Pitting and Micro Pitting (Grey Staining, Frosted Areas) Resistance of Case Carburized Gears – Test Procedures." AGMA.

A.3 Paper C

R. Martins, J. Seabra, A. Brito, C. Seyfert, R. Luther, and A. Igartua, "Friction coefficient in fzg gears lubricated with industrial gear oils: Biodegradable ester vs. mineral oil", Tribology International, vol. 39, no. 6, pp. 512-521, 2006.

Friction coefficient in FZG gears lubricated with industrial gear oils: Biodegradable ester vs. mineral oil

R. Martins^{a,*}, J. Seabra^b, A. Brito^c, Ch. Seyfert^d, R. Luther^d, A. Igartua^e

^aINEGI, Instituto de Engenharia Mecânica e Gestão Industrial, Porto, Portugal

^bDEMEGI, Faculdade de Engenharia da Universidade do Porto, Portugal

^cA. Brito, Indústria Portuguesa de Engrenagens L.da, Porto, Portugal

^dFUCHS Petrolub AG, Mannheim, Germany

^eFundación TEKNIKER, Eibar (Gipuzkoa), Spain

Received 16 November 2004; received in revised form 10 March 2005; accepted 17 March 2005

Available online 3 June 2005

Abstract

Two industrial gear oils, a reference paraffinic mineral oil with a special additive package for extra protection against micropitting and a biodegradable non-toxic ester, were characterized in terms of their physical properties, wear properties and chemical contents and compared in terms of their power dissipation in gear applications [Höhn BR, Michaelis K, Döbereiner R. Load carrying capacity properties of fast biodegradable gear lubricants. *J STLE Lubr Eng* 1999; Höhn BR, Michaelis K, Doleschel A. Frictional behavior of synthetic gear lubricants. *Tribology research: from model experiment to industrial problem*. Elsevier 2001; Martins R, Seabra J, Seyfert Ch, Luther R, Igartua A, Brito A. Power Loss in FZG gears lubricated with industrial gear oils: biodegradable ester vs. mineral oil. *Proceedings of the 31th Leeds-Lyon symposium on tribology*. Elsevier; to be published; Weck M, Hurasky-Schonwerth O, Bugiel Ch. Service behaviour of PVD-coated gearing lubricated with biodegradable synthetic ester oils. *VDI-Berichte Nr.1665 2002*.]. The viscosity–temperature behaviors are compared to describe the feasible operating temperature range.

Standard tests with the Four-Ball machine and the FZG test rig [Winter H, Michaelis K. FZG gear test rig—description and possibilities. In: *Coordinate European Council second international symposium on the performance evaluation of automotive fuels and lubricants*; 1985.] characterize the wear protection properties. Biodegradability and toxicity tests are performed in order to assess the biodegradability and toxicity of the two lubricants.

Power loss gear tests are performed on the FZG test rig using type C gears, for wide ranges of the applied torque and input speed, in order to compare the energetic performance of the two industrial gear oils. Lubricant samples are collected during and at the end of the gear tests [Hunt TM. *Handbook of wear debris analysis and particle detection in liquids*. UK: Elsevier Science; 1993.] and are analyzed by Direct Reading Ferrography (DR3) in order to evaluate and compare the wear particles concentration indexes of both lubricants.

An energetic model of the FZG test gearbox is developed, integrating the mechanisms of power dissipation and heat evacuation, in order to determine its operating equilibrium temperature. An optimization routine allows the evaluation of the friction coefficient between the gear teeth for each lubricant tested, correlating experimental and model results.

For each lubricant and for the operating conditions considered, a correction expression is presented in order to adjust the friction coefficient proposed by Höhn et al. [Höhn BR, Michaelis K, Vollmer T. *Thermal rating of gear drives: balance between power loss and heat dissipation*. AGMA Technical Paper; October 1996. pp 12. ISBN: 1-55589-675-8.] to the friction coefficient exhibited by these lubricants. The influence of each lubricant on the friction coefficient between the gear teeth is discussed taking into consideration the operating torque and speed and the stabilized operating temperature.

© 2005 Elsevier Ltd. All rights reserved.

1. Introduction

The main objective of this study is to compare the energetic performance of two industrial gear oils [1,3]: a reference mineral oil and a biodegradable non-toxic fluid. This comparison will end on the determination and comparison of the friction coefficient between gear teeth promoted by each lubricant.

* Corresponding author.

E-mail address: rcm@fe.up.pt (R. Martins).

Symbols

A_h (m ²)	horizontal surface area of case	T_w (°K)	wall temperature
A_i (m ²)	immersed area	V_{oil} (m ³)	oil volume
A_{rad} (m ²)	radiation surface area of case	X_L (–)	lubricant factor
A_v (m ²)	vertical surface area of case	b (mm)	face width
A_b (m ²)	base support area	d (m)	pitch diameter
F_a (N)	axial force	d_i (m)	shaft diameter
F_{bt} (N)	tooth normal force, transverse section	$f_{0,1}$ (–)	coefficients for bearings losses
F_r (N)	radial force	f_{cn} (–)	conduction coefficient
F_R (–)	Froud number	g_a (m)	length of recess path
L_{ca} (m)	characteristic horizontal length	g_f (m)	length of approach path
P_{fr} (W)	gear friction losses	H (m)	gear immersion depth
P_{in} (W)	input power	h_{ca} (m)	height of case
P_L (W)	total power losses	h_h (W/(m ² K))	natural convection coefficient, horizontal surface
P_{M0} (W)	load independent losses of bearings	h_v (W/(m ² K))	natural convection coefficient, vertical surface
P_{M1} (W)	load dependent losses of bearings	N (rpm)	input rotating speed
P_{sl} (W)	seal losses	p_b (m)	base pitch
P_{spl} (W)	gear churning losses	$V_{\Sigma c}$ (m/s)	sum velocity at pitch point
Q_{cn} (W)	conduction heat	z_i (–)	number of teethes
Q_{cn}^{rad} (W)	conduction heat due to radiation	α_{rad} (W/(m ² K))	radiation heat transfer coefficient
Q_{cn}^{ncv} (W)	conduction heat due to natural convection	ε (–)	case surface emissivity
Q_{cnv} (W)	natural convection heat	η_{oil} (mPa s)	dynamic oil viscosity
Q_H (W)	total heat evacuated	μ_m (–)	mean friction coefficient
Q_{rad} (W)	radiation heat	ρ (kg/m ³)	specific weight
Ra (µm)	mean roughness	ρ_c (mm)	equivalent curvature radius at pitch point
Re (–)	Reynolds number		
T (m)	bearing mean diameter		
T_a (°K)	ambient temperature		

The thermal equilibrium of a gearbox is reached when the operating temperature stabilizes, i.e. when the power dissipated inside the gearbox is equal to the heat evacuated from gearbox to the surrounding environment. The equilibrium temperature is dependent of the gearbox characteristics and of the lubricant properties [7–10]. The higher the power losses the higher will be the equilibrium temperature of the gearbox. A lower stabilization temperature means higher efficiency, lower friction coefficient, smaller oil oxidation and longer oil life [2].

2. Lubricants

Environmental awareness leads to a growing interest in biodegradable non-toxic lubricants. However, the key aspect for any industrial application is technical performance and technical advantages proved in dedicated tests.

Environmental compatibility is usually viewed in respect to biodegradability and toxicity. While the first issue is reached by using a suitable bio-degradable base fluid, low toxicity requires an additivation that is environmentally friendly [4], too. However, lubricant performance (friction, wear, lifetime, load bearing, efficiency, etc.) has a major

impact on its overall environmental compatibility. Premature wear, high energy needs are as well harmful to the environment.

Two industrial gear lubricants are tested and compared: a reference ISO VG 150 mineral oil, containing an additive package to improve micro-pitting resistance, and an ISO VG 100 biodegradable ester lubricant with a low toxicity additivation. Both oils are specified as CLP gear oils according to DIN 51517. The main properties of the two lubricants are shown in Table 1.

2.1. Chemical properties

The reference gear oil is based on a paraffinic mineral oil with significant residual sulphur content. It contains an ashless antiwear additive package based on phosphorous and sulphur chemistry and metal–organic corrosion preventives.

In contrast, the biodegradable product uses a fully saturated ester based on harvestable materials. The absence of unsaturated bonds in this base fluid leads to excellent thermal and oxidative stability. To combine the desired low toxicity with superior gear performance, environmentally compatible, highly efficient additives have been selected. Metal–organic compounds have been completely avoided.

Table 1
Lubricants properties

Parameter (unit)	Desig.	Method	Lubricating oils	
Base oil (<i>l</i>)	/	DIN 51451	paraffinic mineral oil	saturated ester
<i>Physical properties</i>				
Density at 15 °C (g/cm ³)	ρ_{15}	DIN 51757	0.897	0.925
Kinematic viscosity at 40 °C (cSt)	ν_{40}	DIN 51562	146	99.4
Kinematic viscosity at 100 °C (cSt)	ν_{100}	DIN 51562	14.0	14.6
Viscosity index (<i>l</i>)	VI	DIN ISO 2909	92	152
Pour point (°C)		DIN ISO 3016	–21	–42
Thermal expansion [15] (g/cm ³ °C)	α_v		7.16×10^{-4}	8.05×10^{-4}
<i>Wear properties</i>				
VKA weld load (N)	/	DIN 51350-2	2200	2200
VKA wear scar (1 h/300 N) (mm)	/	DIN 51350-3	0.32	0.35
Brugger (N/mm ²)	/	DIN 51347-2	68	37
FZG rating (<i>l</i>)	K_{FZG}	DIN 513540	> 12	> 12
<i>Biodegradability and toxicity properties</i>				
Ready biodegradability (%)		OECD, 301 B	< 60	≥ 60
Aquatic toxicity with <i>Daphnia</i> (ppm)	EL ₅₀	OECD, 202	-	> 100
Aquatic toxicity with <i>Alga</i> (ppm)	EL ₅₀	OECD, 201	-	> 100

2.2. Physical properties

The physical properties of both industrial gear oils display a significant difference in rheology between the two oils: they have almost identical viscosities at 100 °C but the ester gear oil has much lower viscosity at lower temperatures. This is caused by the higher viscosity index of the ester product. This beneficial property leads to a wider range of operational temperature compared to the mineral oil. This can also be seen from the pour point that is 20 °C lower for the ester than for the mineral oil.

Thermal expansion and density of the ester gear oil are higher than those of the mineral oil.

The pressure–viscosity parameter is always larger for the mineral oils than for the ester oils and must be accounted [11,12].

2.3. Standard mechanical tests

The VKA weld load is an extreme pressure test to determine the additives response at welding conditions. Both lubricants withstand a mean pressure of approximately 5500 N/mm² (for a four-ball load of 2200 N) without seizure.

Considering the extreme pressure performance judged by the Brugger test, there is a considerable higher value for the mineral oil than for the ester. Both values are higher than the value considered sufficient for hydraulic oils (30 N/mm²) but only the mineral supersedes the value usually stated for transmission oils (50 N/mm²).

Summarizing these mechanical tests (see Table 1), both lubricants have almost the same performance and can both be considered suitable for a wide range of gear applications.

2.4. Biodegradability and toxicity properties

Standardised and internationally recognised test methods are available for determining the biodegradability (OECD

301B) and environmental toxicity (OECD 201, OECD 202) of lubricants and their components.

The mineral oil did not match the minimum requirements of 60% biodegradability in 28 days, thus any toxicity test were performed for this lubricant.

The ester based oil exceeded the minimum requirements of 60% biodegradability in 28 days and pass both toxicity tests, OECD 201 and OECD 202 as shows Table 1.

3. Gear power loss tests

3.1. FZG gear test rig and type C gears

Fig. 1 shows a schematic view of the FZG back-to-back spur gear test rig [5].

FZG type C gears, made of 20MnCr5 steel, carburised, quenched and oil annealed are used. Their characteristics are shown in Table 2. Both gears are run-in before

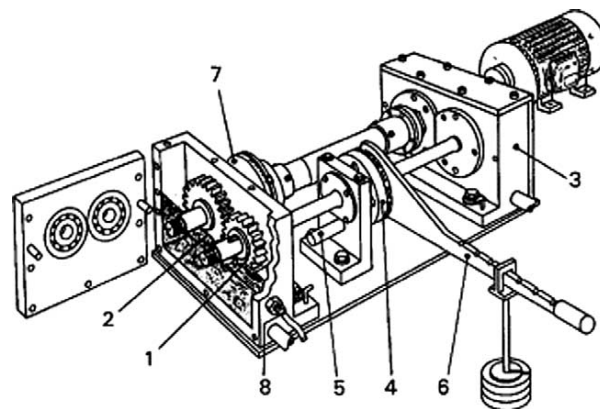


Fig. 1. Schematic view of FZG gear test rig.

Table 2
Characteristics of FZG type C gears

Parameter (unit)	Pinion	Wheel
Number of teeth (<i>i</i>)	16	24
Module (mm)	4.5	
Center distance (mm)	91.5	
Addendum diameter (mm)	82.45	118.35
Pressure angle (°)	20	
Addendum modification (<i>i</i>)	+0.182	+0.171
Face width (mm)	14	
Ra ($\lambda_c=0.25$ mm) (μm)	0.2	
Hardness (HRC)	58 a 62	
Young module (Pa)	206×10^9	
Poisson coefficient (<i>i</i>)	0.3	
Specific heat (Nm/(kg K))	450	
Thermal conductivity (N/(s K))	50	
Specific weight (kg/m^3)	7850	

performing the power loss tests. The gears are dip lubricated with an oil volume of 1.5 l.

3.2. Operating conditions

Each lubricant is submitted to a set of gear tests performed in a wide range of speed and torque conditions, as well as input power, as shown in Table 3.

The first 3 tests are performed at very low torque (*no-load tests*) corresponding to FZG load stage 1 ($T_2=4.95$ Nm) and three different speeds, in order to evaluate the influence of the oil on the churning losses. The no-load tests lasted for 2 h at each operating speed. The initial oil bath temperature is approximately room temperature ($\cong 20$ °C).

The other nine tests (*load tests*) are performed at three different speeds (1000, 2000 and 3000 rpm) and three increasing torque levels, corresponding to FZG load stages 5, 7 and 9 and to Hertzian contact pressures (at pitch point) of 0.92, 1.29, 1.65 GPa, respectively. Each load test lasted 4 h, in order to attain the equilibrium temperature. Each load test began at approximately 40 °C and the oil sump temperature is free.

Table 3
Operating conditions used in the power loss tests

Test type	Wheel speed (rpm)	Wheel torque (Nm)	Input power (kW)	No. of cycles ($\times 10^6$)
No load tests	1000	4.95	0.52	0.72
	2000		1.04	
	3000		1.56	
Load tests	1000	141.15	14.78	0.72
		275.10	28.81	
		453.00	47.44	
	2000	141.15	29.56	1.44
		275.10	57.62	
		453.00	94.88	
	3000	141.15	44.34	2.16
		275.10	86.43	
		453.00	142.31	

A maximum oil sump temperature of 180 °C is imposed for protection of the test rig.

During the load tests and after each testing speed (1000, 2000 and 3000 rpm) lubricant samples are collected for direct reading ferrometry and viscosity measurements.

3.3. Stabilisation temperature

Fig. 2 displays the evolution of the oil sump temperature during the tests performed at 3000 rpm with mineral and ester oils.

At low torque (5 Nm) the oil temperature evolution and stabilization is very similar for both oils.

At higher torques the mineral lubricant always shows a faster rise temperature than the ester lubricant. This difference increases with the increasing torque.

The largest difference in stabilization temperature occurred for the highest torque (453 Nm), when the mineral oil reached the limiting temperature of 180 °C after 112 min, while the ester oil attained 156 °C in the same period and reached a stabilized temperature of 170 °C after 240 min.

Fig. 3 displays the stabilized temperature measured in each test in function of the input speed and torque.

The difference in stabilization temperature between the two oils goes from 2 to 15 K, depending on the operating conditions. For the highest input power (142 kW) the difference is above 30 K and the mineral oil reached the limiting temperature.

In the case of the no-load tests, performed at very low torque (5 Nm), such difference depends mainly on the viscosity and specific weight of the lubricants. The tests performed at 1000 and 2000 rpm generate low stabilization temperatures at which the viscosity of the mineral oil is significantly higher than that of the ester oil, making its stabilized temperature higher. For the test performed at 3000 rpm, the stabilization temperature reaches approximately 75 °C. At this temperature the viscosities of both oils

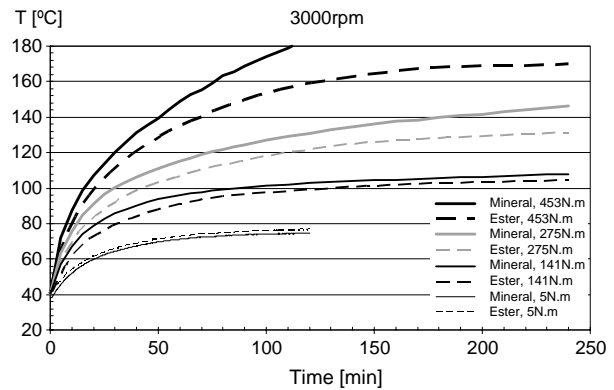


Fig. 2. Oil sump temperature for mineral and ester oils at 3000 rpm for different input torque values.

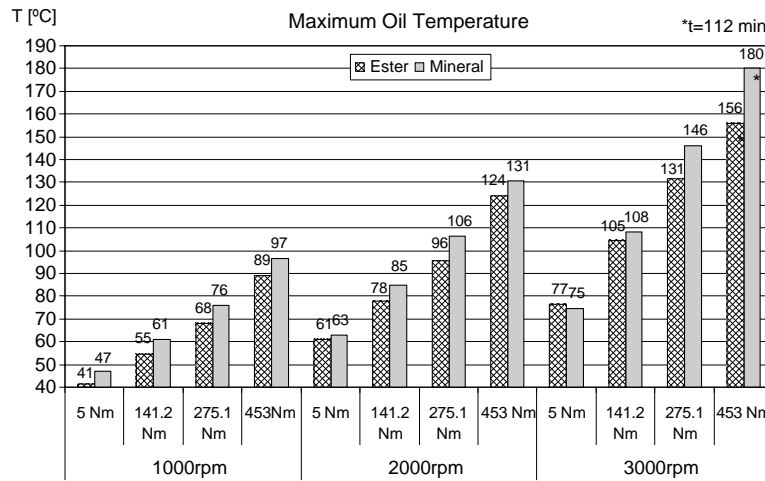


Fig. 3. Stabilized oil sump temperature vs. input speed and torque for ester and mineral industrial gear oils.

are similar, but the ester oil has a higher specific weight leading to a higher stabilization temperature than the mineral oil.

These results indicate that the churning losses are similar for both oils at typical gearbox operating temperatures (between 70 and 80 °C) and for the same operating speed.

For all the other tests at higher operating torques the stabilized temperature of the mineral oil is always higher than that of the ester oil, suggesting that the friction power loss inside the contact between gear teeth is considerably smaller for the ester oil.

These differences in stabilisation temperature and in friction power losses between the two oils, at identical operating conditions, are due to the smaller friction coefficient between the gear teeth and in the bearings provided by the ester oil. The increasing differences in stabilisation temperatures with increasing torques, between the mineral and ester oils, suggests that the difference in friction coefficient between the oils also increases with increasing torques.

3.4. Oil analysis

For each lubricant three samples were collected after the load tests at 1000, 2000 and 3000 rpm. These samples were analysed by direct Reading Ferrometry to evaluate the amount of particles and their sizes. The results are the ferrometric parameters D_1 (large wear particles index) and D_s (small wear particles index). The values of D_1 and D_s are used to evaluate the concentration of wear particles index (CPUC) and the severity of wear particles index (ISUC), defined as $CPUC = D_1 + D_s/d$, $ISUC = D_1^2 - D_s^2/d^2$, where d stands for the oil sample dilution. The CPUC grows when the sum of the small and the large particles increase, while the ISUC index grows when the difference between large particles and small particles increase.

Fig. 4 shows the evolution of CPUC and ISUC indexes along tests. It is clear that the mineral oil presents significantly higher CPUC and ISUC values than the ester

oil, meaning that the wear particles released with the mineral oil have a larger size and are in major number. This difference becomes larger for the tests performed at 2000 and 3000 rpm.

Elemental analysis of both oils, performed at the end of the tests using RFA [13], show that the iron content of both oils is rather low. However, the mineral oil shows 2–3 times higher iron contents than the ester product. This corroborates the higher wear rate of the mineral oil in these tests.

An important reason for the higher wear rate of the mineral oil is that its higher friction leads to oil temperatures well above those indicated for mineral oils. The stabilized temperature reached 131 °C at 2000 rpm and supersedes

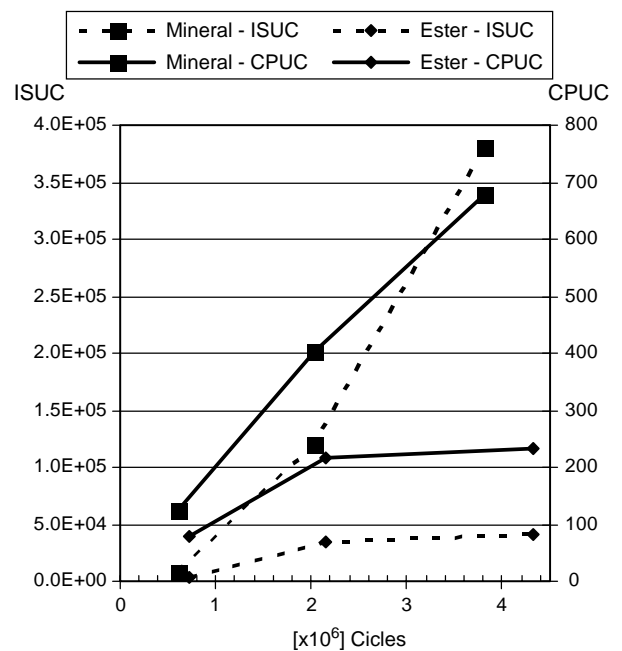


Fig. 4. Evolution of CPUC and ISUC index during the power loss tests for both industrial gear oils.

Table 4
Viscosity [14], viscosity index and Iron content (RFA [13]) values, measured before and after power loss tests for both lubricants

		Fresh oil	Used oil	Variation (%)
Mineral	ν_{40}	144.5	145.8	+0.9
	ν_{100}	14.0	14.1	+0.7
	VI	92	94	+3
	Fe	0	18 ppm	n.d.
Ester	ν_{40}	99.4	100.2	+0.8
	ν_{100}	14.6	14.6	0
	VI	150	150	0
	Fe	0	5 ppm	n.d.

180 °C at 3000 rpm for the highest applied torque ($T_2 = 453$ Nm), as indicated in Fig. 3, which are significantly above the maximum temperature a mineral oil can stand.

The kinematic viscosity [14] of both lubricants was measured before and after the power loss tests and the results are presented in Table 4. No significant change can be observed, indicating that both oils show no sign of oxidative degradation.

4. Energetic balance of the FZG test gearbox

Fig. 5 shows a schematic view of the FZG test gearbox. The different mechanisms of power dissipation and heat evacuation are also indicated. The thermal equilibrium of a gearbox is attained when the power losses are equal to the evacuated heat.

The main mechanisms of power dissipation inside a gearbox are the churning losses and the frictional losses [7–10], in which the lubricant has capital influence. These power losses are usually called the no-load power losses and the load power losses, respectively. The no-load losses are related with moving parts immersed in the lubricant and the load power losses result from contacting bodies with relative movement (see Fig. 5).

The heat evacuation is made essentially by three modes: conduction, radiation and convection.

The churning losses are related with moving parts immersed in the lubricant which depends mainly on the lubricant, speed and parts geometry. The main sources of churning losses are the gear, the bearings and the seals.

The gear churning losses are dependent of gear geometry, immersion depth, rotating speed and gears immersed area as well as lubricant viscosity and density. Other influencing parameters are the gearbox geometry and the fluid flow inertial, viscous and gravitational forces [8]. The gear churning losses (P_{spl}) are defined as

$$P_{spl} = \frac{\pi}{30} \cdot n \cdot \left(\frac{1}{2} \cdot \rho \cdot \left(\frac{\pi \cdot n}{30} \right)^2 \cdot A_i \cdot \left(\frac{d}{2} \right)^3 \right) \cdot \left(\left(\frac{2 \cdot h}{d} \right)^{0.45} \cdot \left(\frac{V_{oil}}{d} \right)^{0.1} \cdot F_R \cdot Re^{-0.21} \right) \quad (1)$$

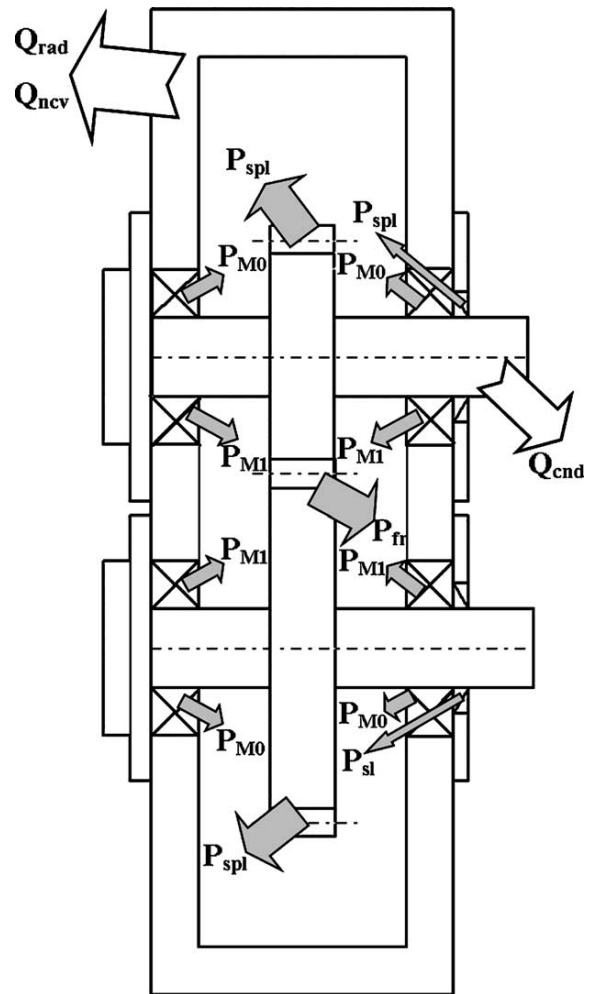


Fig. 5. Schematic view of the FZG test gearbox and of the different mechanisms of power dissipation and heat evacuation.

The bearing churning losses (P_{M0}) depend mainly on the rotating speed, mean diameter, bearing type and lubricant viscosity [10], that is,

$$P_{M0} = \frac{\pi}{30} \cdot n \cdot (f_0 \times 10^{-7} \cdot (n \cdot \eta_{oil})^{2/3} \cdot T^3) \cdot 10^{-3} \quad (2)$$

The seal losses (P_{sl}) depend on the rotating speed and seal interior diameter [6], and may be represented as

$$P_{sl} = 7.69 \times 10^{-6} \cdot d_i \cdot n \quad (3)$$

The frictional losses are related with moving parts in contact between them. The main sources of frictional losses are the gears and the roller bearings.

The gear friction losses (P_{fr}) depend on the gear geometry, the numbers of teeth, the operating conditions and the friction coefficient between the contacting teeth [7,8], being

defined as

$$P_{fr} = \pi \cdot \left(\frac{1}{z_1} + \frac{1}{z_2} \right) \cdot \left(1 - \left(\frac{g_f + g_a}{p_b} \right) + \left(\frac{g_f}{p_b} \right)^2 + \left(\frac{g_a}{p_b} \right)^2 \right) \cdot P_{in} \cdot \mu_m \quad (4)$$

The rolling bearing friction losses (P_{M1}) depend on the applied load, type of bearing, bearing diameter and friction coefficient in bearing contact [10], that is

$$P_{M1} = \frac{\pi}{30} \cdot n \cdot \left(\sqrt{F_r^2 + F_a^2} \cdot f_l \cdot T \right) \quad (5)$$

Thus the total power loss inside the FZG test gearbox is given by

$$P_L = P_{fr} + P_{M1} + P_{spl} + P_{M0} + P_{sl} \quad (6)$$

The main mechanisms of heat evacuation from the FZG test gearbox are conduction, radiation and convection. All these heat evacuation mechanisms depend on the case temperature which in the case of FZG test gearbox is almost the same as the oil temperature (when dip lubrication is used).

The natural convection of the test gearbox is split in two parts, the vertical wall and the horizontal wall. The convection coefficient is dependent on a characteristic dimension and on the wall and ambient temperatures. The vertical and horizontal coefficients of natural convection (h_v and h_h) are, respectively [8],

$$h_v = 11.06 \cdot h_{ca}^{-0.1} \cdot \left(\frac{T_w - T_a}{T_a} \right)^{0.3} \quad (7)$$

$$h_h = 12.87 \cdot L_{ca}^{-0.04} \cdot \left(\frac{T_w - T_a}{T_a} \right)^{0.32} \quad (8)$$

The total heat evacuated by natural convection (Q_{ncv}) is defined by

$$Q_{ncv} = h_v \cdot A_v \cdot (T_w - T_a) + h_h \cdot A_h \cdot (T_w - T_a) \quad (9)$$

The heat evacuated by radiation (Q_{rad}) is based on the Stefan Boltzmann law using a radiation coefficient [7]. The radiation coefficient (α_{rad}) and the evacuated heat are, respectively,

$$\alpha_{rad} = 0.23 \times 10^{-6} \cdot \varepsilon \cdot \left(\frac{T_w + T_a}{2} \right)^3 \quad (10)$$

and

$$Q_{rad} = \alpha_{rad} \cdot A_{rad} \cdot (T_w - T_a) \quad (11)$$

The heat conduction is the most complex form of heat transfer on the FZG test gearbox because the heat transfer is bidimensional and the gearbox support geometry is very complex. An accurate solution for this problem requires a complex numerical solution.

Winter et al. [9] proposes the substitution of the heat conduction calculation by an increase of convection and

radiation areas by 1.5–2.5 times (f_{cn} factor) the gearbox base contact area (conduction area, A_b).

Then increase of radiation heat due to conduction is expressed as:

$$Q_{cn}^{rad} = \alpha_{rad} \cdot (T_w - T_a) \cdot (f_{cn} \cdot A_b) \quad (12)$$

The area increase in the natural convection term must be split in two parts (vertical convection and horizontal convection). This separation is done proportionally to the original areas, i.e. the increase of vertical wall surface is proportional to its relation with total surface area submitted to natural convection ($A_v + A_h$), so the proportion factor is ($A_v / (A_v + A_h)$). The same rule is applied to the top horizontal surface, resulting in a proportion factor of ($A_h / (A_v + A_h)$). Thus the increase in natural convection heat due to conduction becomes:

$$Q_{cn}^{ncv} = h_v \cdot (T_w - T_a) \cdot f_{cn} \cdot A_b \cdot \left(\frac{A_v}{A_v + A_h} \right) + h_h \cdot (T_w - T_a) \cdot f_{cn} \cdot A_b \cdot \left(\frac{A_h}{A_v + A_h} \right) \quad (13)$$

Thus the total heat evacuated by conduction is given by,

$$Q_{cn} = Q_{cn}^{rad} + Q_{cn}^{ncv} \quad (14)$$

So, the total heat evacuated from the FZG test gearbox becomes:

$$Q_H = Q_{rad} + Q_{cnv} + Q_{cn} \quad (15)$$

The energetic equilibrium of the FZG test gearbox is reached when the power dissipated equals the heat evacuated, that is $P_L = Q_H$, or

$$P_{fr} + P_{M1} + P_{spl} + P_{M0} + P_{sl} = Q_{rad} + Q_{cnv} + Q_{cn} \quad (16)$$

Eq. (16) establishes an approximated model for the energetic behavior of the FZG test gearbox, allowing the determination of the oil temperature in permanent conditions (stabilized temperature) for any combination of the operating conditions imposed to the FZG test rig.

Eq. (16) depends on five unknown variables: the oil stabilized temperature (T_{oil}), the gearbox wall temperature (T_w), the ambient temperature (T_a), the heat conduction factor (f_{cn}) and the friction coefficient between the gear teeth (μ_m).

The three temperatures, (T_{oil} , T_w and T_a), are measured during the FZG gear tests. The heat conduction factor and the friction coefficient between gear teeth can be obtained from the correlation between experimental and model oil temperature results.

A parameter adjustment routine using the least squares method has been implemented in order to optimize the heat conduction parameter f_{cn} and the lubricant friction coefficient μ_m using the experimental results obtained in the FZG power loss tests.

Other parameters may also be optimized from the correlation between experimental and model results, but

their influence on the overall result is much smaller. This is the case of the rolling bearing parameters (f_0 and f_1) and of the natural convection coefficients (h_v and h_h).

5. Friction coefficient between gear teeth

5.1. Optimized heat conduction factor

The optimization of the heat conduction factor (f_{cn}) is performed using the No-Load power loss experimental results obtained for both lubricants. Using the set of results obtained for each lubricant, the f_{cn} factor is determined in order to minimize the difference between the power losses and the heat evacuation. The optimized value is $f_{cn}=2.5$, that was validated for both sets of experimental results. This result also allows a first validation of the energetic model implemented.

Fig. 6 shows the stabilized oil bath temperatures measured at the end of the No-Load power loss tests and the corresponding values determined using the model developed and the optimized value of heat conduction factor f_{cn} . The correlation coefficient is above 99%. Fig. 6 also shows that the churning losses are correctly evaluated using the model implemented.

5.2. Optimized friction coefficient between gear teeth

According to Höhn et al. [7], the average friction coefficient between gear teeth may be defined as:

$$\mu_m = 0.048 \cdot \left(\frac{F_{bt}/b}{v_{\Sigma c} \cdot \rho_c} \right)^{0.2} \cdot \eta_{oil}^{-0.05} \cdot Ra^{0.25} \cdot X_L \quad (17)$$

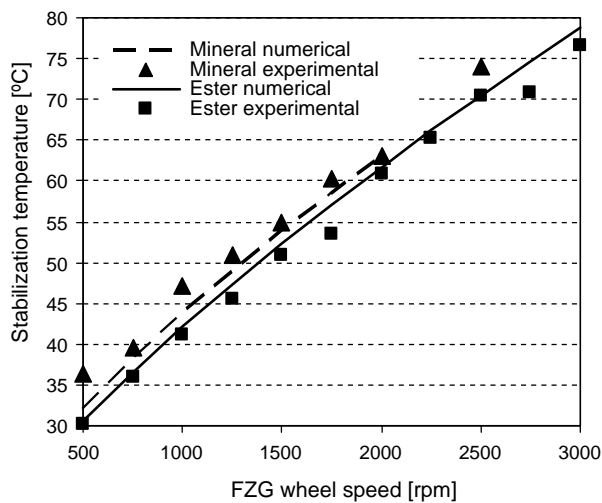


Fig. 6. Experimental vs. simulation stabilized oil sump temperature in No-Load tests. Influence of wheel input speed and oil type (ester or mineral).

where X_L is a parameter that allows the correction of the friction coefficient for each lubricant. Typically $X_L=1$ for additive free mineral oils. This lubricant parameter has different values for different commercial lubricants, since each lubricant is made of a given base oil and contains a particular additive package. This is the case of the two lubricants considered in this work.

Fig. 7 shows the stabilized oil temperatures measured in the power loss tests for both lubricants and calculated using the energetic model implemented, considering a lubricant factor $X_L=1$. A significant difference is observed between experimental and model results, mostly for the highest loads. These results clearly indicate that the load (applied torque) is one of the most important parameters to be considered and that the oil type and the additive package have a significant influence in the results obtained.

Considering that the lubricant parameter X_L is defined as

$$X_L = \frac{a}{(var_1)^{b1} \dots (var_n)^{bn}} \quad (18)$$

it can be optimized for each lubricant correlating the model to the experimental results. The optimization process takes into account all the variables 'var', that is, the applied load (F_{bt}) the oil viscosity (η) and the rolling speed ($v_{\Sigma c}$).

Within the range of operating conditions used, the best correlations are obtained for a load dependent lubricant parameter X_L , independent of the oil viscosity and rolling speed, that is,

$$X_L = \frac{1}{(F_{bt}/b)^{b1}} \quad (19)$$

The constant a (see Eq. (16)) is equal to 1 for both oils and the power constant $b1$ is equal to 0.0651 for the mineral

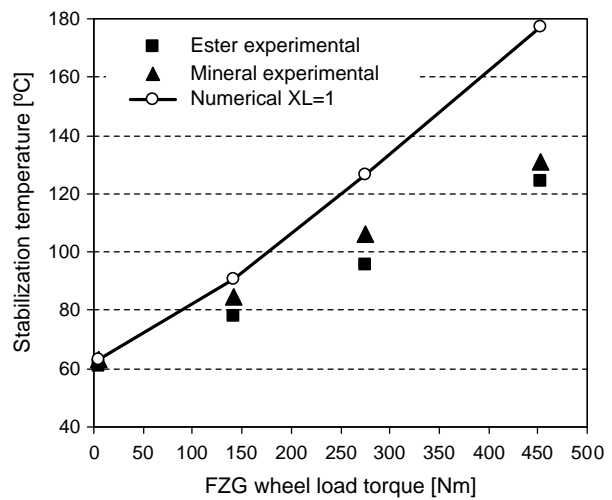


Fig. 7. Experimental stabilization temperature at 2000 rpm vs. numerical result considering the lubricant parameter $X_L=1$.

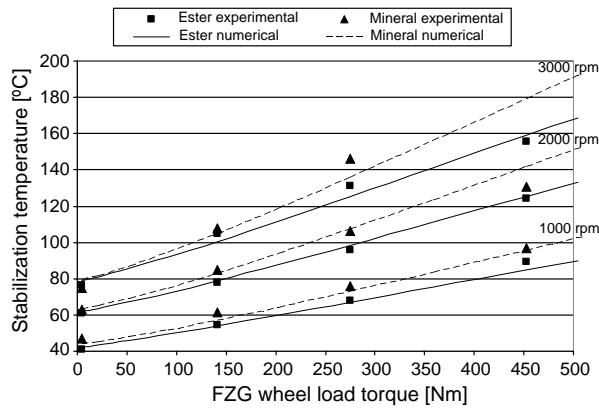


Fig. 8. Experimental vs. numerical stabilization temperatures. Influence of applied torque and speed.

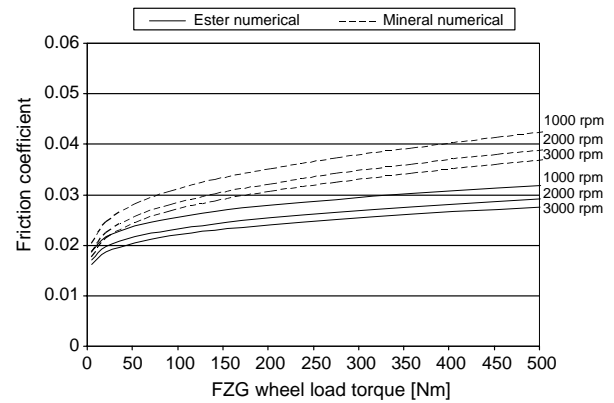


Fig. 9. Predicted friction coefficient between gear teeth for ester and mineral oils at predicted stabilization temperatures, depending on the wheel applied torque and speed.

oil and equal to 0.1055 for the ester oil. The overall correlation coefficient between the experimental and numerical results is above 99% for both lubricants. This X_L lubricant parameter represents a reduction of the influence of the load on the friction coefficient between gear teeth.

The optimized value for the average friction coefficient between gear teeth for the mineral and ester oils tested become, respectively,

$$\mu_m = 0.048 \cdot \left(\frac{F_{bt}/b}{v_{\Sigma c} \cdot \rho_c} \right)^{0.2} \cdot \eta_{oil}^{-0.05} \cdot Ra^{0.25} \cdot \frac{1}{(F_{bt}/b)^{0.0651}} \quad (20)$$

$$\mu_m = 0.048 \cdot \left(\frac{F_{bt}/b}{v_{\Sigma c} \cdot \rho_c} \right)^{0.2} \cdot \eta_{oil}^{-0.05} \cdot Ra^{0.25} \cdot \frac{1}{(F_{bt}/b)^{0.1055}} \quad (21)$$

5.3. Discussion

Fig. 8 shows the experimental stabilization temperatures obtained in the FZG gear power loss tests and the corresponding numerical results obtained using the optimized friction coefficients. It is clear that the agreement between experimental and numerical values is quite good.

Fig. 9 shows the predicted friction coefficient between gear teeth using expressions (20) and (21) for the mineral and the ester oils. The friction coefficient displayed is calculated at the determined stabilization temperature for each load and speed operating condition. The gap in friction coefficient between the two lubricants increases with increasing torques and the mineral oil always presents the highest friction coefficient for the same operating conditions.

These results are totally in agreement with the stabilized temperatures measured in the FZG power loss tests performed, justifying the lower temperatures obtained with the ester oil.

Höhn et al. [2] made measurements of friction coefficient on the FZG test rig for different lubricants, among them are a mineral and an ester base fluid, both ISO VG 150. Fig. 10 displays the results of those measurements, as well as the corresponding results obtained with the model developed in this work and the result corresponding to the reference oil ($X_L=1$).

The agreement between the experimental values obtained by Höhn and the results predicted by the model are quite good, taking into account that the base oils and the corresponding additive packages used by Höhn are not the same used in this work.

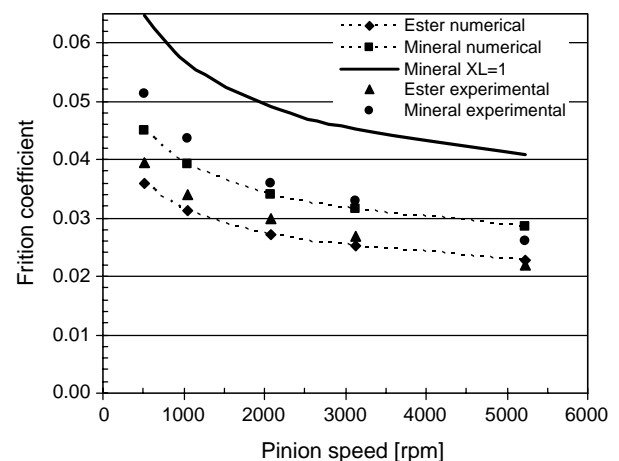


Fig. 10. Friction coefficient measurements [2] (mineral/ester experimental, both ISO VG 150) and numerical results using expressions (20) (mineral), (21) (ester) and (17) using $X_L=1$ (mineral lubricant). $T_{oil}=90$ °C, $p_H=1.1$ GPa.

6. Conclusions

The following conclusions may be drawn from this work:

1. Both lubricants present excellent results in standard mechanical tests.
2. The churning losses at the FZG power loss tests are identical for both lubricants.
3. The ester oil presented a smaller stabilized oil temperature on the FZG power loss tests for the same operating conditions, suggesting it promotes a smaller friction coefficient between the gear teeth.
4. The difference in the stabilization temperature between the two lubricants increases with increasing torques.
5. The mass loss along tests is larger for the mineral oil. This fact is confirmed by Direct Reading Ferrometry and by RFA.
6. The mineral oil operated for a large period at temperatures above 100 °C, leads to the excessive amount of wear particles when compared with the ester oil in the same conditions.
7. The energetic balance model developed simulates quite well the power dissipation vs. heat evacuation behavior of the FZG test gearbox.
8. The optimization process developed allows the correction of the friction coefficient between gear teeth, through the X_L parameter, adapted to the physical and chemical properties of each lubricant.
9. The friction coefficient reduction promoted by the ester oil, when compared with the mineral lubricant used, exceeds 20% for the highest contact pressures.
10. The optimized friction coefficient of each lubricant is significantly smaller than predicted by Höhn et al. for the reference lubricant. These results are in agreement with the measurements made on an FZG machine by Höhn et al. [2].

Acknowledgements

The authors express their gratitude to the European Union for the financial support given to this work

through the GROWTH Project No. GRD2-2001-50119, Contract No. G3RD-CT-2002-00796-EREBIO, 'EREBIO—Emission reduction from engines and transmissions substituting harmful additives in biolubricants by triboreactive materials'.

References

- [1] Höhn B-R, Michaelis K, Döbereiner R. Load carrying capacity properties of fast biodegradable gear lubricants. *J STLE Lubr Eng* 1999.
- [2] Höhn B-R, Michaelis K, Doleschel A. Frictional behavior of synthetic gear lubricants. *Tribology research: From model experiment to Industrial Problem*. Amsterdam: Elsevier; 2001.
- [3] Martins R, Seabra J, Seyfert Ch, Luther R, Igartua A, Brito A. Power loss in FZG gears lubricated with industrial gear oils: Biodegradable ester vs. Mineral oil, *Proceedings of the 31th Leeds-Lyon Symposium on Tribology*, Elsevier Science; to be published.
- [4] Weck M, Hurasky-Schonwerth O, Bugiel Ch. Service behaviour of PVD-coated gearing lubricated with biodegradable synthetic ester oils, *VDI-Berichte*. Nr. 1665; 2002.
- [5] Winter H, Michaelis K. FZG gear test rig—description and possibilities. *Coordinate European council second international symposium on the performance evaluation of automotive fuels and lubricants 1985*.
- [6] Hunt TM. *Handbook of wear debris analysis and particle detection in liquids*. UK: Elsevier Science; 1993.
- [7] Höhn B-R, Michaelis K, Vollmer T. Thermal rating of gear drives: balance between power loss and heat dissipation, *AGMA Technical Paper*; October 1996, pp. 12, ISBN: 1-55589-675-8.
- [8] Chagnenet Chr, Pasquier, M. Power losses and heat exchange in reduction gears: numerical and experimental results, *VDI-Berichte*, NR. 1665; 2002, pp. 603–613.
- [9] Winter H, Michaelis K. Investigation on the thermal balance of gear drives. *ASME* 1979.
- [10] Eschmann P. *Ball and roller bearings—theory, design and applications*. New York: Wiley; 1985.
- [11] Pettersson A, Larson R, Norrby T, Anderson O. Properties of base fluids for environmentally adapted lubricants. *Proc World Tribol Cong* 2001.
- [12] Pettersson A. Tribological characterization of environmentally adapted ester base fluids. *Tribol Int* 2003;36.
- [13] DIN 51396 part 2 Testing of lubricants—Determination of wear elements—Part 2: Analysis by wavelength dispersive X-ray spectrometry.
- [14] IP 212/92 Standard, Determination of Viscosity of Bitumen Emulsions—Engler Method, UK: Institute of Petroleum; 1992.
- [15] Denis J, Briant J, Hipeaux J-C. *Physico-Chimie des Lubrifiants—Analyses et Essais*, Éditions Technip; 1997.

A.4 Paper D

R. C. Martins, P. S. Moura, and J. O. Seabra, “MoS₂/Ti low-friction coating for gears”, *Tribology International*, vol. 39, no. 12, pp. 1686-1697, 2006.

MoS₂/Ti low-friction coating for gears

R.C. Martins^{a,*}, Paulo S. Moura^a, J.O. Seabra^b

^aINEGI, Instituto de Engenharia Mecânica e Gestão Industrial, Porto, Portugal

^bFEUP, Faculdade de Engenharia da Universidade do Porto, Portugal

Received 26 July 2005; received in revised form 7 February 2006; accepted 23 February 2006

Available online 18 April 2006

Abstract

The applicability of a multilayer composite surface coating in gears is discussed in this work, mainly in what concerns to gear efficiency at normal operating conditions and to scuffing load capacity. The average friction coefficient between gear teeth is discussed and compared with uncoated steel gears.

The disulfide molybdenum/titanium (MoS₂/Ti) composite coating is studied and the deposition procedure is described.

Several screening tests, like Rockwell indentations, ball cratering, pin-on-disc and reciprocating wear, were performed to evaluate the adhesion to the substrate, the tribological performance of this coating and his applicability in heavy loaded rolling-sliding contacts, such as found in gears.

FZG gear efficiency tests were performed using type C gears in order to evaluate the influence of the surface coating in gear efficiency, for a wide range of operating conditions. These tests in conjunction with a numerical model for the energetic balance of the FZG gearbox allowed the determination of the average friction coefficient between gear teeth, taking into account the presence of the surface coating.

FZG gear scuffing tests were also performed using type C gears in order to evaluate the coating anti-scuffing performance, which proved to be very significant.

© 2006 Elsevier Ltd. All rights reserved.

Keywords: Gear efficiency; Gear scuffing; Friction coefficient; Composite surface coating; Disulfide molybdenum/titanium

1. Introduction

In the last decades, surface coating technology was important to achieve increased performance, allowing lower friction coefficients, higher protection against surface failures and higher load capacity. In applications with frequent start–stop operations such protection against surface failures, mainly scuffing, is very important.

Multilayer composite surface coatings made of MoS₂/titanium [1–3], exhibit good mechanical and tribological properties in several industrial applications.

The application of low-friction surface coatings to power transmission equipments can improve their efficiency and might represent a significant reduction of energy consumption. In the near future, surface coatings will probably contribute to the reduction/elimination of non-biodegrad-

able and toxic lubricant additives and consent the use of environment friendly lubricants.

There are several types of coatings that can be used in gears, for instance, MoS₂ (molybdenum disulfide) [4], WC/C (tungsten carbide–carbon) [5] or the B4C (boron carbide–carbon) [5,6] among others.

The MoS₂ coatings can be improved with the co-deposition of other metals such as Ti (titanium) [2,7] or Cr (chromium) [8].

The MoS₂/titanium coating [2,7] is harder, more resistant and less sensitive to atmospheric water vapor than other common DLC coatings. It has already given excellent results in a wide range of forming and cutting tools applications [1,3,7].

2. MoS₂/Ti low-friction surface coating

The MoS₂/Ti composite coating [1–3,9] is deposited by DC magnetron sputtering using a standard CFUBMSIP

*Corresponding author. Tel.: +351 225081742; fax: +351 225081584.
E-mail address: rcm@fe.up.pt (R.C. Martins).

Symbols	
A_h (m ²)	horizontal surface area of case
A_i (m ²)	immersed area
A_{rad} (m ²)	radiation surface area of case
A_v (m ²)	vertical surface area of case
A_b (m ²)	base support area
F_a (N)	axial force
F_{bt} (N)	tooth normal force, transverse section
F_r (N)	radial force
F_R	Froud number
G	material parameter
K_f (W/mK)	fluid thermal conductivity
L_{ca} (m)	characteristic horizontal length
P_{fr} (W)	gear friction losses
P_{in} (W)	input power
P_L (W)	total power losses
P_{M0} (W)	load-independent losses of bearings
P_{M1} (W)	load-dependent losses of bearings
P_{sl} (W)	seal losses
P_{spl} (W)	gear churning losses
Q_{cn} (W)	conduction heat
Q_{cn}^{rad} (W)	conduction heat due to radiation
Q_{cn}^{ncv} (W)	conduction heat due to natural convection
Q_{cnv} (W)	natural convection heat
Q_H (W)	total heat evacuated
Q_{rad} (W)	radiation heat
R_a (μm)	average roughness
Re	Reynolds number
R_x (m)	equivalent curvature
T (m)	bearing average diameter
T_a (°K)	ambient temperature
T_w (°K)	wall temperature
U	speed parameter
U_1 (m/s)	surface speed
U_2 (m/s)	surface speed
V_e (m/s)	sliding rate
V_{oil} (m ³)	oil volume
W	load parameter
X_L	lubricant factor
b (mm)	face width
d (m)	pitch diameter
d_i (m)	shaft diameter
$f_{0,1}$	coefficients for bearings losses
f_{cn}	conduction coefficient
g_a (m)	length of recess path
g_f (m)	length of approach path
h (m)	gear immersion depth
h_0 (μm)	center film thickness
h_{0c} (μm)	corrected center film thickness
h_{ca} (m)	height of case
h_h (W/m ² K)	natural convection coefficient, horizontal surface
h_v (W/m ² K)	natural convection coefficient, vertical surface
n (rpm)	input rotating speed
p_b (m)	base pitch
$V_{\sum c}$ (m/s)	sum velocity at pitch point
z_i	number of teeth
α_{rad} (W/m ² K)	radiation heat transfer coefficient
ϵ	case surface emissivity
ϕ_T	inlet shear heating parameter
η_{oil} (mPas)	dynamic oil viscosity
μ_m	average friction coefficient
η (kg/m ³)	specific weight
μ_c (mm)	equivalent curvature radius at pitch point

[10] Teer Coatings PVD system, with four targets (one Ti and three MoS₂ targets). The coating procedure starts with an ion cleaning, followed by a 70 nm Ti layer, a 200 nm MoS₂/Ti multilayer, a 900 nm MoS₂/Ti (non-multilayer) and a last step of 50 nm layer of MoS₂ for coloration. Further details about the coating deposition may be found in Refs. [1–3,9].

The MoS₂/Ti coating was deposited on M42 polished 1200 SiC steel, and several tribological tests were performed in order to evaluate its performance. The thickness of this coating is about 1.2 μm, measured using the Ball Crater technique [3,7].

Rockwell C indentation (Daimler Test) has been performed to assess qualitative coating adhesion to the substrate, showing a very small plastic deformation. The hardness test indicated that the MoS₂/Ti coating had a plastic hardness of HP ≈ 1200 kg/mm² and the scratch test showed that no failure occurred at loads up to 100 N [2,3,7].

Pin-on-disc tests performed at 200 mm/s and 50% r.h. (dry) during 1 h have shown low-wear and low-friction

coefficient. For the highest load (80 N), the friction coefficient is rather small (0.04–0.045) and with the decrease of load the friction coefficient increases reaching the value of 0.1 for a load of 10 N. Coating wear is evaluated as the percentage of coating thickness reduction, measured by the Ball crater technique on the disc track, its value being 10% for a load of 10 N, reaching 24% for a load of 80 N [7].

The reciprocating wear test was carried out using a sliding speed of 150 mm/min under 100 N load at 50% r.h. (dry) and at room temperature. After 10,000 cycles, only 19% of coating was worn away with a specific wear rate of 3.1×10^{-17} m³/mN and a friction coefficient of 0.04 [7].

The MoS₂/Ti coating also presents excellent adhesion to steel substrates tested in twin-disc tests at high contact pressure, high slide-to-roll ratio and low specific film thickness [2].

The MoS₂/Ti coating improves the efficiency of a transfer gearbox in about 0.5% at the low-speed-high-load operating conditions [2].

3. FZG test rig and gears

Fig. 1 shows a schematic view of the FZG back-to-back spur gear test rig where gear efficiency tests and scuffing tests are performed. The geometrical characteristics of FZG type C gears used in both tests are presented in Table 1 and the mechanical properties of the gears are presented in Table 2.

The efficiency and scuffing gear tests are performed using dip lubrication with an oil volume of 1.5 l.

The gears used in both tests are manufactured in DIN 20 MnCr 5 steel, being carburized, quenched and oil annealed before the final grinding operation. The surfaces have a very high hardness, typically around 60 HRC, while the core keeps a very high strength and a considerably high elongation. The MoS₂/Ti composite surface coating is deposited on the carburized gears after the grinding operation.

4. GEAR efficiency tests

4.1. Lubricant

The gear efficiency tests were performed using an ISO VG 100 biodegradable fully saturated ester, based on harvestable materials with a low-toxicity additivation, being free of metal-organic compounds. The main properties of this ester lubricant are presented in Table 3.

4.2. Operating conditions in gear efficiency tests

The uncoated gears and the MoS₂/Ti-coated gears perform a set of tests in a wide range of speed and torque conditions, as well as input power, as shown in Table 4. The Hertzian contact pressures at the pitch point for each FZG load stage are also presented in Table 4.

The test program consists of nine load tests, performed at three different speeds (1000, 2000 and 3000 rpm) and three increasing torque levels, corresponding to FZG load stages 5, 7 and 9. Each load test begins at approximately 40 °C and the oil sump temperature is set free.

Each test lasts for 5 h, the input conditions being kept constant (torque and speed). This test duration is defined in order to attain the stabilization in oil sump temperature. The test is stopped if the oil sump reaches 180 °C.

The arithmetic average roughness value of tooth surface is $R_a = 1 \mu\text{m}$ for the MoS₂/Ti-coated gears and has the value of $R_a = 0.9 \mu\text{m}$ for the uncoated gears (see Table 5).

Table 1
Geometry of the FZG type C test gears

Parameter	Units	Pinion	Wheel
Number of teeth		16	24
Module	mm	4.5	
Center distance	mm	91.5	
Addendum diameter	mm	82.45	118.35
Pressure angle	°	20	
Addendum modification	/	+0.182	+0.171
Face width	mm	14	

Table 2
Mechanical properties of DIN 20 MnCr 5 steel

Properties	Unit	20 MnCr 5
Modulus of elasticity	10 ³ N/mm ²	210
Density	g/cm ³	7.85
Poisson's ratio	/	0.3
Surface hardness	HRC	58–62
Tensile strength	N/mm ²	1300
Yield strength 0.2%	N/mm ²	550
Elongation	%	8

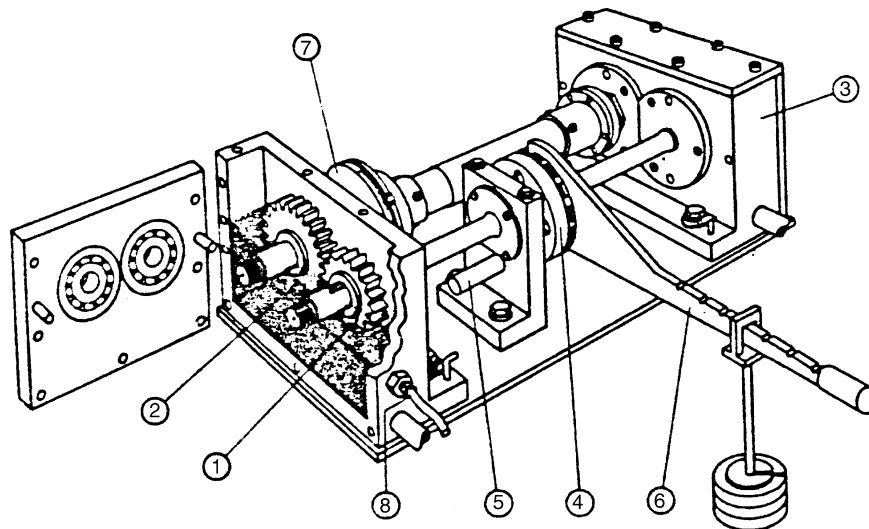


Fig. 1. Schematic view of the FZG test rig.

Table 3
Properties of the saturated ester gear oil

Parameter	unit	Desig.	Method	Value
Base oil	/	/	DIN 51451	Saturated ester
<i>Physical properties</i>				
Density @ 15 °C	g/cm ³	ρ_{15}	DIN 51757	0.925
Kinematic viscosity @ 40 °C	cSt	ν_{40}	DIN 51562	99.4
Kinematic viscosity @ 100 °C	cSt	ν_{100}	DIN 51562	14.6
Viscosity index	/	VI	DIN ISO 2909	152
Pour point	°C		DIN ISO 3016	−42
Piezoviscosity [20]	Pa ^{−1}	$\alpha(p, T) = \frac{1}{a_1 + a_2 T + (b_1 + b_2 T)p}$		
Constant	bar	a_1	—	526
Constant	bar/°C	a_2	—	3.845
Constant	/	b_1	—	4.90×10^{-2}
Constant	1/°C	b_2	—	1.14×10^{-4}
<i>Wear properties</i>				
VKA weld load	N	/	DIN 51350-2	2200
VKA wear scar (1 h/300 N)	mm	/	DIN 51350-3	0.35
Brugger	N/mm ²	/	DIN 51347-2	37
FZG rating	/	K_{FZG}	DIN 51354	> 12
<i>Biodegradability and toxicity properties</i>				
Ready biodegradability	%		OECD, 301 B	≥ 60
Aquatic toxicity with <i>Daphnia</i>	ppm	EL ₅₀	OECD, 202	> 100
Aquatic toxicity with <i>Alga</i>	ppm	EL ₅₀	OECD, 201	> 100
<i>Chemical content</i>				
Zinc	ppm	Zn	ASTM D-4927	—
Calcium	ppm	Ca	ASTM D-4927	—
Phosphor	ppm	P	ASTM D-4927	146
Sulphur	ppm	S	ASTM D-4927	180

Table 4
Operating conditions in gear efficiency tests

Speed (rpm)	Torque (Nm)	Input power (kW)	Hertz pressure (MPa)	No of cycles (wheel) ($\times 10^6$)
1000	141.2	14.8	994	0.9
	275.1	28.8	1388	
	453.0	47.4	1781	
2000	141.2	29.6	994	2.7
	275.1	57.6	1388	
	453.0	94.9	1781	
3000	141.2	44.3	994	5.4
	275.1	86.4	1388	
	453.0	142.3	1781	

After each group of tests at constant speed, a lubricant sample is collected for post-test oil analysis by Direct Reading Ferrometry.

4.3. Oil stabilization temperature

The power dissipated inside the gearbox (P_L), once the oil temperature has stabilized, is equal to the power (heat) evacuated from the FZG gearbox (Q_H). The power evacuated is proportional to the difference between the

oil temperature (T_{oil}) and the room temperature (T_a), assuming that the wall temperature of FZG gearbox is equal to the oil temperature, which is reasonable at stabilized operating conditions.

In Appendix A and in Ref. [11] a detailed analysis of the energetic balance of FZG test gearbox is presented.

The difference between oil temperature and room temperature ($\Delta T = T_{oil} - T_a$) is shown in Fig. 2 for all the operating conditions used. In general, the MoS₂/Ti-coated gear has lower ΔT values, suggesting it dissipates less power than the uncoated gear. At 1000 rpm, ΔT is 5–6 °C lower in the case of the coated gear and at 2000 rpm, ΔT is 1–5 °C lower. At 3000 rpm this tendency is not so clear.

4.4. Gear wear

The Direct Ferrometry measurements (CPUC index) performed during gear efficiency tests are presented in Fig. 3. The CPUC index gives an indication of the total number of particles present in a lubricant sample, growing when the total number of particles increases.

This figure shows that, after the tests at 1000 rpm, the CPUC index of the coated gear is smaller than the one corresponding to the uncoated gear. After the tests at 2000 rpm they are very similar and at 3000 rpm the uncoated gear presents a smaller CPUC index.

Table 5
Average roughness parameters of the gears used on efficiency tests, both uncoated and coated

		R_{max} (μm)	R_{z-D} (μm)	R_a (μm)	R_{pk} (μm)	R_k (μm)	R_{vk} (μm)
MoS ₂ /Ti coated	New	4.7	4.0	0.8	0.5	2.0	1.1
	Used	1.6	1.0	0.2	0.1	0.3	0.5
	Reduction %	67	74	79	79	85	51
Uncoated	New	5.6	4.7	0.9	0.3	1.9	1.8
	Used	1.7	1.0	0.2	0.0	0.2	0.5
	Reduction %	70	79	82	86	89	72

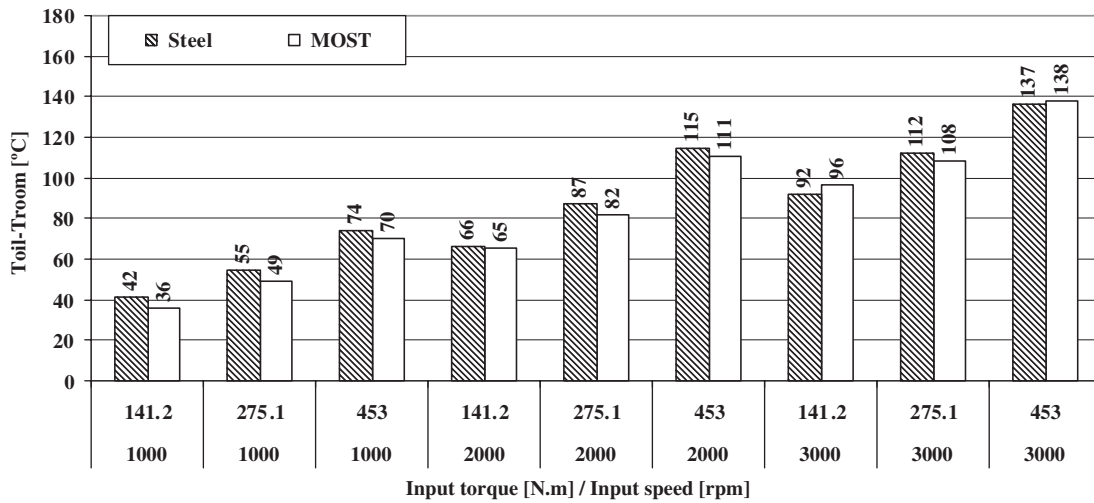


Fig. 2. Difference between stabilized oil bath temperature and room temperature in gear efficiency tests.

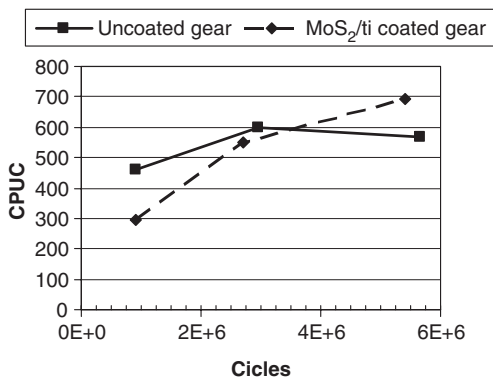


Fig. 3. Evolution of CPUC wear index during gear efficiency tests.

This result is related to the progressive wear of the surface coating due to the film thickness reduction throughout the test.

The EHD center film thickness is determined according to Dowson et al. [12], that is,

$$h_0 = 0.975R_X U^{0.727} G^{0.727} W^{-0.091} \tag{1}$$

The influence of inlet shear heating in the film thickness is according to Gohar [13] given by

$$\phi_T = \left\{ 1 + 0.1 \left[(1 + 14.8 V_e^{0.83}) \left(\frac{\beta \eta_0 (U_1 + U_2)^2}{20K_f} \right)^{0.64} \right] \right\}^{-1} \tag{2}$$

Finally the corrected film thickness becomes:

$$h_{0C} = \phi_T h_0 \tag{3}$$

Fig. 4 shows the film thickness at stabilized temperature for each test. In fact, the increase of speed, at constant load, produces an increase of the film thickness related to the hydrodynamic effect. However, the same speed increase generates a higher operating temperature and consequently a lower dynamic viscosity and lower film thickness. These two antagonist effects result in a slight decrease of the film thickness when the speed increases, as shown in Fig. 4.

The very low operating film thickness (bellow 0.1 μm) generated at 2000 and 3000 rpm, for the highest torque (453 Nm), has a more detrimental effect on the MoS₂/Ti-coated gear than on the uncoated gear.

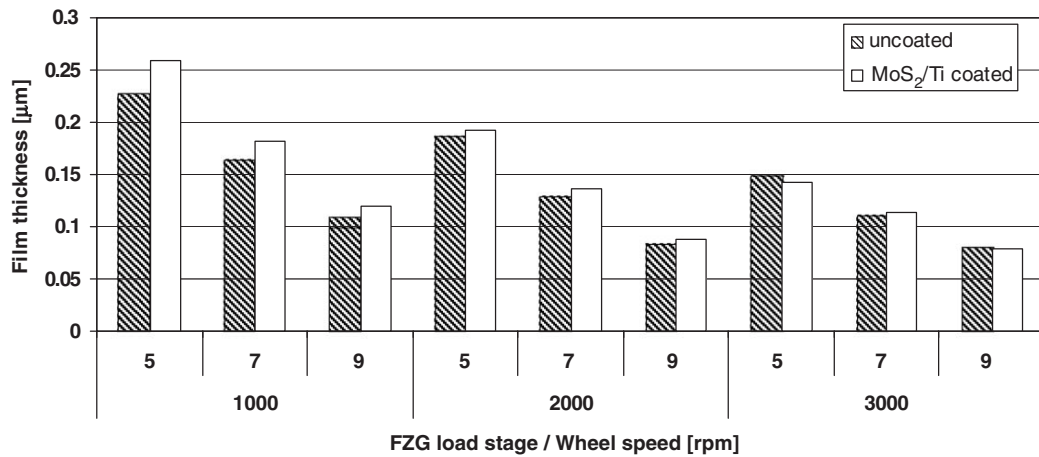


Fig. 4. Evolution of the film thickness between gear teeth, at stabilized oil bath temperature, in gear efficiency tests.

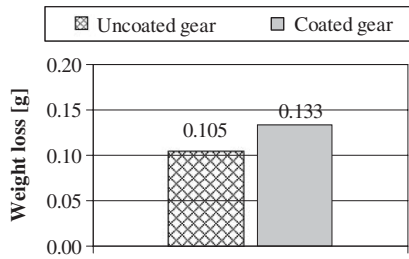


Fig. 5. Total mass loss after gear efficiency tests.

Fig. 5 shows the total mass loss measurement after the efficiency tests with uncoated and coated gears. The weight loss with MoS₂/Ti-coated gears displays a larger value (+27%) than the uncoated gear. This result confirms the CPUC index result displayed in Fig. 3.

Surface wear is clearly visible on the roughness profiles presented in Fig. 6, confirmed by the roughness parameters shown in Table 5. The R_{z-D} parameter decreases 3 μm during the MoS₂/Ti-coated gear test, while its reduction reaches 3.7 μm on the uncoated gear test. This reduction is also evident in Fig. 6 where the new profiles show that the surface peaks were removed, resulting in a smoother plateau-type surface.

4.5. Friction coefficient between gear teeth

In the case of additive free mineral lubricants, the friction coefficient between gear teeth might be calculated from empiric equations based on experimental results. However, few results are available for commercial gear oils with particular base fluids and additive packages [14].

As mentioned above, the thermal equilibrium of a gearbox is attained when the power loss is equal to the evacuated heat. This equilibrium generates a constant operating temperature of the mechanical component and of the lubricant fluid (see Appendix A).

The main mechanisms of power dissipation inside a gearbox are the churning losses and the frictional losses [14–19], the lubricant of capital influencing in both. The total power dissipation (P_L) can be expressed as

$$P_L = P_{fr} + P_{M1} + P_{spl} + P_{M0} + P_{sl}, \quad (4)$$

where P_{fr} represents the friction losses between gear teeth, P_{M1} , represents the load-dependent bearings losses, P_{spl} , represents the gear churning losses, P_{M0} represent the bearing no-load losses and P_{sl} represents the seals power losses.

The heat evacuation from the gearbox to the surrounding environment is made by three mechanisms: conduction, radiation and convection. The heat evacuation is expressed as

$$Q_H = Q_{cn}^{rad} + Q_{cn}^{ncv} + Q_{cn}, \quad (5)$$

where Q_{cn}^{rad} represents the radiation, Q_{cn}^{ncv} represents the natural convection and Q_{cn} represents the conduction.

So the gearbox energetic balance becomes

$$P_{fr} + P_{M1} + P_{spl} + P_{M0} + P_{sl} = Q_{rad} + Q_{cnv} + Q_{cn} \quad (6)$$

or $P_L = Q_H$. More detailed calculation is presented in Annex A and in Martins et al. [11].

The energetic balance of a gearbox at the stabilized (equilibrium) temperature allows the determination of the average friction coefficient between gear teeth for each lubricant, material or coating pair. Correction parameters are proposed to the existing friction coefficient expression in order to take into account the influence of gear materials and lubricant characteristics.

These correction factors are determined using a numerical model for the energetic balance of the FZG gearbox that allows the optimization of friction coefficient parameters in order to maximize the correlation between experimental and numerical equilibrium temperatures (see Appendix A).

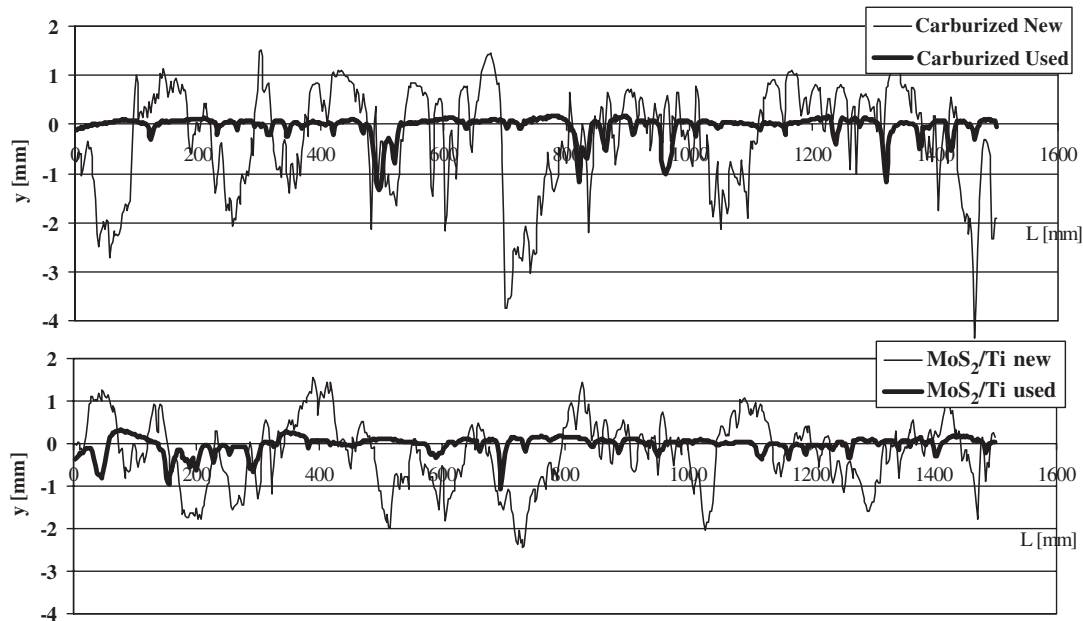


Fig. 6. Roughness profile of MoS₂/Ti-coated gear and carburized gear before (new) and after (used) efficiency test.

Höhn et al. [15] define the average friction coefficient between gear teeth as

$$\mu_m = 0.048 \left(\frac{F_{bt}/b}{v_{\Sigma c} \rho_c} \right)^{0.2} \eta_{oil}^{-0.05} R_a^{0.25} X_L, \quad (7)$$

where F_{bt} stands for the tooth normal force on the transverse section, b is the gear width, $v_{\Sigma c}$ is the sum velocity at pitch point, ρ_c is the equivalent curvature radius at pitch point, η_{oil} is the oil dynamic viscosity, and R_a is the composite surface roughness of the teeth contacting flanks.

X_L is a correction parameter that takes into account the influence of a particular lubricant, material or surface coating. It has the value of 1 for mineral additive free lubricants and steel gears.

The best correlation of the X_L parameter is obtained for a load-dependent parameter, that is,

$$X_L = \frac{1}{(F_{bt}/b)^{b1}}. \quad (8)$$

This X_L parameter only affects the influence of the load on the friction coefficient between gear teeth, and the optimized equation for the average friction coefficient between gear teeth becomes:

$$\mu_m = 0.048 \frac{(F_{bt}/b)^{0.2-b1}}{(v_{\Sigma c} \rho_c)^{0.2}} \eta_{oil}^{-0.05} R_a^{0.25}. \quad (9)$$

The results obtained for the uncoated steel gear and the MoS₂/Ti-coated gear, both lubricated with a fully saturated ester gear oil, are represented in Table 6, indicating that the MoS₂/Ti coating promotes an additional reduction

Table 6
Exponent $b1$ for X_L parameter and load exponent ($0.2 - b1$)

Exponent $b1$		Exponent ($0.2 - b1$)	
Steel	MoS ₂ /Ti	Steel	MoS ₂ /Ti
0.0855	0.0914	0.1145	0.1086

of the influence of the load on the friction coefficient. The load exponent is reduced from 0.1145 to 0.1086.

Fig. 7 shows for the experimental conditions tested the numerically determined tooth friction losses P_{fr} (see Appendix A) based on the equilibrium temperatures determined by the numerical model for both the uncoated and the MoS₂/Ti-coated gears.

The MoS₂/Ti surface coating promotes a slight reduction of the friction power loss, which increases when the speed and the load increases while the film thickness is decreasing (see Fig. 4), meaning that the coating acts as a friction reducer.

Fig. 8 shows the influence of the lubricant and of the MoS₂/Ti surface coating on the average friction coefficient between gear teeth. The curves displayed are determined according to expression 1 for the mineral additive free lubricant ($X_L = 1$) and according to expression 3 and Table 6 for the MoS₂/Ti-coated and uncoated gear lubricated with ester lubricant. It is clear that the lubricant type (saturated ester) has a very significant influence on the friction coefficient [11] and that the surface coating acts as friction reducer.

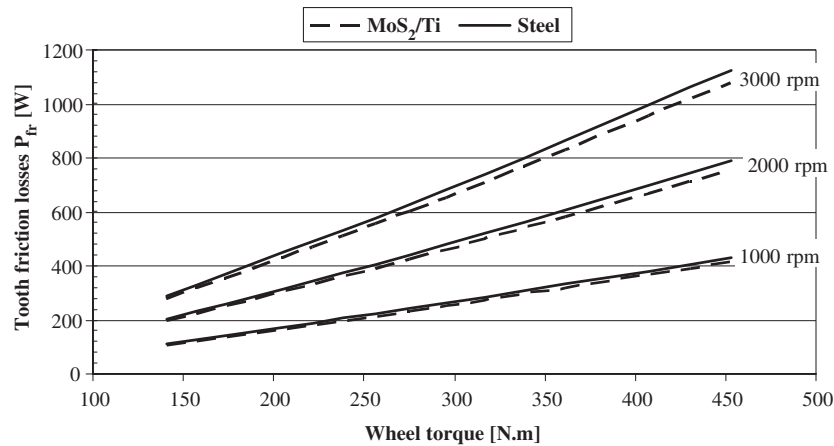


Fig. 7. Comparison of tooth friction losses (P_{fr}) in gear efficiency tests.

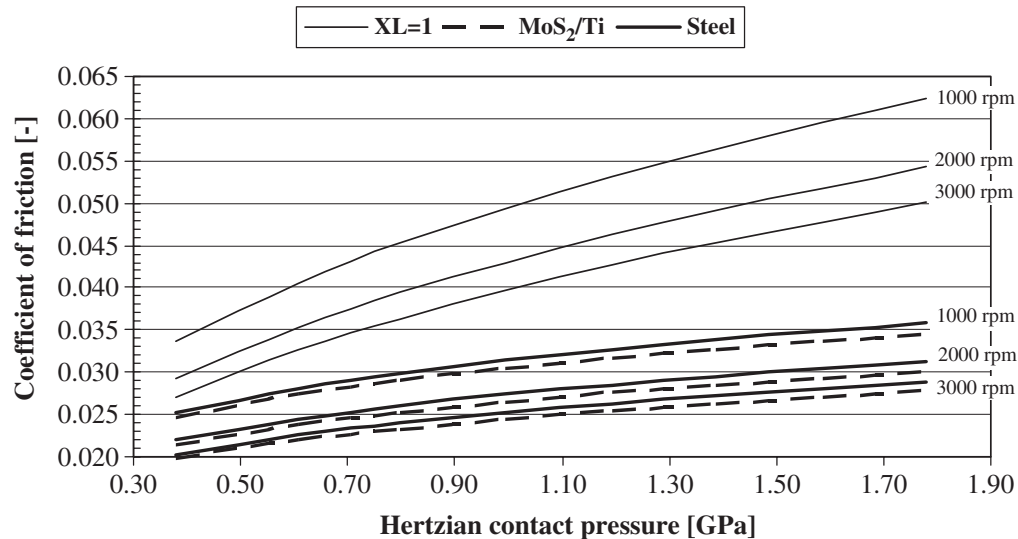


Fig. 8. Estimated friction coefficient for uncoated and MoS_2/Ti -coated gears, lubricated with saturated ester gear oil and with additive free mineral oil ($X_L = 1$) ($T_{oil} = 90^\circ\text{C}$).

5. Gear scuffing tests

5.1. Lubricant and gears

The gear efficiency tests showed that MoS_2/Ti surface coating reduces the friction between gear teeth and, consequently, it should also provide increased scuffing load capacity.

However, the gear efficiency tests (Paragraph 4) were performed using a saturated ester containing anti-wear (AW) and extreme-pressure (EP) additives, which have a very significant influence on load carrying capacity of gears, perhaps as important as the surface coating. This means that the gear scuffing tests must be performed with an additive free lubricant, otherwise scuffing will not be reached within the load and speed limits of FZG machine.

So, in order to evaluate the scuffing protection conferred by MoS_2/Ti coating, FZG gear scuffing tests are performed, using an ISO VG 100 mineral oil without EP and AW additives, and type C gears. The lubricant properties are presented in Table 7.

Three different gear sets were tested: one uncoated gear (NC) and two MoS_2/Ti -coated gears (MST and MST*). The major difference between the two coated gear sets is the surface roughness of the teeth flanks and the ISO quality grade, as presented in Table 8. The MST gear set has current quality grade and surface roughness, while the MST* has an excellent quality grade and surface roughness. This difference in surface finishing is helpful to understand the interaction between surface roughness and surface coating on gear scuffing.

5.2. Gear scuffing testing conditions

For each gear two tests were performed (using both tooth flanks), one at 1500 rpm and the other at 3000 rpm (wheel speeds).

Dip lubrication is used and during the tests the oil is kept at a constant temperature of 90 °C.

Table 7
Physical properties of the additive free mineral gear oil

Parameter	unit	Desig.	Method	Value
Base oil	/	/	DIN 51451	Additive free mineral oil
<i>Physical properties</i>				
Kinematic viscosity @ 40 °C	cSt	v_{40}	DIN 51562	100.0
Kinematic viscosity @ 100 °C	cSt	v_{100}	DIN 51562	11.1
Viscosity index	/	VI	DIN ISO 2909	95
Piezoviscosity at 40 °C	Pa^{-1}	α	—	2.785×10^{-8}
Piezoviscosity at 100 °C	Pa^{-1}	α	—	1.642×10^{-8}
Oil operating temperature	°C			90 ± 2

Table 8
Codification of gear sets used in gear scuffing tests: coating type, gear quality and flank roughness

Gear reference	Coating	Gear quality grade (ISO 1328)	Roughness of tooth flanks R_a (μm)
NC	Uncoated	9	2.4
MST	MoS ₂ /Ti	9	2.4
MST*	MoS ₂ /Ti	5	0.4

Each gear set is run-in during 4 h in FZG load stage 6, corresponding to a wheel torque of 203 N m at 1500 rpm (wheel speed).

The gear scuffing test is based on DIN 51354 standard. The gear scuffing test procedure starts on FZG load stage 7 ($T_{\text{wheel}} = 275 \text{ Nm}$), the torque being progressively increased until FZG load stage 12 ($T_{\text{wheel}} = 801 \text{ Nm}$) or 13 ($T_{\text{wheel}} = 940 \text{ Nm}$), or until any type of surface failure of the teeth flanks is detected.

During each load stage, which lasts for 15 min, the operating conditions (temperature, torque and speed) are kept constant.

After each load stage the pinion and wheel teeth flanks are visually inspected, searching for surface failures, specially scuffing marks or excessive wear.

The maximum Hertzian pressure and the film thickness between gear teeth, corresponding to each load stage and for both testing speeds, are presented in Fig. 9.

5.3. Gear scuffing test results

The results of the gear scuffing tests, in terms of the scuffing load stage and of the transmitted power at scuffing, are presented in Fig. 10. An arrow above a bar indicates that test surpassed the last load stage without scuffing failure.

At 1500 rpm (wheel speed), the uncoated gear reached scuffing in load stage 11 ($T_{\text{wheel}} = 675 \text{ Nm}$), while both MoS₂/Ti-coated gears did not reach scuffing. The MST* gear was even tested in load stage 13 and also did not reach scuffing. Thus, the scuffing load capacity increased at least two load stages due to the MoS₂/Ti coating and at least three load stages due to the MoS₂/Ti coating when applied to high-quality gears with very low teeth surface roughness.

In the tests at 3000 rpm the uncoated gear (NC) reached scuffing in load stage 7, the MST gear on load stage 12, while the MST* gear overcome load stage 12 without failures. These results show that at 3000 rpm the application of MoS₂/Ti coating on gears promotes an increase of scuffing load capacity of at least 5 FZG load stages [2].

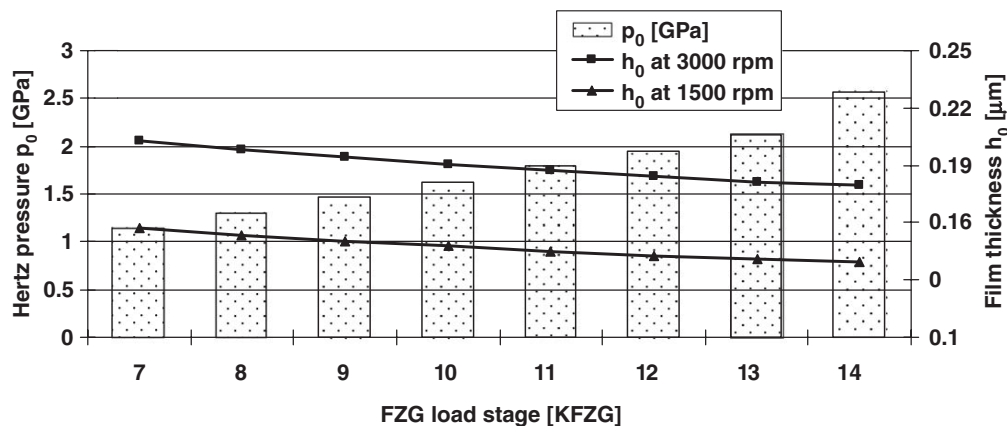


Fig. 9. Hertzian contact pressure and film thickness at wheel tip/pinion root contact point.

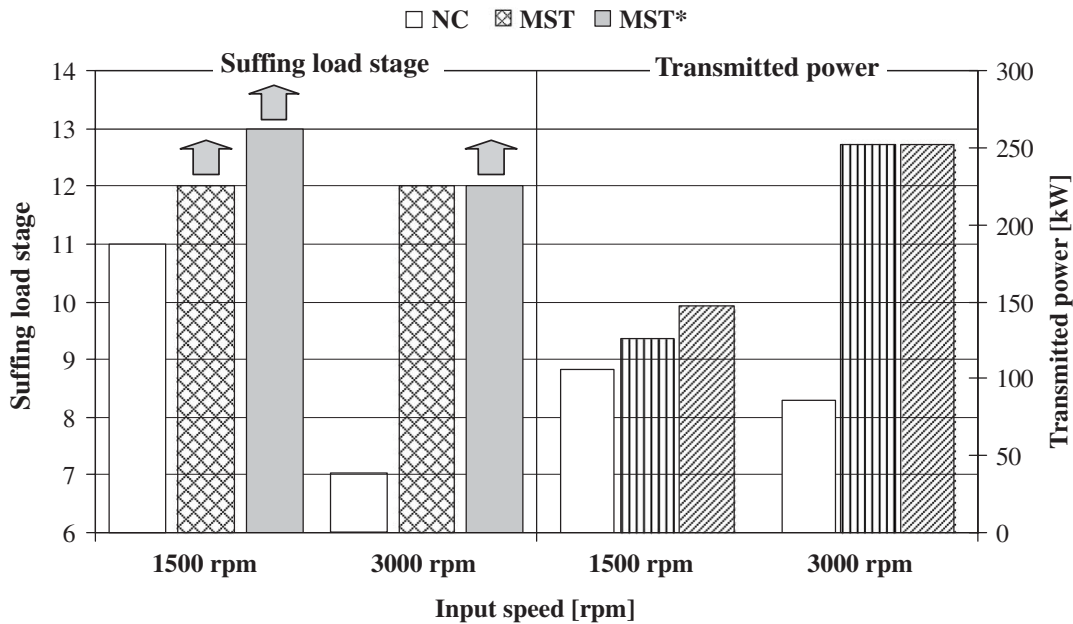


Fig. 10. FZG scuffing load stage and corresponding transmitted power in gear scuffing tests.

Joachim et al. [6] obtained a similar improvement in scuffing resistance (2 FZG load stages) in standard FZG scuffing tests A/8,3/90 lubricated with Mobil Jet Oil II, between uncoated and coated gears, using WC/C (tungsten carbon carbide) and B4C (boron carbide) coatings. Weck et al. [5] also obtained an improvement in scuffing resistance (1 FZG load stage) in standard FZG scuffing tests A/8,3/90 lubricated with COE 100 base oil, between uncoated and coated gears, using WC/C (tungsten carbon carbide) coating.

The transmitted power at the scuffing load stage (or at the highest load stage performed in the cases where scuffing did not occur) is also shown in Fig. 10. The improvement in transmitted power due to MoS₂/Ti surface coating attains at least 40% at 1500 rpm and 190% at 3000 rpm [2].

The use of high-quality grade–low roughness gears promotes an improvement in scuffing resistance of at least 1 load stage, while the improvement in transmitted power attains at least 17% [2]. Joachim et al. [6] also obtained a similar improvement in scuffing resistance (1 FZG load stage) in standard FZG scuffing tests A/8,3/90 lubricated with Mobil Jet Oil II, between the usual and super-finished uncoated FZG gears. They noticed that the influence of the surface coating on scuffing resistance is more important than the influence of surface super-finishing.

6. Conclusions

The main conclusions that might be withdrawn from this work are:

- (1) MoS₂/Ti surface coating applied to gears promotes a significant decrease of their operating temperature.

- (2) MoS₂/Ti coating promotes a decrease of coefficient of friction between gear teeth, putting into evidence by the reduction of load exponent on coefficient of friction equation.
- (3) MoS₂/Ti-coated gears generate a larger wear volume than uncoated gears.
- (4) MoS₂/Ti coating increases, very significantly, the scuffing load carrying capacity of FZG type C gears: up to 5 load stages at 3000 rpm, corresponding to an increase of 190% in transmitted power.
- (5) The low roughness and high-quality gears also promote an increase of scuffing load capacity, although in a smaller proportion.

Acknowledgements

The authors would like to thank the European Comission for the financial support given to this study throught the projects:

“Reduction of fluid lubricant use in heavily loaded motion transmission systems through the application of sel-lubricating coatings”. Project no. BE-S2-5389, Contract no. BRST-CT97-5363, 1998–2000.

“EREBIO—Emission reduction from engines and transmissions substituting harmful additives in biolubricants by triboreactive materials”, Proposal No. GRD2-2001-50119, Contract No. G3RD-CT-2002-00796-EREBIO.

Appendix A. Energetic balance of the FZG test gearbox

Fig. 11 shows a schematic view of the FZG test gearbox. The different mechanisms of power dissipation and heat

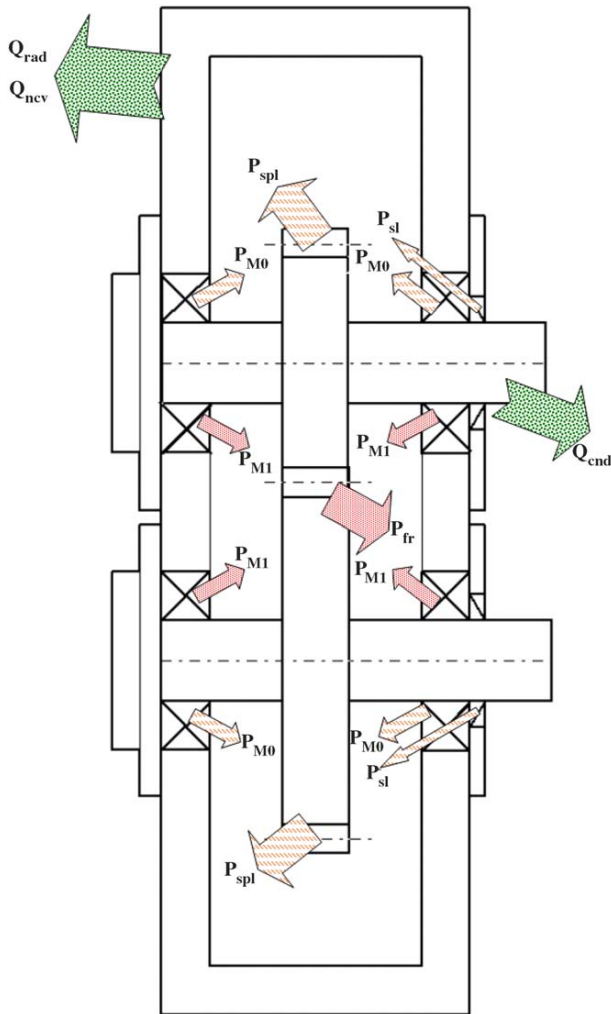


Fig. 11. Schematic view of the FZG test gearbox and of the different mechanisms of power dissipation and heat evacuation.

evacuation are represented. The thermal equilibrium of a gearbox is attained when the power losses are equal to the evacuated heat.

The main mechanisms of power dissipation inside a gearbox are the churning losses and the frictional losses [15,17–19], in which the lubricant has capital influence. These power losses are usually called the no-load power losses and the load power losses, respectively. The no-load losses are related with moving parts immersed on the lubricant and the load power losses result from contacting bodies with relative movement (see Fig. 11).

The heat evacuation is made essentially by three modes: conduction, radiation and convection.

The churning losses are related with moving parts immersed in the lubricant which depends mainly on the lubricant, speed and parts geometry. The main sources of churning losses are the gear, the bearings and the seals.

The gear churning losses (P_{spl}) are defined as

$$P_{spl} = \frac{\pi}{30} n \left(\frac{1}{2} \rho \left(\frac{\pi n}{30} \right)^2 A_i \left(\frac{d}{2} \right)^3 \right) \times \left(\left(\frac{2h}{d} \right)^{0.45} \left(\frac{V_{oil}}{d} \right)^{0.1} FR^{-0.6} Re^{-0.21} \right). \quad (A.1)$$

The bearing churning losses (P_{M0}) are defined as

$$P_{M0} = \frac{\pi}{30} n (f_0 10^{-7} (m_{oil})^{2/3} T^3) 10^{-3}. \quad (A.2)$$

The seal losses (P_{sl}) are defined as

$$P_{sl} = 7.69 \cdot 10^{-6} d_i^2 n. \quad (A.3)$$

The frictional losses are related with moving parts in contact between them. The main sources of frictional losses are the gears and the roller bearings.

The gear friction losses (P_{fr}) are defined as

$$P_{fr} = \pi \left(\frac{1}{z_1} + \frac{1}{z_2} \right) \times \left(1 - \left(\frac{g_f + g_a}{p_b} \right) + \left(\frac{g_f}{p_b} \right)^2 + \left(\frac{g_a}{p_b} \right)^2 \right) P_{in} \mu_m. \quad (A.4)$$

The rolling bearing friction losses (P_{M1}) are defined as

$$P_{M1} = \frac{\pi}{30} n \left(\sqrt{F_r^2 + F_a^2} f_1 T \right). \quad (A.5)$$

Thus the total power loss inside the FZG test gearbox is given by

$$P_L = P_{fr} + P_{M1} + P_{spl} + P_{M0} + P_{sl}. \quad (A.6)$$

The main mechanisms of heat evacuation from the FZG test gearbox are conduction, radiation and convection. All these heat evacuation mechanisms depend on the case temperature which in the case of FZG test gearbox is almost the same as the oil temperature (when dip lubrication is used).

The natural convection of the test gearbox is split into two parts, the vertical wall and the horizontal wall. The convection coefficient is dependent on a characteristic dimension and on the wall and ambient temperatures. The vertical and horizontal coefficients of natural convection (h_v and h_h) are, respectively [17],

$$h_v = 11.06 h_{ca}^{-0.1} \left(\frac{T_w - T_a}{T_a} \right)^{0.3}, \quad (A.7)$$

$$h_h = 12.87 L_{ca}^{-0.04} \left(\frac{T_w - T_a}{T_a} \right)^{0.32}. \quad (A.8)$$

The total heat evacuated by natural convection (Q_{ncv}) is defined by

$$Q_{ncv} = h_v A_v (T_w - T_a) + h_h A_h (T_w - T_a). \quad (A.9)$$

The heat evacuated by radiation (Q_{rad}) is based on the Stefan–Boltzmann law using a radiation coefficient [15]. The radiation coefficient (α_{rad}) and the evacuated heat are,

respectively,

$$\alpha_{\text{rad}} = 0.23 \cdot 10^{-6} \varepsilon \left(\frac{T_w + T_a}{2} \right)^3 \quad (\text{A.10})$$

and

$$Q_{\text{rad}} = \alpha_{\text{rad}} A_{\text{rad}} (T_w - T_a). \quad (\text{A.11})$$

Winter et al. [18] proposes the substitution of the heat conduction calculation by an increase of convection and radiation areas by 1.5–2.5 times (fcn factor) the gearbox base contact area (conduction area, A_b). An optimized value of fcn = 2.5 was obtained based on experimental tests performed in the FZG test rig [11].

Then increase of radiation heat due to conduction is expressed as

$$Q_{\text{cn}}^{\text{rad}} = \alpha_{\text{rad}} (T_w - T_a) (\text{fcn } A_b). \quad (\text{A.12})$$

The area increase in the natural convection term must be split into two parts (vertical convection and horizontal convection). This separation is done proportionally to the original areas, i.e. the increase of vertical wall surface is proportional to its relation with total surface area submitted to natural convection ($A_v + A_h$), so the proportion factor is ($A_v / A_v + A_h$). The same rule is applied to the top horizontal surface, resulting in a proportion factor of ($A_h / A_v + A_h$). Thus the increase in natural convection heat due to conduction becomes:

$$Q_{\text{cn}}^{\text{ncv}} = h_v (T_w - T_a) \text{fcn } A_b \left(\frac{A_v}{A_v + A_h} \right) + h_h (T_w - T_a) \text{fcn } A_b \left(\frac{A_h}{A_v + A_h} \right). \quad (\text{A.13})$$

Thus the total heat evacuated by conduction is given by

$$Q_{\text{cn}} = Q_{\text{cn}}^{\text{rad}} + Q_{\text{cn}}^{\text{ncv}}. \quad (\text{A.14})$$

So, the total heat evacuated from the FZG test gearbox becomes:

$$Q_{\text{H}} = Q_{\text{cn}}^{\text{rad}} + Q_{\text{cn}}^{\text{ncv}} + Q_{\text{cn}}. \quad (\text{A.15})$$

The energetic equilibrium of the FZG test gearbox is reached when the power dissipated equals the heat evacuated, that is, $P_L = Q_{\text{H}}$, or

$$P_{\text{fr}} + P_{\text{M1}} + P_{\text{spl}} + P_{\text{M0}} + P_{\text{sl}} = Q_{\text{rad}} + Q_{\text{cnv}} + Q_{\text{cn}}. \quad (\text{A.16})$$

Eq. (16) establishes an approximated model for the energetic behavior of the FZG test gearbox, allowing the determination of the oil temperature in permanent conditions (stabilized temperature) for any combination of the operating conditions imposed to the FZG test rig.

A.1. Optimized friction coefficient between gear teeth

Considering that the lubricant parameter X_L is defined as

$$X_L = \frac{a}{(\text{var}_1)^{b1} \dots (\text{var}_n)^{bn}}, \quad (\text{A.17})$$

it can be optimized for each lubricant correlating the model to the experimental results. The optimization process takes

into account all the variables “var”, that is, the applied load (F_{bt}) the oil viscosity (η) and the rolling speed ($v_{\Sigma c}$).

Within the range of operating conditions used, the best correlations are obtained for a load-dependent lubricant parameter X_L , independent of the oil viscosity and rolling speed, that is,

$$X_L = \frac{1}{(F_{bt}/b)^{b1}}. \quad (\text{A.18})$$

References

- [1] Renevier N, Fox V, Lobiondo N, Teer D, Hampshire J. Performance of MoS₂/metal composite coatings used for dry machining and other applications. Surf Coat Technol 2000(123).
- [2] Amaro R, Martins R, Seabra J, Renevier NM, Teer DJ. Molybdenum disulfide/titanium low friction coating for gears application. Tribol Int 2004;38–4:423–34.
- [3] Renevier N, Hampshire J, Fox V, Witts J, Allen T, Teer D. Advantages of using self-lubricating, hard, wear-resistant MoS₂-based coatings. Surf Coat Technol 2001;142–144.
- [4] Holmeberg K, Mathews A, Roncainem H. Friction and wear mechanisms of coated surfaces. Fin J Tribol 1998.
- [5] Weck M, Hurasky-Schonwerth O, Bugiel C. Service behaviour of PVD-coated gearing lubricated with biodegradable synthetic ester oils. VDI-Berichte 2002(1665).
- [6] Joachim F, Kurz N, Glatthaar B. Influence of coatings and surface improvements on the lifetime of gears. VDI-Berichte 2002.
- [7] Renevier N, Fox V, Teer D, Hampshire J. Performance of low friction MoS₂-titanium composite coatings used in forming applications. Mater Des 2000(21).
- [8] Su Y, Kao W. Tribological behaviour and wear mechanisms of MoS₂-Cr coatings against various counterbodies. Tribology International 2003;36.
- [9] Amaro R, Martins R, Seabra J, Brito A. MoST low friction coating for gears application. In: GEARS 2003—Gears and Transmissions Workshop, 2003. FEUP, Porto, Portugal.
- [10] Teer D, UK patent no. GB 2258343B, USA patent no. 5556519, 1996.
- [11] Martins R, Seabra J, Brito A, Seyfert C, Luther R, Igartua A. Friction coefficient in FZG gears lubricated with industrial gear oils: biodegradable ester vs. mineral oil. Tribol Int 2006;39(6):512–21.
- [12] Dowson D, Higginson GR. Elastohydrodynamic lubrication, S.I. ed. Pergamon Press Ltd; 1977.
- [13] Gohar R. Elastohydrodynamics. San: Ellis Horwood Ltd; 1988.
- [14] Höhn B-R, Michaelis K, Doleschel A. Frictional behavior of synthetic gear lubricants. In: Dalmaz G, Lubrecht A, Dowson D, Priest M, editors. Tribology research: from model experiment to Industrial Problem, 2001.
- [15] Höhn B-R, Michaelis K, Vollmer T. Thermal rating of gear drives: balance between power loss and heat dissipation. AGMA technical paper, 1996.
- [16] Höhn B-R, Michaelis K, Döbereiner R. Load carrying capacity properties of fast biodegradable gear lubricants. J STLE—Lubrication Eng 1999.
- [17] Changenet C, Pasquier M. Power losses and heat exchange in reduction gears: numerical and experimental results. VDI-Berichte 2002(1665).
- [18] Winter H, Michaelis K. Investigations on the thermal balance of gear drives. In: Fifth World Congress on Theory of Machines and Mechanisms. American Society of Mechanical Engineers, 1979.
- [19] Eschmann P. Ball and roller bearings—theory, design and applications. New York: Wiley; 1985.
- [20] Gold JW, Schmidt A, dicke H, Loos H, Aßmann C. Viscosity–pressure–temperature behaviour of mineral and synthetic oils. J Synth Lubrication 2001;18(1).

A.5 Paper E

R. Martins, J. Seabra, and L. Magalhães, “Austempered Ductile Iron (ADI) Gears: Power Loss, Pitting and Micropitting”, WEAR, Vol.264 no. 9-10, pp. 838-849, 2008.



Austempered ductile iron (ADI) gears: Power loss, pitting and micropitting

R. Martins^a, J. Seabra^{b,*}, L. Magalhães^c

^a INEGI-CETTRIB, Instituto de Engenharia Mecânica e Gestão Industrial, Rua Dr. Roberto Frias s/n, 4200-465 Porto, Portugal

^b Faculdade de Engenharia, Universidade do Porto, Rua Dr. Roberto Frias s/n, 4200-465 Porto, Portugal

^c Instituto Superior de Engenharia, Instituto Politécnico do Porto, Rua Dr. António Bernardino de Almeida, 431, 4200-072 Porto, Portugal

Available online 18 June 2007

Abstract

This work is a systematic experimental evaluation of austempered ductile iron (ADI) as a gear material. The evaluation of this ADI as a gear material concerns two main aspects: power loss and contact fatigue resistance (pitting and micropitting). All gear tests were performed on the FZG test rig. For the micropitting and power loss evaluation two gear lubricants were considered.

The results show that ADI is a material to be considered by gear designers, once the energetic behavior of ADI gears is similar to carburizing gears, being although slightly worst at high input power. The pitting life is infinite for contact pressures below 1.2 GPa. The best wear behavior of ADI is attained if combined with ester biodegradable lubricant, both on power loss and micropitting tests, so the best overall behavior of ADI gears is obtained with biodegradable ester lubricant.

© 2007 Elsevier B.V. All rights reserved.

Keywords: Gears; Austempered ductile iron ADI; Efficiency; Micropitting; Pitting; Biodegradable lubricant

1. Introduction

Austempered ductile iron (ADI) has been used since the late 1970s and significant developments have been made since then, being now possible to produce high-resistance ADIs. Among the Fe–C alloys products, ADI presents a very interesting combination of mechanical properties. Actually, some ADIs are only surpassed by high-resistance alloyed steels when tensile strength is considered [1].

Replacing conventional steel parts by ADIs results in several advantages which strongly promoted the acceptance and use of these materials, namely in the automotive industry. The first economical reason to use ADIs is that the base material (nodular iron) is cheaper than steel, the second is that ADIs are casting materials, thus products can be molded, allowing significant cost reduction of the manufacturing process when compared to conventional steel machining [2]. The heat-treatments are also low-energy consumers (austempering is done at about 300 °C) and allowing cost-savings when compared to steel quenching or

other conventional heat-treatments [2]. ADIs are also very interesting for the automotive industry as they allow considerable weight reduction (10% lighter than steel), high vibration absorption (more than 6 dB attenuation can be achieved in a gearbox, per instance [3]) and a very high wear and scuffing resistance, avoiding malfunctions under unpredicted unfavorable working conditions (a momentaneous failure of a lubrication system, per instance) [4]. ADIs' tribological performance is not dependent of the presence of AW and EP additives in the lubricants, allowing the use of slightly doped oils [5,6], a major ecological benefit.

The use of ADIs is limited when extreme tensile strength is required (most of the power-transmission gears are still made of steel) but some ADIs can now reach more than 1600 MPa (ultimate tensile strength), according to ASTM normalization, thus being able to support the efforts imposed by the majority of the mechanical applications [4].

In this work ADI gears were tested with two gear lubricants, a mineral oil and a biodegradable ester. Power loss tests were performed at several speeds and torques in order to evaluate the equilibrium temperature of the oil bath and the gear power losses. An energetic balance model of the gearbox is used to access the friction coefficient both for materials and lubricants. The wear behavior is also analyzed and the results are compared with carburizing gears.

* Corresponding author. Tel.: +351 22 508 1742; fax: +351 22 508 1584.

E-mail addresses: rmartins@inegi.up.pt (R. Martins), jseabra@fe.up.pt (J. Seabra), llm@isep.ipp.pt (L. Magalhães).

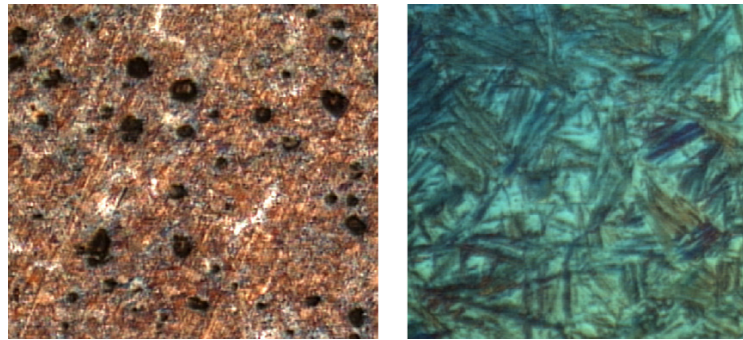


Fig. 1. ADI microstructure (100 \times ; 1000 \times).

The contact fatigue behaviour of ADI as a gear material is also analysed, being for such purpose performed pitting tests at different loads to obtain the S–N curve of the material. The ADI micropitting performance on gears was also evaluated and compared to carburized steel.

2. Austempered ductile iron—ADI

The ductile iron used in this work had the following chemical composition (in weight percent): 3.38% C, 2.43% Si, 0.55% Mn, 1.11% Cu, 0.015% P, 0.020% S [5–8].

The as-cast material suffered a homogenising annealing prior to the test pieces manufacturing. This pre heat treatment was conducted in an electrical muffle furnace at the temperature of 1000 °C, with a soaking time of 30 min, followed by furnace cooling at a rate of 20 °C/min in the pearlitic domain. An essentially pearlitic microstructure was obtained in the end of this pre heat treatment [5–8]. The austempering heat treatment consists on sample austenitisation at 875 °C during 30–40 min, followed by austenite isothermal transformation at 300 °C during 210 min in a salt bath crucible furnace, to produce the ausferritic microstructures (acicular ferrite plus carbon stabilized austenite), as shown on Fig. 1. Graphite nodules are evenly distributed in the ausferritic structure [5–8].

Table 1 shows the main mechanical properties of ADI material used in this work. Quite high tensile and yield strengths were obtained together with a reasonable total elongation. The same mechanical properties are given for the 20MnCr5 carburized steel, which is widely used for gears and other highly stressed parts, allowing the carburizing of the gear surface while the

core keeps up high ductility, having also a considerably high elongation.

3. Gear oils

Two industrial gear lubricants were used on this work: an ISO VG 150 mineral oil, containing an additive package to improve micropitting resistance, and an ISO VG 100 biodegradable fully saturated ester lubricant with a low toxicity additivation. Both oils are specified as CLP gear oils according to DIN 51517.

The main properties of the two lubricants are shown in Table 2. Their kinematic viscosities are almost equal at 90 °C.

The mineral gear lubricant is based on paraffinic oil with significant residual sulphur content and it contains an ashless antiwear additive package based on phosphorous and sulphur chemistry and metal-organic corrosion preventives. In contrast, the biodegradable ester fluid uses a fully saturated ester based on harvestable materials incorporating environmentally compatible and highly efficient additives, being the metal-organic compounds completely avoided. The additive content of the mineral oil is considerably higher than that of the ester oil, mainly in what concerns the sulphur compounds. The “ultimate” biodegradability of lubricants is assessed using a “ready” biodegradability test as published by the OECD and adopted by European Union. The mineral oil didn’t match the minimum requirements of 60% biodegradability in 28 days, as shown in Table 2. Thus, no toxicity tests were performed for this lubricant. The ester based oil exceeded the minimum requirement of 60% biodegradability in 28 days and passed both toxicity tests, OECD 201 “Alga growth inhibition test” and OECD 202 “Daphnia Magna acute immobilization”, as show in Table 2.

4. Power loss of ADI gears

Power transmission equipments using gears dissipate significant amounts of power and the evaluation of their energetic performance is very important, since it might represent a considerable reduction in energy consumption. So, gear power loss and efficiency are of fundamental importance for any application and it depends on gear material and lubricant characteristics [9–11]. The equilibrium temperature of a gearbox is reached when the power losses inside the gearbox are equal to the evacuated heat

Table 1
Mechanical properties of 20MnCr5 and ADI materials

Properties	Unit	ADI	20MnCr5
Modulus of elasticity	10 ³ N/mm ²	170	210
Density	g/cm ³	7.06	7.85
Poisson’s ratio		0.25	0.3
Surface hardness	HRC	42	58–62
Tensile strength	N/mm ²	1433	1300
Yield strength 0.2%	N/mm ²	1178	550
Elongation	%	6	8

Table 2
Physical and chemical properties of the lubricants

Parameter	Method	Desig.	Units	Lubricating oils	
Base oil	DIN 51451	–	–	Paraffinic mineral oil	Fully saturated ester
Physical properties					
Density @ 15 °C	DIN 51757	ρ_{15}	g/cm ³	0.897	0.925
Kinematic viscosity @ 40 °C	DIN 51562	ν_{40}	cSt	146	99.4
Kinematic viscosity @ 100 °C	DIN 51562	ν_{100}	cSt	14.0	14.6
Viscosity index	DIN ISO 2909	VI	–	92	152
Pour point	DIN ISO 3106	–	°C	–21	–42
Wear properties					
KVA weld load	DIN 51350-2	–	N	2200	2200
KVA wear scar (1 h/300 N)	DIN 51350-3	–	mm	0.32	0.35
Brugger crossed cylinder test	DIN 51347-2	–	N/mm ²	68	37
FZG rating	DIN 513540	K _{FZG}	–	>13	–
Chemical content					
Zinc	ASTM D-4927	Zn	ppm	–	–
Calcium	ASTM D-4927	Ca	ppm	40	–
Phosphor	ASTM D-4927	P	ppm	175	146
Sulphur	ASTM D-4927	S	ppm	15040	180
Biodegradability and toxicity properties					
Ready biodegradability	OECD, 301 B	–	%	<60	≥60
Aquatic toxicity with Daphnia	OECD, 202	EL ₅₀	ppm	–	>100
Aquatic toxicity with Alga	OECD, 201	EL ₅₀	ppm	–	>100

from the gearbox to the surrounding environment. This equilibrium is dependent of the gearbox geometry, gear material, lubricant properties and environmental conditions [10,12–14]. The equilibrium temperature at constant operating conditions is a direct indication of power losses, since a lower equilibrium temperature indicates higher energetic efficiency, lower friction coefficient, smaller oil oxidation and a longer oil life [9].

The gear efficiency tests had two main objectives: (i) measurement of the equilibrium temperature of the lubricant, at different operating conditions (torque and speed), and (ii) the evaluation of the wear protection provided by each gear oil. The results obtained were compared with similar results obtained with carburized steel gears.

4.1. Operating conditions in gear power loss tests

All the gear tests were performed on the well known FZG back-to-back spur gear test rig, shown in Fig. 2, and the gears used are similar to standard FZG type C gears [15] (pinion, 16 teeth; wheel, 24 teeth; modulus, 4.5 mm; center distance, 91.5 mm).

The tests were performed with both gear oils using a wide range of speed and torque conditions, corresponding to input powers between 0.5 and 86.4 kW, as shown in Table 3. The hertzian contact pressures at the gear pitch point, corresponding to each FZG load stage (or torque level), and the number of cycles for each combination of torque and speed are also presented. Austempered ductile iron gears have lower contact pressure at the pitch point than carburized steel gears. Such difference is directly related to the difference in Young modulus between the two materials ($E_{ADI} = 170$ GPa and $E_{steel} = 210$ GPa).

The initial surface roughness (R_a) of the teeth flanks of the ADI gears was between 0.6 and 0.7 μm .

The overall gear efficiency test program consisted of nine tests, performed at three different speeds and three torque levels, corresponding to FZG load stages 1, 5 and 7. The tests performed at very low torque (on load stage 1 at 4.95 Nm), usually designated as no-load tests, were used to evaluate the churning losses inside the FZG test gearbox, since in those conditions the friction losses between the gear teeth were reduced to a minimum.

Each one of the nine tests started at approximately 40 °C and the oil sump temperature was set free. During each test the operating conditions were kept constant, so that the equilibrium lubricant temperature was reached. The test was stopped if the oil sump reached 180 °C. The no-load tests duration was 2 h

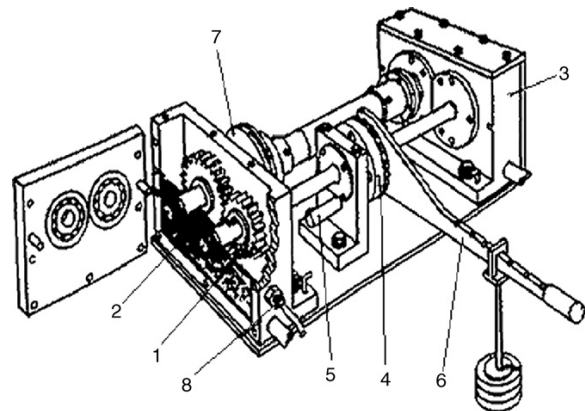


Fig. 2. Schematic view of the FZG gear test rig.

Table 3
Operating conditions in FZG gear power loss tests for carburizing and ADI gears

Test type	Speed (wheel) (rpm)	Torque (Nm)	Input power (kW)	Hertz pressure (MPa)		No. of cycles (wheel) ($\times 10^3$)	
				ADI	Steel		
No-load tests	1000	4.95	0.5	165	186	120	
	2000		1.0			240	
	3000		1.6			360	
Load tests	1000	141.2	14.8	881	994	300	
			28.8	1230	1388	300	
			29.6	881	994	600	
	2000	141.2	57.6	1230	1388	600	
			44.3	881	994	900	
			86.4	1230	1388	900	
	3000	141.2	141.2	141.2	141.2	141.2	141.2
			141.2	141.2	141.2	141.2	141.2
			141.2	141.2	141.2	141.2	141.2

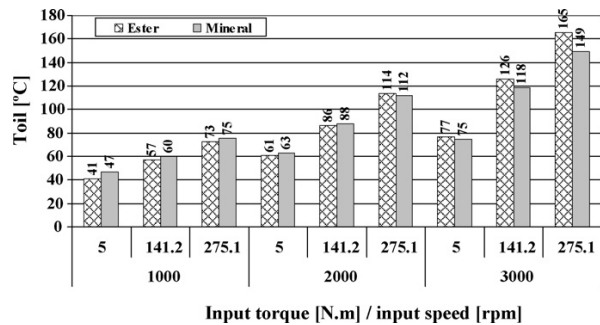


Fig. 3. Stabilization temperature for ADI gears lubricated with mineral and ester gear oils.

(enough to reach the equilibrium temperature) and the load tests lasted 5 h.

After each group of load tests at constant speed a lubricant sample was collected for post-test oil analysis by direct reading ferrometry, in order to evaluate gear wear.

4.2. Gear power loss results

Fig. 3 shows the equilibrium temperatures reached by ester and mineral gear oils in the efficiency tests with ADI gears. In the no-load tests ($T = 5$ Nm) the ester oil always generated a lower equilibrium temperature than the mineral oil. For such low torque values, the most important sources of power dissipation

inside the FZG gearbox were the churning losses, which mainly depend on the lubricant viscosity. So, since the ester oil has lower viscosity than the mineral oil below 100°C it generates less power dissipation and lower equilibrium temperatures.

In the load tests ($T = 141$ and 275 Nm), the friction losses between the gear teeth become much more important than the churning losses, the overall power loss increases, and the gear oil equilibrium temperatures are significantly higher.

At 1000 and 2000 rpm the ester oil had lower equilibrium temperatures than the mineral oil (except the test at 2000 rpm/275 Nm) while at 3000 rpm the opposite was observed. For the highest torque and speed (input power of 86.4 kW) the two gear oils reached very high equilibrium temperatures, around or above 150°C .

The oil samples collected during the gear power loss tests were analyzed by direct reading ferrography [16] to measure the ferrometric parameters D_1 (large wear particles index: size greater than $5\ \mu\text{m}$) and D_s (small wear particles index: size smaller than $5\ \mu\text{m}$) and to determine the concentration of wear particles index—CPUC $((D_1 + D_s)/d)$ and the severity of wear particles index—ISUC $((D_1^2 + D_s^2)/d^2)$.

Fig. 4 presents the evolution of CPUC and ISUC wear indexes for each lubricant, during the FZG power loss tests with ADI gears. The ester gear oil showed lower CPUC and ISUC values than the mineral oil in the first two lubricant samples (collected after the load tests at 1000 and 2000 rpm), while the opposite was observed for the last lubricant samples obtained after the tests at 3000 rpm. However, the evolution during the tests and

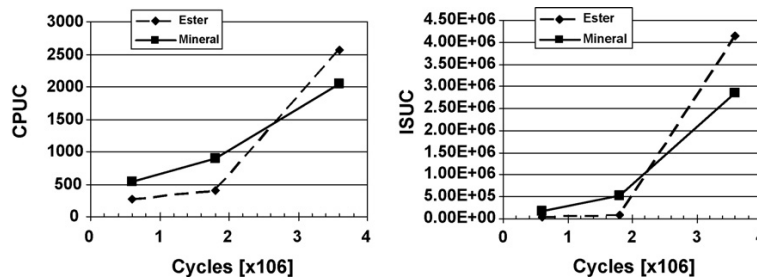


Fig. 4. Evolution of CPUC and ISUC wear indexes during FZG gear power loss tests.

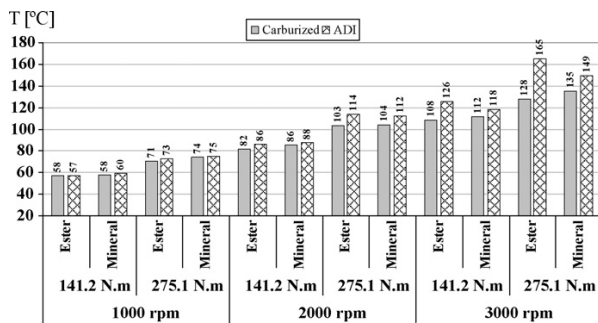


Fig. 5. Stabilization temperature in the FZG gear power loss tests for both lubricants, comparing ADI material with carburized steel.

final values of the CPUC and ISUC wear indexes were similar for both lubricants and typical of normal gear operation.

The total mass loss of each gear (sum of pinion and wheel mass loss) after the gear power loss tests is: 73 mg for the gear lubricated with ester oil and 150 mg for the gear lubricated with mineral oil. Both mass losses were too high, compared with similar gears made of carburized steel. The mass loss corresponding to the mineral oil was twice that of the ester oil.

In the last two load tests at 3000 rpm both gears operated at high torque (141.2 and 275 Nm) and high speed during 5 h, reaching high and abnormal lubricant temperatures for this kind of applications. These high temperatures were related to the high increase of wear indexes after tests at 3000 rpm and agree with the final values of mass loss measured.

4.3. Comparison with carburized steel gears

Fig. 5 compares the oil equilibrium temperatures of ADI gears with similar results obtained in a previous work with carburized steel gears [11,17], which had the same geometry and were tested in the same conditions and with the same gear oils.

In the tests with carburized gears the ester lubricant has always lower stabilization temperature than the mineral lubricant. In the tests with ADI gears the ester lubricant also displays lower stabilization temperatures until the test at 2000 rpm and 275 Nm, from then on the mineral lubricant displays lower stabilization temperatures.

In general, ADI gears exhibited higher oil equilibrium temperatures than carburized gears, whatever the lubricant and the operating conditions. For the highest torque ($T = 275$ Nm), ADI gears showed oil equilibrium temperatures 8–18 °C above those measured for carburized gears, meaning that ADI gears had higher friction power losses than carburized gears, since the churning losses measured in no-load conditions were the same for both gear materials.

4.4. Friction coefficient between gear teeth

In a previous work [11], an energetic balance model was developed for the FZG test gearbox, quantifying the power losses inside the gearbox and the power evacuated to the surrounding

Table 4

Lubricant and material dependent exponent α for the friction coefficient

		Carburized steel	ADI
Gear oil	Mineral	0.145	0.184
	Ester	0.124	0.163

environment. Such model established that,

$$P_{fr} + P_{MI} + P_{spl} + P_{M0} + P_{sl} = Q_{rad} + Q_{cnv} + Q_{cn}, \quad (1)$$

where P_{fr} represented the friction power dissipated by the gears, P_{MI} the friction power dissipated by the bearings, P_{spl} the power dissipated by the seals, P_{M0} the churning power dissipated by the bearings, P_{sl} the churning power dissipated by the gears, Q_{rad} the power evacuated by radiation, Q_{cnv} the power evacuated by convection and Q_{cn} represented the power evacuated by conduction.

Eq. (1) could be used to establish the relation between the oil equilibrium temperatures measured in gear power loss tests and the friction coefficient between gear teeth [11]. The correlation between experimental and model oil equilibrium temperatures, using the energetic balance model of the FZG test gearbox, allowed the definition of an expression for friction coefficient between gear teeth, depending on gear material and gear oil, that is,

$$\mu = 0.048 \frac{(F_{bt}/b)^\alpha}{(v_{\sum c} \rho_c)^{0.2}} \eta_{oil}^{-0.05} Ra^{0.25}, \quad (2)$$

where α is the material and lubricant dependent, F_{bt} the tooth normal force in transverse section, b the face width of the gear, ρ_c the equivalent radius of curvature at pitch point, $v_{\sum c}$ the sum velocity at pitch point and η_{oil} is the oil dynamic viscosity at operating temperature.

The values of exponent α are given in Table 4 for each combination of gear material and gear oil tested. The tests performed at 3000 rpm were not considered in this correlation due to the very high temperature and wear occurred.

The α exponent is smaller for carburized steel with both lubricants tested, meaning that the increase of friction coefficient with the increase of load is larger for ADI gears, as observed during the gear tests. The value of the exponent α proposed for mineral additive free lubricants is 0.2 [10].

4.5. Discussion on ADI gear power loss

In power loss tests ADI gears always presented higher stabilization temperature than carburized steel gears, although on the tests at 1000 rpm (at all load stages) and 2000 rpm (excluding higher load stage) the stabilization temperatures are very similar. In the tests performed at higher speed and load (higher input power) the ADI gears displayed considerably higher stabilization temperatures than carburizing steel. This behavior is similar for both lubricants.

The stabilization temperature is an indication of the power losses inside a gearbox, since higher power losses generate higher operating temperature. The application of an energetic

model allowed the definition of a friction coefficient expression for each combination of material-lubricant. The friction coefficient is always smaller for carburizing steel whichever the lubricant and the ester lubricant promoted lower friction coefficient for both materials. These friction coefficients are coherent with the lubricant stabilization temperatures observed during gear power loss tests.

ADI gears lubricated with ester oil generated significantly smaller mass loss (50% less) than when lubricated with mineral oil and the ferrometric wear indexes measured on the ester oil samples were smaller than those corresponding to equivalent mineral oil samples.

However, during the last test with ester oil at 3000 rpm, the ADI gear exhibited very significant wear and reached very high lubricant temperatures. After this test the ferrometric wear indexes measured on the ester oil samples were higher than those measured in the mineral oil samples.

5. Pitting load carrying capacity of ADI gears

Austempered ductile iron is a material family with an increasing applicability on gears and other highly stressed mechanical components, mainly due to the combination of high strength, ductility, toughness, fatigue strength and wear resistance they offer [18]. However, spalling, pitting and micro-pitting are typical surface failures in ADI gear tooth flanks [5–8], meaning that the contact fatigue performance of ADI is fundamental in gear design.

Magalhães et al. [6] defined a contact fatigue severity parameter based on the fact that higher contact pressure reduces contact fatigue life and high strength material increases fatigue life. This parameter, p_0^2/σ_r , presented a very good correlation when analyzing the contact fatigue resistance of disc and gears for different ADI's.

Gear pitting tests were performed to evaluate the contact fatigue performance of the present ADI and determine its S–N curve.

5.1. Operating conditions in gear pitting tests

The gear pitting tests were also performed in the FZG test rig, under dip lubrication conditions, using 1.5l of fully saturated

ester gear oil. Each test was performed twice, except the test at 1000 rpm that was only performed once.

Table 5 shows the operating conditions used in the gear pitting tests. The tests at 3000 rpm were all performed at constant temperature (90 °C), and in the test at 1000 rpm, the oil temperature was set free (starting at 40 °C), increasing until stabilization occurred, around 92 °C.

5.2. Gear pitting results

Table 5 presents the number of cycles performed by the pinion on each gear pitting test, until a contact fatigue failure occurs. The types of surface fatigue damage considered were micro-pitting and pitting. Micropitting surface failure was hard to detect, especially *in situ*, without dismounting the gears, although when detected it was registered.

The tests where micro-pitting was detected were carried out onwards until the pitting failure occurred, or up to 20 million cycles. Beside the number of cycles, torque, contact pressure and severity parameter (p_0^2/σ_r) of each test are also given in Table 5.

Table 5 shows that micropitting failure occurred at contact pressures of 1.19, 1.33 and 1.48 GPa, although not in all tests performed at those contact pressures.

5.3. Discussion on ADI gear pitting

In Fig. 6 the severity parameter (p_0^2/σ_r) is plotted against the number of cycles (N) until pitting occurs. As expected, as the contact pressure at the pitch point decreased the number of cycles until gear pitting increased. When the severity parameter was lower than 1.2 GPa, no pitting failures were observed and the tests exceeded 20 million cycles. In some tests gear micropitting occurred before the pitting failure.

The correlation between the severity parameter and the number of cycles till gear pitting was very good (correlation factor $R^2 = 0.98$) and could be represented by the following expression:

$$\frac{p_0^2}{\sigma_r} = 5.541 - 2.778 \times \ln(N). \quad (3)$$

Fig. 6 also shows the correlation (slash dot line) obtained by Magalhães et al. [6] for the severity parameter (p_0^2/σ_r)

Table 5
Number of cycles of gear pitting tests, until fatigue failure or test end

Speed (wheel)	Input Power	Torque	Hertzian pressure	p_0^2/σ_r	Number of cycles (pinion)		
					Total	Micropitting	Pitting
[rpm]	[kW]	[N m]	[GPa]	[GPa]	[x10 ⁶]		
3000	124.9	397.5	1.48	1.71	1.08	-	1.08
		397.5	1.48	1.71	0.81	0.54	0.81
	101.6	323.3	1.33	1.39	3.24	-	3.24
		323.3	1.33	1.39	2.97	1.62	2.97
	80.9	257.4	1.19	1.11	20.00	3.78	-
		257.4	1.19	1.11	21.60	-	-
	62.4	198.7	1.05	0.86	24.00	-	-
		198.7	1.05	0.86	27.00	-	-
1000	47.4	453.0	1.58	1.95	0.45	-	0.45

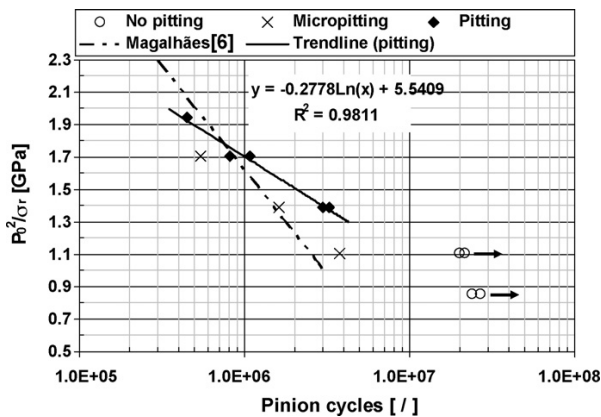


Fig. 6. Gears pitting tests: severity parameter (p_0^2/σ_r) vs. number of cycles (N).

versus number of cycles (N) in gear pitting tests performed with different varieties of ADI's, austempered at several different temperatures (from 260 to 340 °C) and using single and double step austempering heat treatments. The slopes of the curves are different, because the present results only concern the ADI austempered at 300 °C using a conventional single step austempering heat treatment. However, as in the present case, Magalhães did not find pitting failures in gear tests when the contact severity parameter was lower than 1.2 GPa [6].

6. GEAR micropitting tests

In spur gears, pure rolling exists only at the pitch point. Above and below this point there is a combination of rolling and sliding, and the sliding speed increases as the contact point moves away from the pitch line. The more critical contact condition leading to micropitting occurs when sliding and rolling directions are opposite, which always takes place below pitch diameter, both for driving and driven gears [19].

The micropitting tests with ADI gear were also performed in the FZG test rig.

Two different lubricants were tested and the behavior of ADI gears is compared with that of carburized steel gears.

Gear micropitting was assessed during the tests, using accurate mass loss measurements, ferrometric oil analysis and roughness measurements of active teeth flanks.

Micropitting failures appear firstly on pinions, as they perform 33% more cycles than wheels, being the results presented

concerning micro-pitted area, photographs and surface roughness referred to the pinion.

6.1. Test gears and operating conditions

Table 6 shows gear quality grade of tested steel and ADI gears according to ISO 1328 standard in comparison with the standard FZG type C gear for micropitting. The test code and the lubricant used on each test are also shown.

The tested gears have a quality grade considered “current” while the standard gears have a “fine” quality grade. This difference is clearly expressed in terms of the average roughness of the teeth flanks.

Micropitting tests were based on the DGMK-FZG micropitting short test procedure (abbreviated as GFKT-C/8.3/90) [20], which is a short term test, similar to the FVA-FZG-micropitting test [21], able to classify candidate lubricants in terms of gear micropitting. According to this test procedure, carburized gears are tested in load stages k7 and k9, as shown in Table 7 (gears CM and CE).

The GFKT-C/8.3/90 test procedure was adapted to the ADI gears under analysis since they have higher tooth surface roughness, lower geometric quality and lower contact resistance than standard carburized steel gears, thus, ADI gears (AM and AE) were tested in load stages k5 and k7 and one ADI gear (AM*) was also tested in load stages 7 and 9, for comparison.

The test procedure for the assessment of gear micropitting resistance can be resumed as follows:

1. Test the gear in load stage k3 (running-in);
2. Collect a lubricant sample for analysis;
3. Test the gear in load stage k5 (for ADI) or k7 (for steel and AM* ADI gear);
4. Collect a lubricant sample for analysis;
5. Dismount the gear, measure tooth flank roughness and photograph the tooth surface;
6. Mount the gear with fresh lubricant;
7. Test the gear in load stage k7 (for ADI) or k9 (for steel and AM* ADI gear);
8. Repeat steps 4 and 5.

6.2. Comparison of ADI with carburized steel

Fig. 7 represents the mass loss measurements after each load stage during the gear micropitting tests performed with carbur-

Table 6
Gear reference, quality grade and average surface roughness

	Test code	Lubricant type	Gear quality grade (ISO 1328)	Average roughness of teeth flanks (R_a) (μm)
Standard gear	–	–	5	0.5
20MnCr5 carburized	CM	Mineral	9	0.9
	CE	Ester	9	1.1
ADI austempered at 300 °C	AM*	Mineral	9	1.0
	AM	Mineral	9	0.7
	AE	Ester	9	0.7

Table 7
Test procedure and operating conditions for micropitting tests with ADI gears and carburized steel

	Torque stages							
	$K_{FZG} = 3$ running in		$K_{FZG} = 5$		$K_{FZG} = 7$		$K_{FZG} = 9$	
	Pinion	Wheel	Pinion	Wheel	Pinion	Wheel	Pinion	Wheel
Temperature (°C)	80		90					
Torque (Nm)	28.8	43.2	70	104.9	132.5	198.8	215.6	323.4
Rot speed (rpm)	2250	1500	2250	1500	2250	1500	2250	1500
V_t (m/s)	8.3							
Hertzian stress (Mpa)								
ADI	487		760		1046		1334	
Steel	550		857		1180		1505	
Power (kW)	6.8	16.5	31.2	50.8				
Duration (h)	1	16	16	16				
N cycles ($\times 10^3$)	135	90	2160	1440	2160	1440	2160	1440
ADI-AM* Carb. Steel-CM, CE	X				X		X	
ADI-AM, AE	X		X		X			

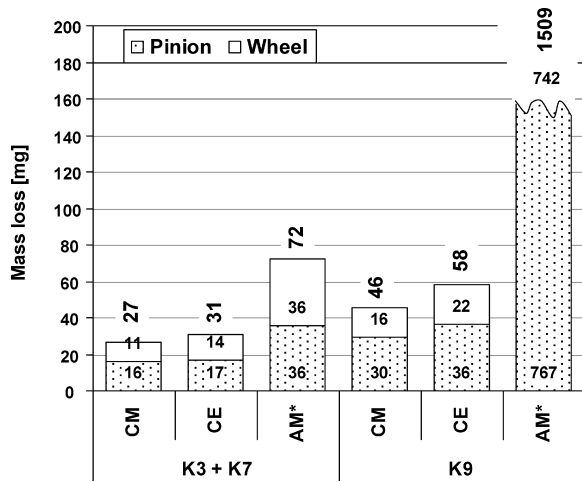


Fig. 7. Gear mass loss during micropitting tests: carburized steel (CM and CE) vs. ADI (AM*).

ized steel and ADI gears. These results clearly differentiate the two materials, as the ADI gear (AM*) displayed a huge mass loss (1509 mg) after the last load stage (k9), approximately 30 times more than carburized gears. Carburized steel gears had a very moderate mass loss (around 50 mg), taking into account the manufacturing quality of the gears (ISO 9) and the initial surface roughness ($R_a \approx 1 \mu\text{m}$). Carburized steel gears had a higher mass loss when lubricated with the ester based gear oil, compared to the reference mineral oil (+25%, +8 mg).

After each load stage, gears were dismantled and cleaned, and pictures of pinion teeth flanks were captured as shown in Table 8. On these pictures the micropitting area below the pitch line is surrounded by a red line for easier reading.

Carburized steel gears had a higher micropitting area when lubricated with the ester based gear oil, compared to the reference mineral oil: +3% after load stage k7 and +7% after load stage k9.

Images from the active flanks of AM* ADI gear, after load stage k7, showed acceptable micropitting area (21%) and mass loss (72 mg). After load stage K9, AM* ADI gear showed an overall failure on tooth flank, showing very severe wear, scuffing

Table 8
Pictures of carburizing steel (CM, CE) and ADI (AM*) pinion teeth after micropitting tests

	CE – Steel, ester oil	CM – Steel, mineral oil	AM* – ADI, mineral oil
K7			
$T_1 = 132.5\text{Nm}$ $n_1 = 2250\text{rpm}$ $P = 31.2\text{kW}$	Micropitted area (%) = 13	Micropitted area (%) = 10	Micropitted area (%) = 21
K9			
$T_1 = 215.6\text{Nm}$ $n_1 = 2250\text{rpm}$ $P = 50.8\text{kW}$	Micropitted area (%) = 31	Micropitted area (%) = 24	

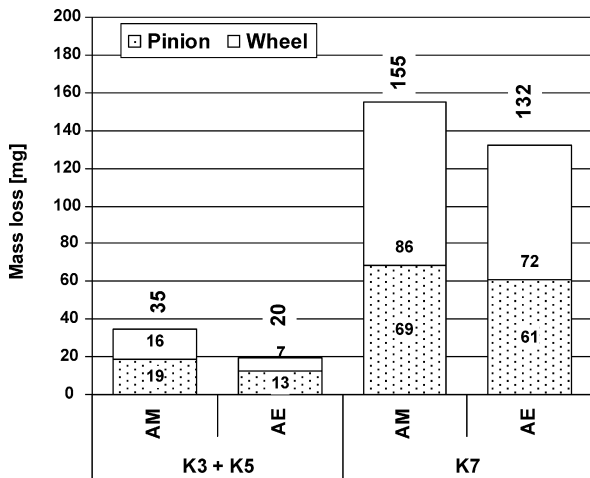


Fig. 8. Gear mass loss during ADI gear micropitting tests: mineral oil (AM) vs. ester (AE) fluid.

marks and pitting on surface, indicating that an excessive contact pressure was used. The AM* gear, suffered a total weight loss of more than 1.5 g and a global destruction of the teeth flanks. These results clearly show that ADI gears did not support the operating conditions proposed by the GFKT-C/8.3/90 test procedure, normally imposed to carburized steel gears, requiring an adapted test procedure.

Thus, the GFKT-C/8.3/90 test procedure was revised and lower contact pressures, corresponding to load stages k5 and k7, were adopted for the micropitting tests with ADI gears, as presented in Table 7.

6.3. ADI micropitting test results

The mass loss results for ADI gears, lubricated with both gear oils using the updated operating conditions are presented in Fig. 8. ADI gears when lubricated with ester oil presented a slightly smaller weight loss than when lubricated with mineral oil (–15% after load stage k7).

Table 9 shows images of ADI teeth flanks after the gear micropitting tests performed with both lubricants (AM and AE). After load stage k5, the micropitting area was very small in both pinions, between 8% and 9% of the tooth flank surface. After load stage k7 the micropitting area increased significantly in both cases, having the same width of the teeth flanks (14 mm) and more than 2 mm of height, as can be observed in Table 9. The micropitting areas measured after load stage k7 increased to 23% in the case of the mineral oil (AM gear) and to 29% in the case of the ester oil (AE gear).

Lubricant samples were collected after each load stage and analysed by direct reading (ferrometry) and analytical ferrography. Fig. 9 displays the wear particles concentration index—CPUC and the wear particles severity index—ISUC

Table 9 Pictures of ADI (AM, AE) pinion teeth flanks after gear micropitting tests

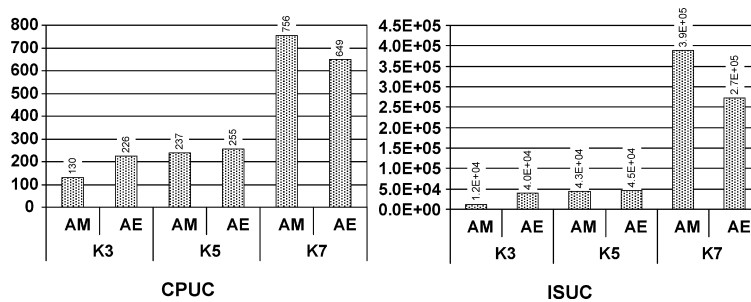
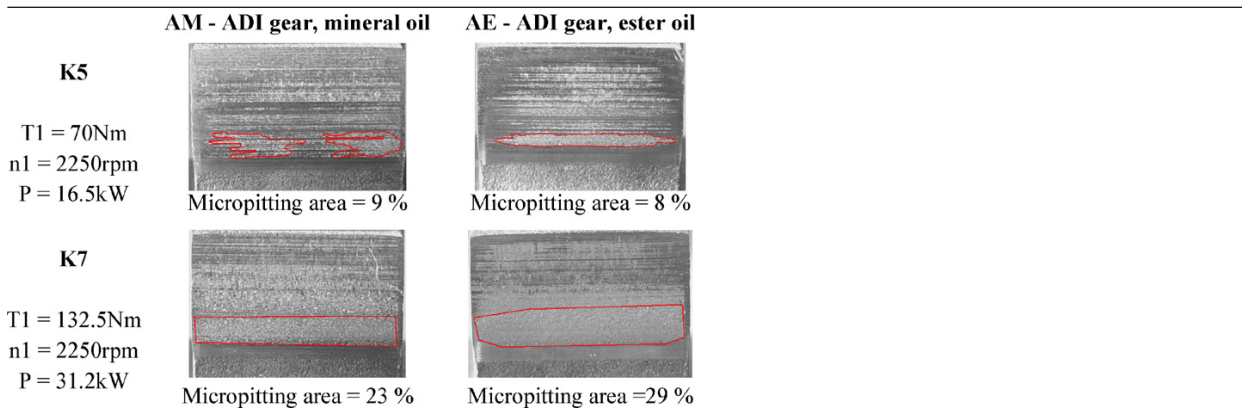
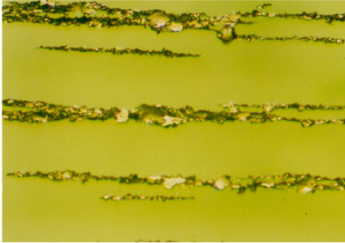


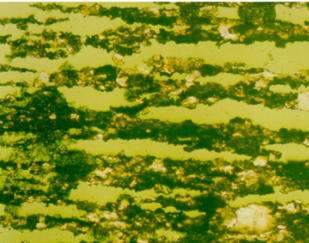


Fig. 9. Ferrometric indexes (CPUC and ISUC) during AM and AE gear micropitting tests.

Table 10
Ferrogram pictures after each load stage of AM and AE gears

	AM - ADI gear, mineral oil	AE - ADI gear, ester oil
Load stage K5		
	$d = 0.1$; $D_1 = 21.0$; $D_s = 2.8$; CPUC = 237; ISUC = 4.3E4	$d = 0.1$; $D_1 = 21.6$; $D_s = 3.9$; CPUC = 255; ISUC = 4.5E4
Load stage K9		
	$d = 0.1$; $D_1 = 63.5$; $D_s = 12.1$; CPUC = 756; ISUC = 3.9E5	$d = 0.1$; $D_1 = 53.4$; $D_s = 11.5$; CPUC = 649; ISUC = 2.7E5

Magnification = 200 \times .

measured for each ADI gear after each load stage. The lubricant was replaced after each load stage, and so the wear particle indexes refer to each load stage test period.

The general behaviour of the ADI gears was similar with both lubricants. The amount (CPUC) and severity (ISUC) of the wear particles generated during running-in (k3) and load stage k5 were very similar, but increased very significantly during load stage k7, as shown in Fig. 9. At the end of the micropitting tests the ADI gear lubricated with ester oil (AE gear) generated a smaller amount of wear particles than the gear lubricated with mineral oil (AM gear).

The ferrograms obtained by analytical ferrography, corresponding to each lubricant sample, are presented in Table 10. The amount, size and shape of the wear particles produced during load stage k5 were very similar for both gear oils, as shown by the ferrograms on Table 10 and confirmed by the D_1 and D_s indexes, related to the amount of large and small particles, respectively.

After load stage k7 the amount of particles increased very significantly, as observed on the ferrograms, and the ADI gear lubricated with the mineral oil generated wear particles of larger size than the gear lubricated with the ester fluid ($D_{1\text{ mineral}} = 63.5$ and $D_{1\text{ ester}} = 53.4$). Typical contact fatigue particles, related to gear micropitting, were observed in both ferrograms and their amount increased when the load stage also increased.

Surface roughness measurements were made on the teeth flanks of both gears, in the radial direction, after each load stage. An assessment length of 1.5 mm and a cut-off length of 0.25 mm. were used. Two different zones were measured, one

below the pitch line, where micropitting generally occurs, and another above the pitch line, where typical mild wear is frequently observed. The as manufactured surface is designated original.

Table 11
Roughness parameters of ADI gear AM (values in μm)

Pinion	R_{max}	R_{z-D}	R_{pk}	R_{vk}
Original	6.6	4.7	0.7	1.5
Below pitch line				
K5	7.6	4.7	0.3	1.9
K7	10.4	6.0	0.8	3.2
Above pitch line				
K5	7.4	4.2	0.3	2.3
K7	7.6	4.8	0.7	2.7

Table 12
Roughness parameters of ADI gear AE (values in μm)

Pinion	R_{max}	R_{z-D}	R_{pk}	R_{vk}
Original	7.5	5.7	1.3	1.1
Below pitch line				
K5	4.7	3.4	0.5	1.3
K7	10.1	6.0	0.7	2.8
Above pitch line				
K5	7.2	3.5	0.3	1.5
K7	7.2	4.5	0.2	2.5

Tables 11 and 12 show the roughness parameters measured on the teeth flanks of AM and AE gears, respectively. The values given are the average of three measurements on each gear.

Below the pitch line, a significant increase of the R_{vk} and R_{max} roughness parameters was observed, indicating the presence of deep valleys related to the micro-pits generated on the teeth flanks. Above the pitch line a significant reduction of the R_{pk} and R_{z-D} roughness parameters was observed, indicating the occurrence of mild wear and the elimination of the most significant roughness peaks.

The occurrence of gear micropitting below the pitch line is clearly observed on the pictures of the tooth flanks shown in Table 9. In the same pictures the wear of the tooth flanks above the pitch line, suggested by the analysis of the surface roughness measurements, can also be observed.

6.4. Discussion on ADI gear micropitting

In the gear micropitting tests, the ADI gear combined with the ester lubricant (AE gear) had 15% less mass loss than with mineral oil (AM gear). This fact is confirmed by the oil analysis results, since the wear particles concentration index (CPUC) and the large particles index (D_1) for AE gear were 15% lower than for AM gear.

The visual inspection of the micropitting areas below the pitch line showed that they were similar for both lubricants (AM and AE gears) after load stage k5. At the end of the micropitting test, AE gear had a micropitting area 26% larger than AM gear. However, the surface roughness measurements made below the pitch line of each gear did not reveal significant differences, as both gears had similar roughness. This indicated that the depths of the micro pits generated were very similar in both gears.

The visual inspection of the teeth flanks above the pitch line showed that the original transversal grinding marks were progressively worn out in both gears during the tests. At the end of the micropitting tests, the degradation of the teeth flanks of AM gear was more severe than that of AE gear, as shown in Table 9. The surface roughness measurements above the pitch line and the corresponding roughness parameters confirm this assessment, in particular the R_{pk} value.

Above the pitch line, the ester oil has a slightly better wear behaviour than the mineral oil, confirmed by the visual inspection and the surface roughness measurements of teeth flanks. This justifies why the ADI gear lubricated with ester oil generated less wear particles than the gear lubricated with mineral oil, as shown by the mass loss and oil analysis results, and is related to the lower friction between gear teeth promoted by the ester oil, as shown in the gear power loss tests.

7. Conclusions

1. The ADI gear presented always higher stabilization temperature than carburized steel gears, although the operating temperature was roughly the same for input powers up to 50 kW. Above that value of input power carburized gears displayed lower stabilization temperature.

2. The tests with carburized gears displayed lower stabilization temperature if ester lubricant is used while ADI gears displayed lower stabilization temperature with mineral lubricant in the tests performed at 3000 rpm.
3. The ester oil promoted smaller weight loss than mineral oil when ADI gears are used, especially for the lowest speeds.
4. The coefficient of friction, determined using an energetic model, has a smaller load exponent (less load dependent) for both materials when ester lubricant is used. The load exponent is smaller for carburized steel, whatever lubricant is used.
5. The pitting tests performed with ADI gears showed that for contact pressures below 1.2 GPa the contact fatigue life of ADI gears is infinite, although micropitting may occur.
6. The S/N curve for the ADI, austempered at 300 °C, was determined, showing very good correlation with the experimental results.
7. The GFKT-C/8.3/90 test procedure for gear micropitting, used for carburized steel gears, cannot be applied to ADI gears, because premature failures may occur. An updated test procedure was developed.
8. The parameters used to assess the micropitting behaviour of ADI gears were adequate and a good correlation was obtained between all test results: mass loss, ferrometry, analytical ferrography and surface roughness measurements.
9. The micropitting behaviour of ADI gears lubricated with mineral and ester oils was very similar and micropitting always occurs below the pitch line, as in the case of carburized steel.
10. Above the pitch line the teeth flanks suffered mild wear. In this region, the ADI gear lubricated with mineral oil had higher wear than the gear lubricated with ester oil.
11. The gear micropitting tests performed with ADI gears showed that the biodegradable non-toxic ester had an overall better performance than the mineral oil.

Acknowledgements

The authors express their gratitude to the European Union for the financial support given to this work through the Project: “EREBIO—Emission reduction from engines and transmissions substituting harmful additives in biolubricants by triboreactive materials” (Proposal no. GRD2-2001-50119, Contract No. G3RD-CT-2002-00796-EREBIO).

The authors would like to thank all the partners involved in EREBIO project for their cooperation, and in particular, FUCHS PETROLUB, AG, (Dr. Rolf Lutther) for supplying the biodegradable gear oil, FERESPE, Fundação de Ferro e Aço L. da (Mr. Joaquim Santos) for supplying the nodular iron and A. BRITO, Industria Portuguesa de Engrenagens L. da (Mr. Álvaro Brito) for machining and grinding the gears.

References

- [1] Mullins, J.D., Ductile Iron Data for Design Engineers. SOREMETAL. 1990. Rio Tinto Iron & Titanium inc.

- [2] R. Harding, The Use of Austempered Ductile Iron for Gears in 2^o World Congress of Gears, Paris, 1986.
- [3] P. Salonen, Improved Noise Damping and Reduced Weight in Truck Components With KYMENITE ADI, in: International ADI and Simulation Conference, Finland, 1997.
- [4] L. Magalhães, Caracterização Tribológica de um Ferro Nodular Austemperado em Ensaio Disco-Disco e de Engrenagens FZG, in: Faculdade de Engenharia, Universidade do Porto: Porto, 2003.
- [5] L. Magalhães, J. Seabra, Contact properties of Cu–Mn austempered ductile iron gears, in: Experimental evaluation using the FZG test rig. Proceedings of the International Conference on Gears, Garching, Germany. VDI-Berichte 1904, 2005.
- [6] L. Magalhães, J. Seabra, Artificial indentations for the study of contact fatigue of austempered ductile iron (ADI) discs, WEAR 258 (11–12) (2005) 1755–1763.
- [7] L. Magalhães, J. Seabra, C. Sá, Experimental observations of contact fatigue crack mechanisms for austempered ductile iron (ADI) discs, WEAR 246 (1/2) (2000) 134–148.
- [8] L. Magalhães, J. Seabra, Wear and scuffing of austempered ductile iron gears, WEAR 215 (1/2) (1998) 1237–1246.
- [9] B.-R. Höhn, K. Michaelis, A. Doleschel, Frictional behavior of synthetic gear lubricants, in Tribology research: From model experiment to Industrial Problem, G. Dalmaz, et al., Editors. 2001, Elsevier.
- [10] B.-R. Höhn, K. Michaelis, T. Vollmer, Thermal Rating of Gear Drives: Balance Between Power Loss and Heat Dissipation. AGMA Technical Paper, 1996.
- [11] R. Martins, et al., Friction coefficient in FZG gears lubricated with industrial gear oils: biodegradable ester vs. mineral oil, Tribol. Int. 39 (6) (2006) 512–521.
- [12] C. Changenet, M. Pasquier, Power losses and heat exchange in reduction gears: numerical and experimental results, VDI-Berichte (2002) 1665.
- [13] H. Winter, K. Michaelis, Investigations on the thermal balance of gear drives, in: Proceedings of the Fifth World Congress on Theory of Machines and Mechanisms, American Society of Mechanical Engineers, 1979.
- [14] P. Eschmann, Ball and Roller Bearings—Theory, Design and Applications, ed. Wiley. 1985.
- [15] H. Winter, K. Michaelis, FZG gear test rig—description and possibilities, in: Coordinate European Council Second International Symposium on The performance Evaluation of Automotive Fuels and Lubricants, 1985.
- [16] D. Scott, W. Seifert, V. Westcott, Ferrography—an advanced design aid for the 80's, WEAR 34 (1975) 251–260.
- [17] R. Martins, et al., Power loss in FZG gears lubricated with industrial gear oils: biodegradable ester vs. mineral oil, in: Proceedings of the 31th “Leeds-Lyon Symposium” on Tribology, Leeds, UK, 2004.
- [18] K. Aslantas, S. Tasgetiren, Y. Yalçın, Austempering retards pitting failure in ductile iron spur gears, Eng. Failure Anal. 11 (6) (2004) 935–941.
- [19] F. Antoine, J.M. Besson, Simplified modellization of gear micropitting, in: Proceedings of the Institution of Mechanical Engineers Part G-Journal of Aerospace Engineering V 216(G6), 2002, pp. 291–302.
- [20] DGMK Information sheet, Short Test Procedure for the investigation of the micropitting load capacity of gear lubricants. 2002.
- [21] Forschungsvereinigung Antriebstechnik E.V, FVA Research Project Nr. 54/I-IV. 1993.

A.6 Paper F

R. Martins, P. Moura, and J. Seabra, “Power loss in fzg gears: Mineral oil vs. biodegradable ester and carburized steel vs. austempered ductile iron vs. MoS₂-Ti coated steel”, VDI Berichte, no. 1904 II, pp. 1467-1486, 2005.

Power loss in FZG gears:

Mineral oil vs. biodegradable ester and carburized steel vs. austempered ductile iron vs. MoS₂-Ti coated steel

R.C. Martins, INEGI – Tribology Unit, Porto, Portugal;

P.S. Moura, INEGI – Tribology Unit, Porto, Portugal;

Prof. J.O. Seabra, Faculdade de Engenharia, Universidade do Porto, Portugal.

Abstract

The aim of this work is the assessment of the energetic behavior in gear applications of two industrial gear oils when combined with three different gear materials: carburized steel, austempered ductile iron (ADI) and MoS₂/Ti coated steel.

Two lubricants, a reference paraffinic mineral oil with an additive package for extra protection against micropitting and a biodegradable non-toxic saturated ester, are selected and characterized in terms of their physical properties.

Power loss gear tests are performed on the FZG test rig using type C gears, for wide ranges of applied torque and input speed, in order to compare the energetic performance of all lubricant/material combinations.

Lubricant samples, collected during and at the end of the gear tests, are analyzed by Direct Reading Ferrography (DR3) and the evolution of wear particles indexes during the tests is assessed. Weigh loss measurements are also performed.

An energetic model of the FZG test gearbox integrating the mechanisms of power dissipation and heat evacuation is used, allowing the determination of its operating equilibrium temperature. The XL parameter, in the average friction coefficient equation proposed by Hohn et al.[1], is determined for each lubricant - material combination, using an optimization routine that correlates experimental and model results.

The influence of lubricants and material / surface coating combinations on the friction coefficient between the gear teeth is discussed taking into consideration the operating conditions (torque, speed and temperature).

1 Introduction

A growing environmental awareness is leading to an increasing interest in biodegradable non-toxic lubricants. Environmental compatibility is usually viewed in respect to biodegradability and toxicity. While the first issue is reached by using a suitable biodegradable base fluid, low toxicity requires an additivation that is environmentally friendly [2], too.

However, lubricant performance (friction, wear, lifetime, load bearing, efficiency etc.) has also a major impact on its overall environmental compatibility, since premature wear, high energy needs are as well harmful to the environment.

2 Lubricants

Two industrial gear lubricants are tested and compared: a reference ISO VG 150 mineral oil, containing an additive package to improve micro-pitting resistance, and an ISO VG 100 biodegradable ester lubricant with a low toxicity additivation. Both oils are specified as CLP gear oils according to DIN 51517. The main properties of the two lubricants are shown in Table 1.

2.1 Chemical properties

The reference gear lubricant is based on a paraffinic mineral oil with significant residual sulphur content. It contains an ashless antiwear additive package based on phosphorous and sulphur chemistry and metal-organic corrosion preventives.

Table 1 – Lubricant properties.

Parameter	[unit]	Desig.	Method	Lubricating Oils	
Base oil	[/]	/	DIN 51451	paraffinic mineral oil	saturated ester
Physical properties					
Density @ 15°C	[g/cm ³]	ρ_{15}	DIN 51757	0.897	0.925
Kinematic Viscosity @ 40 °C	[cSt]	ν_{40}	DIN 51562	146	99.4
Kinematic Viscosity @ 100 °C	[cSt]	ν_{100}	DIN 51562	14.0	14.6
Viscosity Index	[/]	VI	DIN ISO 2909	92	152
Pour point	[°C]		DIN ISO 3016	-21	-42
Thermal expansion [15]	[g/cm ³ °C]	α_v		7.16×10^{-4}	8.05×10^{-4}
Wear properties					
VKA weld load	[N]	/	DIN 51350-2	2200	2200
VKA wear scar (1h/300N)	[mm]	/	DIN 51350-3	0.32	0.35
Brugger	[N/mm ²]	/	DIN 51347-2	68	37
FZG rating	[/]	K _{FZG}	DIN 513540	>12	>12
Biodegradability and toxicity properties					
Ready biodegradability	[%]		OECD, 301 B	<60	≥60
Aquatic toxicity with <i>Daphnia</i>	[ppm]	EL ₅₀	OECD, 202	-	>100
Aquatic toxicity with <i>Alga</i>	[ppm]	EL ₅₀	OECD, 201	-	>100

In contrast, the biodegradable fluid uses a fully saturated ester based on harvestable materials. The absence of unsaturated bonds in this base fluid leads to excellent thermal and oxidative stability. To combine the desired low toxicity with superior gear performance, environmentally compatible, highly efficient additives are added and metal-organic compounds have been completely avoided.

2.2 Physical properties

The two gear oils have significantly different physical properties. They have almost identical viscosities at 100°C but the ester gear oil has much lower viscosity at lower temperatures, caused by the higher viscosity index of the ester product. This beneficial property leads to a wider range of operational temperature compared to the mineral oil. This can also be seen from the pour point which is 20°C lower in the case of the ester fluid.

Thermal expansion and density of the ester gear oil are higher than those of the mineral oil.

The pressure-viscosity parameter is always larger for the mineral oils than for the ester oils and must be accounted in terms of EHD film thickness [3].

2.3 Standard mechanical tests

The VKA weld load is an extreme pressure test to determine the additives response at welding conditions. Both lubricants withstand a mean pressure of approximately 5500 N/mm² (for a four-ball load of 2200 N) without seizure.

Considering the extreme pressure performance judged by the Brugger test, both lubricants present values higher than the value considered sufficient for hydraulic oils (30 N/mm²) but only the mineral supersedes the value usually stated for transmission oils (50 N/mm²).

Summarizing these mechanical tests (see Table 2), both lubricants have almost the same performance and can both be considered suitable for a wide range of gear applications [4].

2.4 Biodegradability and toxicity properties

Standardized and internationally recognized test methods are available for determining the biodegradability (OECD 301B) and environmental toxicity (OECD 201, OECD 202) of lubricants and their components. The mineral oil didn't match the minimum requirements of 60% biodegradability in 28 days, thus any toxicity test were performed for this lubricant. The ester based oil exceeded the minimum requirements of 60% biodegradability in 28 days and pass both toxicity tests, OECD 201 and OECD 202 as shows Table 1 [4].

3 Gear Materials

The FZG type C gears used in this work are manufactured in two different materials: carburized steel and austempered ductile iron (ADI). Carburized steel gears coated with molybdenum disulfide - titanium composite coating were also used.

3.1 Carburizing steel

Gears and other highly stressed mechanical components are often manufactured in carburizing steel. In this case the gears are manufactured in DIN 20 MnCr 5 steel, being carburized, quenched and oil annealed before the final grinding operation. The surfaces have a very high hardness, typically around 60 HRC, while the core keeps a very high strength and a considerably high elongation. This is a common solution for gear manufacturing. The main mechanical properties are shown in Table 2.

3.2 Austempered Ductile Iron

Austempered ductile iron (ADI) has been used since the late 1970s. Nowadays, it is possible to produce high-resistance ADIs, materials that are almost impaired in terms of mechanical properties among the Fe-C alloy products. ADIs are only surpassed by high-resistance alloyed steels when tensile strength is considered [5].

The replacement of steel parts by ADI might result widely advantageous, promoting the acceptance and use of these materials. Some of the main advantages are: ADIs base material (nodular iron) is cheaper than steel, ADIs are casting materials, thus components can be molded, allowing significant cost reduction of the manufacturing process when compared to conventional steel machining [6], ADIs have higher vibration absorption than steel (more than 6 dB attenuation can be achieved in a gearbox [7]), have higher wear and scuffing resistance [8] when lubricated with additive free lubricants, and may allow a small weight reduction (density is 10% lighter than steel),.

ADIs present several important tribologic characteristics, most of them dependent on the matrix structure and on the presence of the graphite nodules [8].

ADIs' tribological performance is not dependent of the presence of AW and EP additives in the lubricants, allowing the use of additive free oils, which might represent an ecological benefit. The heat-treatments are also low-energy consumers, since austenitization occurs at 850 °C for a small period (30 to 45 minutes, depending on the size of the component) and austempering is performed at about 300°C, avoiding the use of special equipments and allowing cost-savings when compared to steel carburizing and quenching or other conventional heat-treatments [6].

The use of ADIs is limited when very high tensile strength are required, although some ADIs can now reach more than 1600 MPa u.t.s., according to ASTM normalization, thus being able to support the efforts imposed by the majority of the mechanical applications [8].

Table 2 shows the main mechanical properties of ADI material used in this work.

Table 2 – Mechanical properties of 20 MnCr 5 and ADI materials.

Properties	Unit	20 MnCr 5	ADI
Modulus of elasticity	10^3 N/mm^2	210	170
Density	g/cm^3	7.85	7.06
Poisson's ratio	/	0.3	0.25
Surface hardness	HRC	58-62	42
Tensile strength	N/mm^2	1300	1433
Yield strength 0.2%	N/mm^2	550	1178
Elongation	%	8	6

3.3 Disulfide Molybdenum – Titanium composite surface coating

In the last decades, surface coating technology was important to achieve increased performance, allowing lower friction coefficients, higher protection against surface failures and higher load capacity. In applications with frequent start-stop operations such protection against surface failures, mainly scuffing, is very important.

Multi-layer composite surface coatings made of MoS_2 /Titanium [9-11], exhibit good mechanical and tribological properties in several industrial applications.

The MoS_2 /Titanium composite coatings are deposited by DC Magnetron Sputtering using a standard CFUBMSIP Teer Coatings PVD system, with four targets (one Ti and three MoS_2 targets). The coating procedure starts with an ion cleaning, followed by a 70nm Ti layer, a 200nm MoS_2 /Ti multilayer, a 900 nm MoS_2 /Ti (non multilayer) and a last step of 50 nm layer of MoS_2 for coloration [9].

This coating presents a very high plastic Hardness ($HP=1200\text{kg/mm}^2$) and a friction coefficient as low as 0.04 (on Pin-on-disc tests) [10, 11].

The coating thickness is $1.2\mu\text{m}$, almost not affecting the substrate initial roughness [10].

The MoS_2 /Ti coating also presents excellent adhesion to steel substrates tested in twin-disc tests at high contact pressure, high slide-to-roll ratio and low specific film thickness [10].

This surface coating promoted a huge increase of the scuffing load carrying capacity in FZG type C gears, 2 load stages at 1500 rpm and 5 load stages at 3000 rpm, representing an increase of 40% and 77% of transmitted power, respectively [10].

The MoS_2 /Ti coating improves the efficiency of a transfer gearbox in about 0.5% at the low speed – high load operating conditions [10]. This coating is applied on DIN 20 MnCr 5 carburized gears.

4 Gear efficiency tests

Power transmission equipments using gears dissipate significant amounts of power and any improvement in their performance represents a considerable reduction in energy consumption.

The equilibrium temperature of a gearbox is reached when the power losses inside the gearbox are equal to the evacuated heat from the gearbox to the surrounding environment. This equilibrium temperature depends on the gearbox characteristics, lubricant properties and environment temperature [1, 12-14]. The equilibrium temperature at constant operating conditions is a direct indication of power losses, since a lower equilibrium temperature indicates higher energetic efficiency, lower friction coefficient, smaller oil oxidation and a longer oil life [15].

A test plan has been developed in order to compare the lubricants and materials behavior at different operating conditions (torque and speed), analyzing the equilibrium temperature and the wear protection.

4.1 FZG gear test rig and FZG type C gears

Figure 1 shows a schematic view of the FZG back-to-back spur gear test rig where gear efficiency tests are performed. The geometrical characteristics of FZG type C gears tested are presented in Table 3. All the efficiency gear tests are dip lubricated with an oil volume of 1.5 liters.

The gear codification and the surface roughness of the teeth flanks are defined in Table 4.

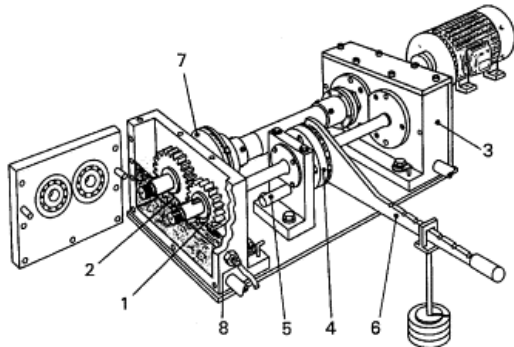


Figure 1 – Schematic view of FZG test rig.

4.2 Operating conditions

Each combination material - lubricant is submitted to a set of gear tests performed in a wide range of speed and torque conditions, as well as input power, as shown in Table 5. The Hertzian contact pressures for each FZG load stage and for both base materials are presented in Table 5, being smaller for the ADI gears due to its lower elastic modulus.

There are three tests performed at load stage 1 with the purpose of evaluating the churning losses generated by each lubricant. These no-load tests lasted for two hours at each operating speed. The initial oil bath temperature is approximately room temperature (20°C).

The other 9 tests (load tests) are performed at three different speeds (1000 rpm, 2000 rpm and 3000 rpm) and three increasing torque levels, corresponding to FZG load stages 5, 7 and 9. Each load test begins at approximately 40°C and the oil sump temperature is free. The ADI gears do not perform the test at load stage 9, corresponding to 1.6GPa of maximum Hertz pressure, since this pressure value is too high for ADI.

Table 3 - Geometry of the test gears.

Parameter	[Units]	Pinion	Wheel
Number of teeth		16	24
Module	[mm]	4.5	
Center distance	[mm]	91.5	
Addendum diameter	[mm]	82.45	118.35
Pressure angle	[°]	20	
Addendum modification	[/]	+0.182	+0.171
Face width	[mm]	14	

Table 4 – Test codification and initial roughness of gear teeth flanks.

Gear Codification	Material	Coating	Lubricant	Flank Roughness Ra [μm]
CM	20MnCr5 carburized	None	Mineral	1.0
CE	20MnCr5 carburized	None	Ester	0.9
AM	ADI	None	Mineral	0.7
AE	ADI	None	Ester	0.6
MM	20MnCr5 carburized	MoS ₂ /Ti	Mineral	1.0
ME	20MnCr5 carburized	MoS ₂ /Ti	Ester	1.0

Table 5 – Operating conditions in efficiency tests for carburizing gears, ADI gears and MoS₂/Ti coated gears (* test not performed).

Test type	Speed	Torque	Input Power	Hertz pressure [MPa]		Nº of cycles (wheel)
	[rpm]	[Nm]	[kW]	ADI	Steel and coated steel	[x10 ⁶]
No load tests	1000	4.95	0.5	165	186	0.72
	2000		1.0			
	3000		1.6			
Load tests	1000	141.2	14.8	881	994	0.9
			28.8	1230	1388	
			47.4	1579 *	1781	
	2000	141.2	29.6	881	994	2.7
			57.6	1230	1388	
			94.9	1579 *	1781	
	3000	141.2	44.3	881	994	5.4
			86.4	1230	1388	
			142.3	1579 *	1781	

Each load test lasts five hours, during which the input conditions (torque and speed) remain constant. The test time is defined in order to attain a stabilized oil sump temperature, consequently reaching the equilibrium between power dissipated inside the gearbox and the evacuated power to the surrounding environment by conduction, convection and radiation.

A maximum oil sump temperature of 180°C is imposed for protection of the test rig.

The monitored variables during the tests are: oil sump temperature, test gearbox temperature, ambient temperature, speed and torque.

During the load tests and after each testing speed (1000 rpm, 2000 rpm and 3000 rpm), lubricant samples are collected for direct reading ferrometry and analytical ferrography.

4.3 Steel gears test results

4.3.1 Stabilization temperature for steel gears

Figure 2 represents the equilibrium temperature reached with carburized gears lubricated with mineral and ester lubricants (refs. CM and CE, respectively). The ester lubricant always generates a smaller equilibrium temperature in all the load tests.

The greatest difference in stabilization temperature between the two oils is observed for the highest speed and torque, where the difference attains over 30°C. The difference observed between the two lubricants became larger for the tests at 3000 rpm, especially at FZG load stage 9, where, in the case of the mineral oil, the beginning of a scuffing failure was noticed and supported by the oil and mass loss analysis shown in Figure 3 and Figure 4.

4.3.2 Oil analysis and mass loss for steel gears

The analysis of the magnetic particles contained in the lubricant gives a quite good indication about the wear of lubricated parts, since those particles in a closed box are generated in the contacting surfaces.

During the gear tests a lubricant sample has been collected after each group of load tests at constant speed, to evaluate lubricant condition. Those samples are analyzed by Direct Reading Ferrography or Ferrometry in order to measure the ferrometric parameters **DI** (large wear particles index - size greater than 5µm) and **Ds** (small wear particles index - size smaller than 5µm). The values of **DI** and **Ds** are used to evaluate the concentration of wear particles index - CPUC and the severity of wear particles index - ISUC, defined as,

$$CPUC = \frac{DI + Ds}{d}, \quad ISUC = \frac{DI^2 - Ds^2}{d^2}, \quad \text{where } d \text{ stands for the oil sample dilution.}$$

The CPUC index grows when the sum of large and small particles increase, while the ISUC index grows when the number of large particles are present in major number than the small particles.

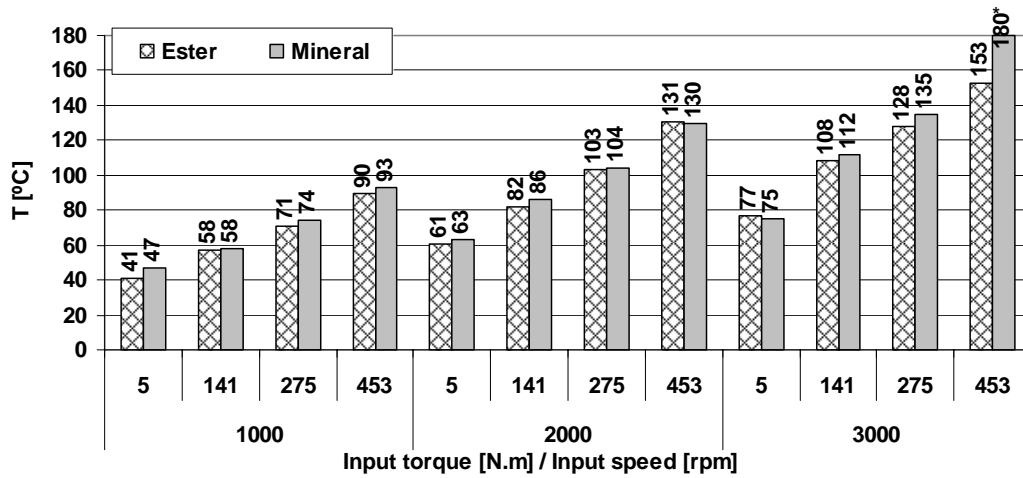


Figure 2 – Equilibrium temperatures in efficiency tests with carburized steel gears, lubricated with mineral and ester oil (* test reached the limit temperature after 133 minutes and was stopped).

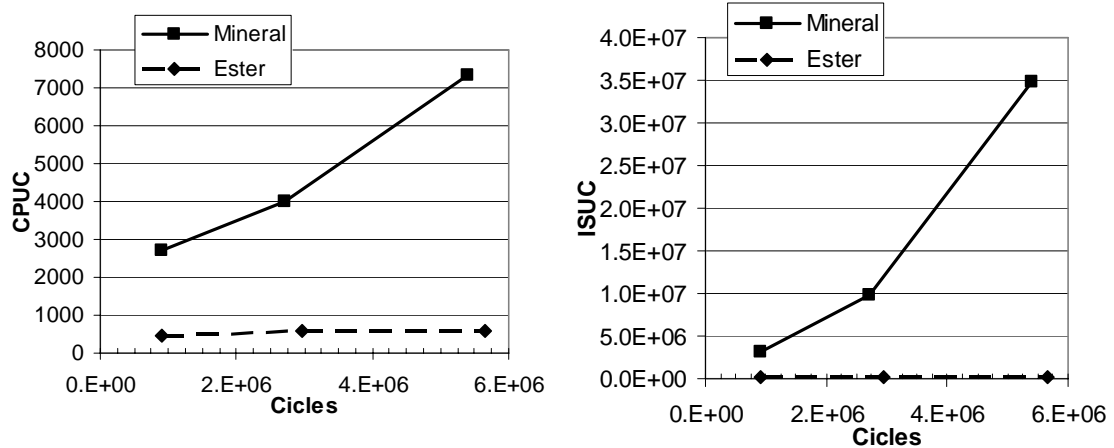


Figure 3 – Evolution of CPUC and ISUC wear indexes during the efficiency tests with carburized steel gears for both lubricants (CM and CE tests).

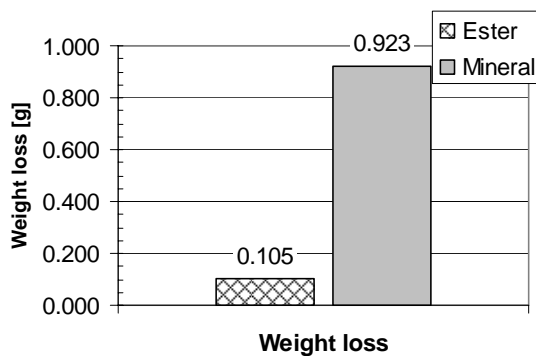


Figure 4 – Total mass loss after the efficiency tests with carburized steel gears for both lubricants (CM and CE tests).

The evolution of the ferrometric indexes during the gear efficiency tests is presented in Figure 3 against the number of load cycles performed, showing that gear wear with the mineral oil is very severe.

The observation of tooth flanks of CM test (steel gear with mineral lubricant) indicates that severe wear of the tooth flanks of both pinion and wheel had occurred. The analysis of temperature evolution along load stage 9 at 3000 rpm shows an abrupt increase of oil sump temperature at 160°C, which is a sign of a surface failure.

The evolution of both wear indexes for CE tests show an increase of both CPUC and ISUC until the end of speed tests at 2000 rpm, stabilizing thereafter.

Figure 4 displays the mass loss measurements after the efficiency tests performed with carburized gears with mineral (CM) and ester (CE) lubricant. This result shows a huge amount of mass loss within test CM, which confirms the results obtained with oil analysis.

4.4 MoS₂-Ti gears test results

4.4.1 Stabilization temperature for MoS₂/Ti coated gears

Figure 5 shows the stabilization temperatures attained in efficiency tests MC and ME. The equilibrium temperature is always lower for the tests performed with the ester lubricant and that difference increases with the increase of load whatever the speed.

The test with mineral lubricant (MM) was stopped after FZG load stage 9 at 2000 rpm because a spall failure occurred in the pinion tooth.

4.4.2 Oil analysis and mass loss for MoS₂/Ti coated gears

The evolution of wear indexes CPUC and ISUC for gear efficiency tests MM and ME are presented in Figure 6. The total concentration of wear particles (CPUC) is quite larger for the mineral lubricant, especially after the tests at 1000 rpm.

The wear particles with large size also appear in larger quantity on lubricant samples from MM test, indicating a more severe form of contact fatigue.

The mass loss measurements for efficiency tests with MoS₂/Ti coated gears with both lubricants are represented in Figure 7. The weight loss represented is larger for the test ME, but the test MM only performed 2.7 million cycles instead of the 5.4 million cycles expected.

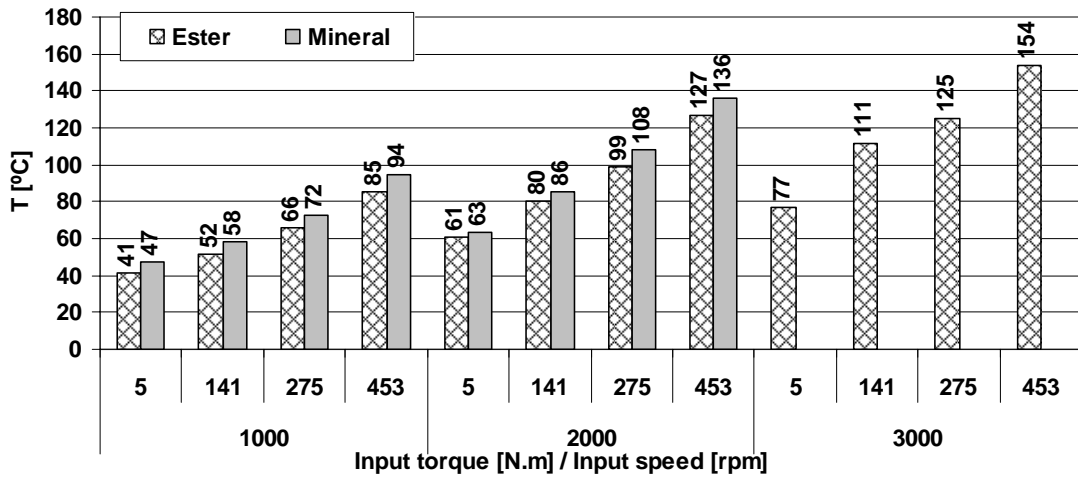


Figure 5 – Equilibrium temperatures in efficiency tests with MoS₂/Ti coated gears, lubricated with mineral and ester oil.

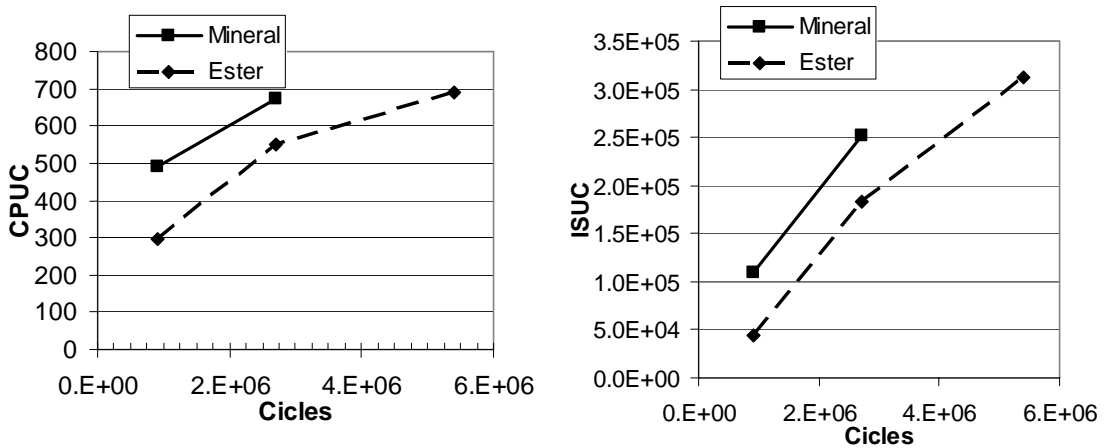


Figure 6 – Evolution of CPUC and ISUC wear indexes during the efficiency tests with MoS₂/Ti coated steel gears for both lubricants (MM and ME tests). MM test performed only 2.7×10^6 cycles.

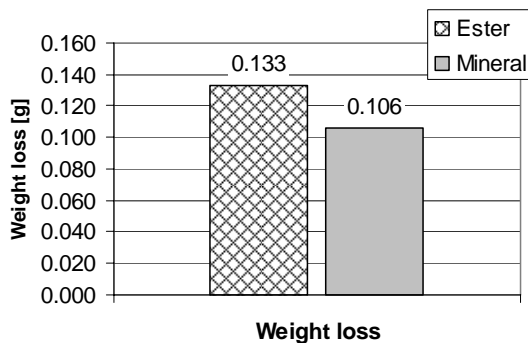


Figure 7 – Total mass loss after the efficiency tests with MoS₂/Ti coated gears for both lubricants (MM and ME tests). MM test performed only 2.7×10^6 cycles.

4.5 ADI gears test results

4.5.1 Stabilization temperature for ADI gears

The equilibrium temperature obtained in efficiency tests with ADI gears is represented in Figure 8. The mineral lubricant promotes smaller equilibrium temperatures for the tests at the highest speeds and load, while the ester lubricant promotes smaller equilibrium temperatures on all the other operating conditions. Abnormal equilibrium temperatures were obtained for load tests at 3000 rpm with the ester fluid, although no sign of failure was observed.

4.5.2 Oil analysis and mass loss for ADI gears

The evolution of wear indexes CPUC and ISUC for efficiency tests AM and AE are represented in Figure 9. The ester oil promotes a smaller wear particles generation for the load tests at speeds of 1000 rpm and 2000 rpm, while at 3000 rpm the opposite is observed. The increase in wear particles from load tests at 2000 rpm to load tests at 3000 rpm is quite important and happens for both the total number of particles as for the large particles.

The mass loss measurement after efficiency tests with ADI gears is represented in Figure 10. The mass loss of ADI gear lubricated with ester oil is around half of the gear lubricated with mineral lubricant.

4.6 Discussion on equilibrium temperatures and weight loss

The ester base oil when used in carburized steel gear promotes a smaller operating temperature and a smaller wear. This is particularly emphasized for the highest operating temperatures for which the ester lubricant has a larger viscosity, generating a higher film thickness. The decrease in oil sump temperature in tests with ester lubricant is up to 7°C (excluding the test at 3000rpm, load stage 9).

The wear protection is not comparable, since in the last gear efficiency test with the mineral oil a scuffing failure occurred resulting in a severe wear of some teeth.

The use of ester lubricant in conjunction with MoS₂/Ti surface coating results in a decrease of operating temperature between 6°C to 9 °C. This combination also confers a better protection against wear, as shown by oil analysis.

The ADI gears present lower operating temperature if lubricated with ester oil, indicating a smaller friction coefficient, although at the highest speeds and highest torques the opposite is verified. On the other hand, the mass loss difference within the ADI gear test is quite important, indicating that the ester base oil promotes a better protection against wear than the mineral base oil. The observation AM test gear teeth surface shows a very polished surface due to the wear. The surface of AE gears present some wear although the cutting marks are still visible.

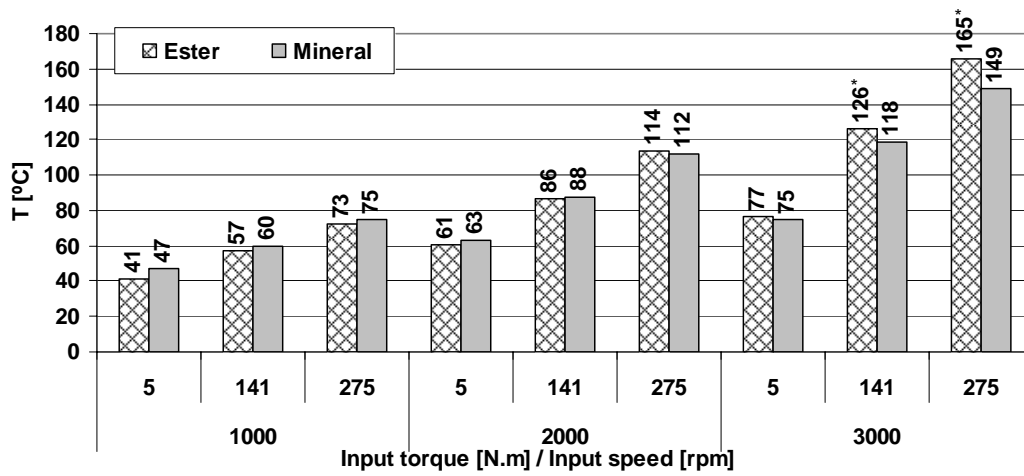


Figure 8 – Equilibrium temperatures in efficiency tests with ADI gears, lubricated with mineral and ester oil. (* abnormal equilibrium temperature).

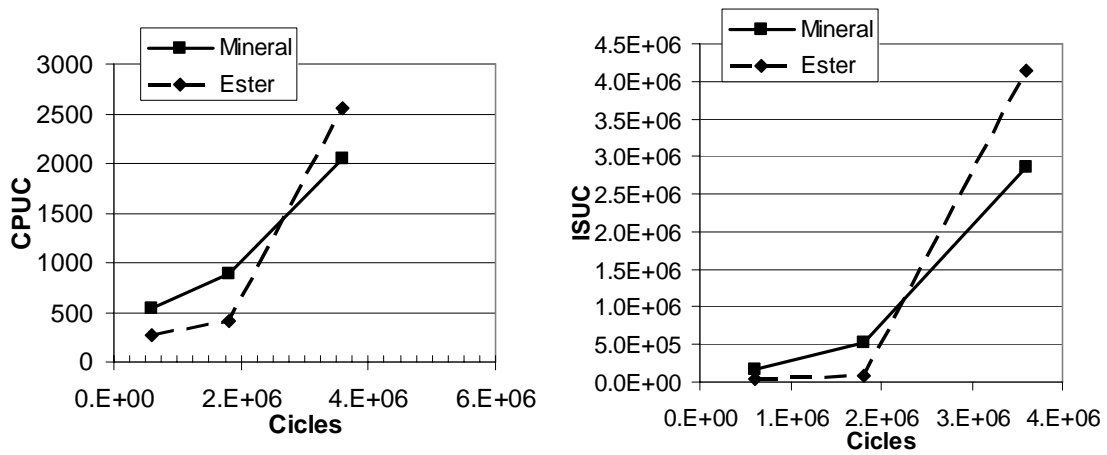


Figure 9 – Evolution of CPUC and ISUC wear indexes during the efficiency tests with ADI gears for both lubricants (AM and AE tests).

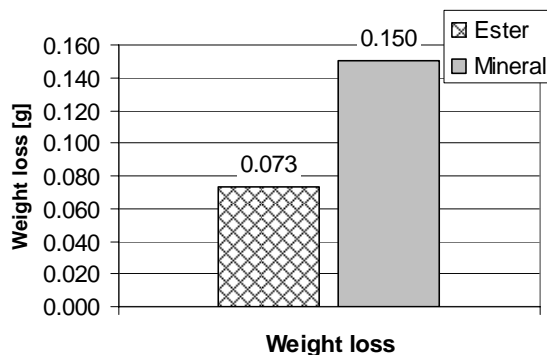


Figure 10 - Total mass loss after the efficiency tests with ADI gears for both lubricants (AM and AE tests).

Figure 11 and Figure 12 show the equilibrium temperature attained with all materials when lubricated with ester and mineral oils, respectively.

On the tests lubricated with ester fluid the gears coated with MoS₂/Ti present the smallest equilibrium temperature. On the other hand the ADI gears present the highest operating temperatures within the operating conditions considered.

On the tests performed with mineral lubricant the ADI gears also display the largest equilibrium temperature. The MoS₂/Ti coated gears lubricated with mineral lubricant show similar equilibrium temperatures to carburized uncoated gears, while if lubricated with ester lubricant show a clear reduction of the equilibrium temperature.

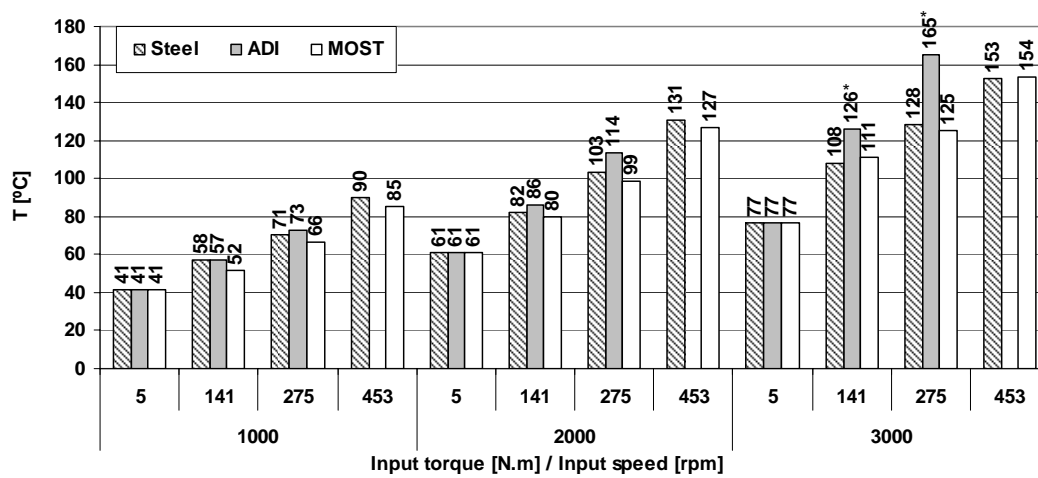


Figure 11 – Equilibrium temperature in efficiency gear tests performed with ester gear oil. (* abnormal equilibrium temperatures).

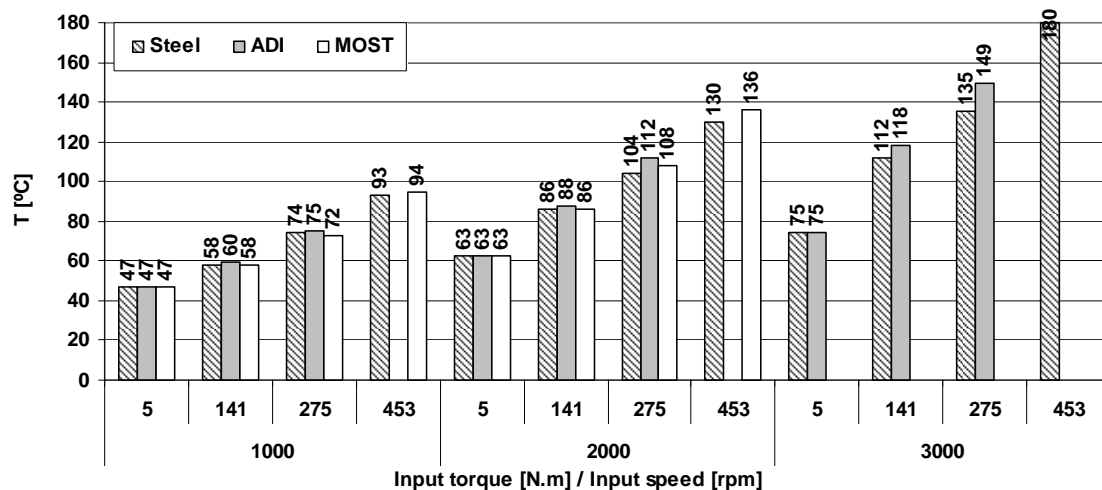


Figure 12 – Equilibrium temperature in efficiency gear tests performed with mineral gear oil.

5 Friction coefficient between gear teeth

In the case of additive free mineral lubricants the friction coefficient between gear teeth might be calculated from empiric equations based on experimental results. However, few results are available for commercial doped lubricants, whatever the base oil, mineral or synthetic [15].

The thermal equilibrium of a gearbox is attained when the power losses are equal to the evacuated heat. This equilibrium generates a constant operating temperature of the mechanical component and of the lubricant fluid.

The main mechanisms of power dissipation inside a gearbox are the churning losses and the frictional losses [1, 12-16], being the lubricant of capital influence in both. These power losses are usually called the no-load power losses and the load power losses, respectively.

The heat evacuation from the gearbox to the surrounding environment is made by three mechanisms: conduction, radiation and convection.

The energetic balance of a gearbox at the stabilized (equilibrium) temperature allows the determination of the mean friction coefficient between gear teeth for each lubricant – material or coating pair. Correction factors are proposed to the existing friction coefficient expression in order to take into account the influence of gear materials and lubricant characteristics.

The energetic balance of the FZG test gearbox is presented in detail in reference [17].

5.1 Energetic balance of the FZG test gearbox

The energetic equilibrium of the FZG test gearbox is reached when the power dissipated equals the power evacuated, that is

$$P_{fr} + P_{M1} + P_{spl} + P_{M0} + P_{sl} = Q_{rad} + Q_{cnv} + Q_{cn} \quad (1)$$

where P_{fr} represents the friction power dissipated by the gears, P_{M1} is the friction power dissipated by the bearings, P_{spl} is the power dissipated by the seals, P_{M0} is the churning power dissipated by the bearings, P_{sl} is the churning power dissipated by the gears, Q_{rad} is the power evacuated by radiation, Q_{cnv} is the power evacuated by convection and Q_{cn} represents the power evacuated by conduction.

Equation (1) establishes an approximated model for the energetic behavior of the FZG test gearbox, allowing the determination of the oil temperature in permanent conditions (stabilized temperature) for any combination of the operating conditions imposed to the FZG test rig [17]. Equation (1) depends on 5 unknown variables: the oil stabilized temperature (T_{oil}), the gearbox wall temperature (T_w), the ambient temperature (T_a), the heat conduction factor (f_{cn}) [17] and the friction coefficient between the gear teeth (μ_m).

The three temperatures, (T_{oil} , T_w and T_a), are measured during the FZG gear tests. The heat conduction factor and the friction coefficient between gear teeth can be obtained from the correlation between experimental and model oil temperature results.

A parameter adjustment routine using the least squares method has been implemented in order to optimize the heat conduction parameter fcn and the lubricant friction coefficient μ_m using the experimental results obtained in the FZG efficiency gear tests.

The fcn parameter was determined using the experimental no-load efficiency gear tests obtained for both lubricants with steel gears (the gear material/coating should not affect heat conduction to the base). The optimized value obtained is **$fcn=2.5$** .

5.2 Optimized friction coefficient

Höhn et al [1] define the average friction coefficient between gear teeth as

$$\mu_m = 0.048 \cdot \left(\frac{F_{bt}/b}{v_{\Sigma c} \cdot \rho_c} \right)^{0.2} \cdot \eta_{oil}^{-0.05} \cdot Ra^{0.25} \cdot X_L, \quad (2)$$

where X_L represents the influence of a particular lubricant on the friction coefficient. It has the value of 1 for mineral additive free lubricants and steel gears.

Using the energetic balance model of the gearbox to calculate the equilibrium temperature of the gearbox, considering $X_L=1$, a significant difference between experimental and numerical results is observed, mainly for the tests at high torque.

The results from the gear efficiency tests clearly show that friction coefficient depends on the base oil type, the additive package and the different gear materials/surface coatings. Three main parameters, variable with the operating conditions used in the gear efficiency tests, affect the friction coefficient: the force between gear teeth (F_{bt}), the sum velocity at pitch point ($v_{\Sigma c}$) and the oil viscosity (η). So the X_L parameter used to express the influence of lubricants and materials/surface coating on the friction coefficient is defined as:

$$X_L = \frac{a}{(var_1)^{b1} \cdot \dots \cdot (var_n)^{bn}}, \quad (3)$$

where “var” represents each one of the three parameters mentioned above.

The search for a lubricant parameter X_L for each material - lubricant combination was done considering the same operating conditions used in the FZG efficiency gear tests (see Table 5). The highest torque (453.0 Nm) was not considered, since it was not used in some of the tests. The tests at 3000 rpm was not considered for ADI and MoS2/Ti tests.

Within the range of operating conditions considered, the best correlations between experimental and model equilibrium temperatures are obtained for a load dependent lubricant parameter X_L , independent of the oil viscosity and rolling speed, that is,

$$X_L = \frac{1}{(F_{bt}/b)^{b1}} \quad (4)$$

Table 6 shows the exponent **b1** in expression (4) obtained for each combination of material and lubricant. The constant **a** in expression (3) is equal to 1 for all tests. Exponent **b1** in expression (4) modifies the load exponent in expression (5).

$$\mu_m = 0.048 \cdot \frac{(F_{bt}/b)^{0.2-b1}}{(v_{\Sigma c} \cdot \rho_c)^{0.2}} \cdot \eta_{oil}^{-0.05} \cdot Ra^{0.25} \quad (5)$$

Table 6 – Lubricant factor exponent (**b1**) and new value for load exponent (**0.2-b1**) for the materials and coating tested.

	Exponent b1			Exponent (0.2-b1)		
	Steel	ADI	MoS ₂ /Ti	Steel	ADI	MoS ₂ /Ti
Ester	0.076	0.037	0.084	0.124	0.163	0.116
Mineral	0.055	0.016	0.047	0.145	0.184	0.153

6 Discussion on the friction coefficient

Table 6 indicates that the ester fluid always generates a larger reduction of friction coefficient than the mineral oil, whatever the gear material used. In the case of the ester fluid, the MoS₂/Ti coated steel promotes the largest reduction of friction coefficient. For the mineral lubricant, the carburized steel promotes the larger reduction of friction coefficient.

The ADI gears always shows the largest friction coefficient, although it generates a significant friction reduction when compared to the reference case ($X_L=1$).

Figure 13 presents the numerical results obtained using the optimized friction coefficient for all the materials and lubricants, as well as, the experimental measurements made by Höhn et al [15] in the FZG test rig with similar lubricants.

The numerical results are in total agreement with the experimental stabilization temperatures measured in the FZG efficiency gear tests performed, as well as, with the measurements made by Höhn et al [15] with steel gears (*Ester experimental / Mineral experimental*).

In Figure 14 the (numerical) friction coefficient is plotted against the load parameter F_{bt}/b , for all the lubricant- material combinations tested. It clearly shows that the influence of the load parameter on the friction coefficient is significantly higher for the mineral oil.

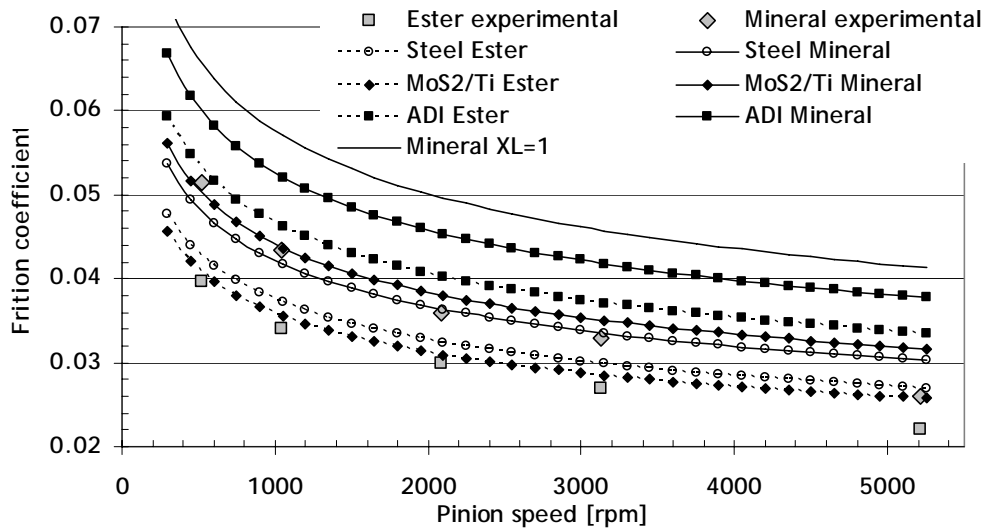


Figure 13 – Friction coefficient measurements [15] and numerical results considering the X_L parameters mentioned in Table 6 ($T_{oil}=90^{\circ}C$, $p_H=1.1GPa$).

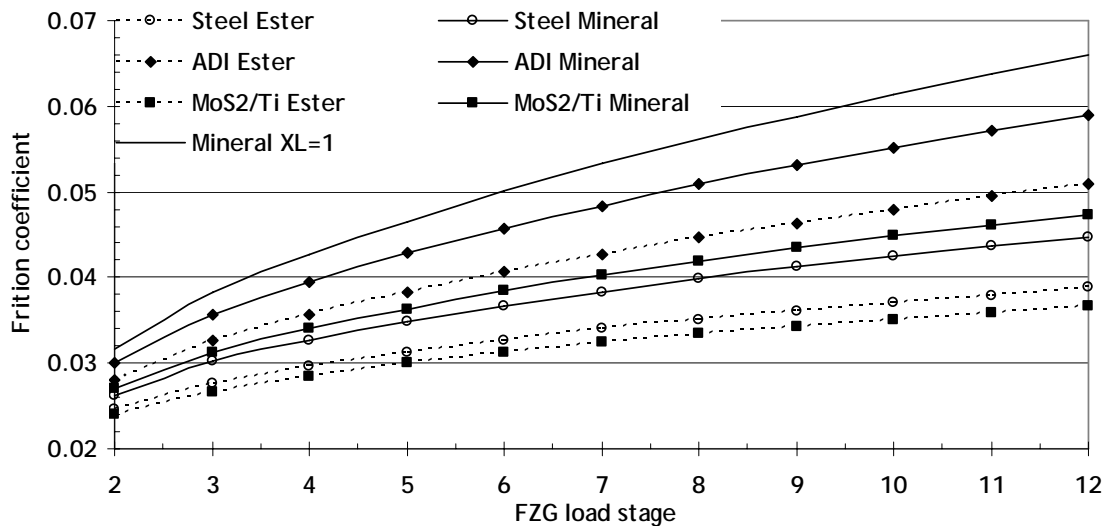


Figure 14 – Numerical results of the friction coefficient between the gear teeth for all the as lubricant-material combinations tested ($T_{oil}=90^{\circ}C$, Pinion speed=2000 rpm).

7 Conclusions

This work allows the statement of following conclusions:

1. The ester biodegradable and non-toxic fluid when used with steel gears (whether coated with MoS_2/Ti or uncoated) exhibit lower equilibrium temperatures than the mineral lubricant.

2. The ester fluid promotes a higher protection against wear within all materials tested, as confirmed by Direct Reading ferrometry and mass loss measurements.
3. At high operating temperatures the mineral lubricant generates a very high wear volume.
4. The ADI material (besides being tested at lower torques) originates higher equilibrium temperatures than the other materials with both lubricants.
5. The MoS₂/Ti coating tested with ester lubricant is the combination that exhibits the smallest equilibrium temperature, although with mineral lubricant its performance is similar to uncoated steel.
6. The calculated friction coefficient for both industrial gear oils is considerably smaller than the one predicted for a reference mineral lubricant (XL=1), mainly for the ester lubricant.
7. The results presented by both lubricants show that the reference friction coefficient overestimates the load influence, being the correction factor a function of load.

ACKNOWLEDGEMENTS

The authors express their gratitude to the European Union for the financial support given to this work through the GROWTH Project “*EREBIO - Emission reduction from engines and transmissions substituting harmful additives in biolubricants by triboreactive materials*”, Proposal N°. GRD2-2001-50119, Contract N° G3RD-CT-2002-00796-EREBIO.

The authors also want to express their gratitude to the following partners in EREBIO project:

- A. BRITO Industria Portuguesa de Engrenagens Lda, for manufacturing the gears,
- FERESPE Fundação de Ferro e Aço Lda, for supplying the nodular iron for ADI gears,
- FUCHS Petrolub A. G., for formulating and supplying the ester fluid, and
- Fundación TEKNIKER for the biodegradability and toxicity lubricant tests.

REFERENCES

- [1]. B.-R. Höhn, K. Michaelis and T. Vollmer, *Thermal Rating of Gear Drives: Balance Between Power Loss and Heat Dissipation*. AGMA Technical Paper, 1996.
- [2]. M. Weck, O. Hurasky-Schonwerth and Ch. Bugiel, *Service Behaviour of PVD-Coated Gearing Lubricated with Biodegradable Synthetic Ester Oils*. VDI-Berichte, 2002(Nr1665).
- [3]. A. Pettersson, *Tribological characterization of environmentally adapted ester base fluids*. Tribology International, 2003. **36**(11).

- [4]. R. Martins, J. Seabra, Ch. Seyfert, R. Luther, A. Igartua and A. Brito. *Power loss in FZG gears lubricated with industrial gear oils: biodegradable ester vs. mineral oil.* in *Proceedings of the 31th "Leeds-Lyon Symposium" on Tribology.* 2004. Leeds, UK.
- [5]. J. D. Mullins, *Ductil Iron Data for Design Engineers.* SOREMETAL. 1990: Rio Tinto Iron & Titanium inc.
- [6]. R. Harding, *The use of austempered ductile iron for gears,* in *2º World Congress of Gears.* 1986: Paris.
- [7]. P. Salonen, *Improved Noise Damping and Reduced Weight in Truck Componentes With KYMENITE ADI,* in *International ADI and Simulation Conference.* 1997: Finland.
- [8]. L. Magalhães, *Caracterização Tribológica de um Ferro Nodular Austemperado em Ensaíos Disco-Disco e de Engrenagens FZG,* in *Faculdade de Engenharia.* 2003, Universidade do Porto: Porto.
- [9]. N. Renevier, V. Fox, N. Lobiondo, D. Teer and J. Hampshire, *Performance of MoS₂/metal composite coatings used for dry machining and other applications.* Surface Coatings Technol, 2000.
- [10]. R. Amaro, R. Martins, J. Seabra, N.M. Renevier and D. J. Teer, *Molybdenium disulfide /Titanium low friction coating for gears application.* Tribology Interational, 2004. 38-4: p. 423-434.
- [11]. R. C. Martins R. I. Amaro, J. O. Seabra and A. T. Brito. *MoST low friction coating for gears application.* in *GEARS 2003 - Gears and Transmissions Workshop.* 2003. FEUP - Porto - Portugal.
- [12]. C. Changenet and M. Pasquier, *Power Losses and Heat Exchange in Reduction Gears: Numerical and Experimental results.* VDI-Berichte, 2002(1665).
- [13]. H. Winter and K. Michaelis. *Investigations on the thermal balance of gear drives.* in *Fifth World Congress on Theory of Machines and Mechanisms.* 1979: American Society of Mechanical Engineers.
- [14]. P. Eschmann, *Ball and roller bearings - Theory, design and applications,* ed. Wiley. 1985.
- [15]. B.-R. Höhn, K. Michaelis and A. Doleschel, *Frictional behavior of synthetic gear lubricants.* Tribology research: From model experiment to Industrial Problem, 2001.
- [16]. B.-R. Höhn, K. Michaelis and R. Döbereiner, *Load Carrying Capacity Properties of Fast Biodegradable Gear Lubricants.* Journal of the STLE - Lubrication Engineering, 1999.
- [17]. R. Martins, J. Seabra, A. Brito, Ch. Seyfert, R. Luther and A. Igartua, *Friction coefficient in FZG gears lubricated with industrial gear oils: biodegradable ester vs. mineral oil.* Tribology International, 2005 (to be published).

A.7 Paper G

R. Amaro, R. Martins, F. Seabra, S. Yang, D. G. Teer, and N. M. Renevier, “Carbon/chromium low friction surface coating for gears application”, *Industrial Lubrication and Tribology*, vol. 57, no. 6, pp. 233-242, 2005.

Carbon/chromium low friction surface coating for gears application

R.I. Amaro

Instituto de Engenharia Mecânica e Gestão Industrial, Porto, Portugal
(presently at RENAULT – C.A.C.I.A., Aveiro, Portugal)

R.C. Martins

Instituto de Engenharia Mecânica e Gestão Industrial, Porto, Portugal

Ĵ.O. Seabra

Faculdade de Engenharia da Universidade do Porto, Porto, Portugal

S. Yang and D.G. Teer

Teer Coatings Ltd, Hartlebury, Worcestershire, UK, and

N.M. Renevier

Teer Coatings Ltd, Hartlebury, Worcestershire, UK (presently at Jost Institute of Tribotechnology,
University of Central Lancashire, Preston, UK)

Abstract

Purpose – Provide tribological information about the applicability of multi-layer carbon-chromium composite coatings to gears. Discuss the protection provided against scuffing failures, wear and the influence on gear power losses.

Design/methodology/approach – Several screening tests, such as Rockwell indentations, ball cratering, pin-on-disc and reciprocating wear tests, were performed in order to evaluate the adhesion to the substrate and the tribological performance of the carbon/chromium composite coating. Afterwards, twin-disc tests were performed at high contact pressure and high slide-to-roll ratios to confirm the good adhesive and tribological properties of the coating under operating conditions similar to those found in gears. Gear tests were performed in the FZG machine in order to evaluate the anti-scuffing performance of the carbon/chromium coating using additive free gear oils. Finally, the carbon/chromium composite coating was also applied to the gearing in a gearbox and its influence on the gearbox efficiency was analysed.

Findings – The C/Cr has got very good adhesion to the steel substrate, provides low friction coefficients between contacting solids in relative movement, gives excellent protection against scuffing and wear reduction in gears, and promotes a slight improvement of the gears efficiency.

Research limitations/implications – The protection of this carbon/chromium coating against gear micro-pitting should be investigated.

Practical implications – This study confirms the applicability of this coating to industrial gear applications, especially in two particular applications: severe applications involving high contact pressures and high sliding, frequent start-ups and inefficient lubrication; and acting as tribo-reactive material and substituting non-biodegradable and toxic additives in environmental lubricants.

Originality/value – This work validates and quantifies the influence of this C/Cr multi-layer composite coating in gear applications in terms of adhesion to the substrate, anti-scuffing performance and efficiency.

Keywords Coatings technology, Tribology, Industrial engineering, Tests and testing

Paper type Research paper

1. Introduction

Power transmission equipments employing gears dissipate significant amounts of power and any improvement in their performance represents a significant reduction in energy

consumption. Beside this, the demands of modern mechanical transmissions require higher operating torques, higher speeds, lower operating noise and lower weight.

Surface coating technology was important to achieve increased energetic performance, allowing lower friction coefficients, higher protection against surface failures and higher load capacity. In applications with frequent start-stop operations such protection against failures, mainly scuffing, is very important.

The Emerald Research Register for this journal is available at www.emeraldinsight.com/researchregister

The current issue and full text archive of this journal is available at www.emeraldinsight.com/0036-8792.htm



Industrial Lubrication and Tribology
57/6 (2005) 233–242
© Emerald Group Publishing Limited [ISSN 0036-8792]
[DOI 10.1108/00368790510622326]

The authors would like to thank the European Commission for the financial support given to this study throughout the project Reduction of fluid lubricant use in heavily loaded motion transmission systems through the application of sel-lubricating coatings. Project no. BE-S2-5389, contract no. BRST-CT97-5363, 1998-2000.

Another important objective to be accomplished by surface coatings in the near future is the reduction/elimination of some toxic lubricant additives and consent the use of environment friendly lubricants.

There are several types of coatings that can be used in gears, for instance, WC/C (tungsten carbide/carbon) (Weck *et al.*, 2002), B₄C (boron carbide/carbon) (Weck *et al.*, 2002; Joachim *et al.*, 2002) or MoS₂/Ti (molybdenum disulphide/titanium) (Amaro *et al.*, 2003; Renevier *et al.*, 2000; Amaro, 2000; Martins, 2002), among others (Su and Kao, 2003; Rigato *et al.*, 2000).

DLC (diamond-like carbon) coatings are very hard and have a lower friction coefficient but tend to be brittle and have poor adhesion. The DLC metallic-carbon coatings tend to be less brittle but are also softer. In order to provide a better wear protection it is interesting that the coating behaves like a true solid lubricant (Fox *et al.*, 2000) like Graphite or MoS₂ (molybdenum disulphide) (Holmberg *et al.*, 1998).

The tribological performance of the sputtered carbon/chromium composite coating is studied in this work. This coating has high hardness, low friction coefficient and a good adhesion conducting to low wear rates and appears to behave like a solid lubricant.

2. Carbon/chromium composite coating

2.1 Deposition procedure

The C/Cr composite coatings (Yang *et al.*, 2000, 2001) is deposited by DC magnetron sputtering using a standard CFUBMSIP (Teer, 1994, 1996, 1997) teer coatings PVD system, with four targets (one chromium and three carbon targets). The coating procedure starts with an ion cleaning, followed by a metal layer deposition (chromium) and a composite deposition of carbon/chromium. Further details about the coating deposition may be found in Yang *et al.* (2000, 2001).

2.2 Physical properties and tribological performance of the carbon/chromium coating deposited onto M42 polished 1200 SiC (Yang *et al.*, 2000, 2001)

This carbon/chromium coating was deposited on M42 polished SiC steel and several screening tests were performed in order to evaluate its performance.

Scratch and Rockwell C indentation tests were performed to assess the adhesion of the carbon – chromium coating to the substrate.

In the scratch test, a 80 N critical load was measured and a hardness of 2200 HV was obtained. In this test there were no cracks, chips or flakes outside the track, indicating an excellent adhesion, as shown in Figure 1. The Rockwell C indentation (Daimler test), shown in Figure 2, also indicates a very good adhesion to the substrate since there is only plastic deformation in the indentation border.

Pin-on-disc and ball cratering tests were performed to assess the tribological performance of the carbon/chromium coating to the substrate.

Pin-on-disc tests performed at 200 mm/s during one hour on a carbon/chromium composite coating indicate that the friction coefficient decreases from 0.1 for a load of 20 N to 0.06 for a load of 140 N, while the bearing load capacity increases from 2.1 to 3.4 GPa for the same load variation, as shown in Figure 3. In these load range the specific wear rate was almost constant at $2.2 \times 10^{-7} \text{ m}^3/\text{mN}$.

Figure 1 Scratch test started with a load of 10 N and ended with a load of 85 N on the carbon/chromium composite coating

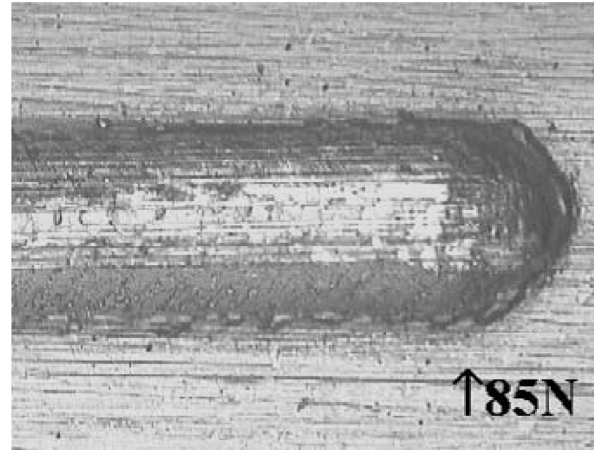
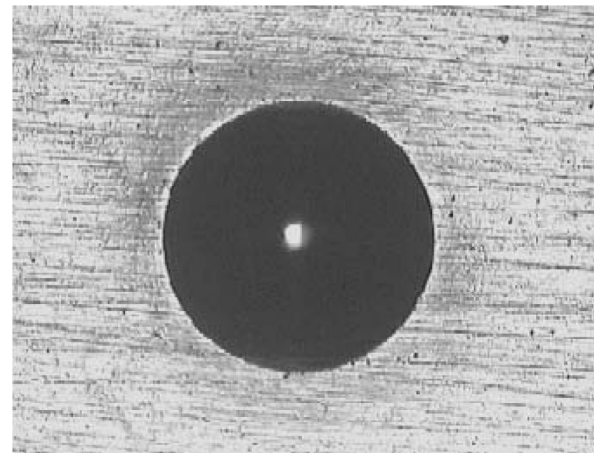


Figure 2 Rockwell hardness test on the carbon/chromium composite coating



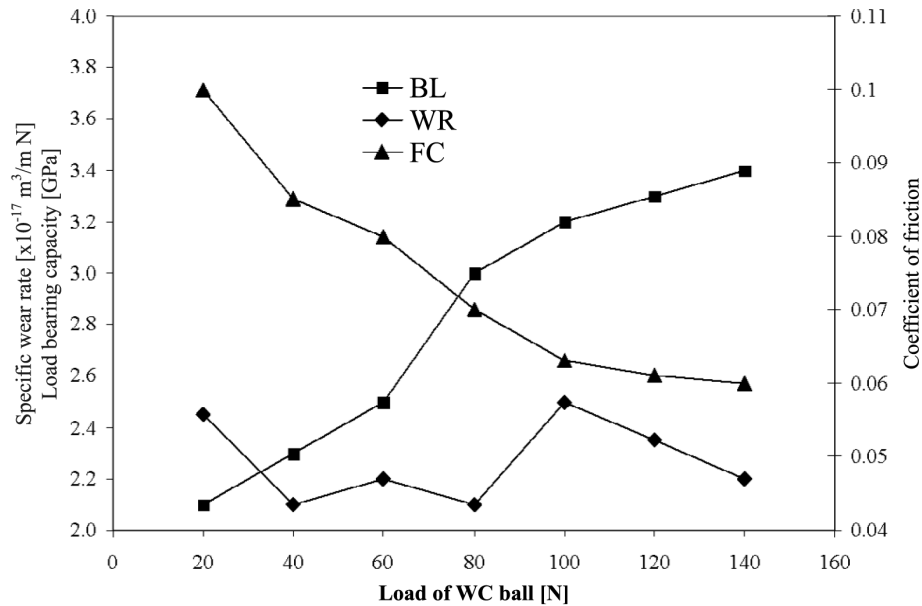
Ball crater technique was used in the worn tracks of the pin-on-disc tests to evaluate the thickness of the remaining coating, as shown in Figure 4. The ball crater traces and optical microscope analysis were used to measure the worn volume, which was very low even for the load of 140 N, corresponding to a contact pressure of 3.4 GPa.

3. Twin-disc tests

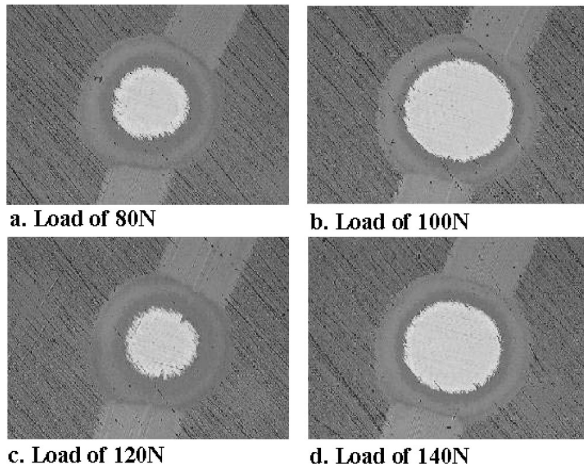
The twin-disc machine (Amaro, 2000) used in this study allows operating conditions of pure rolling or rolling and sliding, different rotating speeds and different contact pressures as well as jet lubrication at controlled temperature.

3.1 Discs geometry, heat treatment and surface roughness

The discs have a diameter of 70 mm and a thickness of 7 mm. The upper disc, called spherical disc, has a transversal

Figure 3 Tribological properties of carbon/chromium vs load

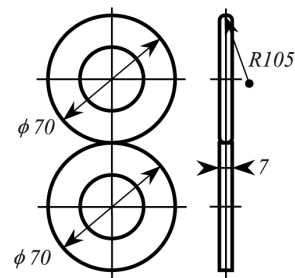
Notes: BL – Bearing Load; WR – Specific wear rate; FC – Friction coefficient

Figure 4 Ball craters in worn tracks of carbon/chromium using loads of 80, 100, 120 and 140 N on the pin

curvature radius of 105 mm (Amaro, 2000). The geometry of the discs is shown in Figure 5.

The discs are manufactured in case hardened DIN 20MnCr5 steel, heat treated and grinded in order to obtain the required surface finishing. The surface hardness has a mean value for all discs of 59 HRC. The surface roughness of each disc was measured in three different locations, before and after the coating deposition, and the corresponding mean values are shown in Table I.

The grinding operation is more difficult in the case of the discs with transverse curvature (spherical discs) and, consequently, they have higher roughness values than the cylindrical discs.

Figure 5 Discs geometry

The surface roughness is similar before and after coating. The roughness parameters of the spherical discs show a slight decrease after coating while those of the cylindrical discs show a slight increase. However, the R_{pk} roughness parameter shows a very significant reduction after coating, for the spherical discs, showing that surface coating may have important effects on the roughness profile.

3.2 Twin-disc testing conditions

Five pairs of carbon/chromium coated discs were tested with increasing load along five load stages and at constant rolling speed ($(U_1 + U_2)/2 = 11 \text{ m/s}$). Each disc pair was tested at a different slide-to-roll ratio, from 0 to 40.9 per cent. The specific film thickness goes from 0.35 to 0.45 depending on pressure and slide-to-roll ratio. Table II presents all the testing conditions.

3.3 Twin-disc tests results

3.3.1 Contact track observation by video microscopy

During each test the contact tracks of both discs were periodically observed using a video microscope, thus avoiding

Table I Disc roughness measurements before and after C/Cr coating deposition

Roughness parameter	After grinding		After C/Cr coating	
	Spherical disc 1	Cylindrical disc 2	Spherical disc 1	Cylindrical disc 2
R_{Z-DIN}	2.550	2.280	2.280	2.387
R_a	0.500	0.310	0.463	0.327
R_q	0.620	0.400	0.587	0.417
R_{pk}	0.420	0.340	0.290	0.363
$\frac{R_{a1} + R_{a2}}{2}$		0.405		0.395
$\sqrt{R_{q1}^2 + R_{q2}^2}$		0.738		0.720

Table II Twin disc testing conditions

Parameter	Desig.	Disc pair				
		C/Cr 1	C/Cr 2	C/Cr 3	C/Cr 4	C/Cr 5
Rolling speed (m/s)	$\frac{U_1 + U_2}{2}$	11.38	11.02	11.05	11.11	11.23
Sliding speed (m/s)	$U_1 - U_2$	0.00	1.42	2.17	3.16	4.60
Slide-to-roll ratio (per cent)	$\frac{2 U_1 - U_2 }{(U_1 + U_2)}$	0.0	12.9	19.6	28.4	40.9
Upper disc cycles/load stage $\times 10^3$	NC ₁	186	192	198	207	221
Lower disc cycles/load stage $\times 10^3$	NC ₂	186	169	163	156	146
Total upper disc cycles $\times 10^3$	N_1	931	960	993	1 038	1 107
Total lower disc cycles $\times 10^3$	N_2	931	843	815	780	731
Maximum Hertz pressure LS1 (GPa)	p_{01}			1.273		
Maximum Hertz pressure LS2 (GPa)	p_{02}			1.511		
Maximum Hertz pressure LS3 (GPa)	p_{03}			1.768		
Maximum Hertz pressure LS4 (GPa)	p_{04}			1.905		
Maximum Hertz pressure LS5 (GPa)	p_{05}			2.024		
Oil reference				ISO VG 22, additive free		
Oil temperature (°C)	T_0			90		

the dismounting of the discs. These systematic observations during all tests showed that the carbon/chromium coating suffered mild and progressive wear. Evidence sustaining the need to stop any of the tests due to catastrophic coating failures were not detected.

3.3.2 Contact track observation by optical microscopy

At the end of each test the contact tracks of both discs were observed using optical microscopy. These observations show that the main wear mechanism of the surface coating is delamination in very thin and long flakes due to the adhesion between the contacting surfaces promoted by the severe operating conditions imposed.

Local wear is not progressive. Small flakes with the coating thickness are pulled out, making the substrate visible and exposed and allowing its quick oxidation.

Wear is higher in the upper spherical discs due to the higher number of cycles performed (fast disc) and the higher value of the initial surface roughness:

$$(R_a^{\text{sph}} = 0.46 \mu\text{m}, \quad R_a^{\text{cil}} = 0.33 \mu\text{m}).$$

The optical microscopy analysis is not always conclusive enough to identify the zones of the contact tracks where the carbon/chromium coating has been completely worn out.

3.3.3 Surface observations by scanning electron microscopy

At the end of each test, both discs were observed by scanning electronic microscopy (SEM) with reflected primary

electrons, at three different locations along the contact track. In each location five images were taken, in order to have a global view of the coating degradation across the contact track.

Figures 6 and 7 show for test C/Cr 3 (slide-to-roll ratio = SRR = 0.196), these five images across the contact track for the upper (spherical) and the lower (cylindrical) discs, respectively.

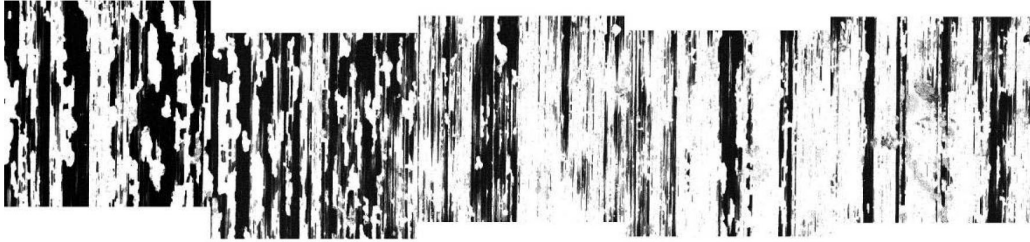
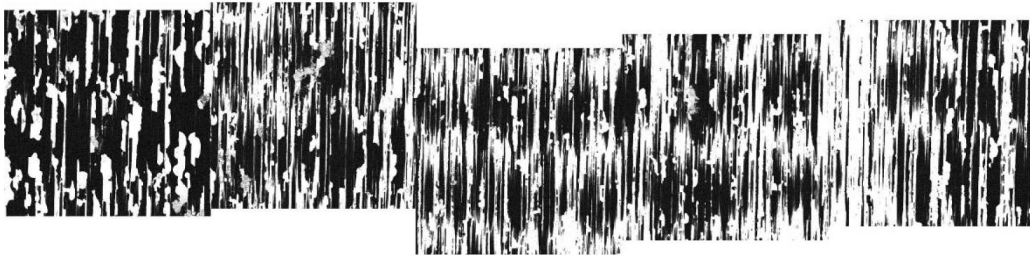
With these SEM observations and analysis it was possible to identify that the dark areas indicate the presence of the carbon/chromium coating while the white areas indicate zones where the C/Cr coating has been completely worn out.

The five images obtained per disc in each location were analysed using image analysis software in order to measure the values of the coated and uncoated areas. The uncoated area was divided by the total area under analysis (coated plus uncoated areas) defining the percentage of coating wear (PCW).

In the case of test C/Cr 3, shown in Figures 6 and 7, the PCW at the end of the test was 61.1 per cent for the upper spherical disc and 42.5 per cent for the lower cylindrical disc.

The average (and also the maximum and minimum) values of the PCW are defined using the values measured in each one of the three locations analysed for each test and are shown in Figure 8.

The PCW for the cylindrical discs is always smaller than 64 per cent in all cases. However, the PCW increases with

Figure 6 Contact track of spherical disc – C/Cr 3; slide-to-roll ratio = 19.6 per cent, uncoated area = 61.1 per cent, total width = 3 mm (50 ×)**Figure 7** Contact track of cylindrical disc-C/Cr 3; slide-to-roll ratio = 19.6 per cent, uncoated area = 42.5 per cent, total width = 3 mm (50 ×)

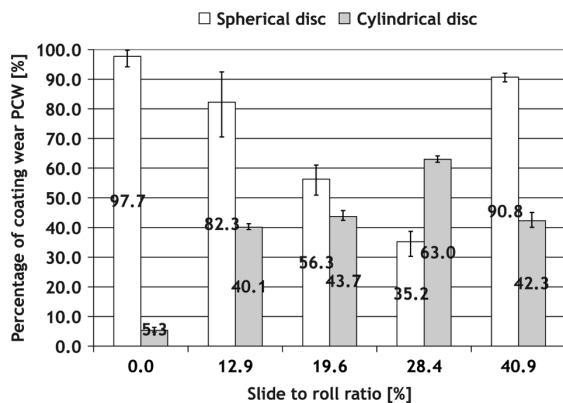
the increasing slide-to-roll ratio and a maximum value of 63 per cent is obtained for a slide-to-roll ratio equal to 0.284.

For the spherical discs the PCW presents an opposite tendency, decreasing from 97.7 per cent in pure rolling to 35.2 per cent for a slide-to-roll ratio equal to 0.284. For the highest slide-to-roll ratio considered (SRR = 0.409) the PCW increases, reaching 90.8 per cent.

The main reason for the different behaviour between the spherical and cylindrical discs, in terms of the PCW parameter, is probably related to their significant difference in surface finishing. The surface roughness of the spherical discs is 60 per cent greater than that of the cylindrical discs:

$$(R_a^{\text{sph}} = 0.50, R_a^{\text{cyl}} = 0.31)$$

and, probably, this has an unfavourable effect on coating adhesion.

Figure 8 Average, minimum and maximum percentage of uncoated area vs slide-to-roll ratio in twin-disc tests with carbon/chromium coated surfaces

The fact that the spherical discs were always used as the fast discs, might be another possible reason for their greater coating wear since they are submitted to a greater number of cycles than the cylindrical discs. On the other hand the fast disc heats considerably less than the slower one.

However, even taking into consideration the different number of cycles performed by each disc in each test (Table II) the remarks made above are still valid as shown in Figure 9, where the PCW is related to the number of cycles.

4. FZG gear tests

4.1 Test rig and FZG type C gears

The gear tests were performed on a FZG machine (Winter and Michaelis, 1985) using FZG type C gears, whose characteristics are shown in Table III.

Two different gears were tested:

- 1 NC – uncoated gear; and
- 2 GC – carbon/chromium coated gear.

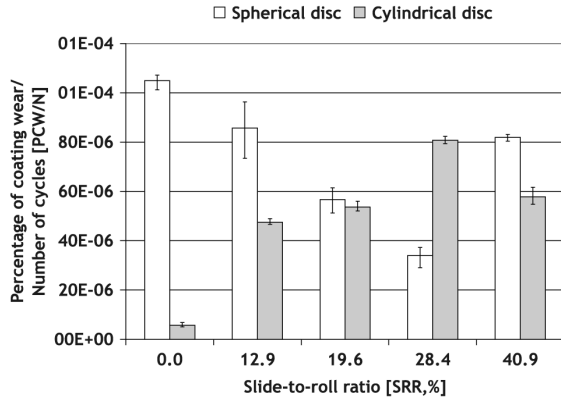
4.2 Physical properties of the lubricant

All tests were performed using an ISO VG 100 mineral oil without extreme-pressure (EP) and anti-wear (AW) additives. The physical properties of the lubricant are presented in Table III. During the tests the oil was kept at a constant temperature of 90°C.

4.3 Gear testing conditions

Before each test the gears were run-in during four hours in FZG load stage 6 at 1,500 rpm ($T_{\text{wheel}} = 203 \text{ N m}$, $n_{\text{wheel}} = 1,500 \text{ rpm}$) with the purpose of softening the surface roughness of the teeth flanks.

After running-in, all gear tests started on FZG load stage 7 ($T_{\text{wheel}} = 275 \text{ N m}$). The torque is progressively increased until FZG load stage 12 ($T_{\text{wheel}} = 801 \text{ N m}$) or until any type of surface failure of the teeth flanks is detected. The duration of each load stage is 15 min, during which both the speed and

Figure 9 Average, minimum and maximum PCW per cycle vs slide-to-roll ratio in twin-disc tests with carbon/chromium coated surfaces

the lubricant temperature are kept constant. At the end of each load stage the teeth flanks are visually inspected looking for surface failures, in particular scuffing and excessive wear.

The tribological operating conditions of the contact between the teeth flanks are extremely severe, as the torque increases from load stages 7-12. At the wheel tip/pinion root contact point, the maximum Hertz pressure increases from 1.13 to 1.92 GPa, while the minimum lubricant film thickness, although remaining almost constant with load, is very thin, 0.15 μm at 1,500 rpm and 0.20 μm at 3,000 rpm.

4.4 Gear tests results

The influence of the carbon/chromium surface coating on the gears performance is very significant, as shown in Figure 10.

Table III Characteristics of FZG Type C gears and physical properties of lubricant

Parameters (units)	Desig.	Pinion	Wheel
Number of teeth (-)	Z	16	24
Tooth width (mm)	b		14
Module (mm)	m		4.5
Pressure angle (°)	α		20
Profile shift factor (l)	x	0.182	0.171
Tip circle (mm)	d_a	82.45	118.35
Center distance (mm)	a_w		91.5
Working pressure angle (°)	α_Ω		22.5
Contact ratio (l)	ϵ		1.47
Material	l	DIN 20MnCr5	
Heat treatment		Case hardened, quenching and annealing	
Surface hardness	HRC		58-62
Surface roughness in teeth flanks (NC) (μm)	R_a	2.4	2.4
Surface roughness in teeth flanks (GC) (μm)	R_a	2.6	2.5
Oil type		ISO VG 100 mineral oil, additive free	
Cinematic viscosity at 40°C (mm^2/s)	ν_{40}		100.0
Cinematic viscosity at 100°C (mm^2/s)	ν_{100}		11.1
Specific gravity at 15°C (-)	Sp Gr		0.891
Viscosity index (-)	VI		95
Oil operating temperature (°C)	T		90 \pm 2

At 1,500 rpm the scuffing load stages of the uncoated and coated gears are, respectively:

$$K_{FZG}^{NC} = 11(T_{\text{wheel}} = 675 \text{ N m}) \quad \text{and}$$

$$K_{FZG}^{GC} = 12(T_{\text{wheel}} = 801 \text{ N m}),$$

representing an improvement in scuffing resistance of one load stage provided by the carbon/chromium coating.

At 3,000 rpm the scuffing load stages of the uncoated and coated gears are, respectively,

$$K_{FZG}^{NC} = 7(T_{\text{wheel}} = 275 \text{ N m}) \quad \text{and}$$

$$K_{FZG}^{GC} = 12(T_{\text{wheel}} = 801 \text{ N m}),$$

representing an improvement in scuffing resistance of five load stages provided by the carbon/chromium coating.

The differences in the scuffing load stages also represent very significant differences in the transmitted power by the FZG type C gear, as shown in Figure 11.

At 1,500 rpm the coated gear GC transmits 19 per cent more power than the uncoated gear NC, corresponding to an increase in input power of 20 kW. At 3,000 rpm the coated gear GC transmits 191 per cent more power than the uncoated gear NC, corresponding to an increase in input power of 165 kW.

5. Tests with a transfer gearbox

5.1 Gearbox test rig

The transfer gearbox tests were performed in a back-to-back test rig with re-circulating power. Thus, the driving electric motor only supplies the power needed to overcome inertia and the frictional and churning losses in order to reach and maintain the desired operating speed. Different types of gearboxes can be tested in this test rig.

Figure 10 Scuffing (or maximum) load stage at 1,500 and 3,000 rpm gear tests (FZG type C gears lubricated with additive free ISO VG 100 mineral oil at 90°C)

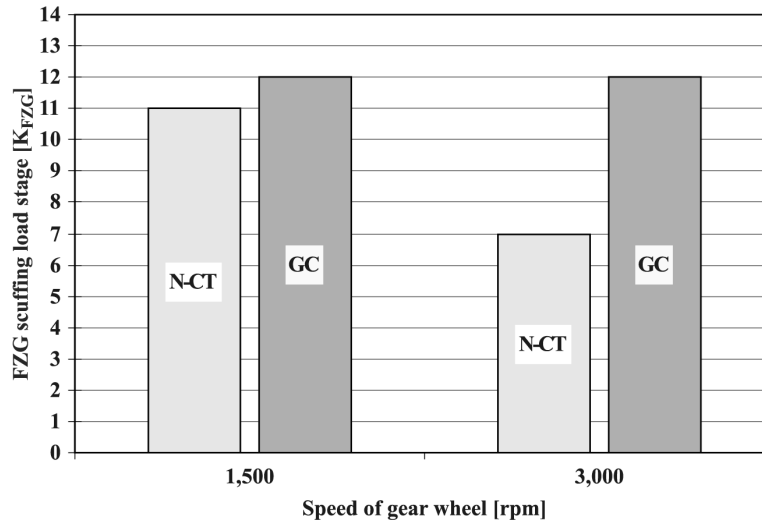
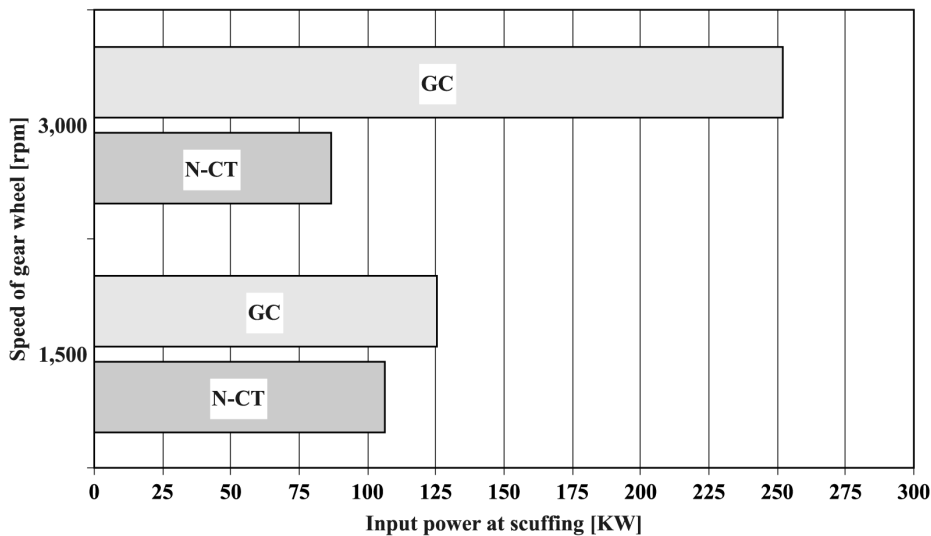


Figure 11 Power transmitted by the FZG type C gear at the scuffing load stage or at the end of the test (additive free ISO VG 100 mineral oil at 90°C)



Torque is applied using a hydraulic cylinder connected to a helical gear. When the cylinder moves forward the helix angle of the helical gear twists the connecting gears and applies the desired torque.

5.2 Transfer gearbox

Figure 12 shows a cross section of the two speeds gearbox used in this study. It is used as a transfer gearbox, mounted after the conventional gearbox of the vehicle, allowing the vehicle to have two drive axles (four wheel drive) and an auxiliary power output.

This transfer gearbox uses five gears mounted in three shafts employing gibs. The gears mounted on the input and output shafts are supported by needle roller bearings.

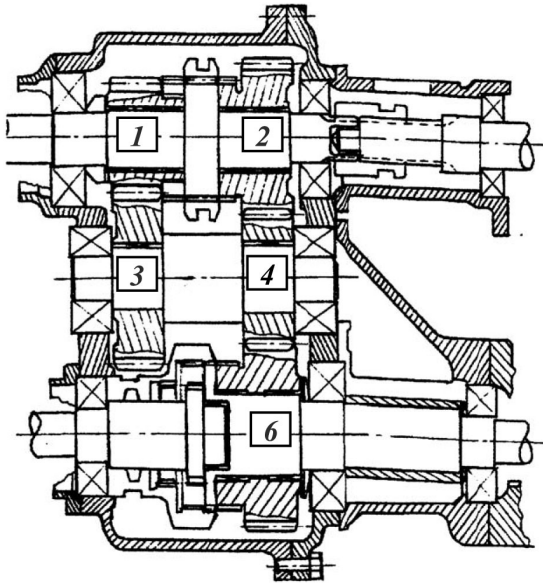
The gears are manufactured with DIN 15CrNi6 steel. After machining, the gears are case hardened, quenched in oil and annealed. The geometric characteristics of the gears are given in Table IV.

The gearbox is lubricated with mineral base industrial gear oil, with a viscosity grade ISO VG 150 and containing EP and AW additives. The transfer gearbox is filled up with 2.85 l of lubricant oil, as recommended by the gearbox manufacturer. The most significant properties of the lubricant are given in Table IV.

5.3 Transfer gearbox testing

Before each test the transfer gearbox is submitted to a running-in period of 5.4 h (0.53 millions cycles), during

Figure 12 Cross section of the two speeds transfer gearbox



which the input power is softly increased from 7.5 to 41 kW. In the end of the running-in period the lubricating oil is changed.

The transfer gearbox was tested in the lower speed range, when it is used as a torque multiplier, considering realistic operating conditions in terms of input speed and torque. The testing programme is defined in Table V and the operating conditions are related to the characteristics of the vehicle using this transfer gearbox (power and torque of the diesel engine and gear ratios of the main gearbox). The test time is 120 min.

The oil temperature when the test starts is 40°C. The oil temperature is measured during the test and depends on the operating conditions in each stage. The test is stopped if the lubricant temperature exceeds 120°C.

5.4 Efficiency of the transfer gearbox

The gearbox tested is equipped with C/Cr coated gears and its efficiency is measured for the input conditions of torque and speed mentioned in Table V.

The efficiency results are shown in Figure 13 and compared with previous data obtained with the same gearbox using uncoated steel gears (Martins, 2002). In both cases the operating conditions are very similar and the oil sump temperature is in the range between 60 and 70°C.

For the operating conditions considered, when the input speed increases from 600 to 1,400 rpm, at constant input power (meaning that the input torque is decreasing), the gearbox efficiency increases, as shown in Figure 13. When the input power increases from 36 to 72 kW, at constant input speed (meaning the input torque is increasing), the gearbox efficiency decreases approximately 0.5 per cent.

At constant speed, the efficiency of the C/Cr coated gears submitted to an input power of 36 kW is similar to that of the non-coated gears submitted to an input power of 30 kW, indicating a slightly better energetic performance of the C/Cr coated gears.

6. Discussion

6.1 Screening tests

The set of results of the screening tests (scratch, Rockwell indentation and pin-on-disc) confirms the excellent adhesion between the carbon/chromium coating and the steel substrate, as well as its interesting tribological properties, in particular, its low friction coefficient and low wear rate.

6.2 Twin-disc tests

The twin-disc tests show that the performance of the C/Cr coating is, in general, very good. The results obtained for the spherical and cylindrical confirm the excellent adhesion of this coating to the substrate, already pointed out by the screening tests. They also indicate that the C/Cr coating has high resistance to sliding at low specific film thickness and high Hertzian contact pressure ($0.35 < \Lambda < 0.45$, $p_0 = 2.0$ GPa).

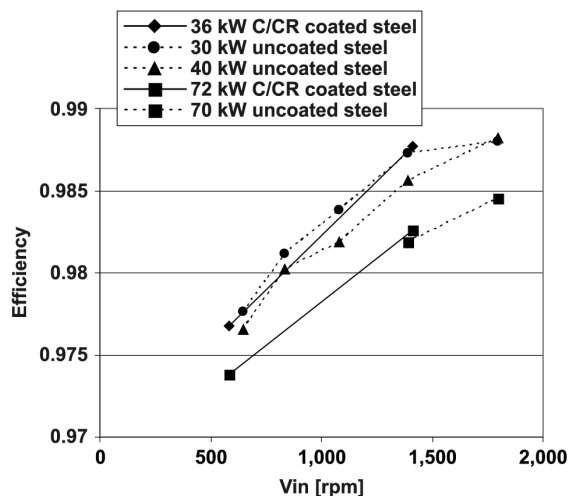
The predominant wear mechanism occurring during the twin-disc tests is coating delamination in the form of thin and long flakes. The coating wear is more intense in spherical discs (except for a SRR of 28 per cent). The larger roughness

Table IV Geometric characteristics of the transfer gearbox gears and lubricant physical properties

Parameter (units)	Design.	Gear wheel no.				
		1	3	2	4	6
Module (mm)	m	4	4	3.5	3.5	3.5
Number of teeth (l)	Z	17	28	27	23	32
Profile shift factor (l)	X	0.051	-0.24	0.161	0.415	0.381
Width (mm)	B	35	33.5	35	35	35
Pressure angle (°)	α	20	20	20	20	20
Helix angle (°)	β	20	20	20	20	20
Max. addendum diameter (mm)	$d_{a\max}$	80.7	125.2	108.4	95.3	128.6
Oil type		ISO VG 150 mineral oil				
Cinematic viscosity at 40°C (mm ² /s)	ν_0	150				
Cinematic viscosity at 100°C (mm ² /s)	ν_1	14.5				
Specific gravity at 15°C (-)	Sp Gr	0.896				
Viscosity index (-)	VI	95				
FZG rating	K_{FZG}	12 >				

Table V Operating conditions of transfer gearbox with carbon/chromium coated gears

Parameter	Design.	Stages	
Input speed to transfer gearbox (rpm)	n	573	1376
Vehicle speed (km/h)	V	5.7	13.6
Input torque (Nm)			
$P \cong 36$ kW	T_{in}	600	250
$P \cong 72$ kW	T_{in}	1,200	500

Figure 13 Efficiency of the transfer gearbox. Influence of input power, input speed and carbon/chromium surface coating

of the spherical discs is probably responsible for the different comportment in what relates to PCW parameter and probably is also responsible for a worst coating adhesion.

The C/Cr coating was able to support the severity of the tribological operating conditions imposed by the twin-disc tests, similar to those found in gears in terms of contact pressures, slide-to-roll ratios and specific lubricant film thickness, giving very good indications about the successful application of this coating in gear sets.

6.3 FZG gear tests

The improvement in scuffing resistance promoted by the C/Cr coating at 1,500 rpm is equal to one FZG load stage, representing an increase in input torque of 19 per cent.

Joachim *et al.* (2002) obtained an improvement in scuffing resistance (2 FZG load stages) in standard FZG scuffing tests A/8,3/90 lubricated with Mobil Jet Oil II, between uncoated and coated gears, using WC/C (tungsten carbon carbide) and B4C (boron carbide) coatings. Weck *et al.* (2002) also obtained a similar improvement in scuffing resistance (1 FZG load stage) in standard FZG scuffing tests A/8,3/90 lubricated with COE 100 base oil using WC/C (tungsten carbon carbide) coating. They also noticed a considerable decrease in the wear of the teeth flanks.

Amaro *et al.* (2003), using the same gears and the same testing and lubrication conditions, also obtained an improvement in scuffing resistance (two FZG load stages) using a MoS₂/titanium surface coating.

The improvement in scuffing resistance promoted by the C/Cr coating at 3,000 rpm is equal to five FZG load stages, representing an increase in input power of 191 per cent. The same result was obtained by Amaro *et al.* (2003), for the same gears and the same testing and lubrication conditions, using a MoS₂/titanium surface coating.

These scuffing results are directly related to the low friction coefficient of the carbon/chromium coating which originates lower contact temperatures between the gear teeth and thus a higher scuffing load carrying capacity.

6.4 Gearbox tests

At constant input power when the speed increases the torque decreases. Consequently, the friction losses inside the gearbox decrease (lower torque) and the churning losses increase (higher speed). However, the increase of the churning losses is smaller than the decrease of the friction losses, and globally, the power dissipated decreases and the gearbox efficiency increases (within the range of operating conditions considered), justifying the experimental results obtained.

At constant input speed when the power increases the torque also increases. Thus, the churning losses remain constant (same speed), the friction losses increase (higher torque) and the gearbox efficiency decreases, as observed in the tests performed.

Comparing the coated and uncoated gears, an increase of the gearbox efficiency between 0.1 and 0.2 per cent is observed when C/Cr coated gears are used, depending on the operating conditions. A similar result was obtained by Amaro *et al.* (2003) using MoS₂/Ti coated gears, where an increase in gearbox efficiency of about 0.5 per cent was observed.

7. Conclusions

The C/Cr coating shows a good tribological performance, confirmed by the results of all tests performed, such as, pin-on-disc tests, twin-disc tests, FZG scuffing tests and gearbox efficiency tests. The carbon/chromium surface coating shows the following characteristics:

- high hardness (2,200 HV) and low friction coefficient (0.06 for a load of 140 N on POD tests);
- excellent adhesion to the steel substrate even at high contact pressure, high slide-to-roll ratio and low specific lubricant film thickness;
- the surface roughness of the substrate is almost unaffected by the coating deposition;
- very significant increase of the load carrying capacity of FZG type C gears against scuffing – 1 FZG load stage at 1,500 rpm and 5 FZG load stages at 3,000 rpm; and
- the efficiency of a transfer gearbox slightly improves when C/Cr coated gears are used.

These characteristics of the C/Cr surface coating are of great interest at least in two particular applications:

- 1 severe applications involving high contact pressures and high sliding, frequent start-ups and inefficient lubrication; and
- 2 acting as tribo-reactive material and substituting non-biodegradable and toxic additives in environmental lubricants.

References

- Amaro, R. (2000), “Comportamento tribológico de revestimentos auto-lubrificantes para engrenagens”, Master of Science thesis, DEMEGI, FEUP (in portuguese).
- Amaro, R., Martins, R., Seabra, J. and Brito, A. (2003), “Most low friction coating for gears application”, paper presented at GEARS 2003 – Gears and Transmissions Workshop.
- Fox, V., Jones, A., Renevier, N. and Teer, D. (2000), “Hard lubricating coatings for cutting and forming tools and mechanical components”, *Surface and Coatings Technology*, Vol. 125.
- Holmberg, K., Mathews, A. and Ronkainen, H. (1998), “Friction and wear mechanisms of coated surfaces”, *Finnish Journal of Tribology*, Vol. 17 Nos 3-4.
- Joachim, F., Kurz, N. and Glatthaar, B. (2002), “Influence of coatings and surface improvements on the lifetime of gears”, *VDI-Berichte*, No. 1665.
- Martins, R. (2002), “Avaliação experimental do desempenho energético de uma caixa transfer para veículos de tracção integral”, Master of Science thesis, DEMEGI, FEUP, 2002 (in portuguese).
- Rigato, V. and Maggioni, G. *et al.*, (2000), “Properties of sputter-deposited MoS₂/metal composite coatings deposited by closed field unbalanced magnetron sputter ion plating”, *Surface and Coatings Technology*, Vol. 131.
- Renevier, N., Fox, V., Hampshire, J. and Teer, D. (2000), “Performance of low friction MoS₂/titanium composite coatings used in forming applications”, *Materials and Design*, Vol. 21.
- Su, Y. and Kao, W. (2003), “Tribological behaviour and wear mechanism of MoS₂-Cr coatings sling against various counterbody”, *Tribology International*, No. 36.
- Teer, D. (1994), “Magnetron Sputter ion plating”, UK Patent No. GB 2 258 343 (1997), EU Patent No. 0 521 045, USA Patent No. 5 554 518 (1996).
- Weck, M., Hurasky-Schonwerth, O. and Bugiel, Ch. (2002), “Service behaviour of PVD-coated gearing lubricated with biodegradable synthetic ester oils”, *VDI-Berichte*, Vol. 1665.
- Winter, H. and Michaelis, K. (1985), “FZG gear test rig – description and possibilities”, paper presented at Coordinate European Council Second International Symposium on the Performance Evaluation of Automotive Fuels and Lubricants.
- Yang, S., Camino, D., Renevier, N., Jones, A. and Teer, D. (2000), “Deposition and tribological behavior of sputtered carbon hard coatings”, *Surface and Coatings Technology*, Vol. 124.
- Yang, S., Li, X., Renevier, N. and Teer, D. (2001), “Tribological properties and wear mechanism of sputtered C/Cr coating”, *Surface and Coatings Technology*, Vol. 142.

A.8 Paper H

R. Martins, N. Cardoso, and J. Seabra, “Influence of lubricant type in gear scuffing”. *Industrial Lubrication and Tribology*, (6) 2008 (to be published).

INFLUENCE OF LUBRICANT TYPE IN GEAR SCUFFING

Ramiro Martins¹, Nuno Cardoso¹, and Jorge Seabra²

¹INEGI, Faculdade de Engenharia, Porto, Portugal

²Faculdade de Engenharia, Universidade do Porto, Portugal

ABSTRACT

This paper investigates the scuffing load carrying capacity of three gear oils: a standard mineral lubricant containing extreme pressure and anti-wear additives (M0) and two biodegradable saturated esters containing low toxicity additives (E1 and E2). The physical, chemical and biodegradability properties of the lubricants are presented and compared.

Four ball wear tests were performed, according to standard ASTM D4172. Results from the wear scar diameter and from ferrographic analysis of the test oil samples are presented and related to the lubricant properties.

FZG gear scuffing tests were performed, according to standard DIN 51535, in order to evaluate the scuffing load carrying capacity of the two oils. Two reference tests were performed, A20/16.6/90 and A10/16.6/90. Test results include scuffing load stage, maximum oil bath temperature, pinion weight loss and surface roughness measurement of the teeth flanks.

Finally, the Critical Temperature Scuffing Criterium (Castro, 2005) for the scuffing failure in FZG gears was used to determine Critical Temperature of characteristic of each lubricant.

1 INTRODUCTION

Scuffing is an instantaneous failure, where gear flanks are welded together under pressure and temperature (Höhn, 2004), it is normally associated with the overall destruction of the gear teeth surfaces with significant modification of the teeth flank geometry. The surfaces protection is promoted by the lubricant and it can be provided by hydrodynamic lubrication through thick oil films, physically adsorbed layers of dipoles from the base fluid or the additives or chemical reaction layers from the additives (Höhn, 2004).

The main objective of this work was to assess the wear properties and the gear scuffing failure protection promoted by two new gear oil formulations, based on biodegradable fully saturated esters with low toxicity additivation, and comparing them with standard mineral gear oil.

Four-Ball Wear Tests, according to ASTM D 4172 (ASTM D 4172, 2004), were performed to evaluate the relative wear preventive properties of lubricating fluids in sliding contact under prescribed test conditions.

Standard FZG gear scuffing tests (FZG A20/16.6/90 and FZG A10/16.6/90), according to DIN 51354 (DIN 51354, 1990)], were performed to determine the scuffing load capacity of the new gear oil formulations.

The results obtained allowed the definition of different oils properties and attributes. The analysis of lubricant behaviour in extreme conditions (high pressure, temperature and

rotations) was used to estimate their performance in real applications.

2 GEAR OILS

Three industrial gear oils were considered: two ISO VG 100 biodegradable fully saturated ester lubricants with low toxicity additivation and an ISO VG 150 mineral oil, containing an additive package to improve micropitting resistance.

The main properties of the three lubricants are shown in Table 1. The ester based oils were formulated so that their viscosities at 100 °C were similar to that of the mineral oil.

Parameter	Method	Desig.	Units	Lubricating Oils		
				M0 paraffinic mineral oil	E1 fully saturated ester	E2 fully saturated ester
Lubricant reference						
Base oil	DIN 51451	/	/			
<i>Physical properties</i>						
Density @ 15°C	DIN 51757	ρ15	g/cm ³	0.897	0.925	0.955
Kinematic Viscosity @ 40 °C	DIN 51562	v40	cSt	146	99.4	114.5
Kinematic Viscosity @ 100 °C	DIN 51562	v100	cSt	14.0	14.6	17.0
Viscosity Index	DIN ISO 2909	VI	/	92	152	162
Pour point	DIN ISO 3106		°C	-21	-42	
<i>Wear properties</i>						
KVA weld load	DIN 51350-2	/	N	2200	2200	-
Kva wear scar (1h/300N)	DIN 51350-3	/	mm	0.32	0.35	-
Brugger crossed cylinder test	DIN 51347-2	/	N/mm ²	68	37	-
FZG rating	DIN 513540	K _{FZG}	/	>13	-	-
<i>Chemical Content</i>						
Zinc	ASTM D-4927	Zn	ppm	-	-	
Calcium	ASTM D-4927	Ca	ppm	40	-	
Phosphor	ASTM D-4927	P	ppm	175	146	
Sulphur	ASTM D-4927	S	ppm	15040	180	
<i>Biodegradability and toxicity properties</i>						
Ready biodegradability	OECD, 301 B		%	<60	≥60	-
Biodegradability	OECD, 301 F		%	-	-	75
Aquatic toxicity with Daphnia	OECD, 202	EL ₅₀	ppm	-	>100	-
Aquatic toxicity with Alga	OECD, 201	EL ₅₀	Ppm	-	>100	-

Table 1 – Physical and chemical properties of the considered lubricants.

The mineral lubricant is based on paraffinic oil with significant residual sulphur content. It contains an ashless antiwear additive package based on phosphorous and sulphur chemistry and metal-organic corrosion preventives. In contrast, the biodegradable ester products use fully saturated esters based on harvestable materials, incorporate environmentally compatible and highly efficient additives and metal-organic compounds were completely avoided. The additive content of the mineral oil is considerably higher than that of the ester oils, mainly in what concerns the sulphur compounds.

The “ultimate” biodegradability of the lubricants was assessed using a “ready” biodegradability test, as published by the OECD and adopted by the European Union. The

mineral oil didn't match the minimum requirements of 60% biodegradability in 28 days, as shown in Table 1. Thus, no toxicity tests were performed for this lubricant. The ester based oils exceeded the minimum requirements of 60% biodegradability in 28 days and pass both toxicity tests, OECD 201 "Alga growth inhibition test" and OECD 202 "Daphnia Magna acute immobilization".

3 FOUR-BALL TESTS

3.1 Standard Test Method for Wear Preventive Characteristic of Lubricating Oils

ASTM Standard¹ D4172 – "Test Method for Wear Preventive Characteristics of Lubricating Fluids, Four-Ball Method", together with ANSI Standard² B3.12 – "Specification for Metal Balls", covers the procedures to do a preliminary evaluation of the anti-wear properties of lubricating oils in sliding contact by means of the Four-Ball Wear Test Machine (see Figure 1).

Three steel balls, 12.7 mm diameter each, were clamped together and covered with the lubricant to be evaluated. A fourth ball with the same dimension, called upper ball, was pressed with the force 392 N [40 kgf] into the cavity formed by the three clamped balls, originating a three-point contact as shown in Figure 2.

The temperature during the test was kept constant at $75\pm 2^{\circ}\text{C}$ with the top ball rotating at 1200 rpm during 60 min. Wear scars were generated in the 3 lower balls and a wear track appeared in the upper ball, during the test.



Figure 1 –Four-Ball Test Machine.

¹ For referenced ASTM standards, visit the ASTM website, www.astm.org, or contact ASTM Customer Service at service@astm.org. For Annual Book of ASTM Standards volume information, refer to the standard's Document Summary page on the ASTM website.

² Available from American National Standards Institute (ANSI), 25 W. 43rd St. 4th Floor, New York, NY 10036

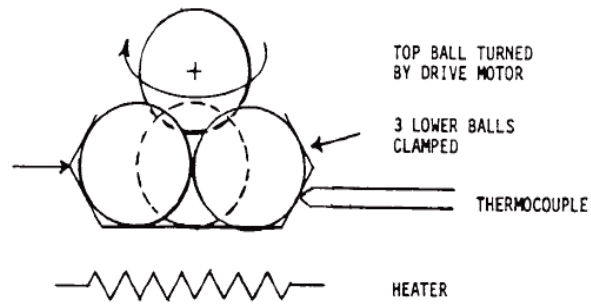


Figure 2– Schematic of a Four-Ball Test Machine.

The wear scars on the three lower balls were measured (± 0.01 mm accuracy) in two directions: one measurement was made along a radial line from the centre of the holder and a second measurement along a line making 90° with the first measurement. The wear scar diameter was the average value from two measurements. The width of the wear track is also measured on the upper ball.

In order to have reliable data two tests were performed for each lubricant. The precision of this test method is determined by the Repeatability - The difference between two test results (the smallest one and the largest one) should not exceed $120 \mu\text{m}$ for lubricating oils.

Additionally, oil lubricant samples were collected after each test and were analyzed by Analytical and Direct Reading Ferrography (Hunt, 1993). The characteristics of the wear particles were determined and the Ferrometric indexes DL, DS, CPUC and ISUC (Hunt, 1993) were obtained. The procedure to collect the lubricant sample at the end of each test was:

1. Drain all the test lubricant (about 8 ml) to a sample bottle;
2. Leaving the three-ball clamped and using an appropriated solvent (petrol benzene) wash the three balls and drain again to the sample bottle;
3. Remove the three balls carefully and flush the oil cup with a solvent jet, draining simultaneously to the sampling bottle.

3.2 Four-Ball wear test results

Table 2 presents the wear scar diameters (lower balls) and the wear track (upper ball) measurements made in all tests. The wear scar diameters shown for each lubricant are the average value of the measurements made on the three balls in two directions on each test (Test 1 and Test 2). Ferrography oil analysis results are shown in Table 3.

3.3 Discussion on Four-Ball test results

The wear scars diameters produced during the Four-Ball Machine wear test are directly related to the anti-wear properties of fluid lubricants in sliding contacts, as well as the wear volume generated and measured by Ferrography. The presence of anti-wear additives and the lubricant film thickness are two important factors to evaluate the wear conditions during the tests.

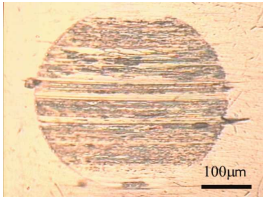
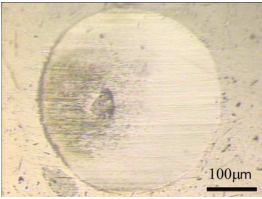
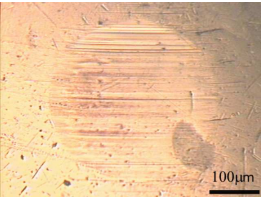
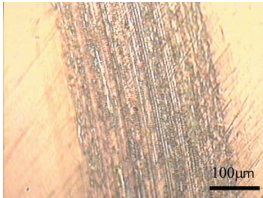
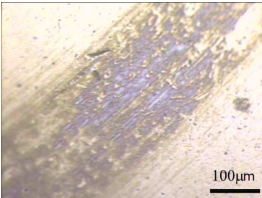
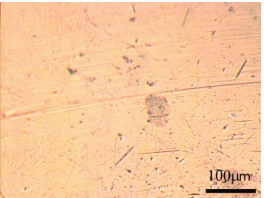
Lubricant		M0	E1	E2
Lower Ball Wear Scar				
Average Wear Scar Diameter	Test1	376 μm	404 μm	364 μm
	Test2	396 μm	392 μm	342 μm
Max. Diff.		30 μm	18 μm	36 μm
Average		386 μm	398 μm	353 μm
Upper Tall Wear Track				
Wear Track Width	Test1	324 μm	360 μm	276 μm
	Test2	420 μm	396 μm	252 μm
Average		372 μm	378 μm	264 μm

Table 2 – Lubricant oil test results.

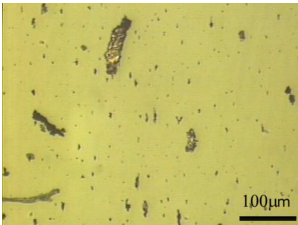

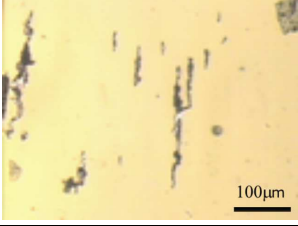
Lubricant		D_L [/]	D_S [/]	CPUC [/]	ISUC [/]	Ferrogram
M0	Test 1	4.9	2.7	7.6	16.7	
	Test 2	3.5	2.4	5.9	6.49	
E1	Test 1	6.6	1.6	8.2	41.1	
	Test 2	1.3	0.8	2.1	1.1	
E2	Test 1	3.7	2.7	6.4	6.4	
	Test 2	2.3	0.6	2.9	4.9	

Table 3 - Ferrography analysis for the lubricants tested.

All the three lubricants (M0, E1 and E2) contain an additive package including anti-wear agents. M0 and E2 lubricants have higher viscosity at the operating temperature (31,47 cSt and 32,57 cSt at 75°C, respectively) than E1 lubricant (27,97 cSt at 75°C) and, probably, also generate higher film thickness than E1. Wear scar diameters (WSD) and wear track widths (WTW) resulting from the tests with M0 and E1 lubricants are in close proximity and those from E2 lubricant are smaller, as presented in Table 2.

In Figure 3, the average wear scar diameter is plotted against the lubricant viscosity at the operating temperature, indicating a tendency for a wear scar diameter decrease when the lubricant viscosity increased, taking into account that all the three lubricants contain anti-wear agents.

The Ferrometry results (D_L , D_S , CPUC and ISUC) from all oil samples presented in Table 3 are similar, with two exceptions: Test 1 with oils M0 and E1, which gave very high severity indexes ISUC. In Figure 4 the average ISUC index is plotted against the average wear scar diameter and a good agreement is obtained and the tendency observed in Figure 3 is the same, with E2 gear oil showing the best result. The ferrograms shown in Table 3 also confirm this analysis, since the sizes of the wear particles corresponding to oil E2 are significantly smaller than those of the other two oils, M0 and E1.

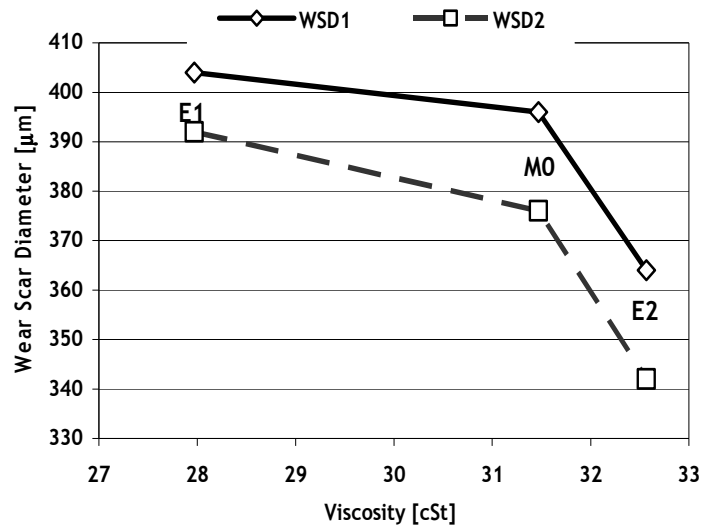


Figure 3 - Relation between Viscosity at 75°C and Wear Scar Diameters [µm].

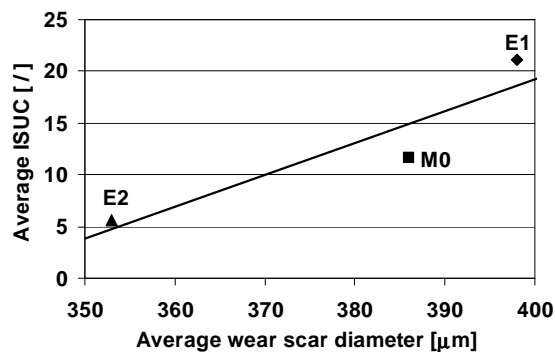


Figure 4 - Average ISUC index vs. average wear scar diameter for the lubricants tested.

Table 2 shows the wear scars corresponding to the three oils tested, being clear that the the one corresponding to lubricant E2 is the smoothest one, thus confirming the correlations established above.

Although not absolutely conclusive, the Four-Ball wear test results indicate a similar performance of gear oils M0 and E1 and a better performance of lubricant E2 when compared with the other two.

4 SCUFFING TESTS

4.1 Gear scuffing

Figure 5 shows the surface roughness evolution of the teeth flanks of a FZG type A gear during a standard FZG A20/8.3/90 test. In this case, the scuffing failure produced a severe modification of the surface roughness without significant modification of the teeth flanks geometry (Michaelis, 2003).

The surface roughness profile of the pinion tooth flank showed several scuffing marks, oriented in the direction of sliding between the gear teeth, from tooth tip to tooth root, indicating that severe adhesion phenomena has occurred, with material removal. At the end of the test these scuffing marks spread over the entire width of the tooth flank, and the corresponding surface roughness (see picture on the right) exhibited a very strong increase of the roughness peaks.

DIN 51354 standard (DIN 51354,1990) considers that scuffing occurred when the sum of all scuffing marks on the flanks of all pinion teeth is greater than the width of one tooth flank (20 mm on the A20 FZG type A gear).

Gear scuffing is influenced by the operating conditions such as temperature, load, speed, sliding, specific film thickness, lubricant additives and surface material as well. Table 4 shows the factors that are reported to interfere in gear scuffing and their influence of the scuffing load capacity of gears.

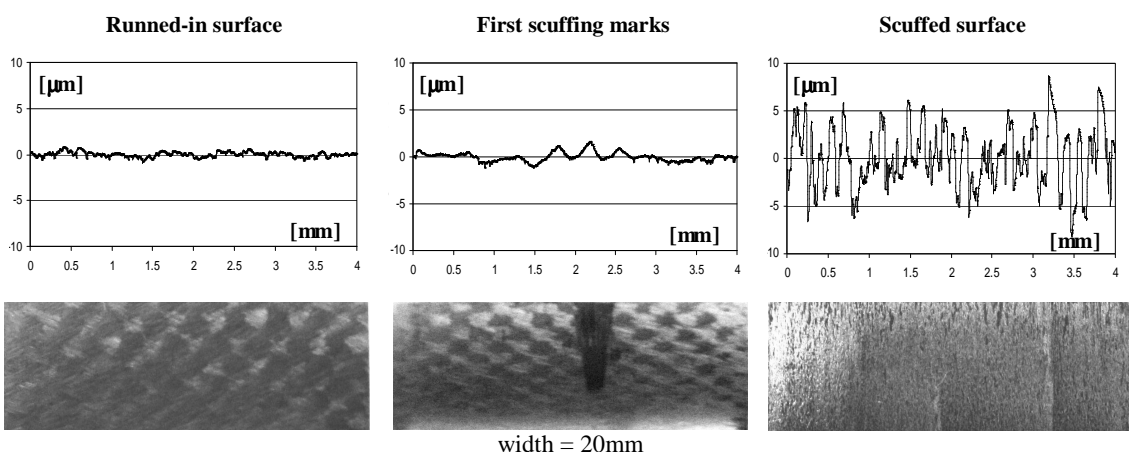


Figure 5 - Evolution of the surface roughness of the teeth flanks during a standard FZG A20/8.3/90 scuffing test (Castro, 2004).

Increasing Factor	Scuffing Load
lubricant viscosity	↗
lubricant additive chemistry	↗
oil sump temperature	↘
speed	↘
coefficient of friction	↘
gear surface roughness	↘

Table 4- Factors influencing gear scuffing: ↗ increase, ↘ decrease (Höhn, 2004).

4.2 FZG gear test rig

The load carrying capacity of gears against scuffing may be evaluated using the FZG gear test rig (Winter, 1985), which is a well known back-to-back spur gear test rig with “power circulation”, as shown in Figure 6. The test pinion (1) and the test wheel (2) are connected by two shafts to the driving gears (3). The front shaft is divided in two parts with the load clutch in between (4). One half of the load clutch can be fixed to the foundation by a locking pin (5) while the other part can be twisted using a load lever and weights (6). After bolting the clutch together the load can be removed and the shaft unlocked.

Now a static torque is applied to the system that can be measured by the torque measuring clutch (7). The maximum speed of the AC-motor is 3000 rpm. The test gears can be dip lubricated or jet lubricated. When dip lubrication is used, the oil may be heated using the electrical heaters mounted in the test gearbox. The heater and cooling coil allows the settling of a constant oil temperature measured by the temperature sensor (8).

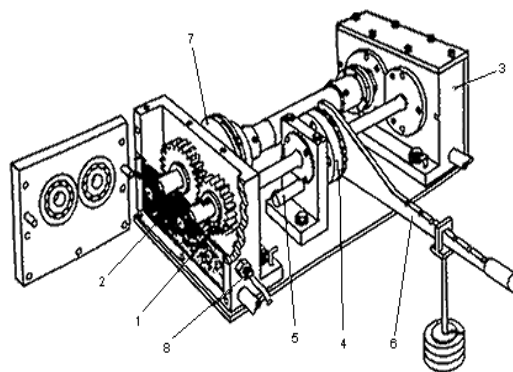


Figure 6 - Schematic view of the FZG Gear Test Rig (Winter, 1985).

4.3 Test gears

The test gears used in these scuffing tests were similar to standard FZG type A gears, but they did not have the manufacturing accuracy grade proposed in standard DIN5134: The surface roughness of the teeth flanks was higher, typically $R_a = 1.0 \mu\text{m}$, generating lower specific film thickness during operation and, thus, making the tests even more severe, and the teeth flanks were grinded at 0° and so didn't have the standard Maag criss-cross grinding (15° method). The geometric characteristics of the test gears are presented in Table 5. They were manufactured in standard carburizing steel (DIN 20 MnCr 5).

4.4 Gear scuffing test procedure

FZG gear scuffing tests give quantitative and qualitative information about the influence of several parameters on gear scuffing, such as, temperature, load, speed, sliding, specific film thickness, lubricant additives, surface roughness and surface material.

In the standard FZG gear scuffing test (FZG A20/8.3/90, DIN 51354) 20 mm wide type A gears are used, allowing very high sliding rates at the end of the meshing line. The operating speed (wheel) is 1500 rpm, under dip lubrication.

Table 6 shows the wheel torque corresponding to each load stage in the standard FZG gear scuffing test. The torque is applied progressively from load stage 1 to load stage 12, until scuffing occurs, and each load stage lasts 15 minutes.

Gear type	A20		A10	
	Pinion	Wheel	Pinion	Wheel
Number of teeth	16	24	16	24
Module [mm]	4.5		4.5	
Centre distance [mm]	91.5		91.5	
Pressure angle [°]	20		20	
Face width [mm]	20		10	20
Addendum modification [/]	+0.853	-0.500	+0.853	-0.500
Addendum diameter [mm]	88.68	112.50	88.68	112.50
Flank roughness (R_a) [μm]	1.0 ± 0.1	1.0 ± 0.1	1.0 ± 0.1	1.0 ± 0.1

Table 5– Geometry of the FZG test gears: Types A10, A20.

FZG load stage - K_{FZG}	1	2	3	4	5	6	7	8	9	10	11	12
Wheel Torque - T [Nm]	3.3	13.7	35.3	60.8	94.1	135.3	183.4	239.0	302.0	372.6	450.1	534.5
Test phases	Running-in				Scuffing stages							

Table 6– Wheel torque for each load stage in the standard FZG gear scuffing test (DIN51354).

Gear running-in takes place during the first 4 load stages, as indicated in Table 6. This running-in period is very important, since it avoids premature scuffing failure of the FZG gear. In these first 4 load stages the initial oil bath temperature is not imposed, typically equal to the ambient temperature. From load stage 4 onward the initial oil bath temperature is set to $90 \pm 2 \text{ }^\circ\text{C}$. During each load stage, the oil temperature increases from the initial value to a final temperature, which is mainly dependent on the applied torque and lubricant properties.

In general, gear oils have a very high scuffing load carrying capacity and they all pass load stage 12 in the standard A20/8.3/90 test, as shown in Table 1. In order to differentiate more clearly the gear scuffing protection provided by the lubricants under analysis, more severe versions of the standard test were used: A20/16.6/90 test, performed at a pitch speed of 16.6 m/s and using 20 mm wide gears and A10/16.6/90 test, performed at the same pitch speed but using 10 mm wide gears. In the first case the input power is twice that of the standard test and in the second case, beside the higher input power, the Hertzian contact pressure between gear teeth is 41.4% higher.

Before and after the tests the roughness of the teeth flanks and the weight of the pinion are measured, in order to assess the evolution of the surface roughness and evaluate the pinion mass loss. During the tests the temperature of the oil bath is monitored continuously.

4.5 Gear scuffing results

Figure 7 shows the scuffing load stage reached by each lubricant in tests A20/16.6/90 and A10/16.6/90. With 20 mm wide gears (test A20/16.6/90) the ester oils E1 and E2 reached scuffing in load stage 12, one load stage more than the mineral oil M0, and with 10 mm wide gears (test A10/16.6/90) all the lubricants reached scuffing in load stage 11. These gear scuffing results are very similar, knowing that the precision of these tests is \pm one load stage.

Figure 8 shows the maximum oil bath temperature reached by each lubricant during the corresponding scuffing load stage, in tests A20/16.6/90 and A10/16.6/90. The results measured for oil E2 were very interesting since it always generated lower temperatures than the other gear oils in both tests. Although lubricants E2 and M0 had the same maximum oil bath temperature in test A20/16.6/90 (156 °C), it must be taken into consideration that E2 reached scuffed in load stage 12 and M0 in load stage 11, meaning that the temperature performance of oil E2 is better.

Once the film breaks down and scuffing occurred the wear amount of the teeth flanks can be very high. Figure 9 shows the pinion mass loss at the end of tests A20/16.6/90 and A10/16.6/90 for each lubricant. However, these pinion mass loss results after scuffing are not significant of the performance of a lubricant.

Taking into account the high severity of the tests performed, the gear scuffing results obtained for the three lubricants are outstanding, confirming the high quality of the biodegradable gear oils, based on saturated esters containing low toxicity additives.

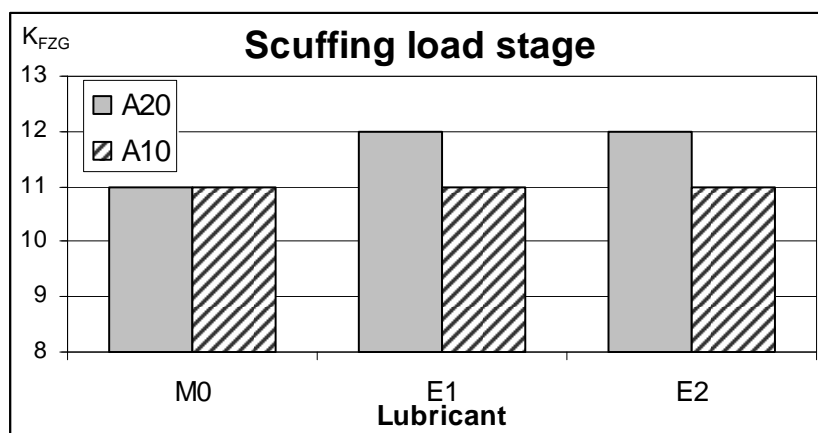


Figure 7 - Scuffing load stage for each lubricant

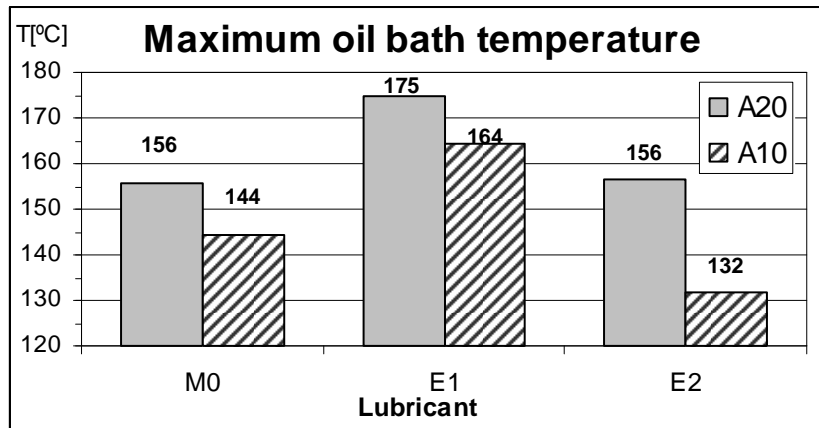


Figure 8 - Oil bath temperature at the end of the scuffing stage.

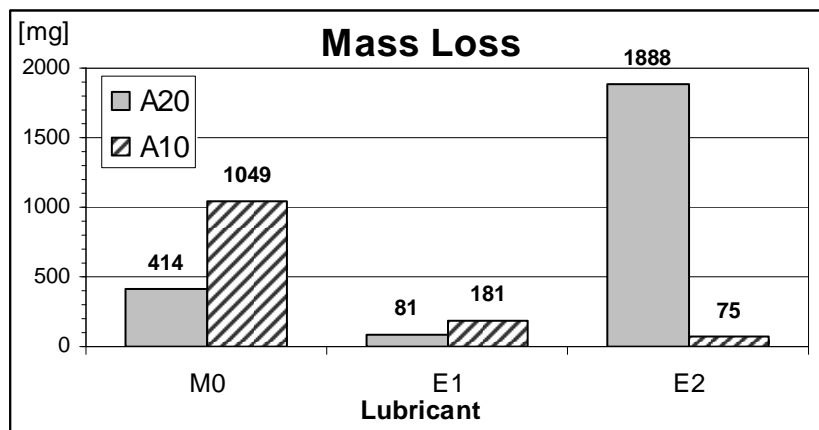


Figure 9 – Pinion mass loss.

4.6 Discussion on gear scuffing test results

4.6.1 Tests A20/16.6/90

Table 7 displays the results obtained for the three lubricants (M0, E1, E2) in FZG A20/16.6/90 gear scuffing tests.

Mineral gear oil M0 reached scuffing in load stage 11, however, the scuffed width was only slightly above the minimum limit (one teeth width = 20 mm). The next load stage ($K_{FZG} = 12$) was performed and a very severe scuffing failure was obtained with a very significant mass loss of 414 mg. This result suggests that the real scuffing load stage of oil M0 is between 11 and 12, but the precision of this test (± 1 load stage) didn't allow a more precise evaluation. The gear lubricant with E2 oil suffered a very destructive scuffing failure with high mass loss (1888 mg) while the gear lubricated with E1 oil had a low mass loss.

Figure 10 shows the oil bath temperatures at the end of each load stage, being interesting to notice that at the end of load stage 11 the oil bath temperatures of the three lubricants were almost the same. During load stage 12 scuffing occurred and several different behaviours

were noticed, the temperatures of oils M0 and E1 increased while the temperature of oil E2 remained the same.

This particular behaviour of gear oil E2, showing maximum oil bath temperatures almost constant at very high load, from load stages 10 to 12, might be related to the type of additives used in its formulation.

Figure 11 shows two flanks of the same gear after test, one undamaged and the other showing significant scuffing marks. The surface roughness of the teeth flanks was measured in two cross directions, axial and radial, before (“Initial”) and after (“Final”) each gear scuffing test as shown in Figure 12. The measurements after test were made both on scuffed and non-scuffed zones.

The average surface roughness on the radial direction is considerably larger than on the axial direction due to the grinding direction (axial), as shown in Figure 12, and the scuffing marks are oriented in the radial direction, as shown in Figure 11. So, the roughness measurements in the radial direction are not suitable to assess the scuffing failure and axial measurements should be used. The evolution of the roughness profiles in the axial direction, shown in Figure 12 (left), demonstrates the degradation of the tooth flanks between initial, undamaged and scuffed surfaces.

A20/16.6/90 gear scuffing test with industrial gear oils				
Lubricant		M0	E1	E2
k_{FZG}		11*	12	12
Weight Loss	[mg]	414*	81	1 888
Maximum Oil Temperature	[°C]	155,5	174,7	156,4
Contact pressure at the scuffing load stage	[GPa]	1,80	1,96	1,96
Oil viscosity at scuffing	[cSt]	4,50	4,16	6,12

Table 7 – A20/16.6/90 gear scuffing test results with lubricants M0, E1 and E2 (*because the scuffing failure on load stage 11 was not very severe, load stage 12 was performed).

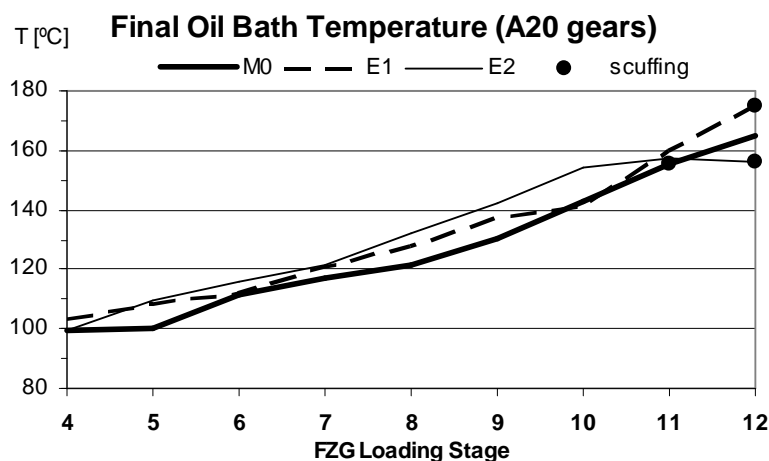


Figure 10 - Oil bath temperature at the end of each load stage on A20/16.6/90 FZG gear scuffing tests.

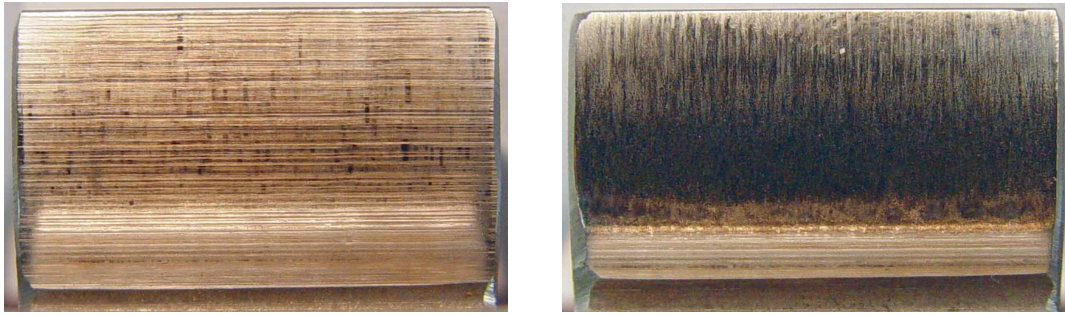


Figure 11 – Gear teeth flanks after scuffing test: right undamaged flank, left scuffed flank (width =20mm).

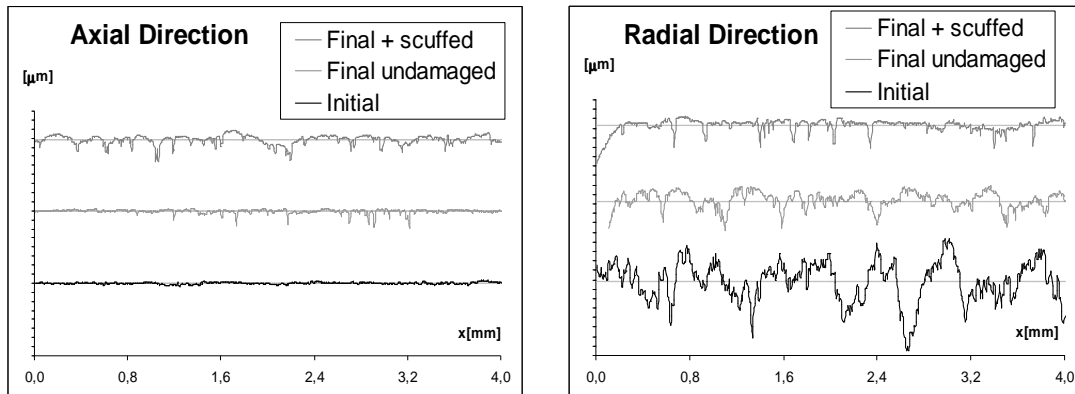


Figure 12 - Typical surface roughness profiles on tooth flanks, measured in the axial (left) and radial (right) directions: new surface (bottom); undamaged used surface (middle); used + scuffed surface (top).

Table 8 shows the surface roughness parameters measured on the tooth flanks in the axial direction for the three gear oils tested. The comparison of R_{max} and R_{z-D} roughness parameters, between initial values (as manufactured after grinding) and final scuffed values, clearly shows the degradation suffered by the tooth flanks after scuffing.

Pinion tooth flank surface roughness parameters in the axial direction [μm] A20/16.6/90 gear scuffing tests							
Oil	Measurement type	R_{max}	R_{z-D}	R_a	R_{pk}	R_k	R_{vk}
M0	Initial	1,9	1,2	0,2	0,3	0,4	0,4
	Final undamaged	1,9	1,4	0,2	0,1	0,4	0,5
	Final scuffed	3,6	2,8	0,5	0,3	1,3	0,8
E1	Initial	1,6	1,0	0,2	0,2	0,4	0,3
	Final scuffed	8,1	5,9	0,8	0,5	1,7	2,4
E2	Initial	1,8	1,1	0,2	0,2	0,4	0,3
	Final scuffed	6,0	4,3	0,7	0,5	1,8	1,6

Table 8 – Surface roughness parameters on tooth flanks, measured in the axial direction, before and after A20/16.6/90 gear scuffing tests.

4.6.2 Tests A10/16.6/90

The FZG gear scuffing test A10/16.6/90 test is a more severe than the previous one because the contact pressures between gear teeth are 40 % higher. Table 9 shows the results obtained for the three lubricants (M0, E1 and E2) in those tests.

All the lubricants reached scuffing on load stage 11, corresponding to a maximum hertzian pressure of 2.54 GPa. The gear lubricated with the mineral oil suffered a very severe surface failure generating a very high mass loss of the pinion (1049 mg). The gear lubricated with the ester based gear oils suffered less severe failures, generating significantly lower mass losses, 181 mg and 75 mg, respectively.

As in the case of the previous test, lubricant E2 presented the lowest oil bath temperature at the end of the scuffing load stage 132 °C, against 144 °C and 164 °C for oils M0 and E1, respectively.

Figure 13 shows the oil bath temperatures at the end of each load stage for the three lubricants tested, all showing a similar behaviour until load stage 9. However, in this more severe test, a clear distinction between the three oils is observed, in terms of oil temperature, after load stage 9, with lubricant E2 always generating significantly lower temperatures.

The degradation of the tooth flanks started between load stages 7 and 8 with oil E1, perhaps explaining the drop in temperature observed at the end of load stage 8, while with M0 and E2 oils it only started on load stage 10. Such differences were probably related to the different chemical compositions and additive packages of the three lubricants.

Table 10 shows the surface roughness parameters measured on the tooth flanks in the axial direction for the three gear oils tested. The comparison of R_{max} and R_{z-D} roughness parameters, between initial values (as manufactured after grinding) and final scuffed values, clearly shows the degradation suffered by the tooth flanks after scuffing. The roughness parameters corresponding to the gear lubricated with the mineral oil M0 ($R_{z-D} = 30.4 \mu\text{m}$) indicate a very severe surface failure in agreement with the very high pinion mass loss measured in this case, while the much lower roughness values measured for the ester based oils ($R_{z-D} = 6.1 \mu\text{m}$ for E1 and $R_{z-D} = 7.5 \mu\text{m}$ for E2) are compatible with their pinion mass losses.

A10/16.6/90 gear scuffing test with industrial gear oils				
Lubricant		M0	E1	E2
k_{FZG}		11	11	11
Weight Loss	[mg]	1049	181	75
Maximum Oil Temperature	[°C]	144,3	164,2	131,7
Contact pressure at the scuffing load stage	[GPa]	2,54	2,54	2,54
Oil viscosity at scuffing	[cSt]	5,41	4,76	9,03

Table 9 – A10/16.6/90 gear scuffing test results with lubricants M0, E1 and E2.

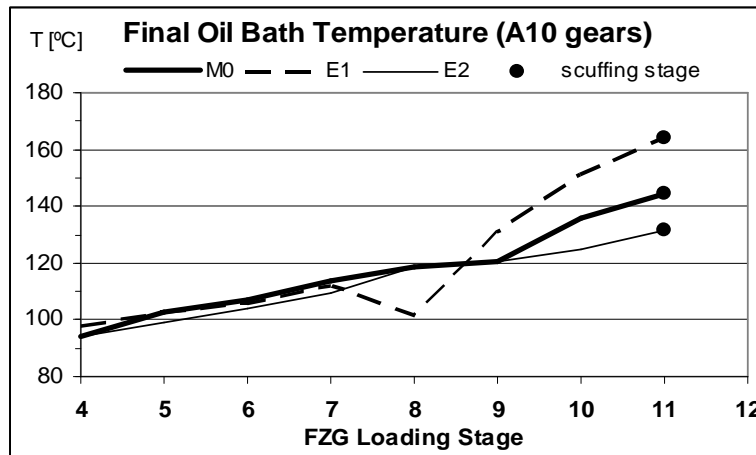


Figure 13- Oil bath temperature at the end of each load stage on A10/16.6/90 FZG gear scuffing tests.

Pinion tooth flank surface roughness parameters in the axial direction [μm] A10/16.6/90 gear scuffing tests							
Oil	Measurement type	Rmax	Rz-D	Ra	Rpk	Rk	Rvk
M0	Initial	1.9	1.2	0.2	0.2	0.4	0.4
	Final undamaged	1.4	1.0	0.1	0.1	0.3	0.3
	Final scuffed	37.2	30.4	6.1	8.5	21.8	2.1
E1	Initial	1.3	0.9	0.2	0.2	0.4	0.2
	Final scuffed	7.8	6.1	0.8	0.9	2.2	2.1
E2	Initial	1.6	1.0	0.2	0.3	0.4	18.9
	Final undamaged	1.6	1.0	0.2	0.1	0.4	0.3
	Final scuffed	19.9	7.5	1.3	1.3	2.2	1.2

Table 10 – Surface roughness parameters on tooth flanks, measured in the axial direction, before and after A10/16.6/90 gear scuffing tests.

5 CRITICAL LUBRICANT TEMPERATURE

Castro (Castro, 2005) proposed a new scuffing criterion for FZG gears, based on the concept of “Critical Lubricant Temperature (T_{CR})” that is the maximum oil bath temperature for which a scuffing failure can happen, whatever the load and the speed. The criterion establishes:

$$T_{CR} - T_0 \leq \frac{\mu \cdot P_0 \cdot V_s \cdot T}{C}$$

where T_0 is the oil bath temperature, C is a constant dependent of oil type and gear material, P_0 is the contact pressure, V_s is the sliding speed, T is the distance from the contact point considered to the pitch point on the meshing line, as shown in Figure 14.

Plotting the 2nd member of the equation $(\mu \cdot P_0 \cdot V_s \cdot T) / C$ against the oil bath temperature, as presented in Figure 15, the critical temperature might be assessed graphically by the intersection of the trend line with horizontal axis.

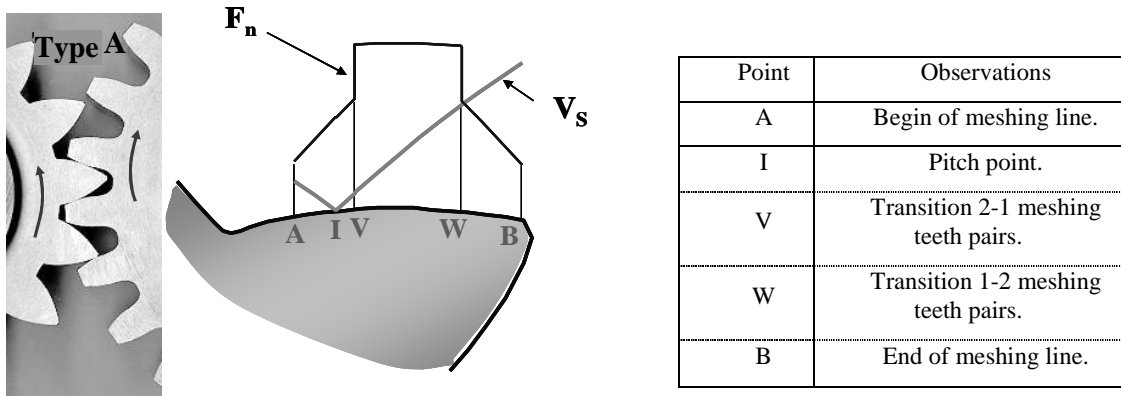


Figure 14 – FZG type A gear geometry and reference points along mesh line.

The critical temperature for each lubricant is displayed in Table 11, and as expected the mineral lubricant has the lowest critical temperature, followed by E1 ester lubricant and the E2 ester lubricant has the highest critical temperature.

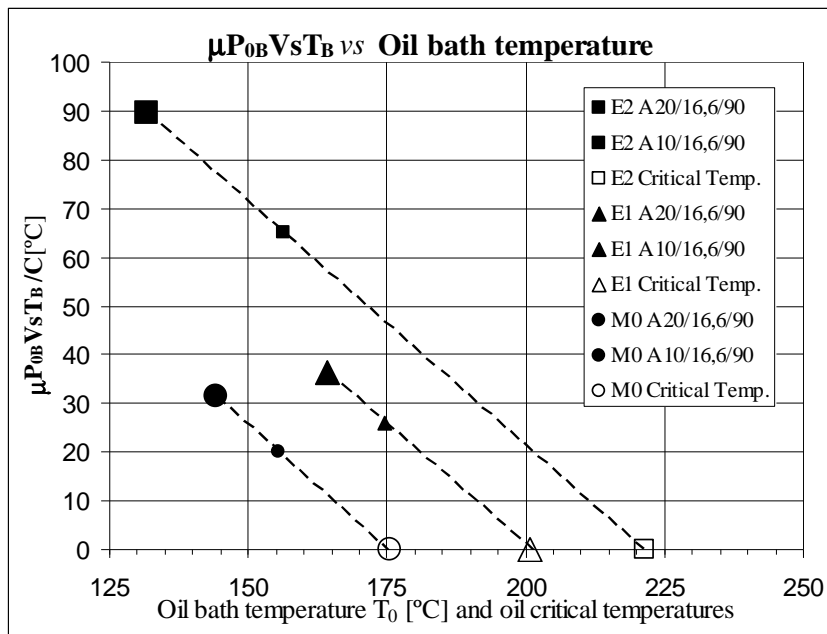


Figure 15– $\mu P_{0B} V_s T_B$ as function of oil bath temperature for point B of contact line (pinion tip – wheel root).

Lubricant	T _{CR} [°C]	C [N/s.°K]
M0	176	8.21x10 ⁵
E1	201	7.16x10 ⁵
E2	221	2.82x10 ⁵

Table 11 – Critical temperature for each industrial gear lubricant tested.

6. CONCLUSIONS

The main conclusions that can be withdrawn from this work are:

- ✓ The best wear preventive properties obtained in the four ball tests are achieved with E2 biodegradable lubricant. The Lubricants M0 and E1 displayed similar behaviours in wear protection, but slightly below gear oil E2.
- ✓ The average wear scar diameter and the ISUC index (severity of wear particles index) show a very good correlation.
- ✓ The scuffing load stages for each lubricant, on FZG A20/16.6/90 test, were: lubricant M0 - K_{FZG} = 11, lubricant E1 - K_{FZG} = 12 and lubricant E2 - K_{FZG} = 12;
- ✓ The scuffing load stage for all lubricants, on FZG A10/16.6/90 test was K_{FZG} = 11;
- ✓ Lubricant E2 generated the lowest oil bath temperatures in both gear scuffing tests.
- ✓ Lubricant E1 generated the lowest mass loss after both scuffing tests.
- ✓ According to the criterion developed Castro (Castro, 2005), the critical lubricant temperatures for each gear oil, in gear scuffing conditions, were: lubricant M0 – T_{CR} = 176 °C, lubricant E1 – T_{CR} = 201 °C and lubricant E2 – T_{CR} = 221 °C.

Globally, the ester based biodegradable gear oils, E1 and E2, showed a very good anti-wear and anti-scuffing performance, above that of the mineral oil in several aspects, thus making them a valid solution for replacing mineral lubricants.

ACKNOWLEDGEMENTS

The authors express their gratitude to the European Union for the financial support given to this work through the Project: “BIOMON – Towards long-life biolubricants using advanced design and monitoring tools” (Proposal n° 508208, Contract n° COOP-CT-2004-508208).

REFERENCES

ASTM International - Standard Test Method for Wear Preventive Characteristics of Lubricating Fluid (Four- Ball Method) Designation: D 4172 – 94 (Reapproved 2004).

Castro, J., Seabra, J., Power dissipation – temperature scuffing criterion for FZG gears, in VDI-Berichte 1904.2: VDI-EKV International conference on gears. 2005: Munchen.

Castro, M.J., Gripagem de engrenagens FZG lubrificadas com óleos base. Novos critérios de gripagem globais e locais. Tese de Doutoramento, Faculdade de Engenharia da Universidade do Porto, Porto, Portugal, 2004, 323 pp (in portuguese). 2004.

DIN 51354 parte 4, Avaliação da capacidade de carga de óleos método standard FZG A/8.3/90. 1990.

Höhn B.-R., K. Michaelis, Influence of oil temperature on gear failures. Tribology International, 37; 2004 p.103-109.

Hunt, T., Handbook of wear debris Analysis and Particle Detection in Liquids, ed. E. Science. 1993.

Klaus L., Gottfried H., Design for Rolling Contac Fatigue, International Journal pf Power Metallurgy, nº39, 2003.

Winter H., Michaelis K., FZG gear test rig - Description and possibilities. In: Coordinate European Council Second International Symposium on The performance Evaluation of Automotive Fuels and Lubricants, 1985.

A.9 Paper I

R. Martins, N. Cardoso, and J. Seabra, “Gear power loss performance of biodegradable low-toxicity ester based oils”, IMech Part J. (to be published).

Gear power loss performance of biodegradable low-toxicity ester based oils

R. Martins ^{a,*} N. Cardoso ^a J. Seabra ^b

^aINEGI, Universidade do Porto, Faculdade de Engenharia, Rua Dr. Roberto Frias s/n, 4200-465 Porto, Portugal

^bFEUP, Universidade do Porto, Rua Dr. Roberto Frias s/n, 4200-465 Porto, Portugal

Abstract

Environmental issues are leading to a growing interest in bio-lubricants, which can have similar or even better performance than mineral and synthetic oils. In this work the power loss performance of two biodegradable, low toxicity, ester based gear oils was evaluated and compared with a commercial mineral oil and an ester based fluid containing ZDDP additives.

Power loss tests were performed on the FZG test rig, using type C carburized gears and the different lubricants under evaluation. The operating temperatures of the oil and of the FZG gearbox wall were measured for different values of the input torque and speed and lubricant samples were periodically collected and analyzed by Direct Reading Ferrography. At the end of the tests, the gear mass loss and the oil viscosity were measured, the teeth flanks were inspected, looking for typical surface failure mechanisms, and the tooth flank surface roughness was measured.

An energetic model of the FZG test gearbox, that took into account the power loss mechanisms inside the gearbox and the heat flow mechanisms from the gearbox to the surrounding environment, was used to calculate the friction losses between the gear teeth, knowing the oil, gearbox wall and room temperatures, in steady-state conditions. Using this model it was possible to analyze the influence of lubricant formulation on the average friction coefficient between gear teeth.

The results obtained showed that one of the biodegradable, low-toxicity, ester based gear oils generated significantly lower mass loss than all the other lubricants, presenting almost no degradation, even when operating at very high temperature for long periods. These bio-lubricants generated friction coefficients between gear teeth up to 27% smaller than the commercial mineral oil, promoted significant reductions of the power loss inside the FZG gearbox, increasing the overall efficiency up to 0.25%.

Key words: Biodegradable lubricants, Non-toxic lubricants, Power losses, Friction coefficient, Gears

1. Introduction

Low operating temperatures, low power losses and high efficiencies are major issues in modern gearboxes, in which gear oils can have significant influence. The most important power loss mechanisms inside a gearbox are the churning losses, generated by

the gears, bearings and seals, and the friction losses, generated in gears and bearings. Churning losses are related to moving parts immersed in the oil sump and friction losses are generated in the contacts between gear tooth and between rolling elements and raceways in rolling bearings [1–5].

The power loss can be related to the equilibrium temperature of the oil sump, for specified operating conditions, which occur when the energetic equilibrium of the gearbox is reached, i.e. when the power

* Tel.: +351225081742; fax: +351225081584
Email address: rcm@fe.up.pt (R. Martins).

loss inside the gearbox is equal to the heat flow evacuated from gearbox to the surrounding environment. The equilibrium temperature is dependent of the gearbox characteristics and of the lubricant properties [1–5]. The higher the power losses the higher will be the equilibrium temperature of the gearbox. A lower equilibrium temperature means higher efficiency, lower friction coefficient, smaller oil oxidation and longer oil life [6,7].

The environmental awareness is leading to a growing interest in biodegradable low-toxicity lubricants. Biodegradability is reached by using a suitable biodegradable base fluid, but low toxicity requires an additivation that is environmentally friendly [8], too. However, the key aspect for any industrial application are technical performance and technical advantages proved in dedicated tests. Lubricant performance (friction, wear, lifetime, load bearing, efficiency, etc.) has a major impact on its overall environmental compatibility, since premature wear or high energy needs are as well harmful to the environment.

Two biodegradable low toxicity ester based oils (E1 and E2, see Table 1), tested in previous works, showed a very high load carrying capacity [9] and a very good micropitting protection [10] in FZG gear scuffing tests and FZG gear micropitting tests, respectively. The same bio oils showed a very good performance in taper roller bearing tests [11], generating significantly lower operating temperatures. Thus, the main objective of this work was the evaluation of the power loss performance of FZG gears lubricated with these bio oils. Gear wear behaviour and lubricant oxidation were also analysed and an energetic model of the FZG gearbox was used to determine the influence of the lubricants on the friction coefficient and on the overall efficiency of the FZG gearbox.

The performance of these bio oils was compared with a commercial mineral gear oil and with another ester based oil containing a special additive package.

2. Lubricants

Two biodegradable low toxicity gear oils (E1 and E2), previously formulated, were tested and compared with a mineral based (M1) and an ester based (E3) gear oils. All the lubricants are classified as CLP gear oils according to DIN 51517, and their main properties are shown in Table 1.

Lubricants E1 and E2 were formulated using

highly biodegradable base oils, a fully saturated ester and a highly saturated ester, respectively. The lack of unsaturated bonds in these two base fluids leads to excellent thermal and oxidative stability. To combine the desired low toxicity with superior gear performance, environmentally compatible, highly efficient additives were added to both oils. In lubricant E1 metal-organic compounds were completely avoided. Lubricants E1 and E2 met both the rapid biodegradability and toxicity criteria specified by the internationally recognised standards, as presented in Table 1. As mentioned above, lubricants E1 and E2 showed a very high performance in gear and taper roller bearing tests [9–11].

Lubricant E3 was based on a fully saturated highly biodegradable ester, and contained special synergistically acting *PD* additives (Plastic Deformation Technology) which create a smoothing effect in gear sets, in machine elements under load. These additives were based on special mild sulphur components, selected surface-active phosphorus components, special zinc dialkyldithiophosphates and liquid mineral oil-soluble molybdenum components. The biodegradability and toxicity characteristics of lubricant E3 were not available.

The mineral gear lubricant M1 was a commercial product, based on a paraffinic oil with significant residual sulphur content. It was formulated with an ashless antiwear additive package based on phosphorous and sulphur chemistry and metal-organic corrosion preventives, providing an improved micropitting resistance. The additive content of this lubricant was considerably higher than those of lubricants E1 and E2. As expected, the mineral lubricant did not accomplish the biodegradability test.

The ester based gear oils (E1, E2 and E3) had a viscosity grade ISO VG 100 while the mineral oil (M1) had a viscosity grade ISO VG 150. The four lubricants had similar viscosities around 100°C, although the ester lubricants had a considerably higher viscosity index. However, the ester based gear oils had considerably lower piezoviscosity coefficient [12]. Those two physical properties have similar contributions to film formation, a higher viscosity as well as a higher piezoviscosity increase the film thickness.

Parameter	Method	Desig.	Units	Lubricating Oils			
Oil type				Industrial gear oil			
				Paraffinic	Fully	Highly	Fully
Base oil	DIN 51451			mineral	saturated	saturated	saturated
				oil	ester	ester	ester
Lubricant reference				M1	E1	E2	E3
Chemical Content							
Zinc	ASTM D-4927	Zn	ppm	-	-	-	na
Calcium	ASTM D-4927	Ca	ppm	40	-	-	na
Phosphorus	ASTM D-4927	P	ppm	175	146	300	na
Sulphur	ASTM D-4927	S	ppm	15040	180	5500	na
Physical properties							
Density @ 15°C	DIN 51757	ρ_{15}	g/cm ³	0.894	0.928	0.962	0.934
Kinematic Viscosity @ 40°C	DIN 51562	ν_{40}	cSt	153.6	98.4	116.6	110.9
Kinematic Viscosity @ 100°C	DIN 51562	ν_{100}	cSt	14.4	13.3	16.9	15.2
Viscosity Index	ISO 2909	VI		96	152	162	156
Pour point	ISO 3106		°C	-27	-42	<-30	na
Wear properties							
KVA weld load	DIN 51350-2		N	2200	2200	-	na
KVA wear scar (1h/300N)	DIN 51350-3		mm	0.32	0.35	-	na
Brugger	DIN 51347-2		N/mm ²	68	37	-	na
FZG rating	DIN 51354	K_{FZG}		>12	>12	>12	na
Biodegradability and toxicity properties							
Ready biodegradability	OECD, 301 F		%	<60	≥60	≥60	na
Aquatic toxicity with Daphnia	OECD, 202	EL₅₀	mg/l	>1000	>100	>100	na
Aquatic toxicity with Algae	OECD, 201	EL₅₀	mg/l	>100	>100	>100	na

Table 1
Lubricant properties.

3. Gear power loss tests

3.1. FZG gear test rig and type C gears

Figure 1 shows a schematic view of the FZG back-to-back spur gear test rig [13]. FZG type C gears, made of DIN 20MnCr5 steel, carburized, quenched in oil and annealed were used, reaching a tooth flank surface hardness around 62 HRC. Their geometrical characteristics are shown in Table 2. The tested gears had a lower gear accuracy grade than standard type C gears, having higher surface roughness, as shown in Table 3, and consequently yielding a lower operating specific film thickness. Table 3 also displays the nomenclature and lubricant used in each test.

The power loss tests were performed using dip lubrication with an oil volume of 1.5 l.

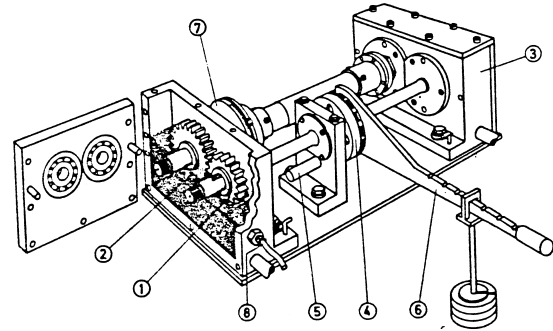


Fig. 1. Schematic representation of FZG test rig.

Type C gear Pinion Wheel		
Number of teeth	16	24
Module [mm]	4.5	
Centre distance [mm]	91.5	
Pressure angle [°]	20	
Face width [mm]	14	
Addendum modification	0.182	0.171
Addendum diameter [mm]	82.64	118.54

Table 2
Geometrical characteristics of FZG type C gears

Gear reference	Gear quality (ISO 1328)	Ra of tooth flanks [μm]	
		Axial	Radial
Standard	5	/	0,5
C-M1	9	0,18	1,20
C-E1	9	0,10	1,09
C-E2	9	0,09	1,09
C-E3	9	0,15	1,21

Table 3
Gear power loss test codification, type C gears quality grade, average surface roughness (pinion and wheel) in axial and radial directions.

3.2. Test procedure

In each gear power loss test, the gear and the lubricant were submitted to a wide range of operating conditions, as shown in Table 4, with an input power going from 0.5 kW to 102 kW. The test was composed by four different load (torque) stages, each one performed at three different speeds, as presented in Table 4. Each torque - speed combination lasted 4 hours, which was the time necessary to reach a stabilized operating temperature. In order to avoid a potential damage of the test rig, the maximum admissible oil temperature was set to 180°C, being the test stopped if reached. Each load (torque) stage started at the wheel speed of 1000 rpm, which was increased to 2000 rpm after 4 hours and to 3000 rpm after another 4 hours.

The first load stage, performed at very low torque ($T = 4.95 \text{ Nm}$), was used to evaluate the churning losses inside the FZG test gearbox, while gear running-in occurred. When the test started the oil was at room temperature, since at low speed (1000 rpm) the stabilized oil operating temperature was slightly above 40°C. The stages performed at higher torques begin at an oil temperature of 40 °C (± 2 °C).

The temperatures of the oil, of the gearbox wall and of the test room were continuously recorded during the tests. Room ventilation was used in order to maintain the room temperature almost constant (28 ± 2 °C).

The lubricant was not changed during the test. At the end of each load stage, a lubricant sample was collected (approximately 40 ml) and the same volume of fresh lubricant was added, in order to keep the total oil volume constant. A gear power loss test represents 48 hours of operation for each lubricant, corresponding to 5.76 million cycles.

3.3. Stabilization temperature

As mentioned above, the equilibrium temperature of the gearbox and of the lubricant occurs when the power loss generated inside the gearbox is equal to the heat flow evacuated from the gearbox to the surrounding environment. The power loss (P) inside the gearbox as well as the heat flow (Q) from it can be directly related to the difference between lubricant temperature and room temperature, that is, ($\Delta T = T_{oil} - T_{room}$). This difference between oil and room temperature will be designated as the stabilization temperature. Figure 2 shows the oil and the stabilization temperature for all the lubricants and operating conditions tested.

At very low torque ($\simeq 4.95 \text{ Nm}$) the churning losses are the most important power loss mechanism, depending mainly on the lubricant viscosity and input speed. Under these conditions the oil temperatures were very similar for all lubricants, 43 to 47°C at 1000 rpm, 62 to 66°C at 2000 rpm and 85 to 93°C at 3000 rpm. The corresponding stabilization temperatures were also very similar, 16 to 18°C at 1000 rpm, 35 to 38°C at 2000 rpm and 57 to 65°C at 3000 rpm. It's interesting to notice that at 1000 and 2000 rpm the mineral oil M1 had a higher stabilization temperature than the ester based fluids, while at 3000 rpm the opposite occurred. The main cause for this behaviour is related to lubricants viscosity, since at 1000 and 2000 rpm the mineral oil temperature was 47 and 66°C, respectively, having higher viscosity than the ester based fluids, while at 3000 rpm the mineral oil temperature was 85°C, having almost the same viscosity of the ester based lubricants. In general, for operating temperatures above 85°C, the mineral oil M1 always generated lower churning losses than the ester based fluids, because it had lower viscosity.

Test type	Wheel Torque [rpm]	Wheel Speed [Nm]	Input Power [kW]	Initial temp. [°C]	Test time [hours]	Number of cycles [x10 ⁶]	Oil samples
No load tests	4.95	1000	0.52	Room	4	0.24	
	4.95	2000	1.04		4	0.48	
	4.95	3000	1.56	temp.	4	0.72	40ml
	105.0	1000	11.00	40 (±2)	4	0.24	
	105.0	2000	21.99	(±2)	4	0.24	
	105.0	3000	32.99	(±2)	4	0.24	40 ml
Load tests	198.8	1000	20.81	40 (±2)	4	0.48	
	198.8	2000	41.63	(±2)	4	0.48	
	198.8	3000	62.44	(±2)	4	0.48	40 ml
	323.4	1000	33.87	40 (±2)	4	0.72	
	323.4	2000	67.73	(±2)	4	0.72	
	323.4	3000	101.60	(±2)	4	0.72	540 ml
Total					48	5.76	

Table 4
Wheel operating conditions of the power loss gear tests.

In the tests performed at higher wheel torque, respectively, 105, 199 and 323 Nm, the friction power losses had a very significant increase, and became higher than the churning losses. At very high torque (323 Nm) and high speed (3000 rpm) the temperatures of the lubricants were always above 150°C and the corresponding stabilization temperatures above 127°C.

At constant speed (e.g. 2000 rpm) the stabilization temperature increased when the applied torque increased, for all lubricants. The mineral oil M1 showed lower stabilization temperature than the ester based lubricants, for an input torque of 105 Nm, and higher stabilization temperature at torques of 199 and 323 Nm, indicating that oil M1 generated higher friction losses than the ester based fluids at higher torques. The stabilization temperatures measured at the highest torque (323 Nm), whatever the speed, also showed that oil M1 always generated the highest stabilization temperatures and thus the highest friction losses, while fluid E2 always produced the lowest stabilization temperatures and friction losses.

The stabilization temperatures measured at the torque of 105 Nm are very interesting, since they put into evidence the balance between churning and friction losses. In fact, at 1000 rpm all lubricants had very similar stabilization temperatures, between 32 and 34°C, meaning that the balance between fric-

tion and churning losses was similar for all lubricants. For 2000 and 3000 rpm, the lubricant temperatures reached 90 and 120°C, respectively, because the churning losses increased. Under these conditions (low torque and high speed) oil M1 showed a lower stabilization temperature than the ester based fluids.

In general the biodegradable low-toxicity oil E2 generated low stabilization temperatures, mainly at high torque, having a better energetic performance than the other 3 oils.

3.4. Gear wear and lubricant degradation

At the end of each test, the gear was dismantled and carefully inspected. The mass loss was measured, the wear particles contained in the oil samples were analyzed and the tooth flanks were inspected, looking for any signs of typical gear failure (micro-pitting, pitting, scuffing, excessive wear, ...).

Figure 3 shows the mass loss of the gear tested with each lubricant. C-E1 gear lost 525 mg, which was an excessive value, indicating the occurrence of a failure. In fact, some tooth flanks presented a scuffing failure as shown in Figure 6, and this mass loss value couldn't be compared with the mass loss of the other gears. However, this failure was not expected, since in previous gear scuffing tests [9] E1 oil showed a very high load carrying capacity, signif-

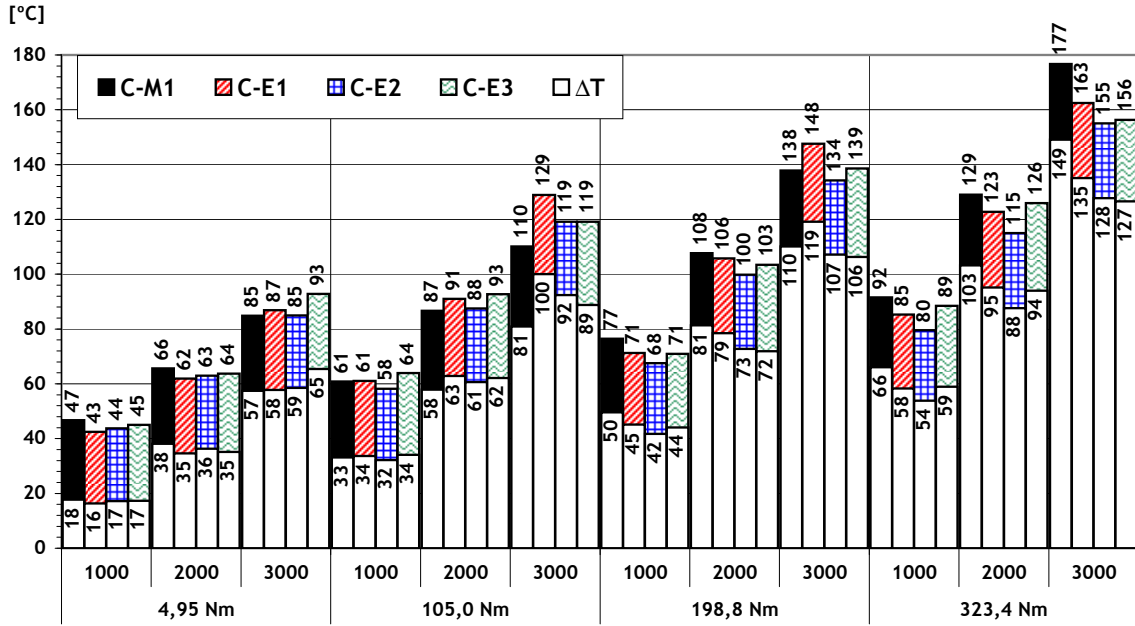


Fig. 2. Equilibrium and stabilization oil bath temperature measured during the tests vs. input speed and input torque.

icantly above that of the mineral oil M1. C-E2 gear presented the lowest mass loss of all gears, 7 mg, while the mass loss of C-E3 gear was 77 mg, higher but similar to that of C-M1 gear, 55 mg. In terms of gear mass loss the performance of E2 fluid was excellent.

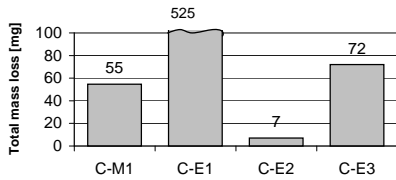


Fig. 3. Total gear mass loss measurements for each lubricant.

The oil samples collected during the power loss tests were analyzed by direct reading ferrometry (DRIII) in order to measure the evolution of the ferrometric indexes (DL, DS, CPUC and ISUC) [14]. The CPUC (concentration of wear particles index) ferrometry values are shown in Figure 4. E2 oil always had lower CPUC values than M1 and E3 during each test stage and the final values measured for all oils were totally in agreement with the mass loss results. E1 and M1 oils had similar CPUC values during the tests. However, the scuffing failure that occurred during the last load stage with gear C-E1 generated a very large amount of wear particles, clearly identified by the final CPUC value of E1 oil.

The ISUC (severity of wear particles index) ferrometry values are shown in Figure 5. ISUC values show exactly the same trends of the CPUC values, confirming the wear performance indicated by the mass loss and CPUC results. In general, the ferrometry results showed an excellent performance of E2 gear oil.

The gears lubricated with E1 and E3 oils performed a slightly higher number of cycles during the running-in load stage due to problems with data acquisition hardware, concerning temperature measurement.

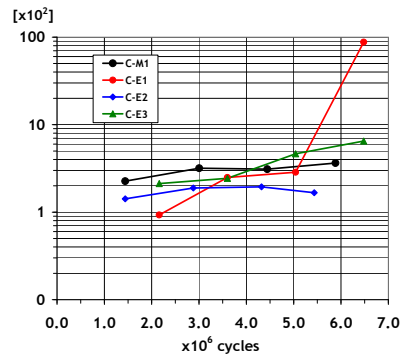


Fig. 4. CPUC wear particles index along gear power loss tests.

At the end of each test an additional oil sample of 500 ml was collected in order to measure the lubri-

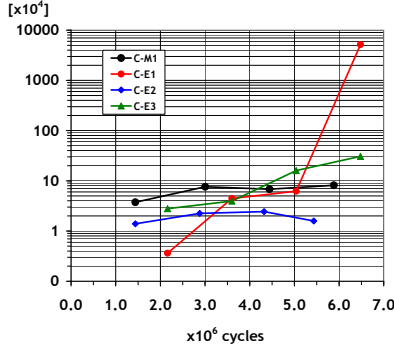


Fig. 5. ISUC wear particles index along gear power loss tests.

cant viscosity and compare it with the corresponding fresh oil value, as shown in Table 5.

The mineral oil (M1) kinematic viscosity increased 10.5% at 40°C and decreased 5.5% at 100°C, leading to a very strong reduction of the Viscosity Index (-26%). This oil was submitted to very high temperatures, well above 100°C, during large periods of time, justifying this strong VI reduction. The ester based oils E1 and E3 had opposite results, since the Viscosity Index of oil E1 decreased 8% and that of oil E3 increased 8%. The kinematic viscosity of oil E2 presented a small increase, both at 40 and 100°C, and the Viscosity Index remained almost constant (-1%).

Test reference	Temp. [C]	kinematic viscosity [cSt]		VI	
		Fresh oil	Used oil	Variation	Variation
C-M1	40	150.0	165.7	10.5%	
	100	14.6	13.8	-5.5%	-26%
C-E1	40	99.4	102.4	3.0%	
	100	14.6	14.1	-3.4%	-8%
C-E2	40	114.5	119.9	4.7%	
	100	17.0	17.4	2.4%	-1%
C-E3	40	108.3	103.2	-4.7%	
	100	15.9	16.2	1.9%	+8%

Table 5

Variation of lubricant viscosities during the power loss tests.

3.5. Tooth flank surface analysis

Gear tooth flanks were carefully inspected at the end of the tests. Figure 6 shows pictures of those tooth flanks for each one of the tested pinions, and in all cases it is possible to observe typical micropitting areas below the pitch line, surrounded by a red

line, and these micropitting areas in the gears lubricated with M1 and E2 oils are smaller than those observed in gears C-E1 and C-E3. Above the pitch line significant differences were also observed. C-E2 gear had very small wear, as confirmed by the mass loss and oil analysis results and almost all the original grinding marks were still visible. The gears lubricated with M1 and E3 fluids showed significant adhesion marks (small polished zones), mainly in the case of gear C-E3, justifying why they had higher mass losses than C-E2. In the case of gear C-E1 a scuffing failure was clearly observed with deep wear grooves in the radial direction of the tooth flanks. It's interesting to notice that in the zones of the tooth flanks closer to the pitch line, where the sliding velocity is very small, the grinding marks were still visible in all gears and significant wear marks were not observed.

Surface roughness measurements were made before and after each gear power loss test, above and below the pitch line, using a measurement length of 4.8 mm and a cut-off of 0.8 mm. Figure 7 and Figure 8 show the roughness measurements performed above and below the pitch line, respectively, after gear manufacturing (thin lines) and after test (thick lines).

In previous gear scuffing tests, performed with the same lubricants, same gear material and same gear geometry [9], it was observed that the scuffing failure always occurred above the pitch line and could be clearly assessed if the tooth flank roughness was measured in the axial direction, as shown in Figure 7. The scuffing failure of C-E1 gear is clearly put into evidence, gear C-M1 and C-E2 showed typical mild wear and gear C-E3 showed a significant amount of adhesion marks.

In previous gear micropitting tests, performed with the same lubricants, same gear material and same gear geometry [10], it was observed that micropitting always occurred below the pitch line and the number of micropits and their depth could be clearly identified if the tooth flank surface roughness was measured in the axial direction, as shown in Figure 8, since in that direction the initial roughness profiles (after grinding) were very smooth and regular. Gear C-E1 showed a very strong modification of roughness profile, indicating that a large modification of the tooth geometry occurred. C-M1 gear showed a few micropits of very small depth (less than 2 - 3 μm), C-E3 gear showed many micropits of very small depth (less than 2 μm) while gear C-E2 had many micropits of larger depth (between

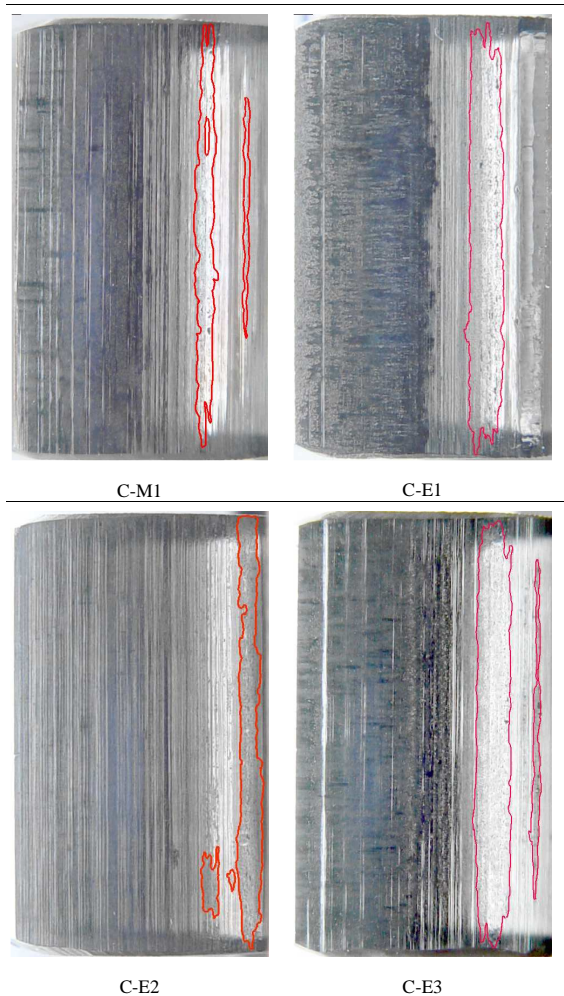


Fig. 6. Pictures of tooth flanks after the power loss tests.

4 - 5 μm).

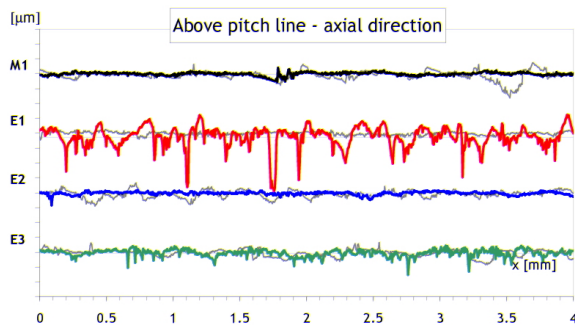


Fig. 7. Roughness profiles above pitch line in the axial direction.

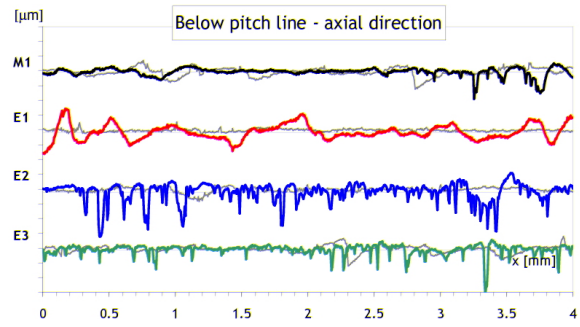


Fig. 8. Roughness profiles below pitch line in the axial direction.

4. Friction coefficient between gear tooth

In a previous work [15] a model for the energetic behaviour of the FZG test gearbox was developed, taking into account all types of power loss and heat flow evacuation mechanisms in presence. Such model is described by equation Equation (1), where P_{fr} represents the friction power dissipated by the gears, P_{M1} is the friction power dissipated by the bearings, P_{spl} is the power dissipated by the seals, P_{M0} is the churning power dissipated by the bearings, P_{sl} is the churning power dissipated by the gears, Q_{rad} is the power evacuated by radiation, Q_{cnv} is the power evacuated by convection and Q_{cn} represents the power evacuated by conduction.

$$P_{fr} + P_{M1} + P_{spl} + P_{M0} + P_{sl} = Q_{rad} + Q_{cnv} + Q_{cn} \quad (1)$$

This equation allows the determination of the oil temperature in permanent conditions (equilibrium temperature) for any combination of the operating conditions imposed to the gearbox, considering both the friction and the churning power loss mechanisms, in particular the friction power loss (P_{fr}) between the gear tooth. Equation (1) depends on 5 unknown variables: the oil equilibrium temperature (T_{oil}), the gearbox wall temperature (T_w), the room temperature (T_{room}), the average friction coefficient between the gear tooth (μ_m) and the conduction factor (f_{cn}) [3].

The energetic model was based on optimization techniques, using the least squares method implemented in Matlab[®] and it could be used to optimize several variables. The optimization function was Equation (1) and the variables to optimize could be any of the model parameters. The main application of the model was the evaluation of the average friction coefficient between gear tooth (μ_m) and of the conduction factor (f_{cn}), which were the param-

eters to be optimized for each lubricant tested, and the temperatures measured were used as input parameters. A detailed description of this model might be found in reference [15].

When lubricant temperature increases it has two opposite effects, promoting higher chemical activity and better tribological layer formation, and, simultaneously, decreasing lubricant viscosity and leading to lower film thickness. Both effects have a direct influence on the friction coefficient between gear tooth. At the same time when the lubricant temperature increases the gearbox wall temperature also increases, affecting the heat flow evacuation mechanisms (radiation, convection and conduction).

One of the main influences of using a different lubricant or a different material in a tooth contact is on the friction coefficient. Hohn et al. [1] developed an expression (see Equation (2)) for the average friction coefficient along the contact line, which already integrates a lubricant factor X_L taking into account the influence of oil formulation. The value of the lubricant factor for additive free mineral oils is $X_L = 1$. All gear oils tested had different formulations in terms of base oils and additives and the lubricant factor X_L was optimized for each gear oil in order to obtain the best correlation with the experimental results.

$$\mu_m = 0.048 \cdot \left(\frac{F_{bt}/b}{v_{\sum c} \cdot \rho_c} \right)^{0.2} \cdot \eta_{oil}^{-0.05} \cdot Ra^{0.25} \cdot X_L \quad (2)$$

The expression used for the lubricant factor X_L was dependent of all variables involved in Equation (2). However, the results obtained showed that the best correlation was obtained for a load (F_{bt}) dependent X_L factor, whatever the lubricant considered, while the other variables had no significant influence. The X_L lubricant factor used is shown in Equation (3).

$$X_L = \frac{1}{(F_{bt}/b)^{b_1}} \quad (3)$$

Table 6 presents the determined values of b_1 exponent of Equation (3). The correlation between experimental and model temperatures were always above 97%, using the X_L lubricant factor determined.

Figure 9 shows the reduction in the friction coefficient between gear tooth promoted by the ester based lubricants, taking as reference the commercial mineral lubricant M1 ($\frac{\mu_{E_i} - \mu_{M1}}{\mu_{M1}}$), at 1000 and 3000 rpm, torques up to load stage K10 (wheel torque = 398 Nm), a room temperature of 25°C and the equi-

Test ref.	Lubricant	b_1
C-M1	Mineral	0.0612
C-E1	Ester	0.0738
C-E2	Ester	0.1055
C-E3	Ester	0.0995

Table 6
Value of b_1 exponent for each lubricant test.

librium oil temperature predicted by the gearbox energetic model. Such reduction in friction coefficient can go from 5% (lubricant E1, on load stage K5 at 3000 rpm) to 27% (lubricant E2, on load stage K10 at 1000 rpm).

These reductions in friction coefficient promoted by the ester based lubricants had a direct influence on the global efficiency of the FZG gearbox, as shown in Figure 10. At the highest load stage (K10) lubricant E2 improved the gearbox efficiency by 0.25% at 1000 rpm and 0.20% at 3000 rpm, in comparison to M1. Such improvement in gearbox efficiency corresponds to a reduction in power loss of 100 W at 1000 rpm and over 250 W at 3000 rpm.

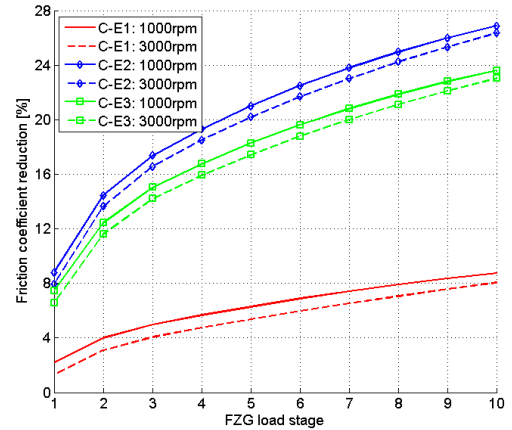


Fig. 9. Reduction in friction coefficient promoted by the ester based lubricants in comparison to M1 lubricant.

5. Discussion

Table 7 summarises the most important results of the gear power loss tests and of the post-testing analysis, for all the tested lubricants.

As shown in Table 7, the experimental and predicted values for the oil and stabilization temperatures were very similar for all lubricants, showing that the energetic model developed for the FZG

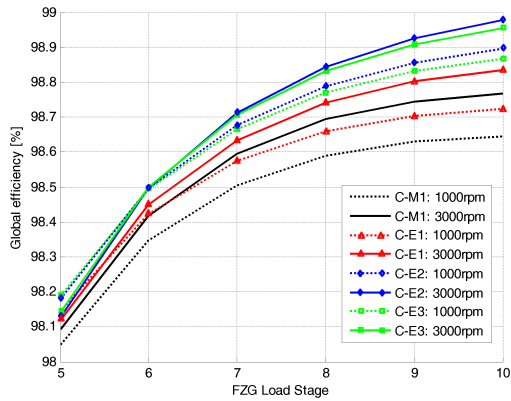


Fig. 10. Comparison of global gearbox efficiency in function of lubricants and load.

gearbox established a very good approximation of the power loss and heat evacuation mechanisms in presence. This good correlation between experimental and model temperature values also showed how the friction coefficient was influenced by the oil formulation and how important was the balance between friction and churning power losses in the model developed.

		Lubricants			
Parameter	units	M1	E1	E2	E3
Load stage K9 at 2000 rpm					
<i>Toil</i> exp.	C	129	123	115	126
<i>Toil</i> model*	C	128	124	115	116
ΔT exp.	C	103	95	88	94
ΔT model*	C	103	99	90	91
Friction coefficient	/	0.37	0.33	0.27	0.28
Power loss	W	880	840	740	760
Efficiency	/	98.70	98.76	98.91	98.88
Overall results					
Mass loss	mg	55	525 ^a	7	72
CPUC	/	364	8780 ^a	167	650
VI variation	/	-26%	-8%	-1%	8%
Micropitting area	/	low	high	low	high
Pits depth	/	low	^a medium	low	low

Table 7
Summary of gear power loss tests results. * - assuming a room temperature of 25 °C. ^a - values after a scuffing failure.

In general, the ester based lubricants generate lower oil temperatures and lower stabilization temperatures than the mineral oil, mainly at high torque

and low speed, that is, when the friction power loss is the most important power loss mechanism. This means that the ester based lubricants generate lower friction coefficient between gear tooth than the mineral oil, and consequently lower friction power loss than the mineral oil. However, if the operating conditions promote high churning power loss and low friction power loss, that is, at high speed and low torque, the mineral oil might generate a global power loss lower than the ester based oils, mainly if the operating oil temperature is over 85 °C. Above this temperature the viscosity of the mineral oil is lower than those of the ester based lubricants, leading to lower churning losses. In almost all operating conditions, but mainly at high torque, the biodegradable low toxicity ester based gear oil E2 had a very good performance generating the lowest oil operating temperatures and stabilization temperatures.

For the operating conditions considered in Table 7, wheel speed of 2000 rpm, wheel torque of 323 Nm and room temperature of 25 °C, oil E2 generated the lowest oil and stabilization temperatures, the lowest friction coefficient, the lowest power loss and the best efficiency.

The mass loss and CPUC oil analysis results showed that the wear performance of oil E2 was outstanding, generating a mass loss of 7 mg in almost 6 million cycles, significantly below the other lubricants tested. In terms of oil degradation the performance of oil E2 was also very good, showing an extremely small variation of the Viscosity Index at the end of the gear power loss test, although the oil operating temperature was above 100 °C for more than 20 hours. In these conditions the behaviour of the mineral oil was poor, as expected, and the lubricant showed significant degradation after the test.

All the tested gears showed some micropitting below the pitch line. However, the depth of the micropits was very small in all cases (less than 4 micrometers). The micropitting area was smaller in the gears lubricated with oils M1 and E2. Oil M1 contained a special additive package that enhances the micropitting protection and oil E2, although formulated with a low toxicity additivation, showed again a very good performance.

The gear lubricated with oil E1 presented a scuffing failure during the last load stage, generating a very high amount of wear and a considerable degradation of the tooth flank surface roughness. The main cause of this failure is not related to the formulation of this lubricant, since in previous gear scuffing tests its behaviour was very good. The main

cause for this failure is related to the low film thickness generated by this lubricant is some operating conditions, because it had the lowest viscosity and also the lowest pressure viscosity coefficient of all lubricants. When formulating gear oils with ester based fluids, it should be taken into account that the piezoviscosity coefficient of the ester fluids is 40% lower than that of a mineral oil and this can have a negative influence in terms of film thickness generation. In fact, the viscosity of oil E1 was always smaller than that of the mineral oil M1, and this together with the lowest piezoviscosity coefficient leads to a significantly smaller film thickness (around 30% less in this case).

6. Conclusions

The results of the gear power loss tests clearly indicate that it is possible to formulate biodegradable low toxicity gear oils that have a better performance than highly doped lubricants, in terms of gear power loss, tooth flank wear and oil degradation. The behaviour of the biodegradable, low toxicity, ester based gear oil E2 was excellent, showing that:

- Lubricant E2 generated lower stabilization temperatures than the other lubricants, mainly at high input torque.
- Lubricant E2 had the best wear protection (mass loss $\bar{7}$ mg) and the best CPUC (concentration of wear particles index) oil analysis result.
- Lubricant E2 presented almost no degradation during the gear power loss test, although it operated above 120 C for more than 10 hours, showing a very slight reduction of the Viscosity Index at the end of the test (-1%).
- Lubricant E2 generated a significant decrease of the friction coefficient between gear teeth (up to 27% when compared with the commercial mineral oil) and, consequently, a decrease of the friction power losses between gear teeth and an improvement of the FZG test gearbox efficiency (up to 0.25% when compared with the commercial mineral oil).
- The temperatures calculated by energetic model, used to assess the power loss and heat flow mechanisms of the FZG test gearbox, showed very good correlation with the experimental results.

Acknowledgements

The authors express their gratitude to the European Union for the financial support given to this work through the Projects: "EREBIO - Emission reduction from engines and transmissions substituting harmful additives in biolubricants by triboreactive materials", (Proposal n° GRD2-2001-50119 Contract n° G3RD-CT-2002-00796-EREBIO). "BIOMON - Towards long-life biolubricants using advanced design and monitoring tools" (Proposal n° 508208, Contract n° COOP-CT-2004-508208).

The authors would also like to thank: Dr. Amaya Igartua from "Fundacion Tekniker" for the biodegradability and toxicity lubricant tests, Dr. Rolf Luther from "FUCHS Petrolub AG. for supplying the ester lubricants and Dr. Harald Bock from "Rowe Mineralölwerk GMBH " for supplying the ester lubricants.

References

- [1] B.-R. Höhn, K. Michaelis, T. Vollmer, Thermal rating of gear drives: Balance between power loss and heat dissipation, AGMA Technical Paper.
- [2] C. Changenet, M. Pasquier, Power losses and heat exchange in reduction gears: Numerical and experimental results, VDI Berichte 2 (1665) (2002) 603–613.
- [3] H. Winter, K. Michaelis, Investigations on the thermal balance of gear drives, in: Fifth World Congress on Theory of Machines and Mechanisms, American Society of Mechanical Engineers, 1979.
- [4] P. Eschmann, Ball and roller bearings - Theory, design and applications, 1985.
- [5] C. Changenet, P. Velex, A model for the prediction of churning losses in geared transmissions - preliminary results, Journal of Mechanical Design 1 (2007) 128–133.
- [6] B.-R. Höhn, K. Michaelis, A. Doleschel, Frictional behavior of synthetic gear lubricants, in: G. Dalmaz, A. Lubrecht, D. Dowson, M. Priest (Eds.), Tribology research: From model experiment to Industrial Problem, Elsevier, 2001.
- [7] B. R. Hohn, K. Michaelis, Influence of oil temperature on gear failures, Tribology International 37 (2) (2004) 103–109.
- [8] M. Weck, O. Hurasky-Schonwerth, C. Bugiel, Service behaviour of pvd-coated gearing lubricated with biodegradable synthetic ester oils, VDI-Berichte (Nr1665).
- [9] R. Martins, N. Cardoso, J. Seabra, Influence of lubricant type in gear scuffing (to be published), Industrial Lubrication and Tribology 60 (6) (2008) 0.

- [10] R. Martins, J. Seabra, Micropitting performance of mineral and biodegradable ester gear oils (to be published), *Industrial Lubrication and Tribology* 60 (6) (2008) 0.
- [11] A. Campos, B. Graça, J. Seabra, H. Bock, Power loss in taper roller bearings: Mineral oils vs. biodegradable esters, in: *IBERTRIB 2007, IK4, Bilbao, 2007*.
- [12] J. W. Gold, A. Schmidt, H. dicke, H. Loos, C. Aßmann, Viscosity-pressure-temperature behaviour of mineral and synthetic oils, *Journal of Synthetic Lubrication* 18 (1).
- [13] H. Winter, K. Michaelis, Fzg gear test rig - description and possibilities, In: *Coordinate European Council Second International Symposium on The performance Evaluation of Automotive Fuels and Lubricants*.
- [14] T. Hunt, *Handbook of Wear Debris Analysis and Particle Detection in Liquids*, 1993.
- [15] R. Martins, J. Seabra, A. Brito, C. Seyfert, R. Luther, A. Igartua, Friction coefficient in fzg gears lubricated with industrial gear oils: Biodegradable ester vs. mineral oil, *Tribology International* 39 (6) (2006) 512–521.